DOCTOR OF PHILOSOPHY

Phosphorylation, ubiquitylation and characterisation of specific inhibitors of AMPK-related kinase NUAK1/ARK5

Banerjee, Sourav

Award date:
2013

DOCTOR OF PHILOSOPHY

Phosphorylation, ubiquitylation and characterisation of specific inhibitors of AMPK-related kinase NUAK1/ARK5

Sourav Banerjee

2013

University of Dundee

Phosphorylation, ubiquitylation and characterisation of specific inhibitors of AMPK-related kinase NUAK1/ARK5

by

Sourav Banerjee

A thesis submitted for the degree of Doctor of Philosophy,

MRC Protein Phosphorylation and Ubiquitylation Unit,

College of Life Sciences,

University of Dundee,

July 2013.

Abstract

LKB1 tumor suppressor is a master upstream protein kinase responsible for activation of 14 different AMPK family members including AMPK and several less studied enzymes such as MARK, BRSK, SIK and NUAK. These enzymes are together thought to play essential roles in controlling cellular energy levels, cell polarity and proliferation. The related NUAK1 and NUAK2 are members of the AMPK family and there is increasing interest in these kinases as recent work suggests they play important roles in regulating key biological processes including Myc driven tumourigenesis, senescence, cell adhesion and neuronal polarity. Recent work from our laboratory has shown that NUAK1 phosphorylates and inhibits the myosin phosphatase complex MYPT1-PP1β following stimuli that induce cell detachment. In this work, I describe the first highly specific protein kinase inhibitors of NUAK kinases namely WZ4003 and HTH-01-015. WZ4003 inhibits both NUAK isoforms (IC50 for NUAK1 20 nM and NUAK2 100 nM), whereas HTH-01-015 inhibits only NUAK1 (IC50 100 nM). These compounds display extreme selectivity and do not significantly inhibit the activity of 139 other kinases tested including 10 AMPK family members. In all cell lines tested, WZ4003 and HTH-01-015 inhibit the phosphorylation of the NUAK substrate MYPT1 at Ser445 which can be rescued by overexpressing drug resistant NUAK1[A195T] which exhibits approximately 50 times more resistance to both the inhibitors. I also demonstrate that administration of WZ4003 and HTH-01-015 significantly inhibit cell migration, proliferation and invasion in cells to a similar extent as NUAK1 knock-out/ knock-down. My data indicate that WZ4003 and HTH-01-015 will serve as useful chemical probes to delineate the biological roles of the NUAK kinases. Furthermore, I present the evidence that NUAK1 interacts with the SCF-βTRCP complex and undergoes phosphorylation mediated degradation. NUAK1 possesses a slightly modified degron sequence that specifically binds to the SCF-βTRCP complex on PLK1 mediated phosphorylation of two serines in the degron. This interaction is lost upon mutating the serine residues on NUAK1 degron. Endogenous NUAK1 gets ubiquitylated and degraded on hyperphosphorylation and subsequently is protected from this degradation in the presence of NEDDylation inhibitor MLN-4924. The knock-out MEFs for the βTRCP1 substrate recognition motif also exhibit double the amount of NUAK1 as compared to the wild-type MEFs. Moreover, I provide evidence showing that NUAK1 is degraded in G2-M stage of the cell cycle, which is mediated by the SCF-βTRCP complex. This degradation is being triggered upon PLK1 mediated phosphorylation of the degron that can be reversed upon treatment with PLK1 inhibitor BI-2536. Thus my data suggests that NUAK1 on being phosphorylated by PLK1 binds to, and is consequently degraded by SCF-βTRCP in the G2-M stage of the cell cycle.

List of Figures

List of Tables

Acknowledgements

First of all I would like to thank my supervisor Prof. Dario Alessi for all his guidance and support and for providing me with the opportunity to be a part of his laboratory. I also would like to acknowledge Sir Philip Cohen and Dr. Vicky Cowling for all the helpful discussions and advice and my thesis committee supervisors Prof. Ron Hay and Dr. Thimo Kurz for important suggestions.

A huge thanks to Maria Deak, Tom Macartney, Mark Peggie, Rachel Toth and James Hastie from the DSTT cloning and protein expression teams, Ryan and Jenny from inhibitor screening and DNA sequencing team. Special thanks to Dave, Bob and Joby who helped tremendously with proteomics, Alan Prescott who spent many hours with me in front of a microscope and Ram, Rosie and Arlene for help with FACS. I also want to thank Kirsten Airey and Janis Stark for always being there for my sudden and unplanned 293 and U2OS flask demands. Judith Hare, Allison Bridges and Alison Hart, who were always there for both formal as well as for potluck support.

I would like to convey my thanks to all the past members of Dario's lab, who were instrumental in helping me develop and learn each day - Anna, Bea, Fatema, Elton, Juanma, Stephan, Laura, Jeremy, Nic, Ciaran, Kei, Fran, Youcef, Akihito, Ayaz and Michale. Of course, no one can deny the roles played by the current members in helping me out through the last few days of my PhD – Chandana (get ready, you are next!), Noor, Piotr (the knock-in blues), Paola (gossips!), Ana, Jenny, Vanessa, Esther, Ning, Francesca, Jinwei, Miratul, Helen, Laia, Ruzica and the evergreen Paul (thanks for the cricket discussions and valuable suggestions, I owe you a litre of prawn curry). A special thanks goes to the girls of my bay, Eeva, Agne and Kris for keeping Bay 3 serene, tranquil, beautiful and with an air of optimism all through (JOKE!)..... Kris, best of luck with organising future DRA lab potlucks!

Dr. Nathanael Gray's laboratory especially Sara, Xiangmeng and David were brilliant with the development of inhibitors, quick despatch and excellent feedbacks and suggestions. Special thanks to Prof. Keichi Nakayama's laboratory for the βTRCP MEF cells.

Last but not the least, my mother, grandparents and my wife Sheelonee for being around listening to and dealing with the rants of a PhD student on a regular basis.

Thank you all for being there for me! Best wishes to all of you!

Declarations

I hereby declare that the following thesis is based on the results of investigations conducted by myself, and that this thesis is of my own composition. Work other than my own is clearly indicated in the text by reference to the researchers or their publications. This dissertation has not in whole, or in part, been previously presented for a higher degree.

Sourav Banerjee

I certify that Sourav Banerjee has spent the equivalent of at least nine terms in research work in the College of Life Sciences, University of Dundee, and that he has fulfilled the conditions of the Ordinance General No. 14 of the University of Dundee and is qualified to submit the accompanying thesis in application for the degree of Doctor of Philosophy.

Dario R. Alessi

Abbreviations

ABL Abelson tyrosine kinase
ACC acetyl-CoA carboxylase
AGC protein kinase A, protein kinase G and protein kinase C
AICAR 5-aminoimidazole-4-carboxamide riboside
AMP adenosine 5'-monophosphate
AMPK AMP activated protein kinase
APS ammonium persulfate
ARK5 AMPK-related kinase 5 (NUAK1)
ATM ataxia telangiectasia mutated protein kinase
ATP adenosine 5'-triphosphate
BRSK brain-specific kinase
BSA bovine serum albumin
βTRCP beta-transducin repeat containing protein
C.elegans Caenorhabditis elegans
CAMK calcium/calmodulin-dependent protein kinase
CAMKK calcium/calmodulin-dependent protein kinase kinase
cAMP cyclic AMP
CDC2 cell division control protein 2
CDK cyclin dependent kinase
cDNA complementary deoxyribonucleic acid
cpm counts per minute
cps counts per second
CREB cAMP-responsive element-binding protein
CRL Cullin RING ligases
CRTC2 CREB-regulated transcription coactivator 2
CT carboxy terminal
Da Dalton
DMEM Dulbecco's modifided Eagle medium
DMP dimethyl pimelimidate
DMPK dystrophia myotonica-protein kinase
DMSO dimethyl sulphoxide
DNA-PK DNA-dependent protein kinase catalytic subunit
doxy doxycyclin

DTT dithiothreitol
DUB deubiquitin enzymes
E. coli Escherichia coli
ECL enhanced chemiluminescence immunoblotting
EDTA ethylenediaminetetraacetate
EGTA ethyle-glycol-tetracetate
ERK extracellular signal-regulated kinase
FBS foetal bovine serum
FLAG DYKDDDDKG peptide
FRT Flp recombination target
GFP green fluorescent protein
GSH glutathione
GSK3 glycogen synthase kinase-3
HA hemagglutinin (YPYDVPDYA peptide)
HECT homologous to E6-associated protein C-terminus
HEK293 human embryonic kidney 293
HeLa Henrietta Lack's cervical cancer derived cells
HILIC hydrophilic interaction liquid chromatography
HPLC high performance liquid chromatography
HRP horseradish peroxidase
IB immunoblot
IgG immunoglobulin G
IκBα nuclear factor of kappa light polypeptide gene enhancer in B-cells inhibitor, alpha
ILK integrin-linked kinase
IMAC immobilised metal affinity chromatography
IMEC immortalised mammalian epithelial cells
IP immunoprecipitation/immunoprecipitate
IPTG isopropyl-β-D-thio-galactopyranoside
JNK C-jun-amino-terminal kinase
kd kinase-dead mutant
LB Luria Bertani broth
LC liquid chromatography
LDS lithium dodecyl-sulfate
LKB Liver kinase B

MALDI matrix-assisted laser-desoprtion ionization

MAP microtubule-associated protein

MAPK mitogen-activated protein kinase

MARK MAP/microtubule affinity-regulating kinase

MBS85 myosin binding subunit of 85 kDa

MEF mouse embryonic fibroblasts

MELK Maternal embryonic leucine zipper kinase

MLC2 myosin light chain 2

MLCK myosin light chain kinase

MOPS 3-(n-morpholino) propane sulphonic acid

MRCK myotonic dystrophy kinase-related CDC42-binding kinase

M-RIP myosin phosphatase Rho-interacting protein

MS mass spectrometry

mTOR mammalian target of rapamycin

MYPT myosin phosphatase targeting subunit

MYPT1 SSS/AAA MYPT1 S445A/S472A/S910A

NDR2 nuclear Dbf2-related kinase 2

NEK2 NIMA-related protein kinase 2

NEM N-ethylmaleimide

NUAK NUAK family SNF1-like kinase

NUAK1 3xIL/KK NUAK1 I400K/L401K/I467K/L468K/I524K/L525K

NUAK1 SSS/AAA NUAK1 Ser476A/Ser480A/Ser481A

OD optical density

PAGE poly-acrylamide gel electrophoresis

PAK p21-activated kinase

Par partition-defective

PBS phosphate buffered saline

PCR polymerase chain reaction

PDB Protein Data Bank

PDK1 3-phosphoinositide-dependent protein kinase 1

PEI polyethylenimine

PI3K phosphatidylinositol-4,5-bisphosphate 3-kinase

PJS Peutz-Jeghers syndrome

PKA cAMP-dependent protein kinase

PKB protein kinase B

PKC protein kinase C

PLK Polo-like kinase

PMSF phenylmethanesulphonylfluoride

QIK Qin-induced kinase

RBX Ring-box

RING really interesting new gene

ROCK Rho-associated protein kinase

rpm rotation per minute

SAD synapses of the amphid-defective kinase

SCF SKP-Cullin-F-box

SDS sodium dodecyl sulphate

shRNA small hairpin RNA

SIK salt-induced kinase

SILAC stable isotope labeling with amino acids in cell culture

siRNA small interfering RNA

SKP S-phase kinase associated protein

SNARK SNF1/AMP kinase-related kinase (NUAK2)

Snf1 sucrose-non-fermenting protein kinase

SNRK SNF1-related protein kinase

SSTK small serine/threonine kinase

STK11 serine/threonine protein kinase 11 (LKB1)

TEMED N,N,N',N'-tetramethylethylenediamine

TET tetracycline

TFA trifluoroacetic acid

TIMAP TGFβ-inhibited membrane-associated protein

Tris Tris(hydroxymethyl)methylamine

TRITC tetramethylrhodamine B isothiocyanate

TSSK testis-specific serine/threonine-protein kinase

UBA ubiquitin associated domain

USP ubiquitin specific protease

WNK with no K(Lys) protein kinase

wt wild type

ZIPK zipper-interacting protein kinase

Amino acid code

Amino acid or residue	Three letter symbol	One letter symbol
alanine	Ala	A
arginine	Arg	R
asparagine	Asn	N
aspartate	Asp	D
cysteine	Cys	C
glutamate	Glu	E
glutamine	Gln	Q
glycine	Gly	G
histidine	His	H
isoleucine	Ile	I
leucine	Leu	L
lysine	Lys	K
methionine	Met	M
phenylalanine	Phe	F
proline	Pro	P
serine	Ser	S
threonine	Thr	T
tryptophan	Trp	W
tyrosine	Tyr	Y
valine	Val	V
any amino acid	Xaa	X
hydrophobic residue	Hyd	Ψ

1. Introduction

1.1. Protein Phosphorylation

The multi-step processes occurring within the cell are very rapid, efficient and tightly controlled . These processes involve replication of its DNA content during cell division, various anabolic and catabolic processes, movement and migration and responses to environmental changes. These various functions are generally controlled and coordinated by a vast array of proteins. In the cell, there is a huge turnover of these proteins with their expressions dependent on the timely requirements within the cell. For the proper synthesis and function of the proteins, evolution has devised multiple methods for protein regulation such as proteolytic cleavage, ligand-binding and post-translational covalent modifications. Amidst the various covalent modifications occurring within the cells, protein phosphorylation one of the major regulatory mechanisms deployed in biology. The majority of eukaryotic proteins are phosphorylated at multiple residues and phosphorylation is likely to control virtually every physiological process. Phosphorylation requires a single ATP molecule per modification which introduces a significant change in the local charge of the substrate leading to the regulation of every conceivable cellular process including signal transduction, anabolism, catabolism, cellular movement, transcription, cytoskeletal rearrangement, cell cycle progression, differentiation and apoptosis.

The concept of reversible protein phosphorylation was first discovered by Fischer and Krebs when they demonstrated that the transfer of a phosphate group from ATP was required for the conversion of glycogen phosphorylase b to phosphorylase a *in vitro* (Fischer and Krebs, 1955, Sutherland and Wosilait, 1955, Krebs and Fischer, 1956). Phosphorylation can cause major conformational changes in the modified protein, thereby directly altering its affinity or

activity towards ligand or substrate. The phosphorylated substrate can also be recognised by other proteins and serve as a docking site for specific phosphate-binding domains. Such modifications might then lead to a change in protein function, localisation within the cell or protein stability. Protein phosphorylation is controlled primarily by two groups of enzymes – protein kinases and protein phosphatases (Fig. 1.1).

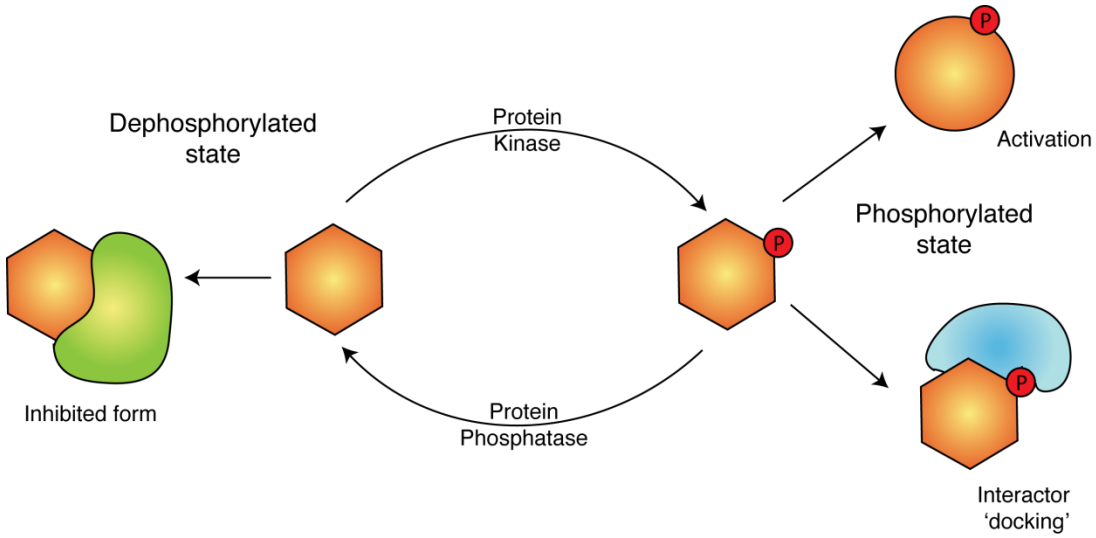

Figure 1.1 Effects of protein phosphorylation. Fundamental outcomes of phosphorylation of proteins by kinases and dephosphorylation by phosphatases are the regulation of the activity and the binding partners.

1.2. Protein kinases

Protein kinases are a large superfamily of enzymes responsible for the catalysis of the γ-phosphate from a molecule of ATP to the hydroxyl group of a residue in the substrate protein. Initial classification of protein kinases were based on the residues that they preferentially phosphorylate: Ser/Thr protein kinases, Tyr protein kinases and dual specificity protein kinases, which phosphorylate Ser, Thr and Tyr residues. Each protein kinase contain a catalytic region called kinase domain (about 250-300 amino acids in length), which performs

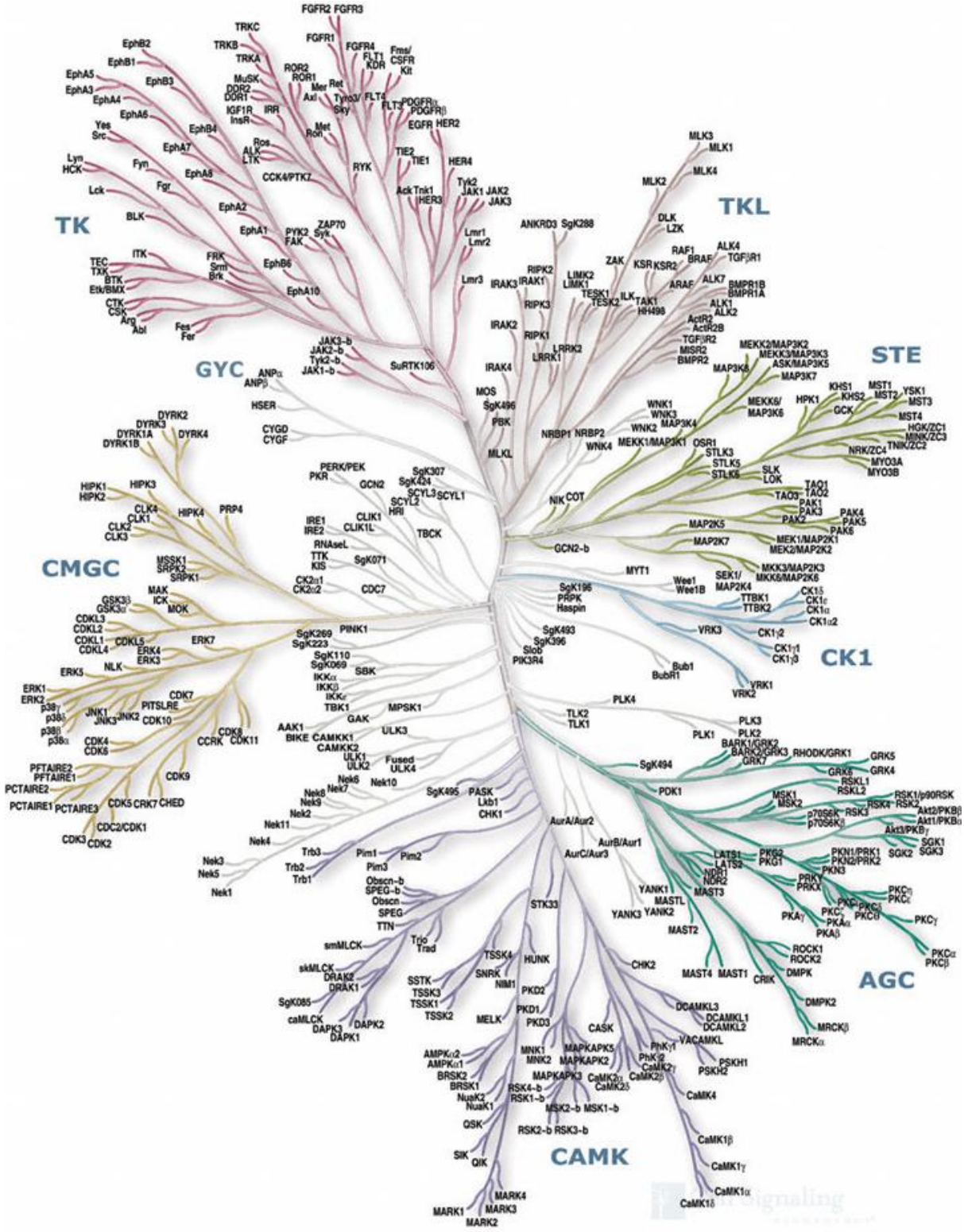

Figure 1.2 The human kinome.
Phylogenetic tree of human protein kinases based on kinase domain sequence similarity. Adapted from (Manning et al., 2002).

the phosphoryl transfer reaction. Besides the kinase domain, the proteins possess additional regions and domains that are unique to each kinase allowing them the ability to perform functions within the cell. The sequencing of the human genome allowed identification of 520 protein kinases, which were constructed and organised in a phylogenetic tree based on their evolutionary divergences of the kinase domain residues, forming the so called kinome (Figure 1.2) (Manning et al., 2002).

The kinase families can be clustered into seven major groups: AGC (containing the PKA, PKG and PKC families), CAMK (calcium/calmodulin-dependent protein kinases), CK1 (Casein kinase 1), CMGC (containing the CDK, MAPK, GSK3, CLK families), STE (containing the homologues of yeast Sterile kinases), TK (Tyrosine kinases), and TKL (Tyrosine kinase–like) (Manning et al., 2002).

The first kinase structure solved was of the catalytic domain of cyclic adenosine monophosphate (cAMP)-dependent protein kinase (PKA) (Knighton et al., 1991). Subsequent structures showed that the fold is highly conserved (Hanks and Hunter, 1995). The kinase domain consists of two lobes which contain several sub-domains with conserved residues that are required for substrate recognition and catalysis. N-terminal lobe contains a GxGxxG motif (where "x" is any amino acid) that binds to and coordinates the α and β phosphates of ATP in subdomain I and a conserved Lys in the VAIK motif located in subdomain II which binds and positions ATP. The C- lobe contains the HRDxxxN motif in subdomain VIB in which Asp is a catalytic base which functions as a proton acceptor for the phosphoryl transfer and the Asn residue stabilises the catalytic loop and chelates the secondary Mg^{2+} ion. In the highly conserved DFG motif of subdomain VII, Asp chelates the primary Mg^{2+} and ensures correct orientation of the γ phosphate of ATP. Subdomain VIII plays a major role in the

recognition of peptide substrates via the conserved APE motif, in which the Glu residue forms a salt bridge with subdomain XI, thereby promoting stability of the C- lobe. Between the DFG and APE motifs, there is a regulatory region called the activation loop (T-loop) (Hanks and Hunter, 1995).

To inactivate a kinase by generating the kinase dead or catalytically inactive mutant version of the kinase, site directed mutagenesis is employed to specifically mutate the VAIK Lys or Asp of DFG motif or the Asp of the HRDxxxN into an alanine residue.

Kinases are known to autophosphorylate themselves, which is often important for their activity and/or stability. Most kinases specifically phosphorylate their substrate at conserved residues and often on studying various substrates of the same kinase, a possible consensus motif sequence can be derived for substrate-recognition for that kinase. The consensus motif sequence represents the amino acid preference for that particular kinase around the Ser/Thr or Tyr site on the substrate(s).

Many kinases employ or require “substrate docking sites”, which are sites or domains on the substrates that are necessary for the recruitment of the upstream kinases. These docking sites play an important role in regulation of substrate specificity. An example for a docking site-dependent kinase-substrate interaction is the recruitment of PLK1 on various substrates after the conserved Polo-box domain on the substrate is phosphorylated by CDKs or related kinases (Neef et al., 2007).

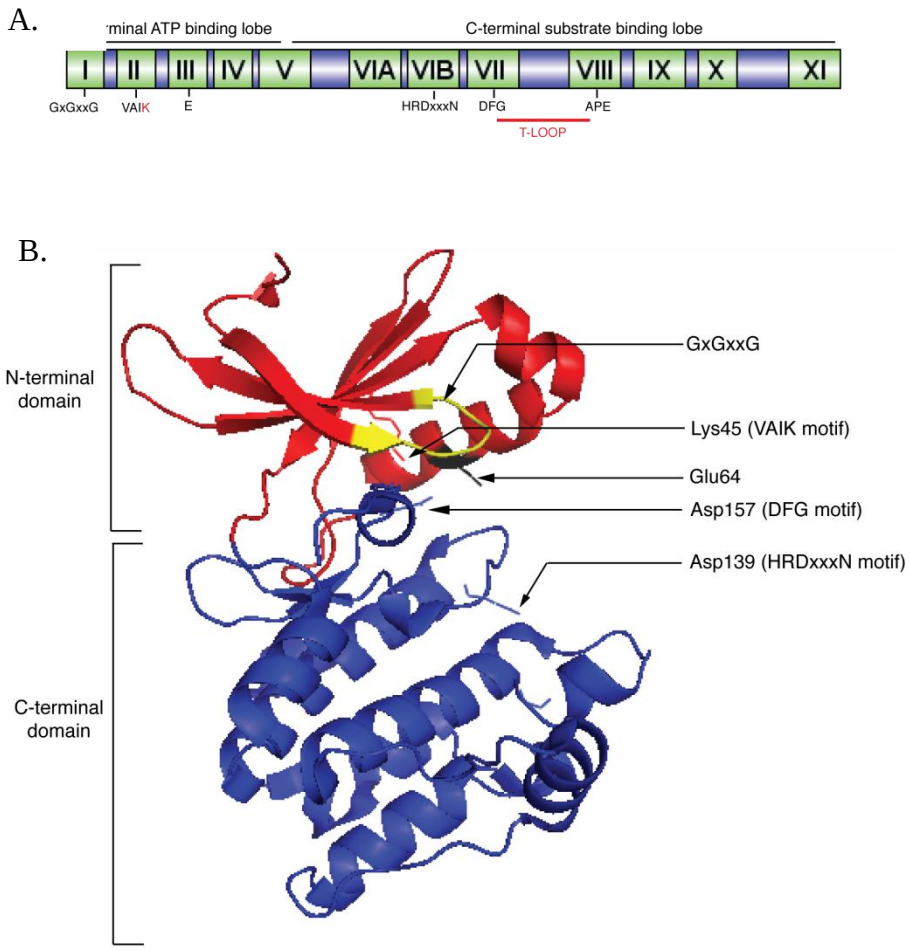

Figure 1.3 Structure of a kinase domain.
(A) Schematic representation of the subdomain structure of a kinase domain. Conserved residues involved in substrate binding and catalysis are indicated. (B) Ribbon representation of the kinase domain of AMPKα2 (PDB ID: 2H6D). The N-lobe is red, the C-lobe is blue, GxGxxG is shown in yellow and the side chains of conserved catalytic and substrate-binding residues are represented by sticks. The Figure prepared using PyMol.

Owing to the varied roles of protein kinases in the cellular signalling pathways, various diseases including cancer are linked to the perturbations of the protein phosphorylation pathways. Various types of cancers have been reported to be caused due to hyperactivation, inactivation and also changes in substrate specificity of the protein kinases. A list of protein kinases involved in human cancer are listed below (Table 1.)

Table 1: Kinases mutated in cancer. Various types of mutations in protein kinases were found to be associated with cancer. Molecular basis key as follows, Act : Activated, Amp : Amplified, Del : Deleted, Exp : Expression, GOF : Gain of function, LOF : Loss of function, LH : Loss of heterozygosity, Meth : Methylation, Mut : Mutation, OE : Overexpression, Splice : Splicing change, SNP : Single nucleotide polymorphism, Trans : Translocation (Adapted from http://www.cellsignal.com/reference/kinase_disease.html).

Kinase name	Mutation type	Cancer caused
Abl1	Trans	Chronic myelogenous leukemia (CML) ; acute lymphoblastic leukemia (ALL)
Abl2	Trans, Exp	Acute Myeloid Leukemia
ACK	Amp	Metastatic potential in primary tumors
ACVR1B	Mut, Splice	Pancreatic carcinoma and pituitary tumors
Akt1	Amp, OE, Act	Various cancers
Akt2	Amp, OE, Mut	Primary ovarian and pancreatic tumors
ALK	Trans	Large cell lymphomas
ALK3	LOF	Juvenile polyposis syndrome
ALK5/ TGFβR1	SNP, Mut	Various cancers
ATM	LOF	Leukemias and lymphomas
ATR	Mut, Splice	Stomach and endometrium
AurB	OE	Various cancers
Axl	OE	Various cancers
Bcr	Trans	Chronic myelogenous leukemia
BMK1/ERK5	Exp	Breast and metastatic prostate cancer
BRAF	GOF, LOF	Malignant melanoma
BRD4	Trans	Juvenile midline carcinomas
BRK	OE	Breast cancer
BTK	LOF	Radiation resistance of tumours
BUB1	LOF	Various cancers
BUB1B	Mut, OE	Various cancers
CaMKIII	OE, Act	Breast cancer
CDK1	Act, Splice	Various cancers
CDK2	Disregulated	Various cancers
CDK4	Act, GOF, Amp, Meth	Various cancers
CDK6	OE, Trans	Leukemias, lymphomas and gliomas
CHEK1	Mut	Stomach, colon and endometrium
CHK2	Mut	Li-Fraumeni's syndrome and various cancers
COT/TPL2	OE, Amp, Mut	Various cancers
c-Raf	Amp	Various cancers
CSF1R/FMS	Mut	Acute myeloid leukemia, chronic myelomonocytic leukemia or myelodysplasia
CSNK1e	Mut, LH	Mammary ductal carcinoma
CSNK2a1/2	OE, Act	Various cancers
CTK/MATK	OE	Breast cancer
DAPK1	Meth, Exp	Various p53 mutated cancers
DNAPK	Mut	Mismatch repair-deficient colorectal cancer
EGFR	Amp, OE, GOF	Various cancers
EphA1	Exp	Various cancers
EphA2	OE	Various cancers
EphB2	OE, Mut	Various cancers

ErbB2/Her2	Amp, OE	Breast cancer
ErbB3/Her3	OE	Breast and prostate cancer
ErbB4/Her4	Exp	Various cancers
FER	Exp	Prostate cancer
FES	Mut, Trans, LOF	Colorectal cancer & acute promyelocytic leukemia
FGFR1	Mut, Trans	Stem cell leukemia lymphoma syndrome
FGFR2	Mut, Amp	Various cancers
FGFR3	GOF, Trans	Multiple myeloma, bladder & cervical cancer
FGR	Amp	Hormone-resistant prostate cancer
FLK1/VEGFR2	Mut	Tumour angiogenesis in various cancers
FLT1/ VEGFR1	Meth, OE	Various cancers
FLT3	GOF, Mut	Acute myeloid leukemia (AML), acute lymphoblastic leukemia, acute promyelocytic leukemia and myelodysplastic syndrome
GUCY2F/CYGF	Mut	Colon, lung, breast and pancreatic tumors
HEK/EphA3	Mut	Point mutations reported in various cancers
HIPK1	OE	Breast cancer
HIPK2	LH, Exp	Breast and thyroid carcinomas
HTK/EphB4	OE	Various cancers
IGF1R	Mut, SNP, OE	Various cancers
IKKα, IKKβ	Exp	Linked to apoptosis
IKKε	Amp, Exp	Breast cancer
ILK	OE	Various cancers
IRAK2	Mut	Anti-apoptotic
ITK	Trans	T-cell lymphomas
Jak1	Mut, Act	Various cancers
Jak2	Trans	Breast cancer & acute lymphoblastic leukemia
Jak3	LOF, Act	Acute megakaryoblastic leukemia
JNK3	Exp	Brain tumours
Kit	GOF, LOF, Act, Mut	Gastrointestinal stromal tumours (GIST)
LATS1	Meth, Exp, Mut	Likely tumour suppressor
LATS2	Exp	Prostate cancer
LCK	Trans, Mut, Exp, Splice	T-cell leukemia, colon and thymus cancers
LIMK1	OE, Amp, LH	Breast and metastatic prostate cancer
LYN	Act	Acute myeloid leukemia
MAP2K1,2	Mut, OE	Various cancers
MAP2K3	Mut, Del	Colon cancer
MAP2K4	LOF, Del	Various cancers
MELK	Exp	Various cancers
Met	GOF, OE, Trans	Renal and gastric carcinomas
MLK4	Mut	Colon cancer
Mst4	OE	Prostate cancer
NEK2	OE	Ewing's tumour & diffuse large B cell lymphoma
NEK8	OE	Breast cancer
NTRK1/TrkA	Mut, Trans	Various cancers
NTRK2/TrkB	Mut	Various cancers
NTRK3/TrkC	Trans, Mut	Various cancers
NUAK1/ARK5	OE	Various cancers
PAK4	OE	Various cancers
PDGFRα	Trans, Del, Mut	Atypical CML and GIST

PDGFRβ	Trans, OE	Various cancers
Pim1,Pim2,Pim3	Trans, OE, Mut	Various cancers
PINK1	Mut, Exp	Ovarian cancer
PKCα	Mut, Del, OE, Act	Various cancers
PLK1	Exp	Various cancers
PRKR	Mut, Exp, Act	Various cancers
PTK2/FAK	OE, Amp, Act	Various cancers
Ret	LOF and GOF, Trans	Endocrine, thyroid, multiple neoplasia and phaeochromocytoma
RON	OE, Splice	Various cancers
ROS	Trans	Glioblastoma
p70S6K	OE, Amp	Breast and colon cancers
SGK1	Exp	Breast cancer
SKY/TYRO3	OE	Multiple myeloma and astrocytoma
SRC	Mut, OE, Act	Colon and various cancers
STK11/LKB1	LOF	Peutz-Jeghers syndrome
Syk	Meth, Splice	Various cancers
TEK/Tie2	Mut, OE	Various cancers
TGFβR2	LOF	Colorectal, gastric and oesophageal cancers
Yes	Amp, Act	Various cancers
ZC1/HGK	OE	Primary tumours

1.3. Protein kinase inhibitors

As listed in Table 1, protein kinases play direct and indirect roles in cancer and various other diseases. Thus, over the last two decades the protein kinase family has been targeted for structure based drug design to generate specific ATP competitive inhibitors. The first protein kinase inhibitors reported were isoquinolinesulphonamide derivatives H7 and H8 developed by Hiroyoshi Hidaka in 1980s which were shown to inhibit the cyclic-nucleotide dependent protein kinases (Hidaka et al., 1984, Cohen, 2002a). Since then various kinases involved in disease have been targeted and in 2001 Imatinib or Gleevec was approved for clinical use for the treatment of chronic myelogenous leukemia by specifically targetting BCR-Abl tyrosine kinase fusion protein (reviewed in (Cohen, 2002a). Till 2012, nearly 25 kinase inhibitors have been approved for clinical use and a further 150 odd compounds are undergoing clinical trials (Cohen and Alessi, 2013). As of 2013, 50-70% of cancer drug discovery programs in

pharmaceutical companies are focussed on the development of protein kinase inhibitors (Cohen and Alessi, 2013).

Besides disease targetting, protein kinase inhibitors are valuable tools to dissect the biochemical and physiological functions of a kinase *in vitro*. They are widely used on cells to identify protein kinase substrates, phosphorylation motifs as well as identifying novel functions of the various kinases. Determining the specificity of an inhibitor is essential before using the compound to study kinase functions (Cohen, 2010). A favourite method amidst biochemists is to exploit the ATP-competitive property of the inhibitors and develop a drug-resistant mutant of the kinase which is a perfect control to study the degree of specificity of the inhibitor *in vivo* as well as to pin-point the exact kinase-substrate functions (Cohen, 2010). A drug-resistant mutant version of a kinase is generally developed either by mutating the conserved gate-keeper Met or Thr into a more bulky residue (Eyers et al., 1999, Clark et al., 2012) or by mutating the residue adjacent to the Mg^{2+} binding Asp of the DFG motif in subdomain VII (Fig 1.3A) into a bulkier residue (Bonn et al., 2006, Nichols et al., 2009, Deng et al., 2011). Previously, studies on Rho-associated protein kinase had revealed that the Ala residue (Ala215) adjacent to the magnesium ion binding DFG motif in subdomain VII played a vital role in binding to the inhibitor H-1152 via Van der Waals interactions (Jacobs et al., 2006). Furthermore it was shown that PKA was almost 50-fold less sensitive to H-1152 as compared to ROCK since it had a Thr (Thr183) at the equivalent position. Mutation of the Thr to an Ala rendered PKA much more sensitive to H-1152 although without affecting the basal activity of PKA (Bonn et al., 2006). Our lab had previously successfully applied this concept to develop drug resistant LRRK2, a kinase mutated in Parkinsons disease, by mutating the Ala2016 to a Thr without altering the intrinsic activity of LRRK2 (Nichols et al., 2009, Deng et al., 2011).

1.4. LKB1 signalling pathway

LKB1 (STK11) Ser/Thr protein kinase is a tumour suppressor which is frequently mutated in a rare autosomal dominant disorder called Peutz-Jeghers cancer syndrome (PJS) (Hemminki et al., 1998, Jenne et al., 1998). Patients suffering from PJS develop multiple benign hamartomatous polyps in their gastrointestinal tract, melanin pigmentation of the lips, palms , face, oral mucosa and genitalia (Hemminki, 1999). Furthermore PJS patients are predisposed to various tumours including gastrointestinal adenocarcinomas, cervical, breast, testicular, ovarian or pancreatic cancers (Katajisto et al., 2008). More than 30% of non-small cell lung carcinomas (Ji et al., 2007) and 20% of cervical cancers (Wingo et al., 2009) have exhibited LKB1 mutations.

LKB1 is ubiquitously expressed but the highest expression is in testis and liver and hence the name Liver Kinase B1. Tissue specific knock-out of LKB1 results in various polyps and carcinomas consistent with PJS phenotype (reviewed in(Shackelford and Shaw, 2009)), while full-body LKB1 homozygous knock-out mice exhibit embryonic lethality (Ylikorkala et al., 2001).

LKB1 has been found to be constitutively active via its interaction with two regulatory subunits, STE20-related adaptor (STRAD) and mouse protein 25 (MO25). The crystal structure of the trimeric LKB1-STRAD-MO25 complex has revealed that the inactive pseudokinase STRAD interacts with LKB1 and allosterically promotes the active conformation while armadillo-repeat adaptor protein MO25 further stabilizes the complex by interacting with the LKB1 activation loop (Figure 1.4) (Zeqiraj et al., 2009). Besides activation, STRAD and MO25 interacts with the predominantly nuclear LKB1 and the trimeric complex re-localises to the cytoplasm (Boudeau et al., 2003, Boudeau et al., 2004).

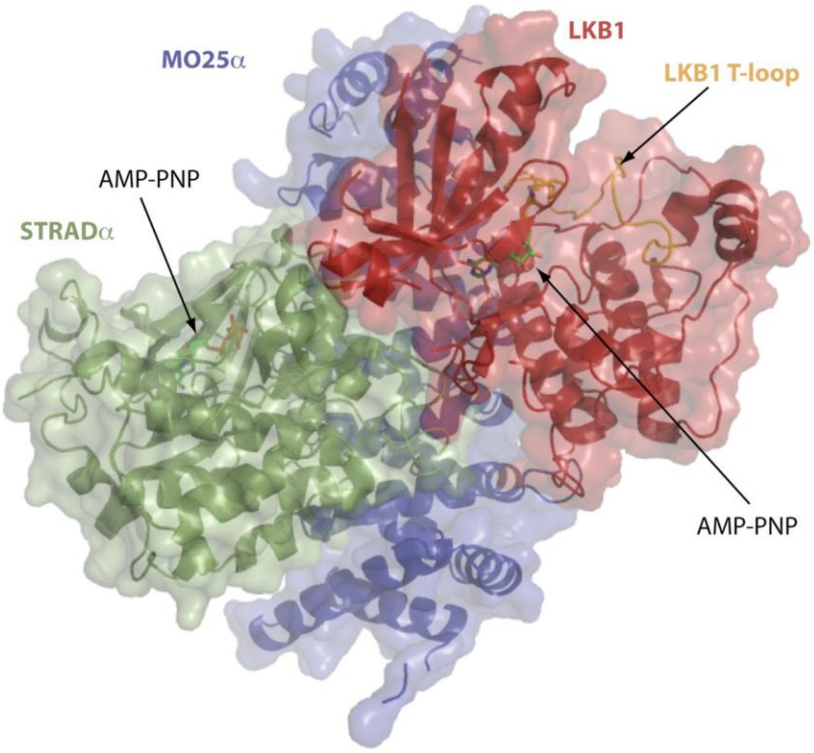

Figure 1.4 Structure of the LKB1-STRAD-MO25 complex. LKB1, STRAD and MO25 are indicated in red, green and blue, respectively (Zeqiraj et al., 2009). LKB1 T-loop is indicated in orange. Non-hydrolysable ATP analogue 5'-adenylylimido-diphosphate (AMP-PNP) that was co-crystallized with the complex are shown by the arrows.

LKB1 has been implicated in the regulation of multiple cellular processes such as energy metabolism, cell polarity, proliferation and apoptosis (Alessi et al., 2006, Fan et al., 2009). These physiological functions of LKB1 are primary brought about by activation of the AMP-activated protein kinase AMPK and AMPK related kinase family (Fig 1.5). LKB1-STRAD-MO25 trimeric complex activates AMPK (Hawley et al., 2003, Woods et al., 2003, Shaw et al., 2004) and AMPK related kinases (Lizcano et al., 2004, Jaleel et al., 2005) by phosphorylating a conserved Thr on the T-loop of the respective kinase domains.

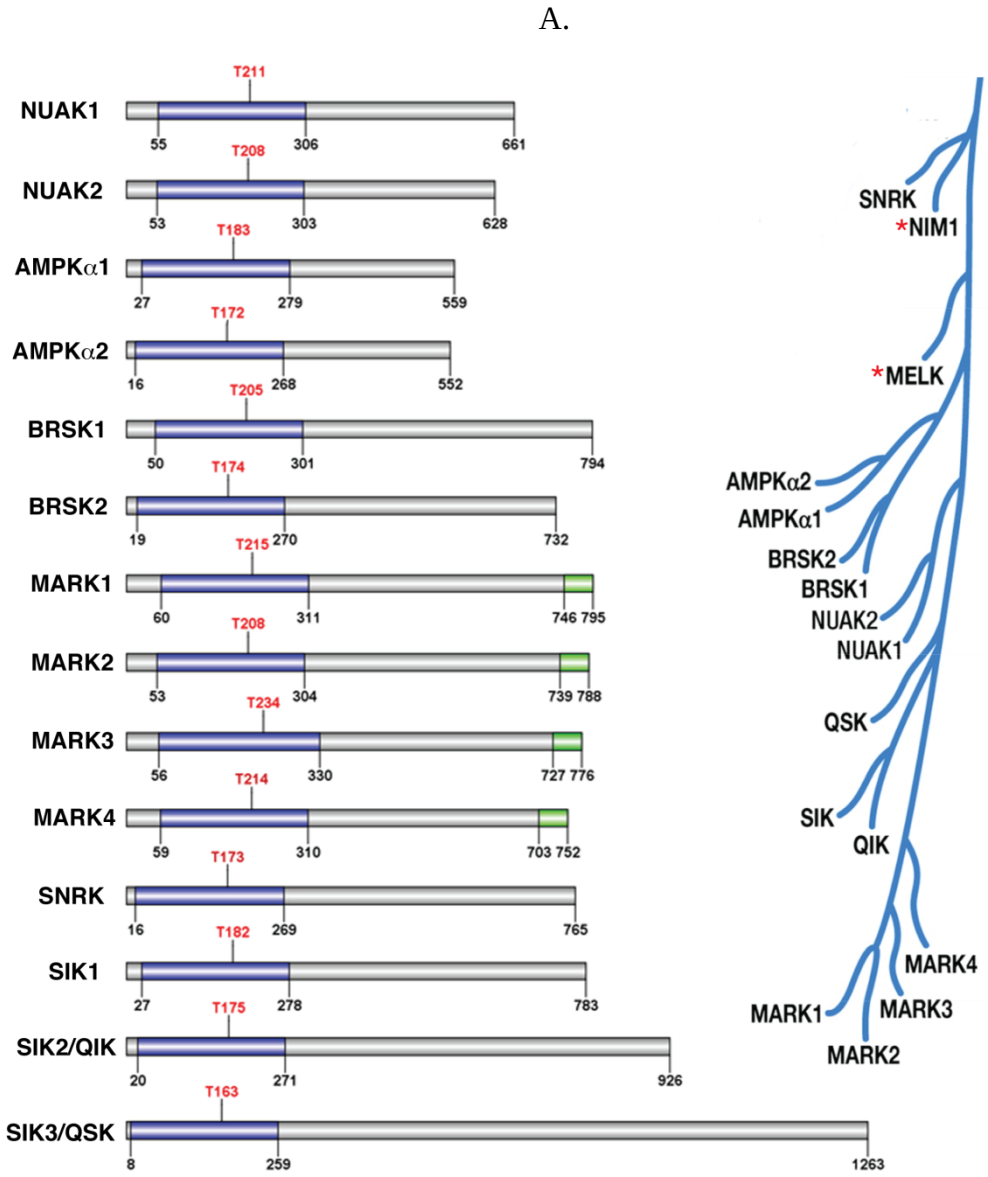

Figure 1.5. AMPK-related kinases : (A) Domain structure of AMPK-related kinases that are phosphorylated by LKB1 at the indicated T-loop (red) residue on the kinase domain (blue). (B) AMPK-family branch from the human kinome. * indicates kinases in the AMPK related family which are not phosphorylated and activated by LKB1 complex.

1.4.1 AMP-activated protein kinase or AMPK

The most extensively studied substrate of LKB1 is AMP-activated protein kinase or AMPK which is the central sensor and regulator of energy homeostasis within a cell (Hardie, 2007, Shackelford and Shaw, 2009). It functions as a heterotrimeric complex consisting of a catalytic subunit, AMPKα (2 isoforms in human) and two regulatory subunits AMPKβ (2

isoforms in human) and AMPKγ (3 isoforms in human). AMPK is allosterically activated by AMP (Yeh and Kim, 1980) upon binding to the AMPKγ submit leading to a conformational change (Scott et al., 2007) and further upon inhibition of dephosphorylation of the T-loop by PP2C phosphatase isoforms (Hawley et al., 1996, Sanders et al., 2007). The primary upstream kinases phosphorylating the T-loop of AMPKα are the LKB1 trimeric complex (Hawley et al., 2003, Woods et al., 2003, Shaw et al., 2004) and CaMKK or Ca^{2+}/calmodulin-dependent protein kinase kinase which activates AMPK in response to tissue-specific calcium signalling (Hawley et al., 1995, Hurley et al., 2005, Woods et al., 2005).

Metabolic stresses which increase the cellular AMP/ATP ratio leads to the activation of AMPK which inhibits the anabolic pathways and activates the catabolic pathways to restore energy balance (Hardie, 2007, Hardie et al., 2012). AMPK plays pivotal roles in glucose metabolism, protein metabolism, lipid metabolism, mitochondrial biogenesis and autophagy (Figure 1.6).

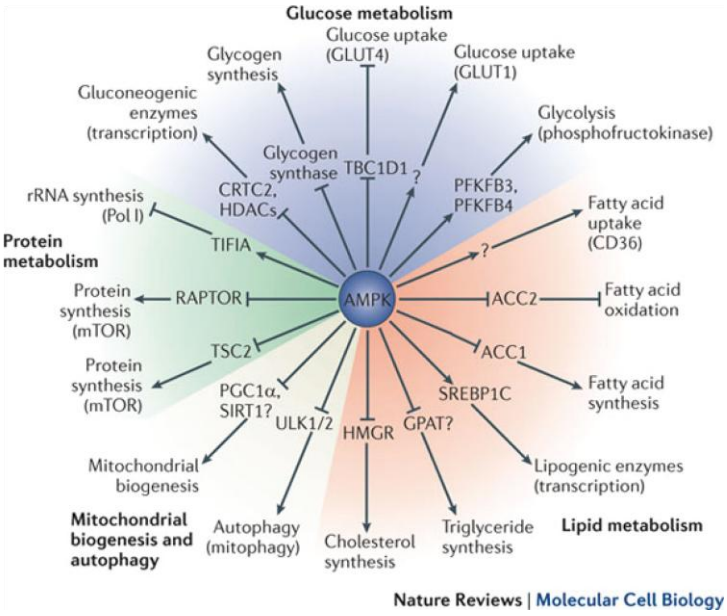

Figure 1.6 : Effects of AMPK activation on the cell metabolism. Adapted from (Hardie et al., 2012)

Besides energy stress, some chemical stimuli like the type 2 diabetes drug metformin activates AMPK (Zhou et al., 2001) possibly by affecting the levels of mitochondrial reactive nitrogen species (Zou et al., 2004). Various other reagents like cytokines such as leptin, ghrelin, adiponectin, interleukin-6 and natural products such as resveratrol, cannabinoids, berberine, salicylate or substances in green tea like epigallocatechin gallate can activate AMPK (Hardie, 2007, Steinberg and Kemp, 2009, Hardie et al., 2012, Hawley et al., 2012). Additionally, potent and specific allosteric activators of AMPK, such as AMP analog AICAR (5-amino-1-β-D-ribofuranosyl-imidazole-4-carboxamide) and A-769662 (also called "Abbott compound") have been developed, which have been extremely helpful in studying the downstream functions of AMPK *in vitro* and *in vivo* (Hardie, 2007, Steinberg and Kemp, 2009).

AMPK substrates generally exhibit a consensus motif for AMPK phosphorylation. The sequence includes hydrophobic residues at the -5 and +4 positions and basic residues at -4 or -3 (or both) positions relative to the Ser/Thr phosphorylation site. A further basic residue at -6 position is often preferred by the more canonical substrates like acetyl CoA carboxylase (ACC). The simplified consensus motif can be written ΨXBXX(S/T)XXXΨ, where Ψ is a hydrophobic residue, B is basic, and X is any residue (reviewed in (Hardie et al., 2012)). However, presence of this motif doesnot predispose a protein to be an AMPK substrate as various factors like protein localisations and tertiary structures play a role.

1.4.2. The family of AMPK-related kinases

The AMPK family belongs to the CAMK Ser/Thr protein kinase superfamily and are the lesser studied downstream substrates of LKB1 (Fig 1.5). LKB1 phosphorylates 12 of the AMPK related kinases at the conserved Thr on the T-loop of the kinase domain (Lizcano et

al., 2004, Jaleel et al., 2005) whereas MELK and NIM1, although belonging to the same family, are not activated by the trimeric tumour suppressor (Fig 1.5B) (Jaleel et al., 2005). The AMPK related kinases possess highly homologous kinase domains (Fig 1.7), very similar substrate specificities and many of them often employ the AMPK consensus motif to phosphorylate their substrates (Zagorska et al., 2010, Hou et al., 2011).

Some of these kinases phosphorylate their substrates and form a RSXS*XP consensus where S* is the phosphorylation residue which leads to the formation of a canonical 14-3-3 adaptor protein docking motif (Mackintosh, 2004, Al-Hakim et al., 2005, Matenia and Mandelkow, 2009, Zagorska et al., 2010).

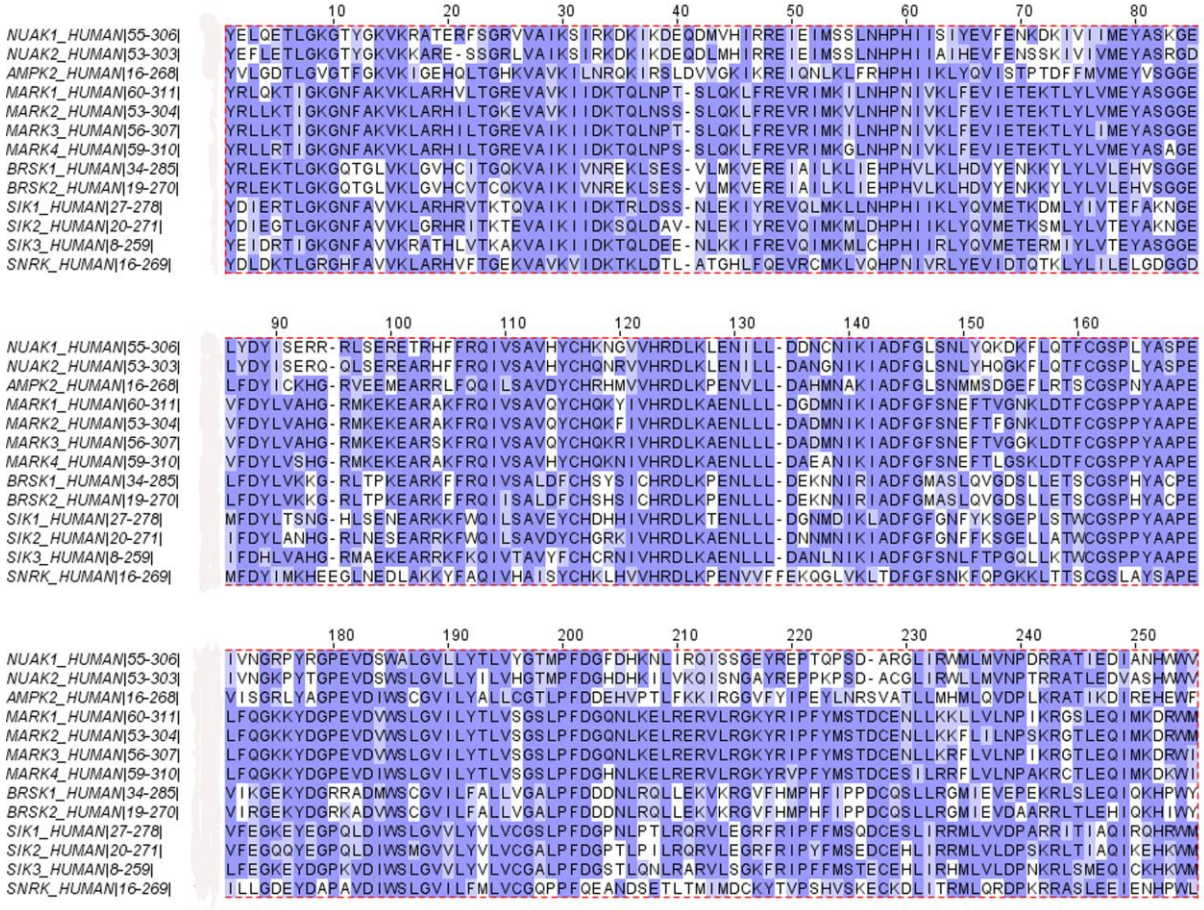

Figure 1.7 : Sequence alignment of the kinase domains of AMPK-related kinases.

The AMPK related kinases regulate various cellular functions like cell polarity, migration and detachment, neuronal polarity, transcription, cell proliferation etc. (Alessi et al., 2006, Bright et al., 2009). As the name suggests, microtubule-affinity regulating kinases or MARKs are associated with the cytoskeletal system of the cells and regulates cell polarity (Kemphues et al., 1988, Tassan and Le Goff, 2004). MARKs recognize and phosphorylate a relatively short consensus motif [K/R]XX[S/T] which forms a 14-3-3 docking site on the phosphorylated substrate (Mackintosh, 2004, Matenia and Mandelkow, 2009). MARKs phosphorylate a microtubular protein called Tau which leads to the disruption of microtubules (Drewes et al., 1997). MARK4 is atypically ubiquitylated by 29/33 linked polyubiquitin chains (Al-hakim et al., 2008) and all four of the MARK isoforms possess a UBA or ubiquitin associated domain which has very low affinity for ubiquitin and instead stabilises the kinase domain by keeping it in an open conformation for LKB1 mediated T-loop phosphorylation (Jaleel et al., 2006, Murphy et al., 2007). Besides cell polarity, various groups have implicated the MARK isoforms in development of neurones, neurite growth, immune system, intracellular transport and also have been suggested as potential therapeutic targets for neurodegeneration (reviewed in (Matenia and Mandelkow, 2009)).

The BRSKs or Brain-specific kinases (also known as SAD or Synapses of Amphids Defective kinases) are exclusively expressed in brain and have been reported to be essential for development of neuronal polarity (Kishi et al., 2005, Barnes et al., 2007, Shelly et al., 2007). BRSKs are activated by LKB1 (Lizcano et al., 2004) and similar to MARKs, BRSKs phosphorylate Tau (Kishi et al., 2005) and BRSK1 has been shown to regulate presynaptic neurotransmitter release by localising into synaptosomal membrane lipid rafts (Inoue et al., 2006, Rodriguez-Asiain et al., 2011).

Of the SIKs or salt-inducible kinase family, SIK1 was first identified as a kinase regulating steroidogenesis (Takemori et al., 2003) in the adrenal glands of rats kept on a high salt diet (Wang et al., 1999). SIK2/QIK is thought to regulate insulin-signalling in adipose tissue by phosphorylating insulin receptor substrate IRS1 (Horike et al., 2003). Both SIK1 and SIK2 has been reported to phosphorylate CRTC2 (CREB-regulated transcription coactivator 2), leading to inhibition of CREB-mediated transcription (Screaton et al., 2004, Katoh et al., 2006). Recently, it has been shown that SIKs phosphorylate and inhibit CRTC3 mediated transcription leading to a marked reduction in formation of regulatory macrophages (Clark et al., 2012) and inhibition of prostaglandin E2 induced macrophage IL-10 production (MacKenzie et al., 2013). Not much is known about SIK3/ QSK except that its thought to be involved in skeletal development (Sasagawa et al., 2012) and glucose and lipid metabolism in mice (Uebi et al., 2012). Selective and highly potent small molecules inhibitors KIN112 and HG-9-91-01 (Clark et al., 2012, MacKenzie et al., 2013) has recently been reported that inhibit all three SIK isoforms without significant off-target effects on any of the other AMPK family kinases (Clark et al., 2012). These two SIK inhibitors are first of its kind to specifically target only a sub-set of kinases within the AMPK-related kinase family.

1.4.3. NUAK family Snf1 like kinases or NUAKs

NUAK1 (also known as AMPK related kinase 5 or ARK5 and OMPHK1 or Omphalocoele Kinase 1) and NUAK2 (also known as SNARK or sucrose non-fermenting AMPK related kinase) are two isoforms, both of which are activated upon phosphorylation by the LKB1-STRAD-MO25 trimeric tumour-suppressor complex at a conserved threonine residue in the respective activation loop of the kinase domain (Lizcano et al., 2004). NUAK1 or ARK5 was first identified by the group of Hiroyasu Esumi in 2003 as a 661 amino acid AMPK related kinase which is activated by Akt upon phosphorylation at Ser600 (Suzuki et al., 2003). Since

then, the same group has reported various upstream kinases like PKB (Suzuki et al., 2003) and NDR2 (Suzuki et al., 2006) as well as various downstream substrates like ATM (Suzuki et al., 2003) and caspase6 (Suzuki et al., 2004a) of NUAK1, but all these data were carried out mostly by overexpression of NUAK1 and hence remains largely controversial. The Akt mediated phosphorylation of NUAK1 upon IGF1 stimulation is also considered thoroughly controversial (Humbert et al., 2010, Hou et al., 2011, Inazuka et al., 2012).

NUAK1 knockout mice show embryonic lethality at E14.5 with the development of omphalocoele (Hirano et al., 2006), a congential abdominal defect where the epithelial lining of alimentary canal is mal-developed. Over the past decade, various groups have reported NUAK1 to be involved in promoting invasiveness and metastatic potential of various cancer cells (Kusakai et al., 2004a, Suzuki et al., 2004b, Chang et al., 2012, Chen et al., 2013b, Lu et al., 2013) perhaps mainly by increased secretion of matrix metalloproteinases (Suzuki et al., 2004b). NUAK1 has been shown to directly phosphorylate p53 and thereby control tumour cell proliferation (Hou et al., 2011) and also regulate cellular ploidy and senescence by mediating phosphorylation and degradation of a genomic stability factor LATS1 (Humbert et al., 2010). Recently, NUAK1 has been reported to be a primary anti-apoptotic factor responsible for the survival of tumours expressing deregulated oncogenic MYC (myelocytomatosis gene) (Liu et al., 2012) and knocking down NUAK1 by RNAi or by treating the MYC driven cancer cells with inhibitor BX-795 triggers apoptosis (Liu et al., 2012).

Previously, our laboratory has shown that NUAK1 is atypically ubiquitylated by a 29/33 linked polyubiquitin chains and interacts with the deubiquitylating enzyme USP9X and this atypical ubiquitylation may result in the inhibition of the NUAK1 kinase activity (Al-hakim

et al., 2008). In 2010, our laboratory reported the first physiological substrate of NUAK1, the MYPT1-PP1β complex wherein, upon cell-detachment agonists NUAK1 phosphorylates MYPT1 at Ser445, Ser472 and Ser910 leading to the inhibition of the phosphatase complex and promoting 14-3-3 binding at the phosphorylation sites (Zagorska et al., 2010). NUAK1 and NUAK2 are the only reported human proteins which possess three GILK motifs which potentially interact with PP1β (Zagorska et al., 2010). The MYPT1 subunit possesses a KVKF motif which directly interacts with the catalytic PP1β while NUAK utilises the 3 GILK motifs to interact with PP1β subunit of the MYPT1-PP1β complex (Zagorska et al., 2010). All 3 GILK motifs are essential for efficient binding of NUAK to the phosphatase complex and association of MYPT1 to PP1β inhibits the catalytic activity of PP1β from dephosphorylating the NUAK activation T-loop phosphorylation (Zagorska et al., 2010). Furthermore, on knocking down NUAK1 by RNAi and also in LKB1$^{-/-}$ and NUAK1$^{-/-}$ mouse embryonic fibroblasts (MEFs) there is significantly higher number of focal adhesion points and accumulation of F-actin stress fibres confirming that inhibition of LKB1-NUAK1 pathway leads to increased cell adhesion (Zagorska et al., 2010).

NUAK2 or SNARK transcripts were first identified in UV irradiated rat keratinocytes and its expression was found to increase upon glucose starvation (Lefebvre et al., 2001). 90% of NUAK2 knockout mice are embryonic lethal at E16.5 owing to the development of exencephaly (Tsuchihara et al., 2008). Heterozygous NUAK2$^{-/+}$ mice develop mature-onset obesity and are more susceptible to chemical carcinogen, azoxymathan (Tsuchihara et al., 2008). NUAK2 has also been studied to have roles in TNFα signalling (Yamamoto et al., 2008), sucrose fermentation (Lefebvre et al., 2001, Rune et al., 2009), upregulation of acto-myosin stress fibres by interacting with myosin phosphatase interacting protein MRIP (Vallenius et al., 2011) and promotion of tumour growth and invasive properties in human

melanoma (Namiki et al., 2011b). Although NUAK1 and NUAK2 possess 53% sequence homology, yet their kinase domains are 82% identical (Fig 1.8). NUAK1 and NUAK2 double knockout mice exhibit severe neural tube defects and development of spina bifida, facial clefting and exencephaly (Ohmura et al., 2012).

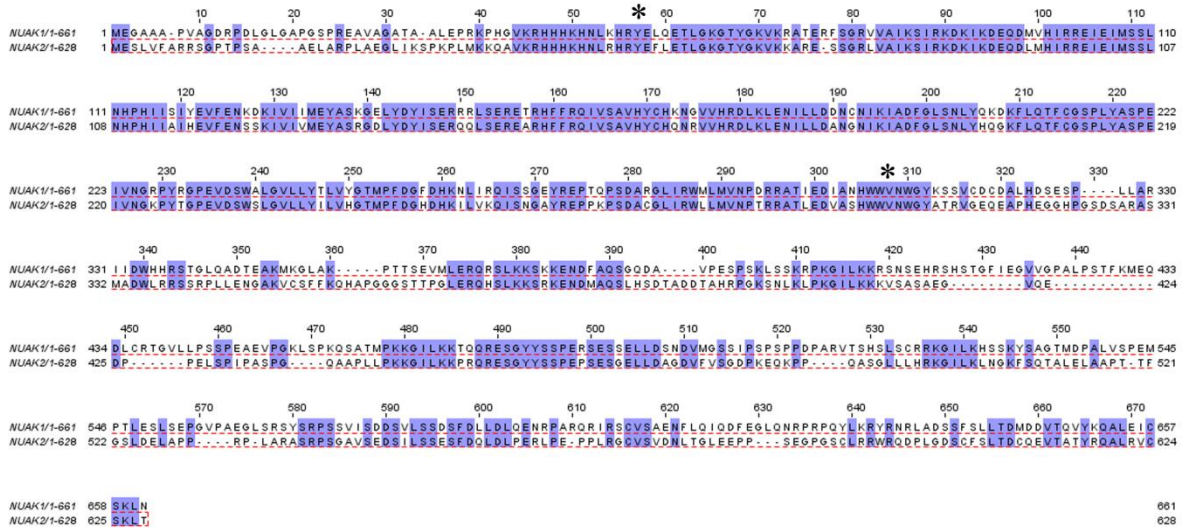

Figure 1.8 : Sequence alignment of human NUAK1 and NUAK2. Alignment of NUAK1 (O60285) and NUAK2 (Q9H093) were carried out using Jalview (Waterhouse et al., 2009). Region within the two * denotes the kinase domains.

Although NUAKs have been found to exhibit links to cancer and tumour progression, the only tool compound available to inhibit the NUAKs is BX-795 (Zagorska et al., 2010, Liu et al., 2012) which has been initially reported as a PDK1 inhibitor (Feldman et al., 2005) and later on as a potent TBK1/IKKε inhibitor (Clark et al., 2009). BX-795 has a NUAK1 IC_{50} of 5nM and it has been further shown to inhibit most of the AMPK-related kinase family members including the MARK isoforms with nanomolar IC_{50} values (Clark et al., 2009). Amidst the more generic inhibitors reported, receptor tyrosine kinase inhibitors Sunitinib (Demetri et al., 2006), Dovitinib (Trudel et al., 2005) and JAK2 inhibitor TG101348 (Lasho et al., 2008) have been shown to inhibit NUAK1with nanomolar IC_{50} values (Davis et al., 2011).

Developing highly specific and potent inhibitors of the AMPK family members were originally deemed a challenging task due to the highly homologous kinase domains of these enzymes (Alessi et al., 2006) (Fig 1.7). The early AMPK family inhibitors that were reported such as Compound C (also known as dorsomorphin) (Yu et al., 2008) and BX-795 were found to significantly inhibit all AMPK family members tested including NUAK isoforms with nanomolar IC_{50} values (Clark et al., 2009). Subsequently a BX-795 derivative termed MRT67307 (Clark et al., 2012) was developed that displayed better specificity but nevertheless still inhibited SIK, NUAK, and MARK isoforms. However, recently, the success of SIK inhibitors KIN112 and HG-9-91-01 (Clark et al., 2012, MacKenzie et al., 2013) signifies that it will ultimately be possible to develop specific inhibitors to each of the AMPK family members.

The concept of specific NUAK inhibitors first arose in our laboratory when in collaboration with Dr. Nathanael Gray (Harvard, USA) it was observed that the 7-membered ring structured inhibitors of LRRK2, a kinase mutated in Parkinsons disease, had off-target effects on NUAK1 at higher concentrations. One of the most potent and selective inhibitors of LRRK2, LRRK2-in-1 inhibited NUAK1 *in vitro* by almost 80% at 10 µM concentration (Deng et al., 2011). Based on the 7-membered ring inhibitor series and the BX-795 derived 2,4,5-trisubstituted pyrimidine series, Dr. Nathanael Gray's laboratory developed various prototypes of potential NUAK inhibitors which shall be further discussed and described in details in Chapter 3.

1.5. Ubiquitylation as a regulatory mechanism

Ubiquitylation is one of the most versatile post translational modifications in the cell which controls various mechanisms like cell cycle, DNA repair, immune responses, transcription,

viral infection, receptor endocytosis, protein stability etc. (reviewed in(Ikeda and Dikic, 2008)). The process involves the covalent attachment of a mono or poly ubiquitin small protein modifier by a cascade of enzymatic reactions on a conserved Lys residue on the substrate which finally determines the fate of the substrate within the cell (reviewed in (Teixeira and Reed, 2013)). Similar to phosphorylation and dephosphorylation, the process of ubiquitylation is reversible by the action of deubiquitylating enzymes or DUBs which play a role in the ubiquitin chain cleavage from substrates (Ikeda and Dikic, 2008).

1.5.1. Ubiquitin

Ubiquitin was first described as a 8.5 kDa 74 amino acid long UBIP or ubiquitous immunopoietic polypeptide involved in thymic lymphocyte differentiation (Goldstein et al., 1975). The first ubiquitylated substrate reported was Histone H2A, wherein a branched polypeptide was found linked via an isopeptide bond at the C-terminus of H2A (Goldknopf and Busch, 1977). It was in the 1980s that the role of ubiquitin in ATP dependent proteolytic cleavage was identified and was termed as ATP-dependent proteolytic factor or APF1 (Ciechanover et al., 1980). Eventually this protein has been identified as ubiquitin, a 76 amino acid highly conserved and heat stable protein which is an essential component of the ubiquitin-proteasome system (UPS) deciding the fate of proteins in the biological processes.

Ubiquitin exhibits a very stable β-grasp fold structure (Vijaykumar et al., 1987) and on its surface there are two conserved hydrophobic patches (Fig 1.9a), the Ile44 patch consisting of Leu8, Ile44, His68 and Val70 and the Ile36 patch consisting of Leu8, Ile36, Leu71 and Leu73. These two patches are essential for polyubiquitin chain formation as well as for the interactions with proteasome, substrates, E3 ligases and DUBs (Komander and Rape, 2012). Recently, crystal structure of an E3 enzyme conjugated with ubiquitin primed E2 has shown

that the Ile44 patch of ubiquitin is essential for its docking into the E2 enzyme prior to substrate catalysis (Plechanovova et al., 2012). Besides the Ile44 and Ile36 patches, the Phe4 patch is required for DUB interactions and the TEK patch is essential for mitotic degradation of ubiquitin (Komander and Rape, 2012).

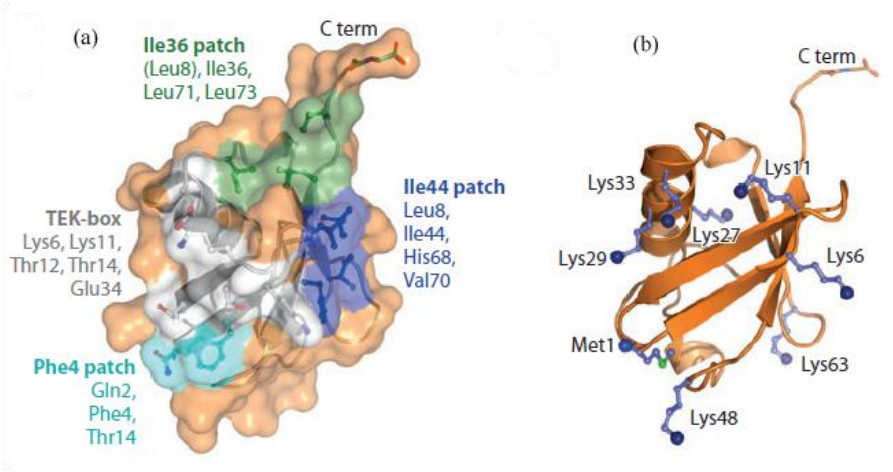

Figure 1.9 : Structure of Ubiquitin : a) The surface topology of ubiquitin structure is shown and the important patches are highlighted. Ile44 patch in blue, Ile 36 patch in green, Phe4 patch in cyan and TEK box in white. b) The structure of ubiquitin highlighting the polyubiquitin chain forming Lys residues and the Met residue (blue spheres). Image taken from (Komander and Rape, 2012).

1.5.2. Polyubiquitin chains

Ubiquitin can modify substrate proteins in its monomeric form (monoubiquitylation) or via polyubiquitylation upon conjugation with preceding ubiquitin moieties to form a chain. Ubiquitin contains seven Lys residues (Lys6, Lys11, Lys27, Lys29, Lys33, Lys48 and Lys63) and the N-terminal Met1 residue (Fig 1.9b) which interact with each other forming isopeptide bonds to form long polyubiquitin chains and each chain architecture determines the subsequent fate of the substrates (Ikeda and Dikic, 2008, Komander and Rape, 2012). Lys48 linked chains are the most abundant form of polyubiquitylation and responsible for targetting the substrate for 26S proteasomal degradation (Ikeda and Dikic, 2008). Lys63 linked chains are markedly different from the Lys48 linked chains and have been reported to have roles in

degradation as well as some essential functions in immune signalling and kinase activation (Komander et al., 2009, Komander and Rape, 2012). Lys11 chains assume a very compact conformation (Bremm et al., 2010) and are preferentially formed in the cell cycle by APC/C E3 ligase enzyme (Komander and Rape, 2012, Teixeira and Reed, 2013). Lys29/33 linked chains seem to inhibit activity of some AMPK related kinases (Al-hakim et al., 2008). Met1 chains or linear ubiquitin chains regulate NFκB signalling pathway (Tokunaga et al., 2009), while very less is known regarding the roles of Lys6 and Lys27 linked chains.

1.5.3. Ubiquitin cascade

The process of ubiquitylation is a three step process involving the E1-E2-E3 cascade (Fig. 1.10) (Scheffner et al., 1995). The E1 activating enzyme utilises ATP to activate and bind to ubiquitin via a ubiquitin -adenylate intermediate. This intermediate further transfers the active ubiquitin to the active site Cys of the E1 via a thiol ester linkage (Schulman and Harper, 2009). Subsequently the active ubiquitin is transferred from E1 to the E2 active site wherein the ubiquitin C-terminal tail docks firmly into the α2 helix of the E2 into a 'folded back' conformation which orientates the ubiquitin Gly76 residue for the incoming substrate Lys (Plechanovova et al., 2012). The substrate is brought in by the E3 ubiquitin ligase complex and the Lys residue on the substrate causes a nucleophillic attack on the Gly76 of the active ubiquitin leading to an isopeptide bond formation and the final transfer takes place (Plechanovova et al., 2012). The combination of E2 and E3 enzymes generally dictate the type of polyubiquitin linkage to be formed on the substrate (Ikeda and Dikic, 2008).

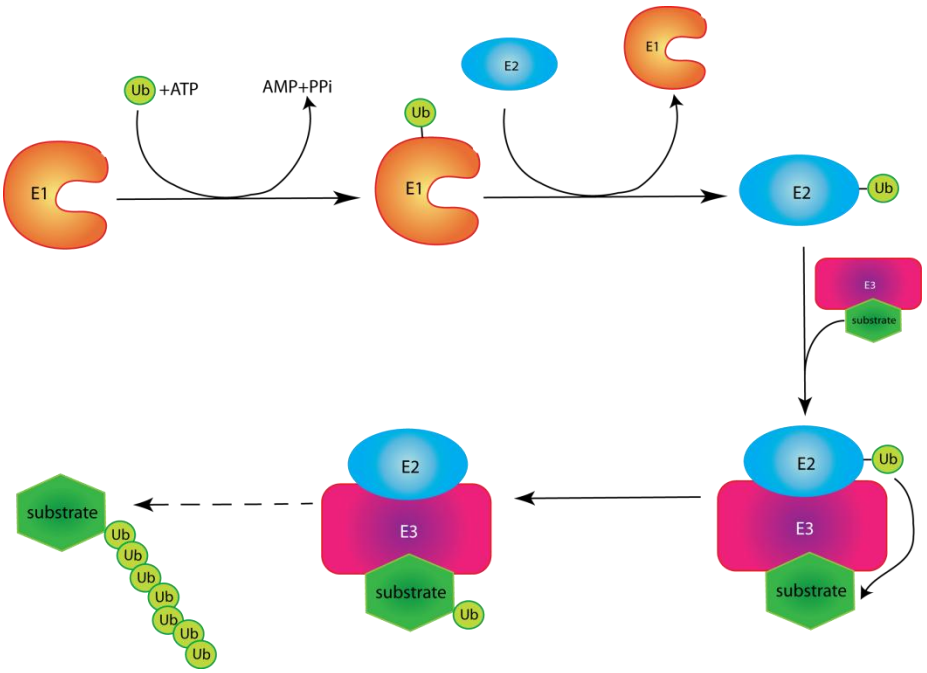

Figure 1.10 The Ubiquitin E1-E2-E3 cascade

1.5.4. Types of E3 ligases

There are over 600 E3 ubiquitin ligases and they are primarily of three types based on their modes of ubiquitin transfer. The Really Interesting New Gene (RING) domain (Fig 1.11b) (Borden, 2000, Joazeiro and Weissman, 2000, Budhidarmo et al., 2012) and closely related U-box domain (Hatakeyama and Nakayama, 2003) families of E3 ubiquitin ligases act as a scaffold to allow the direct transfer of ubiquitin from the E2 to a Lys residue on the target protein. In contrast, the Homologous to the E6-AP Carboxyl Terminus (HECT) domain family forms an ubiquitin-E3 intermediate before transferring ubiquitin from the E3 onto the substrate (Fig 1.11a) (Huibregtse et al., 1995). Recently, a new class of E3 ligases have been identified containing two RING domains referred to as RING-in-between-RING or RBR E3 ligases (Wenzel et al., 2011). RBR E3 ligases like HHARI, parkin, RNF4 etc. act as hybrids between RING and HECT E3 ligases by functioning through an intermediate covalent thioester in a manner similar to HECT E3 ligases (Wenzel et al., 2011, Metzger et al., 2012).

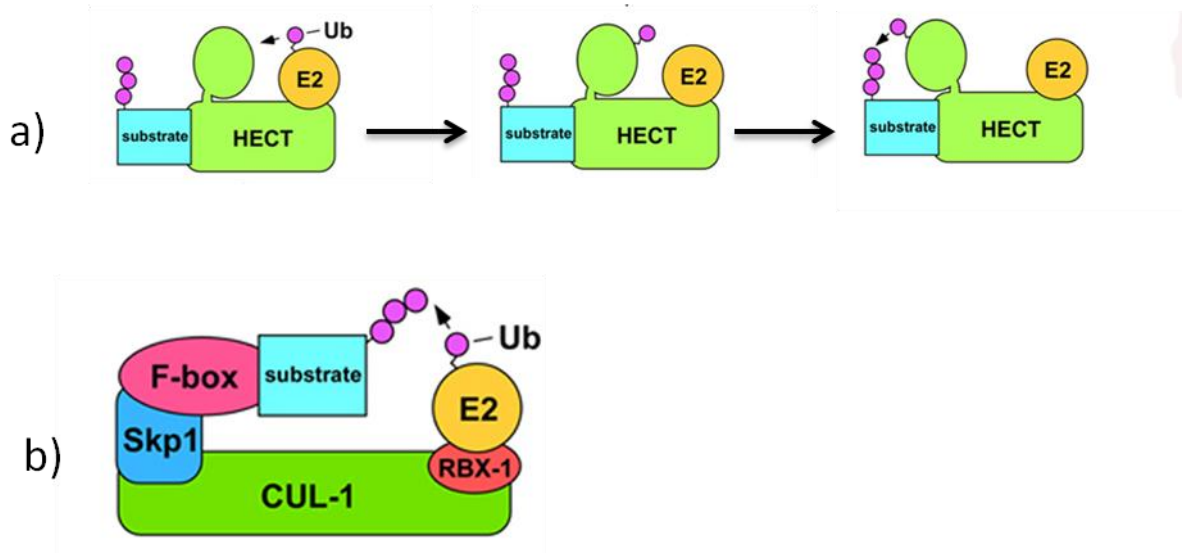

Figure 1.11 : HECT and RING domain E3 ligases a) Mechanism of ubiquitin transfer in HECT domain E3 ligases where an intermediate Ub-E3 conjugate is formed before substrate transfer. b) RING domain E3 ligases (eg. SCF complex) acts as scaffolds which bring E2 and substrate close for direct E2 to substrate ubiquitin transfer. Image adapted from (Kipreos, 2005).

1.6. The Cell Cycle : Cross talk between Phosphorylation and Ubiquitylation

The cell cycle is highly regulated physiological process wherein a cell undergoes duplication of its chromosomes and divides into two daughter cells by a series of phases : G1, S (DNA replication), G2 and Mitosis (M) (cell division). The cell cycle is a perfect physiological scenario to explain how robust post translational modifications like phosphorylation and ubiquitylation cross-talk to success highly regulated processes. Kinases, phosphatases, E3 ubiquitin ligases, helicases and various other proteins play fundamental roles in controlling the progression of the cell through the four phases of cell cycle. This section, however, shall primarily focus on the role of various kinases and E3ubiquitin ligases in each stage of the cell cycle.

For the cell to undergo division, the presence of growth factor stimuli and mitogens are essential. However, upon withdrawal or absence of mitogens, cells enter early G1 stage of

the cell cycle. The E3 ubiquitin ligase APC/C^{Cdh1} is activated during late mitosis and is a central player in the Lys11-linked polyubiquitylation (Jin et al., 2008) and degradation of mitotic proteins and DNA replication agonists which leads to mitotic exit (Bassermann et al., 2013). APC/C^{Cdh1} degrades Cdc6, a DNA replication promoting protein (Mailand and Diffley, 2005) and transcription factor Ets1 which is involved in the expression of Cyclin D downstream of Ras-Raf-MAPK pathway (Albanese et al., 1995, Li et al., 2008). In early G1 stage, APC/C^{Cdh1} keeps the CDK family of kinases in an inactive state by degrading SCF^{Skp2} thereby promoting the expression of CDK inhibitors p21 and p27 (Bashir et al., 2004, Wei et al., 2004). Proteasomal degradation of mitotic cyclins (A and B) and the rapid degradations of mitotic Aurora family and polo-like kinase (PLK) family of protein kinases ensure a fast exit from mitosis and implementation of early G1 phase of the cell cycle (Bassermann et al., 2013).

When growth factors and mitogens become available, cells trigger the late G1 phase for preparations to enter the S-phase or DNA replication phase of the cell cycle. At this point APC/C^{Cdh1} activity decreases owing primarily due to autoubiquitylation of its E2 (Rape and Kirschner, 2004) as well as Cdh1(Listovsky et al., 2004). Reduced activity of APC/C^{Cdh1} triggers dephosphorylation and activation of CDK1 and CDK2 by CDC25A dual specificity phosphatase which promotes entry to S-phase (Donzelli et al., 2002). Activation of CDKs are further enhanced by degradation of the CDK inhibitors p27 by SCF^{Skp2} (Pagano et al., 1995) and p21 by $CRL4^{CDT2}$ (Abbas et al., 2008). Active CDKs further phosphorylate Cdh1 and disrupts the APC/C^{Cdh1} complex (Lukas et al., 1999). Ets1 mediated transcription of Cyclin D leads to the formation of CDK4/6-cyclin D complexes which phosphorylate and inactivate pRb (Retinoblastoma family p107 and p130) dependent cell cycle repression machinery (Malumbres and Barbacid, 2001). Thus, at the G1/S border, inhibition of pRb machinery leads to activation of E2F mediated transcription of Emi1 (Fbxo5) which binds to and

completely inhibits the APC/C^{Cdh1} complex all through S and G2 stage of the cell cycle (Hsu et al., 2002, Miller et al., 2006).

Upon successful entry into S-phase, CDK2-cyclin E and CDK2-cyclin A are the primary exponents which initiate DNA and centrosome duplication (Bassermann et al., 2013). Cyclin D is phosphorylated by GSK3β and consequently degraded by SCF^{Fbxo4} (Lin et al., 2006). CDC7 kinase works along with CDKs to phosphorylate and activate the minichromosome maintenance complexes MCM helicases which leads to establishing proper integrity of replication forks during chromosome duplication (Malumbres, 2011). As DNA replication takes place, various E3 ligases like $CRL4^{CDT2}$ (Abbas and Dutta, 2011) and $CRL4^{DDB1}$ (Senga et al., 2006) play vital roles to limit DNA replication to once per cell cycle. Accurate DNA replication is crucial for the cells, hence besides having a tightly controlled regulation, various kinases and E3 ubiquitin ligases play essential roles in DNA repair mechanism. Upon DNA damage, the checkpoint kinases CHK1 and CHK2 are activated via ATR and ATM upstream kinases (Matsuoka et al., 1998, Zeng et al., 1998). CHKs phosphorylate the dual specificity phosphatase CDC25A which consequently leads to $SCF^{\beta TRCP}$ mediated degradation of CDC25A, thus attenuating CDK activation (Busino et al., 2003). Inhibition of CDK activity leads to a halt in cell cycle progression and provides time for DNA repair. During checkpoint recovery, PLK1 phosphorylates Claspin and targets it for $SCF^{\beta TRCP}$ mediated degradation (Mailand et al., 2006, Peschiaroli et al., 2006). Claspin is an essential upstream component for ATR induced CHK1 activation in response to DNA damage (Liu et al., 2006). Degradation of Claspin via $SCF^{\beta TRCP}$ ensures S-phase checkpoint revival and further progression of cell cycle. As cells progress into S/G2 border, S phase cyclin E is phosphorylated by CDK2 and leads to its degradation via SCF^{Fbw7} (Clurman et al., 1996, Koepp et al., 2001).

After an accurate replication of DNA, the ribonucleotide reductase family member 2 or RRM2 is phosphorylated by CDKs and consequently degraded by $SCF^{CyclinF}$ which leads to reduction in the synthesis of dNTP pool in the cell (D'Angiolella et al., 2012). Besides controlling cellular dNTP pool, $SCF^{CyclinF}$ also regulates centrosome duplication by targetting CP110 for proteasomal degradation (D'Angiolella et al., 2010). PLK4 is an essential kinase responsible for centrosome duplication (Kleylein-Sohn et al., 2007) and to avoid overduplication of centrosomes, PLK4 undergoes robust autophosphorylation followed by $SCF^{\beta TRCP}$ mediated degradation (Mocciaro and Rape, 2012). Aurora A localises to the centrosomes at late S and early G2 stage and plays vital roles like centrosome separation and controlling bipolar spindle dynamics (Barr and Gergely, 2007). As G2 phase progresses, PLK1 activity increases owing to synergistic activity of Bora and Aurora A (Seki et al., 2008). PLK1 phosphorylates CDK1 inhibitory kinase WEE1 which gets degraded by $SCF^{\beta TRCP}$ (Watanabe et al., 2004). Degradation of WEE1 promotes the formation of CDK1-cyclin B complex which further phosphorylates and inhibits assembly of cyclin B degrading SCF^{NIPA} complex (Bassermann et al., 2007, Illert et al., 2012). Thus, a massive upregulation of CDK1-cyclin B complex ensures a proper mitotic entry of the cells. In the event of DNA damage induced G2 checkpoint silencing, $SCF^{\beta TRCP}$ plays a vital role in degrading the translation inhibitory Eukaryotic Elongation factor 2 kinase (eEF2K) upon AMPK phosphorylation (Kruiswijk et al., 2012). This ensures a smooth re-start of the cell cycle post G2 checkpoint DNA repair. At the G2/M border, NIMA-related kinase NEK2A localises to centrosome and along with Aurora A, initiates centrosome separation and microtubule organization (O'Regan et al., 2007).

During early mitosis, nuclear envelope breakdown, chromatin condensation and assembly of mitotic spindles are all carried out by the CDK1-cyclin B complex throughout prophase and metaphase (Bassermann et al., 2013). PLK1 and Aurora A play essential roles in maintaining

the spindle stability and proper tension between the kinetochores (Bassermann et al., 2013). The spindle assembly checkpoint (SAC) complex mediates proper chromosomal attachment of sister chromatids to the spindle fibres. Upon proper attachment of kinetochores, $SCF^{\beta TRCP}$ mediates degradation of APC/C inhibitor EMI1 following CDK1 and PLK1 phosphorylation (Margottin-Goguet et al., 2003). This activates APC/C which interacts with substrate recognition subunit CDC20 and plays a key role in mitotic progression and exit. In the event of unattached kinetochores, SAC complex proteins MAD2, BUBR1 and BUB3 inhibits APC/C^{CDC20} by inhibitory phosphorylation or by mediating CDC20 degradation (Bassermann et al., 2013) thus restricting entry to anaphase. Once proper alignment of sister chromatids have occured, SAC is inhibited and APC/C^{CDC20} degrades Securin which starts the segregation of sister chromatids and hence progresses into anaphase (Zou et al., 1999, Hauf et al., 2001). Degradation of mitotic cyclins are commenced by APC/C^{CDC20} complex in metaphase and is completed by APC/C^{Cdh1} in late mitosis which leads to sister chromatid separation (Acquaviva and Pines, 2006). Aurora B, which functions in the centrometric regions of chromosomes, undergoes Lys63 linked polyubiquitylation via $CRL3^{KLHL9}$ and $CRL3^{KLHL13}$ complexes which results in relocalisation of Aurora B to the spindle midzone to control mitotic chromosome alignment and cytokinesis (Sumara et al., 2007). Post-cytokinesis or during late mitosis APC/C^{Cdh1} degrades Geminin to prevent random re-replication of DNA (McGarry and Kirschner, 1998) and promotes mitotic exit by proteasomal degradation of mitotic kinases PLK1 (Lindon and Pines, 2004), Aurora A (Castro et al., 2002) and Aurora B (Stewart and Fang, 2005). APC/C^{Cdh1} re-establishes G1 stage of cell cycle by degradation of cyclin B and thus significantly inhibiting CDK activity (Acquaviva and Pines, 2006).

1.7. Aims of the study

Over the last decade, LKB1-NUAK1 pathway has been reported to have various links to cancer especially in metastasis, cell proliferation and anti-apoptotic roles in deregulated MYC driven tumours. A specific and potent tool compound to inhibit the NUAKs was also not available to dissect the roles of the NUAKs. In collaboration with Dr. Nathanael Gray (Harvard, USA), I aim to test various small molecule inhibitors of NUAK1 which would ideally be very potent and selective for NUAK isoforms alone with least off-target effects on any of the other kinases tested including the homologous AMPK related kinases which has always been the prime drawbacks of the earlier inhibitors. Chapter 3 discusses in details the story behind the development of NUAK inhibitors.

In chapter 4, the primary focus is to look into any novel functions and regulatory pathways of NUAK1 in cells. The idea is to identify physiological pathways where NUAK1 is regulated and to identify the enzymes responsible in interacting and conferring further post-translational modifications on NUAK1. I would also aim to dissect the functions of any novel modifications or interactors that might regulate NUAK1.

We had previously published that MYPT1-PP1β is the substrate for NUAK1. In chapter 5, I would aim to establish the other myosin phosphatase isoforms MYPT2 and MBS85 as potential substrates of NUAK1 as the phosphosites on the isoforms are all conserved with MYPT1.

2. Materials and Methods

2.1 Materials

2.1.1 Commercial reagents

Adenosine 5'-triphosphate sodium salt (ATP), anti-HA-agarose, anti-FLAG-agarose, ammonium persulphate (APS), ampicillin, benzamidine, bovine serum albumin (BSA), bromophenol blue (BPB), dimethyl pimelimidate (DMP), dimethyl sulphoxide (DMSO), ethidium bromide, hydrogen peroxide, iodoacetamide, insulin, epidermal-growth factor (EGF), hydrocortisone, MISSION™ shRNAs, nocodazole, puromycin, N-ethylmaleimide (NEM), propidium iodide, sodium dodecyl sulphate (SDS), sodium tetraborate, thymidine, N, N, N', N'-Tetramethylethylenediamine (TEMED), Phalloidin-Tetramethylrhodamine B isothiocyanate (TRITCPhalloidin), Triton-X-100 and Tween-20 were from Sigma-Aldrich (Poole, UK). Protein A-agarose, Protein G-sepharose, Glutathione-sepharose, Enhanced chemiluminescence (ECL) kit and Hyperfilm MP were from Merck. Dulbecco's modified eagle medium (DMEM), Opti-MEM reduced serum media, Foetal bovine serum (FBS), tissue culture grade Dulbecco's phosphate buffered serum (PBS), Trypsin/EDTA solution, L-glutamine, non-essential amino acids, vitamins, sodium pyruvate and antibiotic/antimycotic were from GIBCO (Paisley, UK). [γ^{32}P]-labelled ATP were purchased from Perkin Elmer. Acetic acid, acetone, ammonium bicarbonate, ethanol, glycerol, glycine, 4-(2-Hydroxyethyl)piperazine-1-ethanesulfonic acid (Hepes), isopropanol, magnesium chloride, manganese chloride, methanol, 2-mercaptoethanol, orthophosphoric acid, potassium chloride, sodium chloride, sodium ethylenediaminetetraacetic acid (EDTA), sodium ethylene glycol tetraacetic acid (EGTA), sodium fluoride, sodium β-glycerophosphate, sodium orthovanadate, sucrose and Tris(hydroxymethyl)methylamine (Tris) were from BDH (Lutterworth, UK) or Sigma-Aldrich (Poole, UK). CHAPS and okadaic acid were from Calbiochem (Merck Biosciences Ltd, Nottingham, UK). Calyculin A and polybrene were

from Cell Signaling Technology (CST). 6, 24 and 96 well tissue culture plates, cell culture dishes, cryovials and Spin-X columns were from Corning Incorporated (NY, USA). Cellophane films and All Blue Precision Plus pre-stained protein markers were from BioRad (Herts, UK). Cell scrapers were from Costar (Cambridge, USA). 40% (w/v) 29:1 Acrylamide: Bis-Acrylamide solution was from Flowgen Bioscience. Pre-cast NuPAGE Novex SDS polyacrylamide 4-12% Bis-Tris gels, NuPAGE MES and MOPS running buffer (20X), 10X NuPAGE sample reducing agent, 4X NuPAGE LDS sample buffer, Colloidal blue staining kit, Alexa Fluor donkey secondary antibodies were from Invitrogen (Paisley, UK). Instant-Blue stain was from Expedeon, UK. Photographic developer (LX24) and liquid fixer (FX40) were from Kodak (Liverpool, UK). X-ray films were from Konica Corporation (Japan). Agarose, phenylmethanesulphonylfluoride (PMSF), Geneticin (G418) and Isopropyl-β-D-thiogalactopyranoside (IPTG) were from Melford Laboratories (Chelsworth, UK). Restriction enzymes, DNA ligase and DNA ladder were from New England Biolabs (Hertfordshire, UK). Coomassie protein assay reagent (Bradford reagent) was from Pierce (Chester, UK). Hygromycin, blasticidin and polyethylenimine (PEI) were from Polysciences (Warrington, PA). Skimmed milk (Marvel) was from Premier Beverages (Stafford, UK). The CellTiter 96® AQ_{ueous} Non-Radioactive Cell Proliferation Assay kit, Taq DNA polymerase in storage buffer A, sequencing grade trypsin and nucleotide mix (dNTP) were from Promega (UK). Growth-factor-reduced Matrigel™ invasion chambers were from BD Biosciences. Reastain Quick-Diff kit was from Reagena. Sequencing grade AspN was from Roche. P81 paper and 3mm chromatography paper were from Whatman InterInternational Ltd (Maidstone, UK). Plasmid Maxi kits were from Qiagen Ltd (Crawley, UK). Acetonitrile (HPLC grade), trichloroacetic acid (TCA) and trifluoroacetic acid (TFA) were from Rathburn Chemicals (Walkerburn, UK). Protran BA nitrocellulose membrane was purchased from Schleicher and Schuell (Anderman and Co. Ltd., Surrey, UK). HRP-conjugated secondary

antibodies and SuperSignal West Dura extended duration substrate were from Thermo-scientific (Essex, UK).

2.1.2 In-house reagents

Oligonucleotide primers were custom synthesised by the University of Dundee oligonucleotide synthesis service. Bacterial culture medium Luria Bertani broth (LB), autoinduction media and LB agar plates were provided by the College of Life Sciences media kitchen service. Sakamototide substrate peptide [ALNRTSSDSALHRRR], used for AMPK related kinase activity assays, was obtained from the Division of Signal Transduction Therapy (DSTT, University of Dundee). Microcystin-LR was kindly provided by Prof. C. Mackintosh (University of Dundee, MRC-PPU).

2.1.3 Antibodies

2.1.3.1 In-house antibodies

In-house antibodies (Table 2.1) were raised in sheep and affinity purified on the approprate antigen. The polyclonal sheep antibody production was carried out by the Division of Signal Transduction Therapy (DSTT, University of Dundee).

Table 2.1 : List of in-house sheep antibodies

Antibody	Antigen	Sheep	Bleed
anti-MYPT1 phospho Ser445	MYPT1 (437-452) RLGLRKTGS*YGALAEI	S508C	1st
anti-MYPT1 phospho Ser472	MYPT1 (466-478) GVMRSAS*SPRLSS	S509C	2nd
anti-MYPT1 phospho Ser910	MYPT1 (903-917) RLLGRSAS*YSYLEDRK	S516C	1st
anti-MYPT1	Human MBP-MYPT1 (714-1005)	S662B	1st
anti-NUAK1	Human his-NUAK1	S628B	2nd
anti-PP1β	Human PP1β (316-327)	S383B	3rd
anti-GFP	GFP	S268B	1st

* indicate phosphorylated residue

2.3.1.2. Commercial/gifted antibodies

Table 2.2 tabulates antibodies obtained from the indicated commercial sources and used at the concentration recommended by the manufacturer/collaborator.

Table 2.2 : List of commercial antibodies used in this thesis

Antibody	Company/Gift from	Catalogue	Raised in
β-TRCP	Cell Signalling	4394	Rabbit
ACC	Cell Signalling	3662	Rabbit
pSer79 ACC	Cell Signalling	3661	Rabbit
MLC2	Cell Signalling	3672	Rabbit
pSer19 MLC2	Cell Signalling	3671	Rabbit
pSer19/Thr18 MLC2	Cell Signalling	3674	Rabbit
AMPKα	Cell Signalling	2532	Rabbit
pThr172 AMPK	Cell Signalling	2535	Rabbit
p53	Cell Signalling	9282	Rabbit

Cyclin B1	Cell Signalling	4135	Mouse
Cyclin D1	Cell Signalling	2926	Mouse
Cyclin E	Cell Signalling	4129	Mouse
Histone H3 pSer10	Cell Signalling	3377	Rabbit
Histone H3	Cell Signalling	4499	Rabbit
Cyclin A	Cell Signalling	4656	Mouse
PLK1	Cell Signalling	4535	Rabbit
c-MYC	Cell Signalling	9402	Rabbit
N-MYC	Cell Signalling	9405	Rabbit
GAPDH	Cell Signalling	2118	Rabbit
LATS1	Cell Signalling	9153	Rabbit
ZO1	Abcam	ab59720	Rabbit
GST-HRP	Abcam	ab58626	-
HA-HRP	Roche	12013819001	-
FLAG-HRP	Sigma	A8592	-
HA monoclonal	Roche	11867423001	Rat
14-3-3	Santa Cruz	sc-629	Rabbit
ERK	Cell Signalling	4372	Rabbit
pERK	Cell Signalling	9102	Rabbit
Ubiquitin	Dako	Z0458	Rabbit
Caspase3 FITC conjugated	BD Pharmingen	559341	-

2.1.4 Plasmids

Dr. M. Deak, Dr. M. Peggie, Dr. R. Toth and Mr. T. Macartney performed the cloning, subcloning and mutagenesis of the constructs described in this thesis. Table 2.3 summarises all the mammalian constructs used in this work while Table 2.4 lists the constructs used to purify recombinant proteins from E.coli BL21 DE3 cells (2.2.4).

Table 2.3 : Mammalian expression constructs

Protein	Expressed	Plasmid	DU No.
NUAK1	GFP-NUAK1	pBABE.puro-GFP NUAK1	DU41429
NUAK1	HA-NUAK1 A195T	pcDNA5frtTO HA NUAK1 A195T	DU44193
NUAK1	GFP-HA-NUAK1 S476/480/481A	pcDNA5-FRT/TO-GFP HA NUAK1 SSS/AAA	DU41375
NUAK1	GST-HA-NUAK1-Y479/A	pEBG-2T-HA NUAK1-Y479/A	DU38175
NUAK1	GST-NUAK1 D196A SSS/AAA	pEBG6P NUAK1 D196A S/476/480/481A	DU41537
NUAK1	GST-HA-NUAK1-S480/A	pEBG-2T-HA NUAK1-S480/A	DU38176
NUAK1	HA-NUAK1-S476/480/AA	pcDNA5-FRT/TO-HA NUAK1-S476/480/AA	DU38598
NUAK1	HA-NUAK1 A195T	pBabe.hygro.DU HA-NUAK1 A195T	DU40830
NUAK1	GST-NUAK1 D196A S476A	pEBG-6P NUAK1 D196A S476A	DU41622
NUAK1	GST-HA-NUAK1 A195/G	pEBG-2T-HA NUAK1 A195/G	DU38086
NUAK1	GST-HA-NUAK1-S481/A	pEBG-2T-HA NUAK1-S481/A	DU38177
NUAK1	HA-NUAK1-S476/480/AA	pBabe.puro-HA NUAK1-S476/480/AA	DU38599
NUAK1	HA-NUAK1	pBabe.hygro.DU HA-NUAK1	DU40806
NUAK1	GST-NUAK1 D196A S480A	pEBG-6P NUAK1 D196A S480A	DU41623
NUAK1	GST-HA-NUAK1 A195/S	pEBG-2T-HA NUAK1 A195/S	DU38087
NUAK1	GST-HA-NUAK1-P482/A	pEBG-2T-HA NUAK1-P482/A	DU38178
NUAK1	HA-NUAK1 wt	Lentiviral-HA NUAK1 wt	DU13246
NUAK1	HA-NUAK1 A195G	pBabe.hygro.DU HA-NUAK1A195G	DU40827
NUAK1	eCFP-NUAK1	pcDNA5frtTO eCFP NUAK1	DU41878
NUAK1	GST-HA-NUAK1 A195/T	pEBG-2T-HA NUAK1 A195/T	DU38088
NUAK1	GST-HA-NUAK1-E483/A	pEBG-2T-HA NUAK1-E483/A	DU38179
NUAK1	GFP-wt-NUAK1	pGFP NUAK1 wt	DU2153
NUAK1	HA-NUAK1 Kdead	Lentiviral-HA NUAK1 D196/A	DU13247
NUAK1	NUAK1-CFP	pcDNA5 FRT/TO NUAK1-CFP	DU40837
NUAK1	NUAK1 A195G	pcDNA5frtTO NUAK1 A195G	DU41824
NUAK1	HA-NUAK1 wt	pcDNA5-FRT/TO-HA NUAK1 wt	DU13418
NUAK1	GST-HA-NUAK1 A195/N	pEBG-2T-HA NUAK1 A195/N	DU38089
NUAK1	GST-HA-NUAK1-S476/480/AA	pEBG-2T-HA NUAK1-S476/480/AA	DU38180
NUAK1	HA-NUAK1 T211/A	Lentiviral-HA NUAK1 T211/A	DU13248
NUAK1	GST-NUAK1-wt	pEBG-2T-HA NUAK1-wt	DU2108
NUAK1	HA-NUAK1 T211/A	pcDNA5-FRT/TO-HA NUAK1 T211/A	DU13419
NUAK1	FLAG-NUAK1	pCMV-FLAG NUAK1 wt	DU6359
NUAK1	GST-HA-NUAK1 A195/V	pEBG-2T-HA NUAK1 A195/V	DU38090
NUAK1	GST-HA-NUAK1 A195/D	pEBG-2T-HA NUAK1 A195/D	DU38091
NUAK1	HA-NUAK1 D196/A	pcDNA5-FRT/TO-HA NUAK1 D196/A	DU13421

NUAK1	GST-HA-NUAK1 A195/K	pEBG-2T-HA NUAK1 A195/K	DU38092
NUAK1	NUAK1	pBABE.puro NUAK1	DU38884
NUAK1	GST-NUAK1-D196/A	pEBG-2T-NUAK1-D196/A	DU2111
NUAK1	GFP-HA-NUAK1 wt	pcDNA5-FRT/TO-GFP-HA NUAK1 wt	DU13422
NUAK1	HA-NUAK1-S476/480/481/AAA	pcDNA5-FRT/TO-HA NUAK1 SSS/AAA	DU38911
NUAK1	HA-NUAK1 wt	pCMV-HA NUAK1 wt	DU2127
NUAK1	GST-HA-NUAK-Q473/A	pEBG-2T-HA NUAK Q473/A	DU38169
NUAK1	HA-NUAK1 S476/480/481A	pcDNA5-FRT/TO-HA NUAK1 S476/480/481A	DU41249
NUAK1	GST-NUAK1	pCMV5 GST NUAK1	DU41891
NUAK1	GST-HA-NUAK-R474/A	pEBG-2T-HA NUAK R474/A	DU38170
NUAK1	HA-NUAK1 S476/480/481A	pCMV5-HA NUAK1 S476/480/481A	DU41280
NUAK1	FLAG-NUAK1 D196A	pCMV5 FLAG NUAK1 D196A	DU44036
NUAK1	GST-HA-NUAK-E475/A	pEBG-2T-HA NUAK E475/A	DU38171
NUAK1	NUAK1 S476/480/481A	pBabe.puro NUAK1 S476/480/481A	DU41315
NUAK1	HA-NUAK1-D196/A-dead	pCMV-HA NUAK1-D196/A-dead	DU2227
NUAK1	FLAG-NUAK1 A195T	pCMV5 FLAG NUAK1 A195T	DU44028
NUAK1	GST-HA-NUAK-S476/A	pEBG-2T-HA NUAK S476/A	DU38172
NUAK1	HA-NUAK1 W305/A	pCMV-HA NUAK1 W305/A	DU13026
NUAK1	GFP-NUAK1 S476/480/481A	pBabe.puro-GFP NUAK1 S476/480/481A	DU41316
NUAK1	GST-HA-NUAK1 K348/R	pEBG-HA NUAK1 K348/R	DU13256
NUAK1	HA NUAK1-2-425 I400/K	pCMV-HA NUAK1-2-425 I400/K	DU17326
NUAK1	HA-NUAK1 A195T	pCMV5 HA NUAK1 A195T	DU44037
NUAK1	HA-NUAK1 wt	pBabe.puro-HA NUAK1 wt	DU30763
NUAK2	GST-HA-NUAK2	pEBG-2T-HA NUAK2-wt	DU2044
NUAK2	HA-NUAK2-wt	pCMV NUAK2 wt	DU2152
MARK1	HA-MARK1	pCMV5-HA MARK1	DU1265
MARK1	GST-HA-MARK1	pEBG-2T-HA MARK1	DU1200
MARK2	HA-MARK2	pCMV5-HA MARK2	DU1253
MARK2	GST-HA-MARK2	pEBG-2T-HA MARK2	DU1133
MARK3	HA-MARK3-wt	pCMV-HA MARK3-wt	DU2268
MARK3	GST-HA-MARK3	pEBG-2T-HA MARK3	DU2058
MARK4	HA MARK4-wt	pCMV5-HA MARK4-wt	DU2230
MARK4	GST-MARK4-wt	pEBG MARK4 wt	DU2135
BRSK1	HA-BRSK1	pCMV5-HA BRSK1	DU1236
BRSK1	GST-HA-BRSK1	pEBG-2T-HA BRSK1	DU1175
BRSK2	HA-BRSK2 wt	pCMV-HA BRSK2 wt	DU2175
BRSK2	GST-BRSK2 wt	pEBG BRSK2 wt	DU2101
SIK	HA-SIK-wt	pCMV-2HA SIK wt	DU6208

SIK	GST-HA-SIK	pEBG-2T-HA SIK	DU1081
QIK	HA-QIK	pCMV5-HA	DU1079
QIK	GST-HA-QIK	pEBG-2T-HA QIK	DU1078
QSK	HA-QSK	pCMV5-HA QSK	DU1311
QSK	GST-HA-QSK	pEBG-2T-HA QSK	DU1184
MYPT1	FLAG-MYPT1	pCMV-FLAG MYPT1 ppp1r12a	DU17632
MYPT1	GST-MYPT1	pEBG6-MYPT1 ppp1r12a	DU17631
MYPT2	FLAG-MYPT2	pCMV-FLAG MYPT2	DU30286
MYPT2	GST-MYPT2	pEBG6P-MYPT2	DU30285
MBS85	FLAG MBS85	pCMV-FLAG MBS85 wt	DU17960
MBS85	GST-MBS85 wt	pEBG6-MBS85 wt	DU17958
MBS85	FLAG-MBS85 wt	pBabe.puro-FLAG MBS85 wt	DU34833
MYPT3	GST-MYPT3	pEBG6-MYPT3	DU17841
MYPT3	FLAG-MYPT3	pCMV-FLAG MYPT3	DU17799
TIMAP	FLAG-TIMAP	pCMV-FLAG TIMAP	DU17798
PLK1	GST PLK1	pEBG6p PLK1	DU15391
Nek2a	GST Nek2a	pEBG6P-NEK2a	DU15294

Table 2.4 : Bacterial expression constructs

Protein	Expressed	Plasmid	DU No.
NUAK1	GST-NUAK1-wt	pGEX-6-NUAK1-wt	DU2104
NUAK1	GST-NUAK1-D196/A-kinase dead	pGEX-6-NUAK1-D196/A-kin-dead	DU2107
NUAK1	GST-HA-NUAK1 D196A S476/480/481A	pGEX-HA NUAK1 D196A SSS/AAA	DU41207
MYPT1	GST-MYPT1	pGEX-6-MYPT1 ppp1r12a	DU17840
MYPT1- PP1β	His-PP1 beta, GST-rat wt MYPT1	POPH-His-PP1β, GST-MYPT1	DU30200
MYPT1- PP1β	His-PP1 beta, GST-rat wt MYPT1 S445/A+S472/A+S856/A	POPH-His-PP1β, GST-MYPT1 SSS/AAA	DU30200
MYPT2	GST-MYPT2	pGEX-6-MYPT2 wt	DU30287
MYPT2	GST-MYPT2-S447/A+S473/A+S525/A	pGEX-6-MYPT2-SSS/AAA	DU34400
MYPT2- PP1β	His-PP1 beta, GST-MYPT2	POPH-His-PP1β, GST-MYPT2	DU34099
MYPT2- PP1β	His-PP1 beta, GST-MYPT2 S447/A+S473/A+S525/A	POPH-His-PP1β, GST-MYPT1 SSS/AAA	DU34099
MBS85	GST-MBS85 wt	pGEX-6-MBS85 wt	DU17959
MBS85	GST-MBS85-S427/A+S452/A	pGEX-6-MBS85-S427/A+S452/A	DU34094
MYPT3	GST-MYPT3	pGEX-6-MYPT3	DU17842
TIMAP	GST-TIMAP	pGEX-6-TIMAP	DU17580

2.1.5 Buffers

Lysis Buffer: 50 mM Tris/HCl pH 7.5, 1 mM EGTA, 1 mM EDTA, 1% (v/v) Triton X-100 (or 0.3% w/v CHAPS), 1 mM sodium orthovanadate, 50 mM sodium fluoride, 5 mM sodium pyrophosphate, 0.27 M sucrose, 0.1% β-mercaptoethanol, 1 mM benzamidine and 0.1 mM phenylmethanesulphonylfluoride (PMSF). Lysis buffer ensures immediate inhibition of protein kinases, phosphatases and proteases during lysis so that the phosphorylation state of proteins in the extracts are fixed at the levels present *in vivo* at the time of extraction. PMSF and benzamidine are serine protease inhibitors. EDTA chelates divalent cations including Mg^{2+} and thus inhibits metal dependent enzymes such as kinases and many phosphatases. EGTA is a chelator with high affinity towards Ca^{2+}. Sodium fluoride and sodium pyrophosphate inhibit Ser/Thr protein phosphatases and sodium orthovanadate (Na_3VO_4) inhibits protein tyrosine phosphatases. Lysis buffer was stored at 4ºC. β-mercaptoethanol and protease inhibitors were added fresh before each use.

Phosphatase lysis Buffer: 50 mM Tris/HCl pH 7.5, 1 mM EGTA, 1 mM EDTA, 1% (v/v) Triton X-100, 0.27 M sucrose, 0.1% β-mercaptoethanol, 1 mM benzamidine and 0.1 mM phenylmethanesulphonylfluoride (PMSF).

GST bacterial lysis buffer : 50 mM Tris/HCl pH 7.5, 270 mM sucrose, 150 mM NaCl, 0.1 mM EGTA, 1 mM benzamidine 0.2 mM PMSF and 0.1% β-mercaptoethanol.

GST bacterial elution buffer : 50 mM Tris/HCl pH 7.5, 270 mM sucrose, 150 mM NaCl, 0.1 mM EGTA, 50 mM glutathione, 1 mM benzamidine 0.2 mM PMSF and 0.1% β-mercaptoethanol. After addition of glutathione re-pH buffer to 7.5.

Phosphate buffered saline (PBS): 137mM NaCl, 2.7mM KCl, 8.1mM di-sodium hydrogen phosphate, 1.5mM potassium dihydrogen phosphate pH 7.4.

SDS Lysis Buffer (used for detection of MLC2): Lysis Buffer with 1% (w/v) SDS instead of Triton X-100 or CHAPS, and pH adjusted 6.8. SDS is a dentaurating anionic detergent.

Buffer A: 50mM Tris-HCl pH 7.5, 0.1mM EGTA, and 0.1% β-mercaptoethanol.

TBST: 50 mM Tris-HCl pH 7.5, 0.15 M NaCl and 0.1% (v/v) Tween-20.

5X SDS-PAGE Sample Buffer: 5% SDS, 5% (v/v) β-mercaptoethanol, 250mM Tris-HCl pH 6.8, 32.5% (v/v) Glycerol, traces of BPB for adequate color intensity.

SDS-PAGE Running Buffer: 25mM Tris-HCl pH 8.3, 192mM Glycine, 0.1% (w/v) SDS.

Western Blotting Transfer Buffer: 48mM Tris-HCl, 39mM Glycine, 20% (v/v) Methanol.

ECL Solution 1: 0.1M Tris-HCl pH 8.5, 2.5mM Luminol, 0.4mM p-Coumaric acid

ECL Solution 2: 0.1M Tris-HCl pH 8.5, 5.6mM Hydrogen peroxide.

TAE buffer: 40mM Tris-acetate pH 8, 1mM EDTA.

2.1.6 Cell lines

NUAK1$^{+/+}$ and NUAK1$^{-/-}$ mouse embryonic fibroblasts (MEFs) were kindly provided by Dr. Shinichi Aizawa (Kobe, Japan). β-TRCP1$^{+/+}$ and β-TRCP1$^{-/-}$ MEFs were kindly provided by Dr. Keiko Nakayama (Sendai, Japan). TET21N neuroblastoma , P4936 B-cell lymphoma cells (both cell lines stably expressing doxycyclin inducible repressor of MYC) and immortalised mammalian epithelial IMECs (MYC overexpressing and vector control) cells were kindly provided by Dr.Victoria Cowling (MRCPPU, University of Dundee).

2.1.7 Instruments

Countess cell counter, X-Cell SureLock Mini-cell electrophoresis systems and X-Cell II Blot modules were from Invitrogen (Paisley, UK). AE6450 Atto Vertical Dual Mini Slab Kits

were from Genetic Research Instrumentation. Trans-Blot Cells, automatic western blot processors and gel dryer apparatus were from BioRad (Herts, UK). X-omat autoradiography cassettes with intensifying screens were from Kodak. Automatic film processor was from Konica Corporation. The Procise 494C Sequenator was from Applied Biosystems (Foster City, USA). HPLC system components were obtained from Dionex (Camberley, UK). The Vydac 218TP54 C_{18} reverse phase HPLC column was from Separations group. The LTQ-orbitrap mass spectrometer and Nanodrop was from Thermo Scientific. The PCR thermocycler (PTC-200) was from MJ Research. The 96-well Versamax plate reader was from Molecular Devices (Wokingham, UK). Thermomixer IP shakers were purchased from Eppendorf (Cambridge, UK). Centrifuge tubes, rotors and centrifuges were from Beckmann. Biofuge pico microcentrifuge was from Haraeus Instruments (Osterode, Germany). pH meters and electrodes were from Horiba (Kyoto, Japan). Scintillation counter (Tri-Carb 2800 TR) was from Perkin-Elmer. Vibrax-VR platform shaker was from IKA. Balances were from Ohaus. Sonicators were from Sonics and Materials. Speed-vacs were from CHRIST. Gel Electrophoresis System (Horison 11-14) was from Life Technologies. Tissue culture class II safety cabinets were from Medical Air Technology (Oldham, UK). CO_2 incubators were from Mackay and Lynn (Dundee, UK). The LiCOR odyssey infrared imaging system was from LiCOR biosciences (Cambridge, UK).

2.1.8. Inhibitors

Table 2.5 summarises the various small molecule inhibitors used in this thesis. Various protein kinase inhibitors, phosphatase inhibitors and NEDD8 enzyme inhibitor has been used. The inhibitors were either synthesized in house by Dr. Natalia Shpiro (DSTT, University of Dundee) or were purchased from commercial sources.

Table 2.5 : Details of the various small molecule inhibitors used in this work

Compound	Inhibits	Structure	Mol. wt (g/mol)	Publication
401 KuDOS	DNA-PK	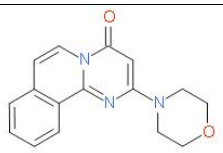	281.31	(Griffin et al., 2005)
AZD8055	mTOR	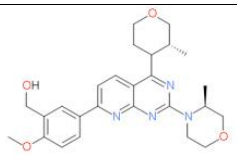	465.5	(Chresta et al., 2010)
BI 2536	PLK1	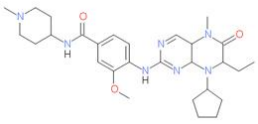	521.65	(Steegmaier et al., 2007)
BIO	GSK3/IKK	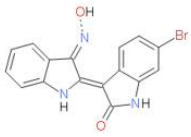	356.2	(Tseng et al., 2006)
BIRB-0796	p38 MAPK	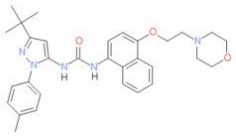	527.66	(Regan et al., 2002)
BX-795	PDK1/TBK1/IKKε	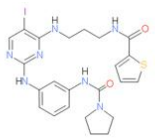	591.47	(Feldman et al., 2005, Clark et al., 2009)
CCT250863	NEK2	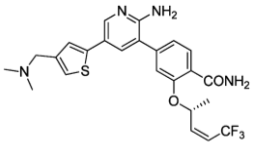	490.17	(Innocenti et al., 2012)
CHIR 99021	GSK3	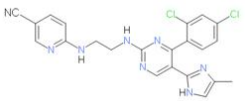	465.34	(Ring et al., 2003)
D4476	CK1	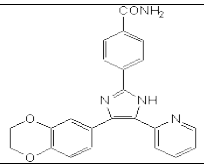	398.4	(Rena et al., 2004)
ETP 46464	ATR	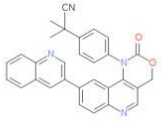	470.52	(Toledo et al., 2011)
GDC-0941	PI3K	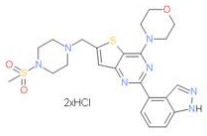	586.57	(Folkes et al., 2008)

H-1152	ROCK	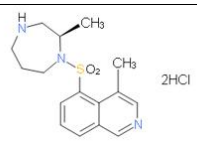	392.3	(Sasaki et al., 2002)
KU 55933	ATM	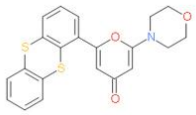	395.49	(Hickson et al., 2004)
MK-2206	PKB	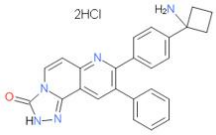	480.39	(Li et al., 2009)
MLN4924	NEDD8 enzymes	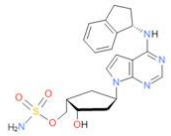	479.98	(Soucy et al., 2009a)
RO 3306	CDK1	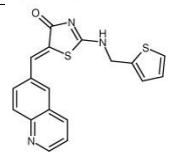	351.5	(Vassilev, 2006)
VX-680	Aurora	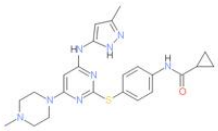	464.59	(Harrington et al., 2004)
Calyculin A	PP1 & PP2	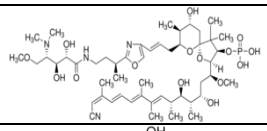	1009.18	(Ishihara et al., 1989)
Okadaic acid	PP1 & PP2	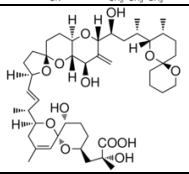	805	(Ishihara et al., 1989)

2.2 Methods

2.2.1 Transformation and plasmid purification from *E.coli*

Competent *E.coli* DH5α and BL21 DE3 cells were provided by Dr. Maria Deak or Dr. Mark Peggie using a previously described method (Inoue et al., 1990). For each transformation, approximately 5-20ng DNA was added to 30µl of competent cells and incubated on ice for 5min. Cells were then directly spread onto LB agar plates containing 100 µg/ml ampicillin and incubated at 37°C overnight. The transformed DH5α *E.coli* colonies were transferred from the plate and cultured in 200ml LB containing 200 µg/ml ampicillin at 30-37°C while shaking at 200rpm for 16-24 hours. Cells were pelleted by centrifugation at 6000g for 15min at 4^{o}C. Plasmid DNA was purified using the Qiagen plasmid Maxi kit according to the manufacturer's instructions. DNA concentration was measured using NanoDrop as per manufacturer's instructions.

2.2.2 Agarose gel electrophoresis

1.7 g of agarose was boiled in 170 ml of 1X TAE buffer. 10 µl of 10 mg/ml ethidium bromide were added after the boiled agarose solution cooled down to approximately 50-60°C and then poured into a the gel casting tray. The gel was allowed to solidify and electrophoresis was carried out at 100V for 45min.

2.2.3 Site-directed mutagenesis and DNA sequencing

Site-directed mutagenesis was performed by Dr. Maria Deak or Mr. Thomas Macartney using QuikChange kit (Stratagene) and KOD polymerase (Novagen). Mutations were verified by DNA sequencing. The sequencing was performed by DNA sequencing service (School of

Life Sciences, University of Dundee) using DYEnamic ET terminator chemistry kit (Amersham Biosciences) on Applied Biosystems sequencers.

2.2.4 Purification of recombinant bacterially expressed proteins

Protein purification from bacteria were either done using the standard LB-IPTG method or by using auto-induction media (Studier, 2005). For standard LB-IPTG method, pGEX6P-MYPT1, pGEX6P-MYPT2, pGEX6P-MLC2, pGEX6P-MBS85, pGEX6P-MYPT3 or pGEX6P-TIMAP constructs were transformed into *E.coli* BL21 DE3. 50 ml of LB containing 100 μg/ml ampicillin was inoculated with a single colony of transformed cells and grown overnight at 37°C. 50 ml of this culture was used to inoculate 500 mL of the same medium. The cells were grown at 37°C in a shaking incubator (200 rpm) until OD_{600} of 0.6-0.7. The temperature was reduced to 16ºC and protein expression was induced by the addition of isopropyl β-D-1-thiogalactopyranoside (IPTG) to 250 μM final concentration. For the polycistronic pOPH-MYPT1-HIS-PP1β, pOPH-MYPT1-HIS-PP1β (Ser445Ala+Ser472Ala+Ser910Ala), pOPH-MYPT2-HIS-PP1β and pOPH-MYPT2-HIS-PP1β (Ser447Ala+Ser473Ala+Ser525Ala) vectors, 250 ml of LB containing 100 μg/ml ampicillin was inoculated with five single colonies of transformed cells and grown overnight at 37°C. 250 ml of this culture was used to inoculate 2 L of autoinduction media containing 200 μg/ml ampicillin and incubated at 16°C for 48-72 hrs. After the incubation in a shaking incubator (200 rpm), cultures were spun for 30 min at 6000g at 4°C. The pellet was resuspended in 25 ml of GST bacterial lysis buffer and was sonicated 4 times for 10 sec with 10 sec breaks at maximum power with a 0.6 cm diameter sonication probe. During the sonication the lysate was maintained on ice. Subsequently, the lysate was clarified by centrifugation for 15 min at 26,000 g at 4°C. The clarified lysate was incubated with 0.5 ml of glutathione-Sepharose (equilibrated in GST bacterial lysis buffer) per 1 L of cultured cells

and the suspension was incubated for 2 h at 4°C with gentle agitation. The beads were washed three times with GST bacterial lysis buffer containing 0.5 M NaCl and twice in Buffer A. For elution of GST-fusion proteins, 25 mM (final concentration) of glutathione in GST bacterial lysis buffer pH 7.5 was added to the slurry of beads and incubated for 10 min at room temperature. Elution by enzymatic cleavage of the GST-tag from the protein was performed where appropriate using PreScission protease (purified at DSTT, University of Dundee). This protease cleaves the protein sequence LGVLFQGP between Q and G at the C-terminal to the GST moiety of the protein expressed using the pGEX6P or pOPH vectors. The cleavage reaction was performed at 4°C overnight with 60 μg of GST-PreScission protease per 1ml of 1:1 slurry under gentle agitation. The PreScission protease has non-cleavable GST tag so it remained bound to the beads. The slurry was transferred on Spin-X column and spun for 1 min at 2,000 g. The flow through containing the eluted protein was collected, aliquoted and stored at -80ºC.

2.2.5 Cell culture

HEK293, HEK293T, HEK293 FLP/IN TREX, U2OS, U2OS FLP/IN, MCF7, MDA-MB-231, MDA-MB-468, HCT116, TET21N, SHSY5Y and T47D cells were grown in Dulbecco's modified eagle medium (DMEM) supplemented with 10% (v/v) foetal bovine serum (FBS), 2mM L-glutamine, antibiotic/antimycotic, 1X non-essential amino acids and 1mM sodium pyruvate. Immortalised mammalian epithelial cells (IMEC) were cultured in DMEM/F12 50:50 media (Sigma) with 2mM L-glutamine, antibiotic/antimycotic, 5 mg/ml insulin, 10 ng/ml EGF and 0.5 mg/ml hydrocortisone. Procedures were done under aseptic conditions meeting biological safety category 2 regulations. Cells were grown at 37°C in a 5% CO_2 water-saturated incubator. For the passaging, adherent cells were washed once with PBS and then incubated with Trypsin/EDTA for 3-5 min at room temperature or at 37°C. For

suspension cells, the cells were centrifuged at 1200g for 3 mins, supernatant was removed, resuspended in fresh media and seeded into fresh T75 flask at 1:4 dilution.

2.2.6 Freeze/thawing of cell lines

Cells in a T75 flask were trypsinised (for adherent culture) and centrifuged at 1000g for 5min at room temperature. The supernatant was aspirated and cells were resuspended in 4ml of FBS containing 10% DMSO. 1ml aliquots were stored in cryovials in a polystyrene rack at -80°C or in liquid nitrogen for long-term storage. Cells were thawed in a water bath at 37°C for 1min and placed into a T75 flask containing 20ml of media.

2.2.7 Transient transfection of cells using polyethylenimine PEI

Cells were transiently transfected using the polyethylenimine (PEI) method (Durocher et al., 2002). PEI stock (1mg/ml) was prepared by dissolving it in 20mM Hepes (pH 7.4) and filter-sterilizing using 0.22um filter. 1ml aliquots were stored at -20°C. Cells were seeded from one T75 flask into 6-8 10cm dishes or into 3-4 15cm dishes 16-24hrs prior to transfection. Transfection mix was prepared as follows: per plate, to 1ml of serum-free DMEM, 5-10 ug of plasmid DNA and 20ul 1mg/ml PEI was added and the mix was immediately vortexed. After incubation for 20min at room temperature, the transfection mix was delivered dropwise onto the cells. Cells were harvested after 48hrs of transfection.

2.2.8 Stable transfections

Cell lines with the stable inducible overexpression of NUAK1wild-type and mutants were generated using Flp-In T-Rex System (Invitrogen) following manufacturer's instructions.

This system allows for either constitutive overexpression of the protein in U2OS FLP/IN cells or tetracycline-inducible expression of the protein of interest in HEK293 FLP/IN TREX cells using the pcDNA5/FRT/TO vector encoding the gene of interest.

Retroviral vectors like pRetroSuperior or pBABE carrying the gene of interest were also used to transfect NUAK1$^{-/-}$ mouse embryonic fibroblasts. 1 μg of retroviral pBABE-puro constructs encoding wild-type or mutants of NUAK1 were co-expressed with CMV-VSVG (0.3 μg) and CMV-Gag/Pol (1 μg) constructs in HEK-293T cells. The culture media containing retroviruses were collected 48 hrs post-transfection and filtered through 0.22 μm filters directly onto the target cells. NUAK1$^{-/-}$ MEFs, plated at ~70% confluency, were infected by transferring the filtered retroviruses directly onto the cells and 10 μg/ml polybrene a cationic polymer was added to aid infection. 24 h post-infection, cells were cultured in the presence of 3 μg/ml puromycin for selection of infected cells.

2.2.9 Generation of stable shRNA knockdown using lentiviral delivery

The MISSION™ shRNA system (Sigma-Aldrich) was used to generate cell lines stable expressing shRNA against NUAK1 or MYPT1 or PLK1. To generate lentiviral particles, HEK293T cells grown on 10-cm dishes were transfected with a plasmid mix containing 3 μg of the shRNA-encoding plasmid pLK0.1, 3 μg of pCMV delta R8.2 (packaging plasmid) and 3 μg of pCMV-VSV-G (envelope plasmid) using the PEI method. 48 hrs post-transfection, the virus-containing medium was collected and filtered through a 0.22-mm filter. Target cells were plated on a 6-well plate 24 h before the viral infection. Cells were then infected with 2 ml per well of virus-containing medium supplemented with 10 μg/ml polybrene. 48 hrs post

infection the virus-containing medium was replaced with normal DMEM medium supplemented with 2-3 µg/ml puromycin. Selected cells were cultured in the presence of 2 µg/ml puromycin or in normal DMEM media.

2.2.10 Inhibitor treatment followed by cell detachment

Inhibitors (final concentrations 10 µM) were dissolved in DMSO and an equivalent volume of DMSO was used as a control. The final concentration of DMSO in the culture medium was never more than 0.1% (v/v). Following inhibitor treatment, to induce cell detachment, the culture media was aspirated and replaced with EDTA-PBS based cell dissociation buffer (GIBCO) supplemented with or without inhibitor and cells were incubated at 37°C in a 5% CO_2 for 15 min. Detached cells were collected by gentle centrifugation for 3 min at 70 g at room temperature and lysed immediately.

2.2.11 Cell lysis

Cells were placed on ice, media was aspirated and lysed using 0.4ml of Lysis Buffer for 10cm dishes or 1 ml for 15 cm dishes using plastic scrappers. Lysates were clarified by centrifugation at 16,000-18,000xg for 15min at 4°C and the supernatants were used for experiments. For SDS lysis, cells were rapidly lysed on ice and sonicated before resolving in SDS-PAGE.

2.2.12 Protein concentration estimation using Bradford assay

Bradford method was employed to estimate the protein concentration of lysates (Bradford, 1976). The assay employs the fact that in an acidic medium Coomassie Brilliant Blue binds to proteins and shifts the absorption maxima from 465nm to 595nm. A standard curve was generated using BSA standards (1, 0.5, 0.25, 0.125, 0.06 mg/ml). 200 µl of Bradford reagent was used per sample and OD_{595} was measured using a 96-well plate reader. Samples were

read in triplicates and concentrations were estimated using the OD_{595} values from the standard curve.

2.2.13 Purification of GST fusion proteins from HEK293 cells

HEK293 cells were transfected GST-tagged constructs by PEI method and harvested 48hrs post-transfection Lysis Buffer. Clarified cell lysates were incubated for 1 hour on a rotating platform with glutathione-Sepharose 4B (20 µl beads/5 mg of cell lysate) previously equilibrated in PBS. The beads were washed three times with Lysis Buffer containing 0.5 M NaCl and two times with Buffer A. GST-tagged proteins were eluted from the resin with an equal volume of Buffer A supplemented with 150 mM NaCl, 0.27M sucrose and 40mM glutathione (pH 7.5-8) for 10min at room temperature on a rotating platform. The elution was repeated and all the elusions were pooled together, filtered through a 0.22um Spin-X column aliquoted, snap-frozen in liquid nitrogen and stored at -80°C.

2.2.14 Non covalent coupling of antibodies

Protein G Sepharose was washed twice in PBS and the antibody was added to the beads at a concentration of 1 µg antibody per 1 µl of protein G-Sepharose. The antibody-beads slurry was incubated on a shaking platform for at least 30 min at 4°C. The beads were then centrifuged and washed three times in PBS to remove any uncoupled antibody, resuspended in PBS with 0.02% (w/v) sodium azide and stored at 4ºC for up to one month.

2.2.15 Covalent coupling of antibodies

Antibodies were covalently coupled to protein G-Sepharose with a dimethyl pimelimidate (DMP) cross-linking procedure (Harlow and Lane, 1999). DMP is a homobifunctional cross-linker that reacts with primary amine groups (Harlow and Lane, 1999). After the non-

covalent coupling step in 2.2.14, the beads were washed 3 times with 0.1 M sodium borate pH 9 and then resuspended in 0.1 M sodium borate pH 9 containing 20 mM freshly added DMP and incubated for 30 min at room temperature with gentle mixing. The 0.1 M sodium borate with DMP step was repeated. The beads were then washed 4 times with 50 mM glycine pH 2.5 to remove all the antibodies that were non covalently coupled to the beads. The were further washed twice with 0.2 M Tris-HCl pH 8 to neutralise the pH and then incubated in this buffer for a further 2 h at room temp with gentle mixing to ensure that any residual DMP was quenched by reaction with the amine group of Tris. The antibody-coupled beads were stored in PBS containing 0.02% (w/v) sodium azide at 4ºC for up to one month.

2.2.16 Immunoprecipitation

For endogenous protein immunoprecipitation, 1 mg of cell lysate was incubated with 5 µg of antibody coupled to 5 µl of protein G-Sepharose for 2-16 hrs at 4°C on a rotating wheel. For overexpressed protein immunoprecipitation, depending on the tag of the protein, 5 µl of FLAG-agarose or HA-agarose or GST-sepharose beads was incubated with 200 µg of cell lysate for 2-4 hrs at 4°C on a rotating wheel. The mixture was centrifuged for 1 min at 8,000 g and the supernatant was removed. The immunoprecipitates were washed twice with 0.5 ml of Lysis Buffer containing 0.15 M NaCl and twice with 0.5 ml of Buffer A. Then either they were used for further assays or 1xLDS buffer was added and subjected to SDS-PAGE.

2.2.17 Sodium Dodecyl Sulphate Polyacrylamide Gel Electrophoresis (SDS-PAGE)

SDS-PAGE allows the resolution of proteins based on their electrophoretic mobility which is a function of their molecular weight. The anionic detergent, sodium dodecyl sulphate (SDS) or lithium dodecyl sulphate (LDS) binds to protein in a constant ratio of about one SDS/LDS molecule per 2 amino acids, thus providing a net negative charge which is proportional to the

mass of that protein. Mobilities of these proteins along the matrix become a linear function of the logarithms of their molecular weights. Resolving gel consisted of 375 mM Tris-HCl pH 8.6, 0.1% SDS and 8-15% acrylamide. N,N,N',N'-tetramethylethylenediamine (TEMED) and ammonium persulphate (APS) were added to initiate polymerisation. The gels were allowed to polymerise for 30-60 min under a layer of isopropanol. Stacking gel contained 125 mM Tris-HCl pH 6.8, 0.1% SDS, 4% acrylamide, TEMED and APS. Purified proteins, cell lysates or immunoprecipitates were resuspended in 1x SDS Sample Buffer containing 1% β-mercaptoethanol and boiled at 90ºC for 5 min. 10-20 µl sample was loaded into each well and electrophoresis was performed in 1x SDS electrophoresis buffer at 90 V for 15 min and then at 180 V for the next 60 min.

2.2.18 Commassie staining of gel

Gels were stained in Instant-Blue (Expedeon, UK) for 15min and then destained in milliQ water until the band staining to background contrast was satisfactory.

2.2.19 Gel drying and autoradiography

Post 2.2.18, gels were incubated in 5% glycerol for 10min and sandwiched between two sheets of pre-wet cellophane avoiding air-bubbles. The gel was then dried in a GelAir Dryer for 1.5hrs. Dried gels were exposed to Hyperfilm MP for 1-24hrs in an X-Omat autoradiography cassette. The cassette was stored in -80°C freezer to improve the signal. Films were developed using a Konica auto-developer.

2.2.20 Transfer of proteins onto nitrocellulose membrane and immunoblotting

After the completion of SDS-PAGE, gels were sandwiched between pre-wet (in Western Blotting Transfer Buffer) nylon sponge pads, Whatman 3mm filter papers and nitrocellulose membrane. The sandwich was loaded into BioRad Trans-Blot Cell transfer tanks and transfer was carried out at 90V for 1.5hrs or at 0.75A for 1hr. After transfer, non-specific binding of antibodies on the nitrocellulose membranes was prevented by "blocking" the membranes with 5% (w/v) skimmed milk in TBST for 15-30 mins at room temperature. Primary antibodies were then diluted to working concentrations in either milk or BSA-TBST solutions and incubated with the membrane at either room temperature for 1 hr (for most HRP conjugated antibodies) or for 4°C overnight. Primary antibodies were collected and frozen at -20^{o}C for future reuse. Membranes were then processed using the BioRad western processor. The processor program was set to three times wash with TBST followed by 1 hr HRP-conjugated secondary antibody incubation and finally a further four times wash with TBST. Membranes were incubated with the enhanced chemiluminescence (ECL) substrate and exposed to X-ray films. Films were developed using a Konica automatic developer.

2.2.21 Kinase assay

2.2.21.1 *In vitro* kinase assays employing a peptide substrate

In vitro NUAK1 wild-type and mutants' activities were measured using Cerenkov counting of incorporation of radioactive ^{32}P from [γ^{32}P]-labelled ATP into Sakamototide substrate peptide [ALNRTSSDSALHRRR]. A typical 50 µl kinase reaction consisted of 10mM magnesium acetate, 0.1mM [γ^{32}P] ATP (450-500 cpm/pmol), 0.1% β-mercaptoethanol, 200 µM of Sakamototide. Control reactions contained either no kinase or IPs with GFP control antibody. Reactions were

incubated at 30°C for 30min and were eventually terminated by pipetting 40 µl onto a 2 square cm of P81 paper (which binds substrates that contain a net basic charge at acidic pH) which was dropped to a beaker containing 50 mM orthophosphoric acid. Papers were washed four times in 50mM orthophosphoric acid to remove any unbound radioactivity. Papers were then washed in acetone for 3min and air dried. Papers were folded and transferred to 1.5ml tubes and Cerenkov counting was done on a liquid scintillation counter. Kinase activity was expressed as specific activity (units of activity per mg of protein or lysate used for IP of the protein). One unit of activity was the amount of kinase which was needed to incorporate 1 µmol of phosphate per 1 µmol of substrate peptide per minute.

2.2.21.2 *In vitro* kinase inhibitor biochemical IC_{50} determination

IC_{50} value of an inhibitor is defined as the concentration of inhibitor required for 50% inhibition of enzyme activity. To determine the IC_{50} values of NUAK inhibitors, active GST-NUAK1, GST-NUAK1[A195T] and GST-NUAK2 enzymes were purified from HEK293 cell as described in 2.2.13. 96 well plates were used to carry out peptide kinase assays, each reaction performed in triplicate. Each reaction was set up in a total volume of 50 µL containing 100 ng NUAK1(wild-type or A195T mutant) or NUAK2 in 50 mM Tris/HCl, pH 7.5, 0.1 mM EGTA, 10 mM magnesium acetate, 200 µM Sakamototide, 0.1 µM [γ-32P]ATP (450-500 cpm/pmol) and various concentrations of inhibitors (from 0.1 nM to 100 µM) dissolved in DMSO. After incubation for 30 min at 30 °C, reactions were terminated by adding 25 mM (final) EDTA to chelate the magnesium. 40 µl of the reaction mix was spotted onto P81 paper and immersed in 50 mM orthophosphoric acid. Samples were washed three times in 50 mM orthophosphoric acid, then a single acetone rinse followed by air

drying. The kinase mediated incorporation of [γ-32P]ATP into Sakamototide was quantified by Cerenkov counting. The values were expressed as % of the DMSO control. IC_{50} curves were developed and IC_{50} values were calculated using GraphPad Prism software using non-linear regression analysis. IC_{50} determination for Aurora kinases were carried out at The International Centre for Protein Kinase Profiling (http://www.kinase-screen.mrc.ac.uk/) using 300 μM substrate peptide [LRRLSLGLRRLSLGLRRLSLGLRRLSLG].

2.2.21.3 *In vitro* kinase assays employing a protein substrate

The quantification of the protein substrate phosphorylation was achieved by measuring the incorporation of radioactive ^{32}P phosphate from [γ-32P]ATP into a protein substrate. The kinases used were HIS-NUAK1 and HIS-ROCK2 (both kinases were purified from insect cells as described previously (Biondi et al., 2002) in the DSTT, University of Dundee). For each reaction, HIS-NUAK1 was used at 100-200 ng and HIS-ROCK2 was used at 0.5-1 μg. The substrates were used at a 5 μg per reaction. Assays were set up in a total volume of 25 μl of Buffer A containing the protein kinase, protein substrate, 10 mM magnesium acetate and 0.1 mM [γ-32P]ATP (450-500 cpm/pmol). Reactions were performed at 30ºC in a Thermomixer at 1000 rpm for indicated times, and terminated by the addition of SDS/LDS Sample Buffer. The incorporation of the phosphate into proteins was determined following SDS-PAGE (see 2.2.17), Coomassie staining (see 2.2.18), destaining and autoradiography of the dried gels (see 2.2.19). If required, the proteins bands of interest were then excised, transferred to microcentrifuge tubes and ^{32}P incorporation was quantified by Cerenkov counting in a scintillation counter. One unit of protein kinase activity is the

amount of enzyme that catalyses the incorporation of 1 nmole phosphate into the substrate in 1 min.

2.2.22 Phosphatase assay

The phosphatase activity of MYPT1-HIS-PP1β (wild-type and mutant) and MYPT2-HIS-PP1β (wild-type and mutant) were carried out using radiolabelled myosin light chain 2 (MLC2) as substrate.

2.2.22.1 Preparation of radiolabelled MLC2 substrate

GST-MLC2 was purified from E.coli BL21 DE3 cells as mentioned in section 2.2.4. Since myosin phosphatases dephosphorylate MLC2 at Thr 18 and Ser19 sites, active HIS-ROCK2 was employed to label the Ser19 site of MLC2 (Totsukawa et al., 2000). 2 mg of purified GST-MLC2 was incubated with 20 µg of active ROCK2 for 3 hrs at 30ºC in the presence of 10 mM magnesium acetate and 0.1 mM [γ-32P]ATP (450-500 cpm/pmol). Glutathione sepharose was added to the reaction mix to re-purify GST-MLC2 and incubated for 30 min at 4 °C. The slurry was loaded onto a column and extensively washed with Buffer A till any unbound residual [γ-32P]ATP was washed away from the slurry. The ^{32}P-labeled GST-MLC2 was eluted using GST elution buffer.

2.2.22.2 Phosphatase assay using MYPT-PP1β complexes

2 µg of each of the recombinant MYPT-PP1β complexes (wild-type and triple serine mutants as in section 2.2.4) was phosphorylated with or without 0.1 µg of active HIS-

NUAK1 for 30 mins at 30ºC in the presence of 3 µg recombinant 14-3-3ε, 10 mM magnesium acetate and 0.1 mM (cold) ATP. Samples were diluted 100 to 500 times in buffer A containing 1 mM $MnCl_2$ and 3 mg/ml BSA. 10 µl of the diluted reaction mix was incubated at 30ºC for 10 min with the previously purified ^{32}P-labeled GST-MLC2 (10 µM final in 30 µl reaction volume). Reactions were stopped by the precipitation of proteins with 100 µl of 20% trichloroacetic acid. Samples were vortexed briefly, and the precipitate was pelleted by centrifugation 14,000g for 10 mins. ^{32}P radioactivity in the supernatants and pellets was measured by Cerenkov counting, and the release of phosphate to the supernatant was calculated.

2.2.23 Mass spectrometry

2.2.23.1 Processing of samples for mass spectrometric analysis

Mass spectrometry samples were processed and handled under a laminar flow hood to minimise keratin contaminations. Samples were prepared in 1xLDS Sample Buffer, reduced by boiling with 1x NuPAGE sample reducing agent, boiled, alkylated with 50 mM iodoacetamide (incubated in dark for 30mins at room temperature) and subjected to electrophoresis on a NuPAGE Bis-Tris 4-12% gel. Gels were stained and destained using Instant Blue. Gel pieces were cut into small cubes of about 1 mm and sequentially washed on a Vibrax shaking platform with 50% acetonitrile/water, 0.1 M NH_4HCO_3 and 50% acenotrile/50 mM NH_4HCO_3. All washes were performed for 10 min using 0.5 ml per gel band and all liquids were removed between washes. Once colourless, the gel pieces were shrunk with 0.3 ml acetonitrile for 15 min, aspirated and gel pieces were dried in a Speed-Vac. Gel pieces were next swollen in 5 µg/ml

AspN or 25mM Triethylammonium bicarbonate with 5 µg/ml of Trypsin and incubated overnight at 30ºC on shaker. After incubation, an equivalent volume of acetonitrile was added to the digest and incubated for a further 15 min. The supernatants were transferred to a clean tube and samples were dried in a SpeedVac. To further extract the peptides, 100ul of 50% acetonitrile / 2.5% formic acid were added to the gel pieces and incubated for 15min at room temperature on a shaking platform. The supernatant was combined with the first dried peptide extract and dried using Speed-Vac. The samples were submitted for mass spectrometry immediately or stored at -20ºC.

LC-MS was performed by Dr. D. Campbell, Mr. R. Gourlay and Mr. J. Varghese. Tryptic peptides were subjected to LC-MS/MS on a Dionex3000 Nano liquid chromatography system coupled with an LTQ-Orbitrap mass spectrometer (for peptide mass fingerprinting) or 4000 QTrap (to identify phosphorylation sites). Extracted Ion Chromatograms (XIC) were obtained manually using the ABSciex Analyst software (Applied Biosystems). Results were searched against the SwissProt or IPI human or mouse databases using the Mascot Daemon (www.matrixscience.com). Peptide mass fingerprinting data analysis was performed using OLMAT (http://www.proteinguru.com/MassSpec/OLMAT).

2.2.23.2 Mapping of phosphosites using HPLC and Edman degradation

Substrate (5 µg) purified from *E. coli* was incubated with active kinase, for 30 min at 30°C in Buffer A containing 10 mM magnesium acetate and 0.1 mM [γ-32P]ATP (11,000-25,000 cpm/pmol) in a total reaction volume of 25 µl. The reaction was terminated by addition of LDS sample buffer with 1x NuPAGE sample reducing

agent, boiled, alkylated (as in section 2.2.23.1) and samples were subjected to electrophoresis, stained, bands were excised and processed for mass spectrometry as in 2.2.23.1. Following digestion, >95% of the ^{32}P radioactivity incorporated in the gel bands was recovered and samples were then subjected to HPLC on a Vydac C_{18} column equilibrated in 0.1% (w/v) trifluoroacetic acid (TFA), with a linear acetonitrile gradient at a flow rate of 0.2 ml/minute. Fractions of 0.1 ml were collected and phosphopeptides were analysed by LC-MS/MS. The resultant data files were searched using Mascot (www.matrixscience.com) run on an in-house system allowing for Phospho (S/T), Phospho (Y), Oxidation (M) and Dioxidation (M) as variable modifications. Individual MS/MS spectra were inspected using Xcalibur 2.2 software. The site of phosphorylation of all the ^{32}P labelled peptides was determined by solid-phase Edman degradation on an Applied Biosystems 494C sequencer of the peptide coupled to Sequelon-AA membrane (Applied Biosystems) as described previously(Campbell and Morrice, 2002). HPLC, LC-MS and Edman degradation was performed by Mr. Robert Gourlay.

2.2.24 Immunofluorescence

Cells were grown on glass coverslips, washed twice with PBS, fixed in 4% paraformaldehyde in PBS at room temperature for 15min, rinsed twice with PBS and permeabilized with 1% NP-40 in PBS for 5-10min. Cells were then "blocked" by incubation with 1% donkey serum in PBS for 20-30min at room temperature. The primary antibodies were diluted to as par user guidelines in 1% BSA in PBS and incubated at either 1 hr at 37^{o}C. Cells were washed thrice with 1% BSA in PBS for 10min at room temperature. Secondary antibodies (raised in donkey) were diluted to 1:500 in 1% BSA in PBS and incubated at room temperature for 1hr.

Cells were washed thrice with 1% BSA in PBS for 10min at room temperature. The slides were rinsed in distilled water, the excess water was drained on a tissue paper and the slides were immediately mounted using ProLong Gold. Slides were allowed to dry for 2-3hrs.

2.2.25 Cell cycle synchronisation

For G1-arrest, cells at ~50% confluency were treated with 2.5mM of thymidine for 16hrs, followed by 3x rinse with PBS, fresh media was added and cells were released for 12hrs, followed by a second thymidine block for 16hrs and final 3x PBS rinse and release after which cells were harvested for western blotting and flow cytometry analysis every 2hrs. For G2/M arrest, the above procedure was performed and cells were released into 10 µM RO-3306 for 20hrs, after which cells were rinsed 4x with PBS, fresh media was added and harvested every 2 hrs.

2.2.26 Flow cytometry

2.2.26.1 Flow cytometric analysis for cell cycle distribution

Cells were trypsinized and the trypsin was quenched using the old medium the cells were present, in order to account for floating dead cells. Cells were then washed once with room temperature PBS (spin: 350xg, 5min) and fixed in 1ml of ice-cold 70% ethanol. After washing twice with PBS, cells were rinsed with 1% FBS in PBS and DNA staining was done using FACS Staining Solution (50 µg/ml propidium iodide, 50 µg/ml RNAse A in 1% FBS in PBS) for 20min in the dark. Cells were analyzed by

Ms Arlene Whigham using FACS Canto (BD Biosciences) or FACS Verse (BD Biosciences).

2.2.26.2 Flow cytometric analysis for active Caspase 3 apoptotic cells

Cells were trypsinized and the trypsin was quenched using the old medium the cells were present, in order to account for floating dead cells. Cells were then washed once with room temperature PBS with 1% FBS (spin: 350xg, 5min) and fixed in 0.5ml 1% (w/v) PFA. The cells were incubated at 37°C for 15min and subsequently washed once in PBS-FBS. Cells were then further fixed in 1ml of ice-cold 70% ethanol. After washing once with 1% FBS in PBS, 20µl FITC-Caspase 3 antibody stock solution was added to 100µl PBS-FBS per sample and add to pelleted cells. The cells were incubated in the dark at room temperature for 30mins. Cells were washed once in PBS-FBS and then 300µl PBS-FBS was added containing 10 µg/ml DAPI. Active Caspase 3 in the cells was analysed by Dr. Rosemary Clarke using FACS Verse (BD Biosciences).

2.2.27 Wound healing assays

U2OS or MEF cells were split and approximately equal number of cells were loaded into the left and right chambers of the IBIDI Self-insertion inserts (IBIDI 80209). Each insert was placed in one well of a 12 well plate and the cells were seeded with or without the treatment of the inhibitors. For the comparison between the NUAK1$^{+/+}$ and NUAK1$^{-/-}$ MEFs, a single insert was used and the NUAK1$^{-/-}$ cells were loaded on the right and NUAK1$^{+/+}$ cells on the left chamber of the insert. For proper quantification of migration, wound-healing assay on NUAK1$^{+/+}$ and NUAK1$^{-/-}$ MEFs were also carried out on separate inserts to avoid any

chemotactic stimulation between two different cell lines. The experiments were done in triplicates. After overnight incubation at 37 °C and 5% CO_2, the insert was removed and the migration of cells into the 500 µm gap between the chambers were observed. The wound-gap healing properties of the cells were observed over a period of 20 hours under a Nikon Eclipse Ti microscope with photography taken every 2 mins by a Photometrics cascade II CCD camera. The first 225 frames of the sequence were imported into Volocity software (Perkin Elmer). This software was used to generate the quantitative kymograph with time as the horizontal parameter and 1 pixel was collected per time point along a line from the edge of the field to the centre of the wound. To compare between videos, the length of the line was kept constant.

2.2.28 MTS cell proliferation assay

Cell proliferation assays were carried out colorimetrically in 96 well plates using the CellTiter 96® AQ_{ueous} Non-Radioactive Cell Proliferation Assay kit (Promega) following the manufacturer's instructions. The solution consists of MTS (3-(4,5-dimethylthiazol-2-yl)-5-(3-carboxymethoxyphenyl)-2-(4-sulphophenyl)-2H-tetrazolium, inner salt) and an electron coupling reagent PMS (phenazine methosulphate). The dehydrogenase enzymes in metabolically active cells reduce MTS reagent into a coloured formazan product that is soluble in the cell culture media. The absorbance of the formazan can be measured at OD_{490} and is directly proportional to the number of live cells in culture.

2.2.29 Cell Invasion assay

The ability of cells to invade with or without the presence of inhibitors was tested in a growth-factor-reduced Matrigel™ invasion chambers according to manufacturer's instructions and as previously described (Sommer et al., 2013). The cells were serum-

deprived for 2 hours with or without the presence of 10 μM inhibitor, detached with cell dissociation buffer and 5 x 10^5 cells suspended in DMEM containing 1% (w/v) BSA were added to the upper chambers in triplicates and chemoattractant (DMEM containing 10% (v/v) FBS) to the lower wells. The chambers were kept at 37°C in 5% CO_2 for 18 hours. Cells that did not invade were removed from the upper face of the filters and cells that had migrated to the lower face of the filters were fixed and stained with Reastain Quick-Diff kit (Reagena) according to manufacturer's instructions and images (×10) were captured.

2.2.30 Kinase inhibitor specificity profiling on a panel of 120-140 protein kinases

Kinase inhibitor specificity profiling assays were carried out at The International Centre for Protein Kinase Profiling (http://www.kinase-screen.mrc.ac.uk/) against the panel of 140 protein kinases as described previously (Bain et al., 2007, Najafov et al., 2011). Results were presented as a percentage of kinase activity in DMSO control reactions. Protein kinases were assayed *in vitro* with 1 μM of the inhibitors and the results were presented as an average of triplicate reactions ± S.D or in the form of comparative bar charts. Kinase abbreviations are as follows: ABL, Abelson tyrosine-protein kinase 1; AMPK, AMP-activated protein kinase; ASK, apoptosis signal-regulating kinase; BRK, breast tumor kinase; BRSK, brain-specific kinase; BTK, Bruton's tyrosine kinase; CaMK, calmodulin-dependent kinase; CaMKK, CaMK kinase; CDK, cyclin-dependent kinase; CHK, checkpoint kinase; CK, casein kinase; CLK, CDC-like kinase; CSK, C-terminal Src kinase; DAPK, death-associated protein kinase; DDR, discoidin domain receptor; DYRK, dual-specificity tyrosine-phosphorylated and regulated kinase; EF2K, elongation-factor-2 kinase; EIF2AK, eukaryotic translation initiation factor 2-alpha kinase*;* EPH, ephrin; ERK, extracellular signal-regulated kinase; FGF-R, fibroblast growth factor receptor; GCK, germinal centre kinase; GSK, glycogen synthase kinase; HER, human epidermal growth factor receptor; HIPK, homeodomain-interacting

protein kinase; IGF1R, IGF1 receptor; IKK, inhibitory κB kinase; IR, insulin receptor; IRAK, Interleukin-1 Receptor-Associated Kinase; IRR, insulin-related receptor; JAK, Janus kinase; JNK, c-Jun N-terminal kinase; Lck, lymphocyte cell-specific protein tyrosine kinase; LKB1, liver kinase B1; MAPK, Mitogen-activated protein kinase; MAPKAP-K, MAPK-activated protein kinase; MARK, microtubule-affinity-regulating kinase; MEKK, MAP kinase kinase kinase; MELK, maternal embryonic leucine-zipper kinase; MINK, Misshapen/NIK-related kinase; MKK, MAPK kinase; MLK, mixed lineage kinase; MNK, MAPK-integrating protein kinase; MPSK, myristoylated and palmitoylated serine/threonine-protein kinase; MSK, mitogen- and stress-activated protein kinase; MST, mammalian homologue Ste20-like kinase; NEK, NIMA (never in mitosis in Aspergillus nidulans)-related kinase; NUAK, novel (NUA) family SnF1-like Kinase; OSR, oxidative stress-responsive kinase; PAK, p21-activated protein kinase; PDGFRA, platelet-derived growth factor receptor-α; PDK, Phosphoinositide-dependent kinase; PHK, phosphorylase kinase; PIM, provirus integration site for Moloney murine leukaemia virus; PINK, PTEN-induced kinase; PKA, cAMP dependent protein kinase; PKB, Protein kinase B; PKC, Protein kinase C; PKD, protein kinase D; PLK, polo-like kinase; PRAK, p38-regulated activated kinase; PRK, protein kinase C-related kinase; RIPK, receptor-interacting protein kinase; ROCK, Rho-dependent protein kinase; RSK, Ribosomal S6 kinase; S6K, p70 ribosomal S6 kinase; SGK, serum- and glucocorticoid-induced protein kinase; SIK, salt-induced kinase; smMLCK, smooth muscle myosin light-chain kinase; SRPK, serine arginine protein kinase; STK, serine/theronine kinase; SYK, spleen tyrosine kinase; TAK, TGFβ activated kinase; TAO, thousand and one amino acid; TBK1, TANK-binding kinase 1; TESK, testis-specific protein kinase; TGFBR, TGFβ receptor; TIE, tyrosine-protein kinase receptor; TLK, tousled-like kinase; TrkA, tropomyocin receptor kinase; TSSK, testis-specific serine/threonine-protein kinase; TTBK, tau-tubulin kinase; ULK, Unc-51-like kinase; VEGFR, vascular endothelial growth factor

receptor; WNK, with no lysine; YES1, Yamaguchi sarcoma viral oncogene homologue 1; ZAP, zeta-chain-associated protein.

2.2.31 Sequence alignments

Sequence alignments were done using the ClustalW algorithm for multiple sequence alignment and visualised using JalView (Waterhouse et al., 2009).

2.2.32 Statistical analysis

All experiments presented in this thesis were performed at least twice and similar results were obtained. Data were analyzed using Student's t test or one-way analysis of variance (ANOVA) followed by multiple pairwise comparisons (*$P < 0.01$). Error bars indicate standard deviation. IC50 curves were generated using non-linear regression (curve fit) and statistical analysis was calculated using GraphPad Prism or Microsoft Excel.

3. Characterisation of novel and highly selective inhibitors of NUAKs

3.1. Introduction

AMPK family members possess highly similar substrate specificities and it is likely that in biochemical and overexpression-analysis, AMPK family kinases are likely to phosphorylate non-physiological substrates. Myosin phosphatase 1 subunit or MYPT1 possess three canonical AMPK consensus phosphorylation motifs which are specifically targeted by NUAKs alone (Zagorska et al., 2010), but in vitro kinase reactions and overexpression studies revealed that AMPK and all the AMPK related family of kinases could phosphorylate MYPT1 at those motifs and provide false-positive results. Hence, to avoid having to rely on overexpression of AMPK family members would be to develop selective inhibitors to each of the AMPK family kinases. This was originally deemed a challenging task due to the highly homologous kinase domains of these enzymes (Alessi et al., 2006) (Fig. 1.7).

To date, the pan-AMPK related kinase family inhibitor BX-795 is the only reported compound used as a tool inhibitor for NUAK isoforms (Zagorska et al., 2010, Liu et al., 2012).

In 2011, our lab in collaboration with Dr. Nathanael Gray (Harvard, USA) published the 7-membered ring structured inhibitor of LRRK2, a kinase mutated in Parkinson's disease, LRRK2-in-1 (Deng et al., 2011). Dr. Nathanael Gray observed that some of the compounds

with the 7-membered ring backbone had significant off-target effects on NUAK1. Based on this observation, Dr. Nathanael Gray's laboratory developed various prototypes of potential NUAK inhibitors and the compounds were screened for kinase inhibitor specificity at The International Centre for Protein Kinase Profiling (http://www.kinase-screen.mrc.ac.uk/) as described in section 2.2.30. Out of all the NUAK1 inhibitor prototypes, the ones deemed relatively selective for NUAK1 were carried forward for further cell based and biochemical assays.

There were in total three families of NUAK1 inhibitors based on their structural similarities:

1. The **7-membered ring series**: JWE-071, XMD-17-51, DLW-01-122-01, DLW-01-125-01, XMD-18-42, XMD-18-83 and HTH-01-015 (Fig 3.1) were chosen for cell based and biochemical assays.

2. The **2,4,5-trisubstituted pyrimidines**: These inhibitors had the same structural backbone as BX-795 and TG101348. Amidst the compounds, SJB4115, HMSL10085, WZ4002 and WZ4003 (Fig 3.1) were chosen for further assays.

3. The **imidizolopyrimidines**, loosely based on the structures of sunitinib and its derivaties. WZ4074 is the only compound used in this series for this thesis.

To study the potency of the NUAK inhibitors in vitro, IC50 values of the inhibitors were analysed either on purified NUAK1 alone or on potential drug resistant mutants of NUAK1 in parallel and on some occasions on purified NUAK2 in parallel to NUAK1 (Section 2.2.21.2). The inhibitors were sent through the kinase panel at the International Centre for Protein Kinase Profiling (http://www.kinase-screen.mrc.ac.uk/) (Section 2.2.30) to ascertain the specificity of the inhibitors and to identify off-target effects on other kinases. Finally, to identify the potency of the compounds towards inhibiting endogenous NUAK activity in cells, various concentrations of the inhibitors were utilised on HEK293 or U2OS or MEFs to check the inhibition of cell-detachment induced (EDTA buffer treated) (Section 2.2.10) phosphorylation of Ser445 of MYPT1 which has been extensively characterised as a bonafide NUAK phosphorylation site in vivo (Zagorska et al., 2010).

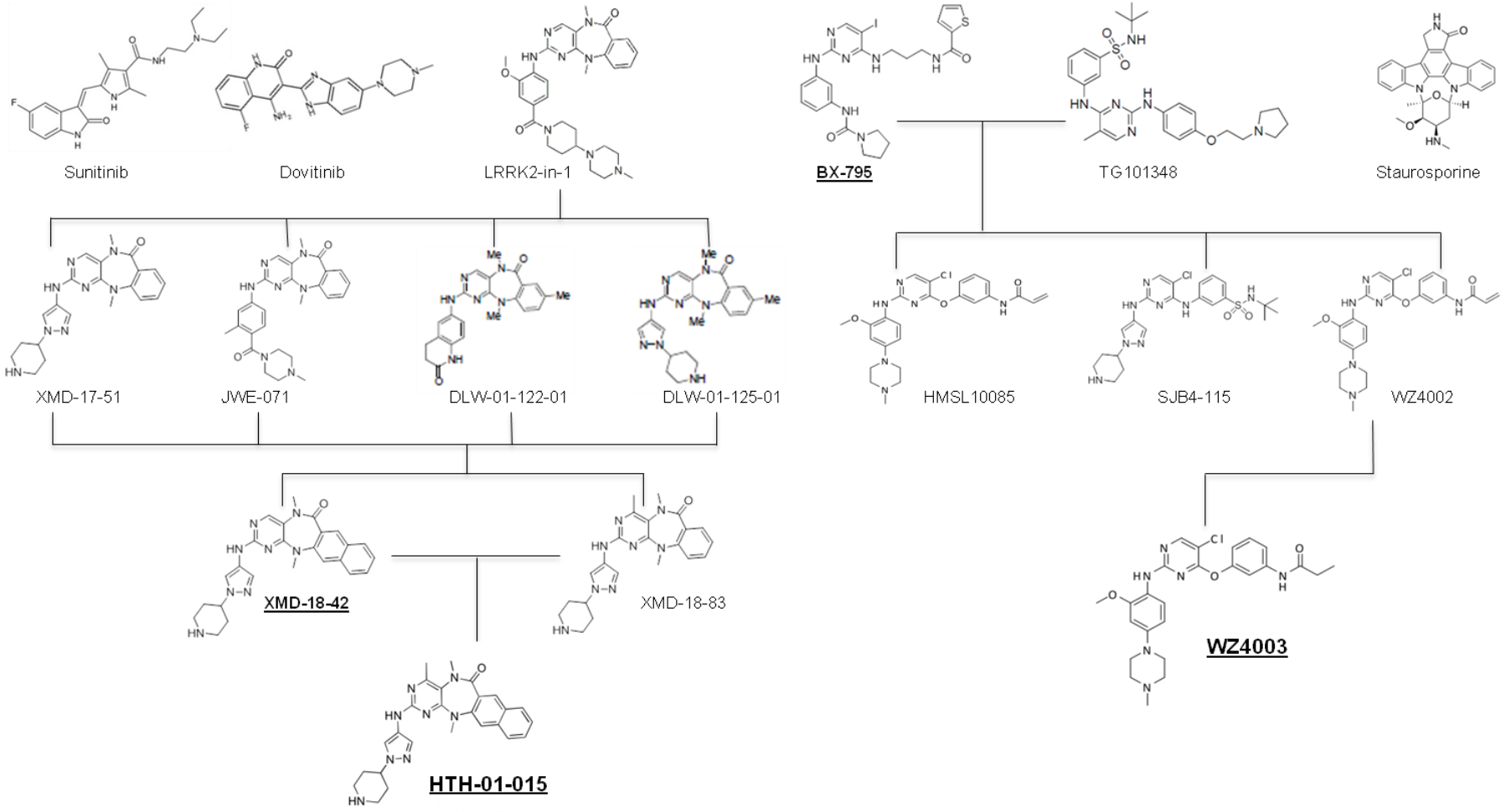

Figure 3.1 : Pedigree chart showing the gradual development of NUAK1 inhibitors from generic structures to the following generations of more potent and selective tool compounds.

3.2. Results

3.2.1. BX-795 is the only reported potent tool inhibitor of NUAK1 to date

BX-795 is a pyrimidine backbone (Fig.3.2A) containing small molecule initially developed as a potent PDK1 inhibitor (Feldman et al., 2005). Later on, it was extensively used in the innate immune signalling system as a very potent TBK1 and IKKε inhibitor which inhibited the production of interferon β in poly (I:C) or lipopolysaccharide stimulated macrophages (Clark et al., 2009). Specificity studies on BX-795 revealed that the tool compound potently inhibited AMPK and many of the AMPK-related kinases at 1 μM including NUAK1, MARK isoforms and SIK isoforms (Clark et al., 2009, Clark et al., 2012). The standard IC50 values previously calculated for various kinases with BX-795 are listed in Table 3.1.

Kinase	IC50 value	ATP conc (μM)
NUAK1	5 nM	100
MARK1	55 nM	100
MARK2	53 nM	100
MARK3	81 nM	100
MARK4	19 nM	100
PDK1	111 nM	100
Aurora B	31 nM	100
ERK8	140 nM	100
TBK1	6 nM	100
IKKε	41 nM	100
MLK isoforms	≤50 nM	100
VEGFR	157 nM	100

Table 3.1 : IC50 values for the inhibition of a few protein kinases by BX-795. (Clark et al., 2009)

BX-795 has been used extensively to identify MYPT1 as a novel and bonafide substrate of NUAK wherein treatment of BX-795 on cells could mimic the effects and phenotypes of the

NUAK1 deficient MEFs including loss of phosphorylation of Ser445 of MYPT1 upon induction of cell detachment (Zagorska et al., 2010). More recently, BX-795 was used to consolidate the RNAi data which suggested that NUAK1 plays a vital antiapoptotic role in deregulated oncogenic MYC expressing tumour cells and is an essential factor for tumour progression (Liu et al., 2012). I repeated the IC50 for BX-795 (Fig. 3.2 B) which was similar to previously reported 5 nM. BX-795 potently inhibited Ser445 phosphorylation of MYPT1 at 1 -10 µM concentrations on HEK293 cells (Fig. 3.2.C). Since BX-795 inhibits AMPK in vitro (Fig. 3.2 D), there was a moderate loss of canonical AMPK substrate phosphorylation Ser79 of ACC between 1-10 µM BX-795 (Fig. 3.2C). Besides the previously mentioned kinases, the major off-targets of BX-795 includes JAK2, GCK, CDK2 and MELK (Fig. 3.2.D).

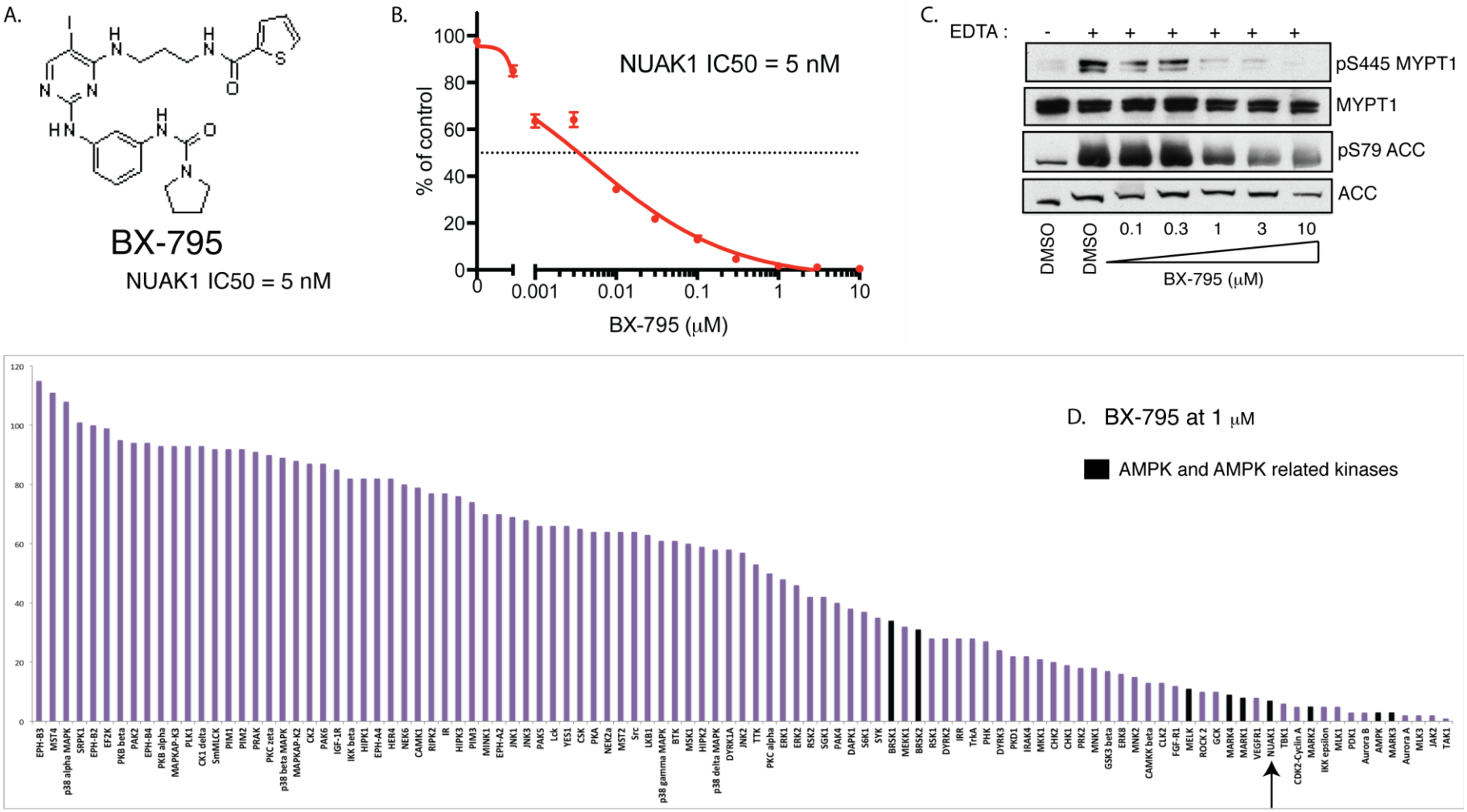

Figure 3.2 : BX-795 is a potent and non selective inhibitor of NUAK1. A) Structure of BX-795. B) NUAK1 IC50 with BX-795 was carried out using NUAK1 WT. C) HEK293 cells were treated with the indicated concentrations of BX-795 and the inhibition of NUAK1 induced pS445 of MYPT1 and AMPK induced pS79 ACC were observed. D) The kinase specificity panel for BX-795 was carried out as described in section 2.2.30. Arrow indicates NUAK1.

3.2.2. Development of potential drug resistant mutants of NUAK1

To study the effect of NUAK1 inhibitors in vivo and in vitro, I developed a NUAK1 drug resistant mutant. By sequence alignment, I observed that NUAK1 possessed an Ala residue (Ala195) adjacent to the DFG motif (Fig 3.3A) similar to ROCK (Bonn et al., 2006, Jacobs et al., 2006) and LRRK2 (Nichols et al., 2009, Deng et al., 2011). Previously, studies on ROCK had revealed that the Ala residue adjacent to the magnesium ion binding DFG motif in subdomain VII played a vital role in binding to the ROCK inhibitor H-1152 via Van der Waals interactions (Jacobs et al., 2006) while PKA which had a Thr at the same position was much more resistant to H-1152 and upon mutating the Thr to an Ala, H-1152 potently inhibited PKA (Bonn et al., 2006). Our laboratory had previously utilised this strategy to develop drug resistant LRRK2 mutants (Nichols et al., 2009, Deng et al., 2011). In order to identify the best possible mutation that would confer maximum drug resistance, we mutated Ala195 of NUAK1 into various amino acids and checked for the expression and activity of the mutants as compared to wild-type (Fig 3.3B). Out of the 7 mutants tested, NUAK1[A195G], NUAK1[A195S] and NUAK1[A195T] had comparable expression and were found to be catalytically active (Fig 3.3B). The NUAK1[A195T] displayed similar intrinsic activity as NUAK1 WT and was also expressed at the same levels as wild-type as shown in Fig 3.3C.

As shown in figure 3.3B, many of the NUAK1 mutants like A195D, A195K, A195N and A195V did not express at comparable levels with the wild-type and owing to either low expression or due to severity of the point mutation, the kinase activities were also negligible.

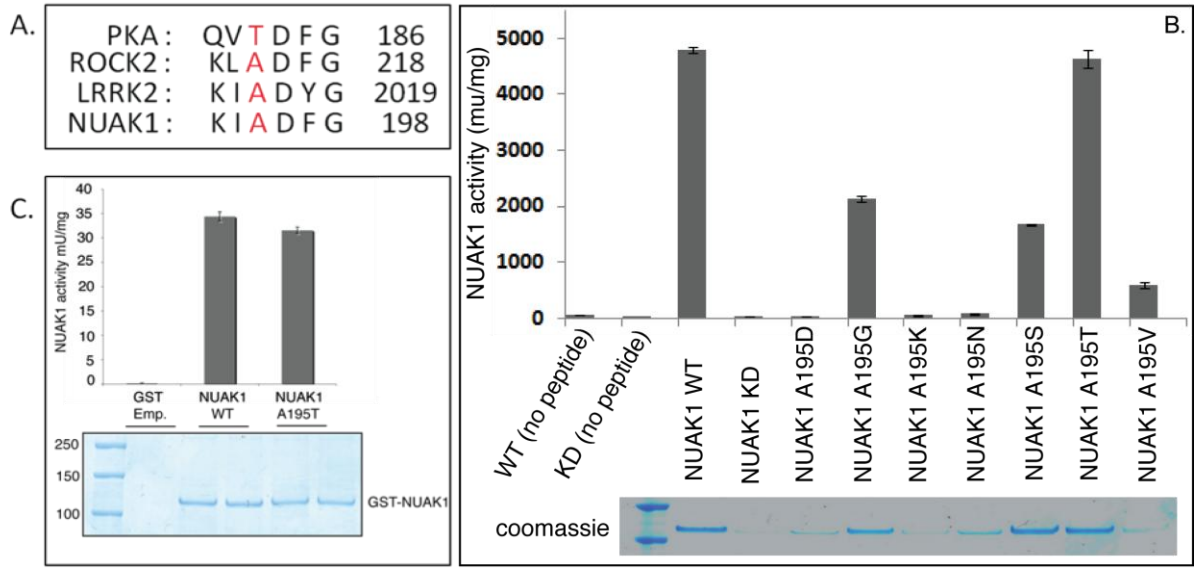

Fig 3.3. Development of potential drug resistant mutants of NUAK1: A) NUAK1 had a Ala residue similar to ROCK2 and LRRK2 adjacent to the subdomain VII DFG motif . B) The various NUAK1 potential drug resistant mutants were purified from transiently transfected HEK293 cells and their activities were compared using Sakamototide substrate peptide and [γ^{32}P] ATP. C) NUAK1 WT and NUAK1 [A195T] mutant protein expression and kinase activity was compared.

3.2.3. The first generation 7-membered ring series inhibitors were potent but less selective for NUAK1

The first generation of 7-membered ring series of NUAK1 inhibitors were JWE-071 (Fig 3.4A), XMD-17-51 (Fig 3.5A), DLW-01-122-01 (Fig 3.7A) and DLW-01-125-01 (Fig 3.6A).

3.2.3.1. JWE-071

JWE-071 was one of the first NUAK1 inhibitors received. It had better kinome selectivity than any of the previously reported inhibitors of NUAK1 especially BX-795. JWE-071 inhibited NUAK1 potently with an IC50 of 6 nM. The drug resistant mutant NUAK1 [A195T] exhibited 250 times more resistance for the inhibitor while NUAK1 [A195S] was 16-17 times more resistant (Fig. 3.4B). Interestingly, mutating Ala195 to a smaller Gly residue rendered the kinase 6 times more sensitive to the inhibitor (NUAK1 [A195G] IC50 1 nM) (Fig 3.4B). JWE-071 clearly inhibited the

NUAK1 mediated phosphorylation of MYPT1 at Ser445 in HEK293 cells at a concentration of 10 μM without significant inhibition of AMPK substrate ACC (Ser79) (Fig. 3.4.C). The major off-targets of JWE-071 were Aurora A, JAK2, ABL and Src and amidst the AMPK related kinases JWE-071 did exhibit some inhibitory activity on AMPK, BRSK1 and some of the MARK isoforms (Fig 3.4.D)

3.2.3.2. XMD-17-51

Along with JWE-071, the closely related inhibitor XMD-17-51 also exhibits high potency towards NUAK1 with an IC50 of 1.5 nM (Fig 3.5B) and inhibited Ser445 phosphorylation on MYPT1 at a concentration of 10 μM in HEK293 cells (Fig 3.5C). The NUAK1 [A195T] mutant was 400 times more resistant while NUAK1 [A195S] was 10 times more resistant to XMD-17-51 (Fig 3.5B). As with JWE-071, the NUAK1[A195G] mutant was approximately twice as sensitive to XMD-17-51 compared with NUAK1 WT (Fig 3.5B). XMD-17-51 had similar off-target effects as JWE-071 suppressing Aurora A & B, Src, JAK2, ABL. Amidst AMPK family kinases, XMD-17-51 had moderate activity on AMPK, BRSK1 and some MARK isoforms (Fig 3.5D).

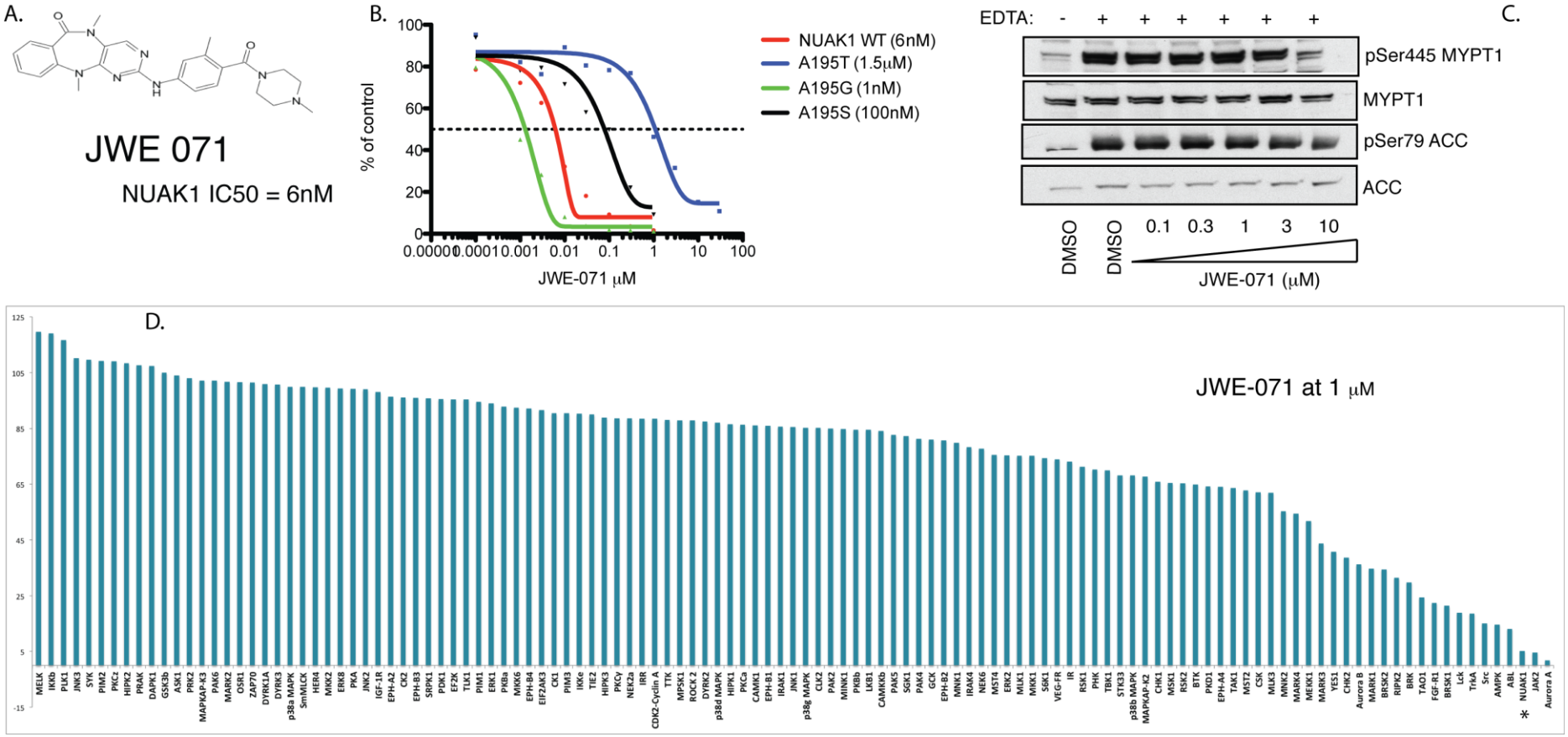

Figure 3.4 : JWE-071 is a potent and moderately selective inhibitor of NUAK1. A) Structure of JWE-071. B) NUAK1 IC50 with JWE_071 was carried out using NUAK1 WT, NUAK1 [A195T], NUAK1 [A195S] and NUAK1 [A195G]. C) HEK293 cells were treated with the indicated concentrations of JWE-071 and the inhibition of NUAK1 induced pS445 of MYPT1 and AMPK induced pS79 ACC were observed. D) The kinase specificity panel for JWE-071 was carried out as described in section 2.2.30.

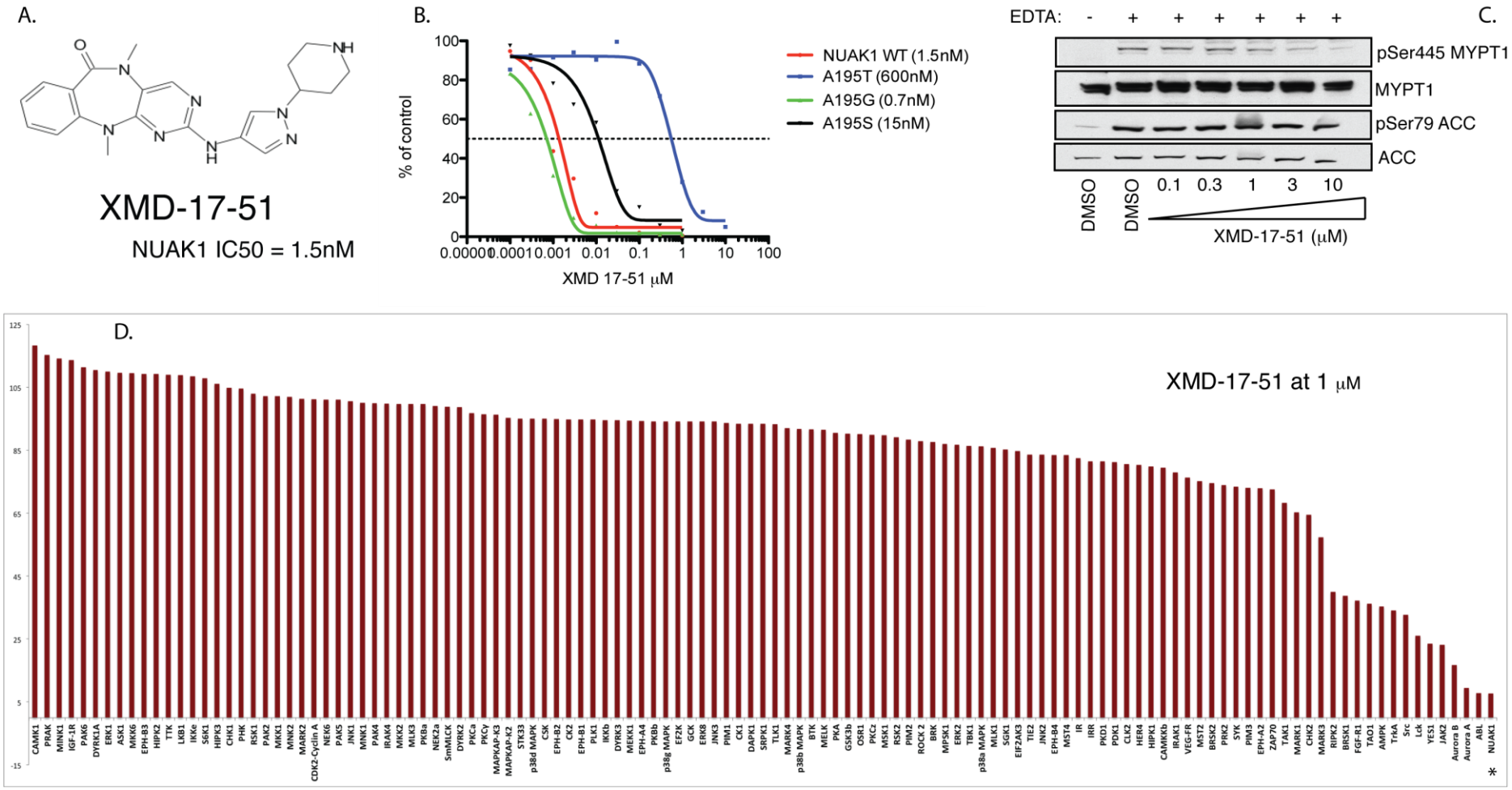

Figure 3.5 : XMD-17-51 is a potent and moderately selective inhibitor of NUAK1. A) Structure of XMD-17-51. B) NUAK1 IC50 with XMD-17-51 was carried out using NUAK1 WT, NUAK1 [A195T], NUAK1 [A195S] and NUAK1 [A195G]. C) HEK293 cells were treated with the indicated concentrations of XMD-17-51 and the inhibition of NUAK1 induced pS445 of MYPT1 and AMPK induced pS79 ACC were observed. D) The kinase specificity panel for XMD-17-51 was carried out as described in section 2.2.30.

3.2.3.3. DLW-01-125-01

DLW-01-125-01 exhibited similar activity as JWE-071 and XMD-17-51 with a NUAK1 IC50 of 7 nM and NUAK1 [A195T] exhibiting over 200 times more resistance (Fig 3.6B). DLW-01-125-01 inhibited Ser445 phosphorylation of MYPT1 at 10 µM (Fig.3.6C). Compared to JWE-071 or XMD-17-51, DLW-01-125-01 had less off-target effects inhibiting Aurora A & B, and exhibiting moderate inhibition of FGFR, Src, ABL and a rather modest inhibition of AMPK or any of the other AMPK-related kinases (Fig 3.6D)

3.2.3.3. DLW-01-122-01

DLW-01-122-01 is by far the most selective of all the first generation 7-membered ring series of NUAK inhibitors. The only drawback being that DLW-01-122-01 inhibited Aurora A & B with similar potency as NUAK1. There was hardly any inhibition of the AMPK-related kinases exhibited (Fig 3.7D) without much compromise for NUAK1 potency (IC50 of 15 nM with NUAK1 [A195T] IC50 of 2 µM) (Fig 3.7B). DLW-01-122-01 inhibited Ser445 phosphorylation of MYPT1 at 10 µM without much effect on Ser79 of AMPK substrate ACC (Fig 3.7C).

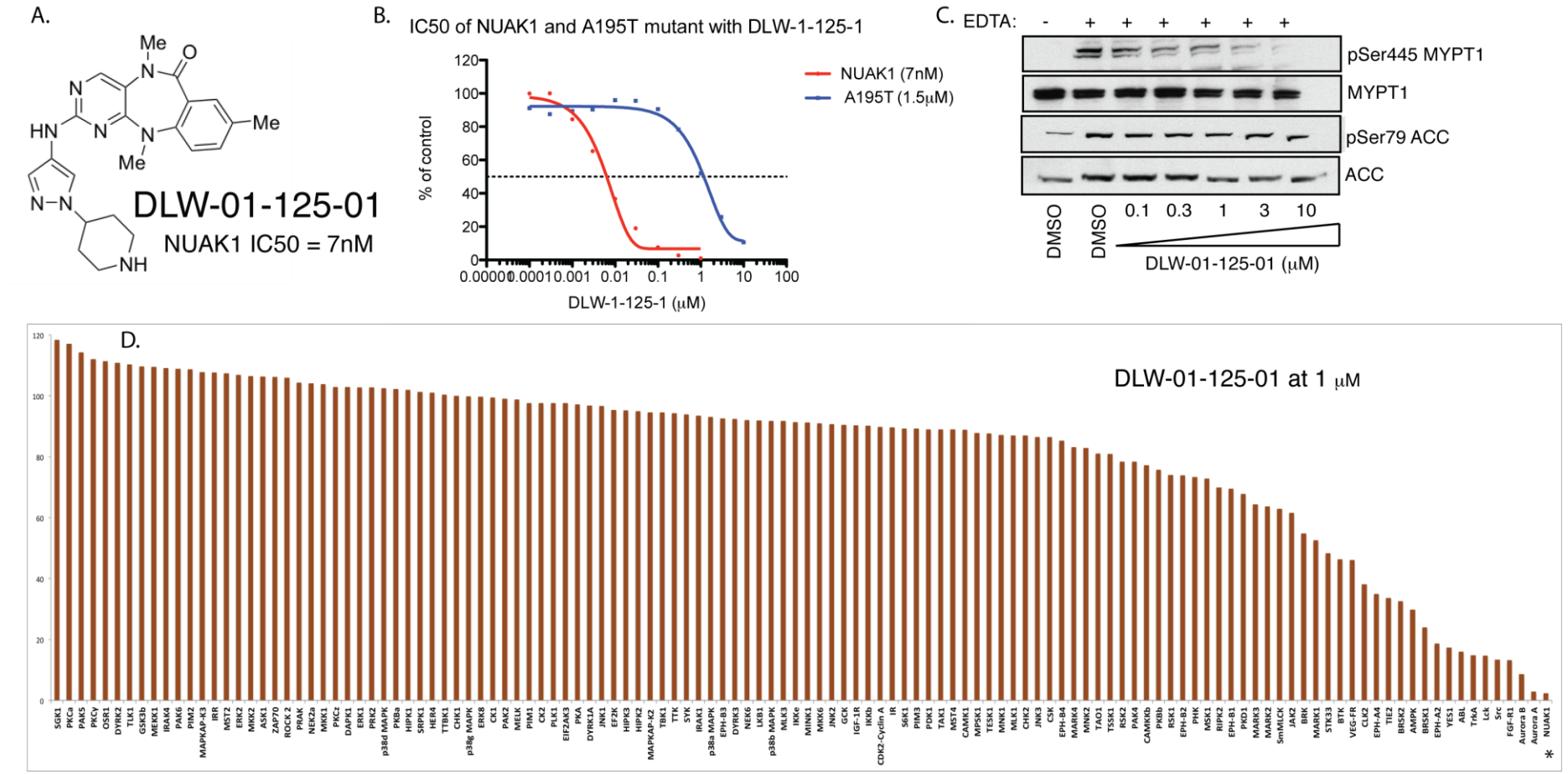

Figure 3.6: DLW-01-125-01 is a potent and selective inhibitor of NUAK1. A) Structure of DLW-01-125-01. B) NUAK1 IC50 with DLW-01-125-01was carried out using NUAK1 WT and NUAK1 [A195T]. C) HEK293 cells were treated with the indicated concentrations of DLW-01-125-01 and the inhibition of NUAK1 induced pS445 of MYPT1 and AMPK induced pS79 ACC were observed. D) The kinase specificity panel for DLW-01-125-01 was carried out as described in section 2.2.30.

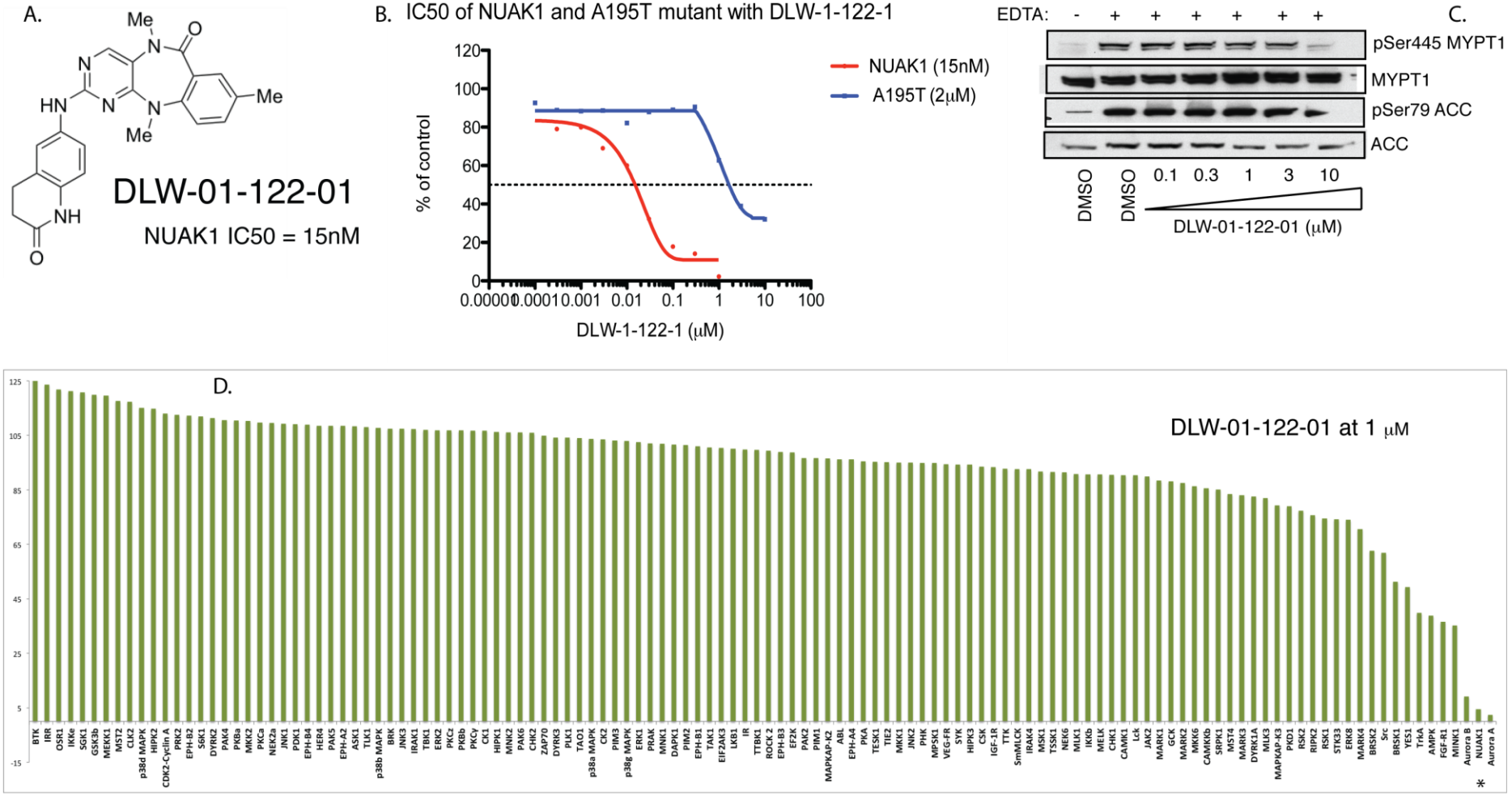

Figure 3.7 : DLW-01-122-01 is a potent and very selective inhibitor of NUAK1. A) Structure of DLW-01-122-01. B) NUAK1 IC50 with DLW-01-122-01 was carried out using NUAK1 WT and NUAK1 [A195T]. C) HEK293 cells were treated with the indicated concentrations of DLW-01-122-01 and the inhibition of NUAK1 induced pS445 of MYPT1 and AMPK induced pS79 ACC were observed. D) The kinase specificity panel for DLW-01-122-01 was carried out as described in section 2.2.30.

3.2.4 . The second generation 7-membered ring series NUAK1 inhibitor XMD-18-42 was highly selective for NUAK1 but still inhibited Aurora C & B

XMD-1842 (Fig 3.10A) was a derivative of the first generation inhibitors and exhibited high potency for NUAK1 in vitro with an IC50 of 30 nM while NUAK1[A195T] mutant was 50 times more resistant (Fig 3.10B). Similar to the earlier generation of 7-membered ring series of inhibitors, XMD-18-42 inhibits Ser445 phosphorylation on MYPT1 at 10 μM in HEK293 cells (Fig 3.10B). The kinase specificity panel for XMD-18-42 (Fig. 3.10D) showed that it potently inhibited Aurora B as well. Furthermore, IC50 analysis of XMD-18-42 for the Aurora kinases showed that the inhibitor potently inhibited Aurora B with an IC50 of 54 nM and Aurora C with an IC50 of 120 nM (Fig 3.8).

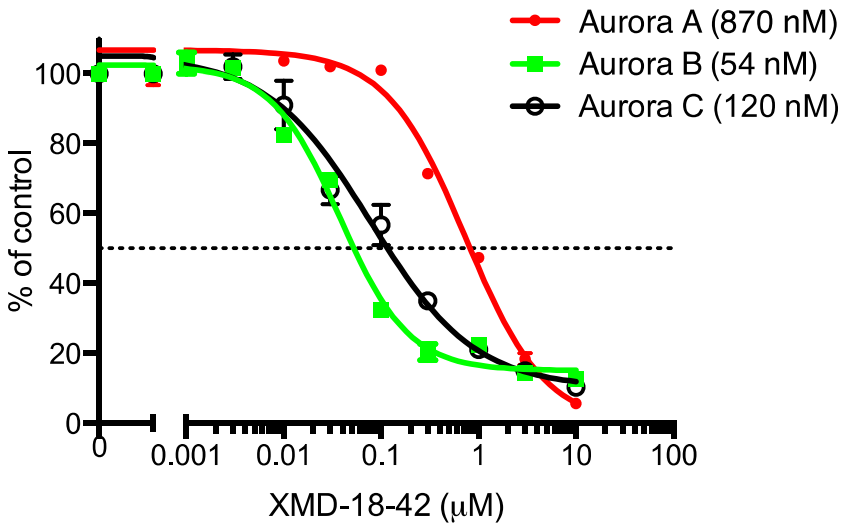

Figure 3.8 : XMD-18-42 inhibits Aurora kinases *in vitro*

In the XMD-18-42 related second generation of the 7-membered ring series, XMD-18- 83 was one of the less selective NUAK1 inhibitor (IC50 17 nM) with off-target effects on ABL, DDR2, Lck, CLK2, Src and JAK2 (Fig 3.9) However, one interesting observation was that it was the first compound of the 7-membered series which had least off-target effects on the Aurora kinases, especially Aurora B.

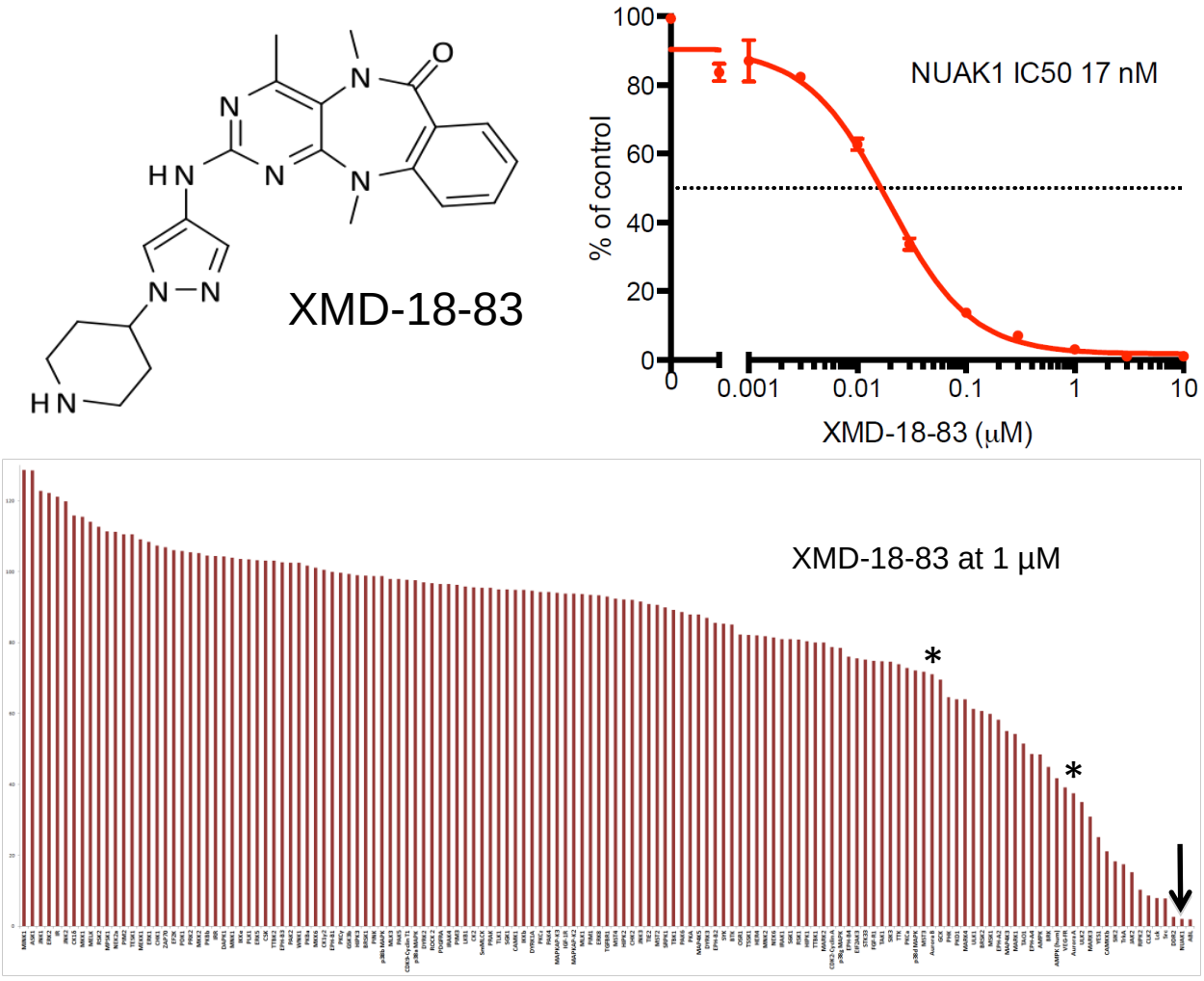

Figure 3.9 : XMD-18-83 was a less selective inhibitor of NUAK1 but did not inhibit the Aurora kinases. (Arrow indicates NUAK1 and * indicates Aurora kinases)

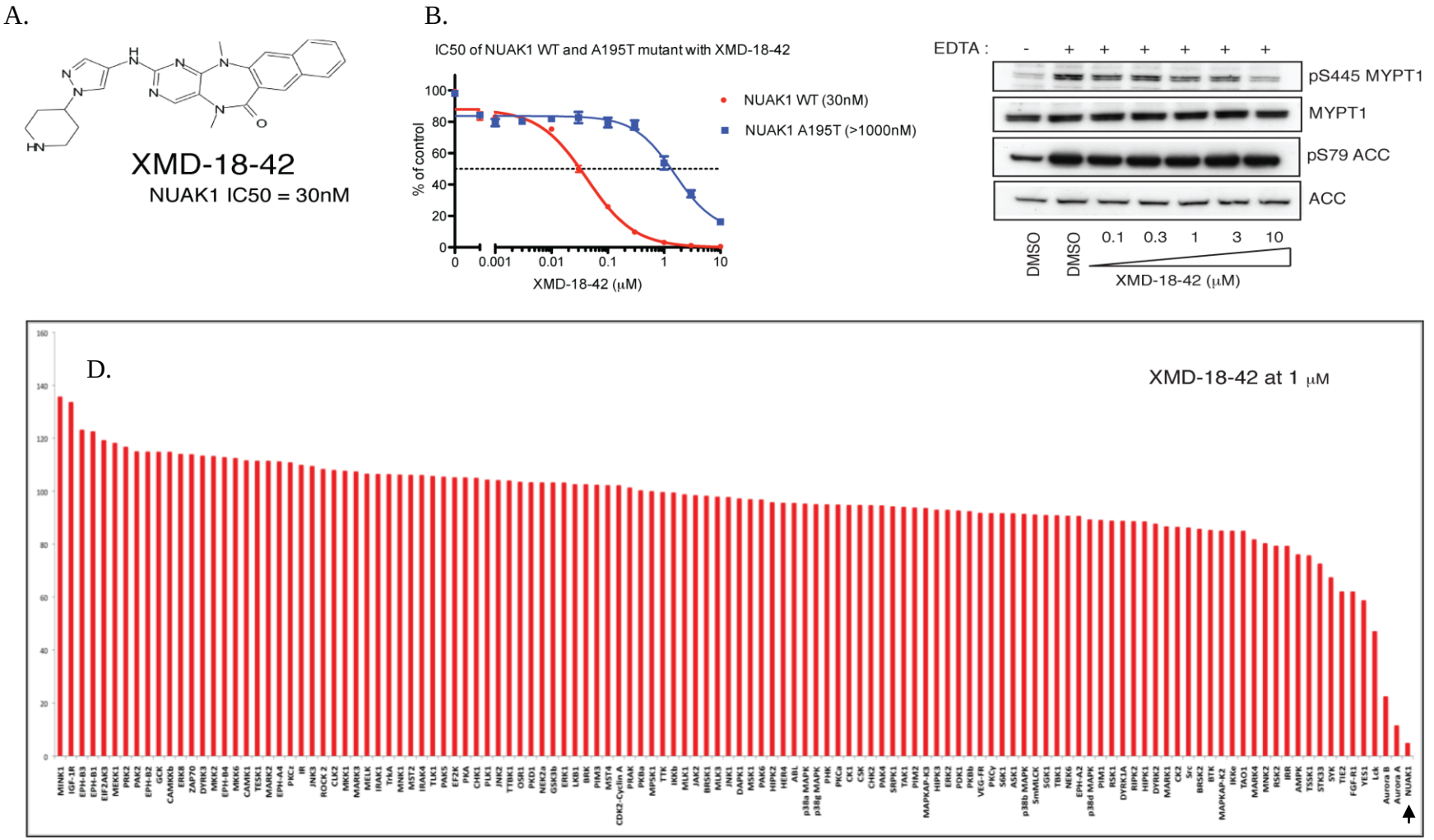

Figure 3.10 : XMD-18-42 is a potent and highly selective inhibitor of NUAK1. A) Structure of XMD-18-42. B) NUAK1 IC50 with XMD-18-42 was carried out using NUAK1 WT and NUAK1 [A195T]. C) HEK293 cells were treated with the indicated concentrations of XMD-18-42 and the inhibition of NUAK1 induced pS445 of MYPT1 and AMPK induced pS79 ACC were observed. D) The kinase specificity panel for XMD-18-42 was carried out as described in section 2.2.30.

3.2.5. The first and second generation 7-membered ring series had very weak activity on NUAK2

Interestingly, DLW-01-122-01 and XMD-18-42 has very weak inhibitory activity on NUAK2 (Fig. 3.11). At 10 µM concentration of XMD-18-42 (>300 times the IC50 of NUAK1), NUAK2 retained >80% of its kinase activity and at 10 µM concentration of DLW-01-122-01 (>650 times the IC50 of NUAK1), NUAK2 retained >50% of its kinase activity.

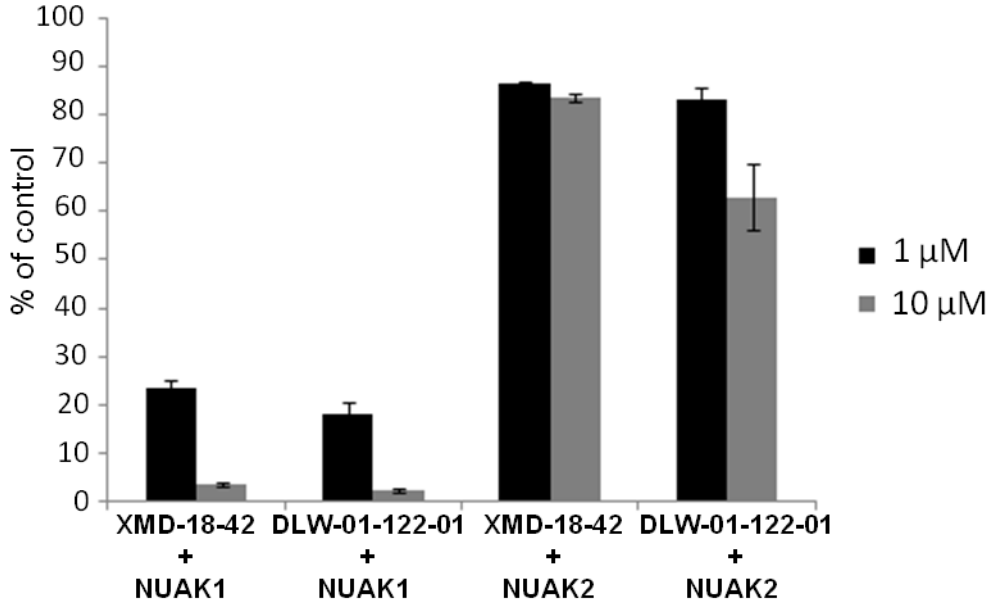

Figure 3.11 : First and second generation 7-membered ring series of NUAK1 inhibitors exhibit very low activity towards NUAK2

3.2.6. The third generation 7-membered ring series HTH-01-015 is a highly potent and remarkably specific inhibitor of NUAK1

To develop the most specific and potent inhibitor of NUAK1 and to negate the activity against the Aurora kinases, a third generation inhibitor was synthesized termed HTH-01-015 (Fig. 3.12A). HTH-01-015 was a hybrid of XMD-18-42 and XMD-18-83 that retained the specificity of XMD-18-42 and exhibited minimal activity towards the Aurora kinases characteristic of XMD-18-83 (Fig.3.12D). HTH-01-015 was remarkably selective for NUAK1 with an IC50 of 100 nM with NUAK1 [A195T] being approximately 60 times more resistant to the inhibitor (Fig. 3.12B). Similar to its 7-membered ring predecessors, HTH-01-015 inhibited NUAK2 with an IC50 of >11 µM (Fig. 3.12C).

HTH-01-015 inhibits Ser445 phosphorylation of MYPT1 at 3-10 µM concentrations in HEK293 cells (Fig. 3.13). Consistent with the screening data (Fig 3.12D), HTH-01-015 does not inhibit AMPK that is evident from the robust Ser79 ACC signal at 3-10 µM concentrations of the inhibitor (Fig. 3.13).

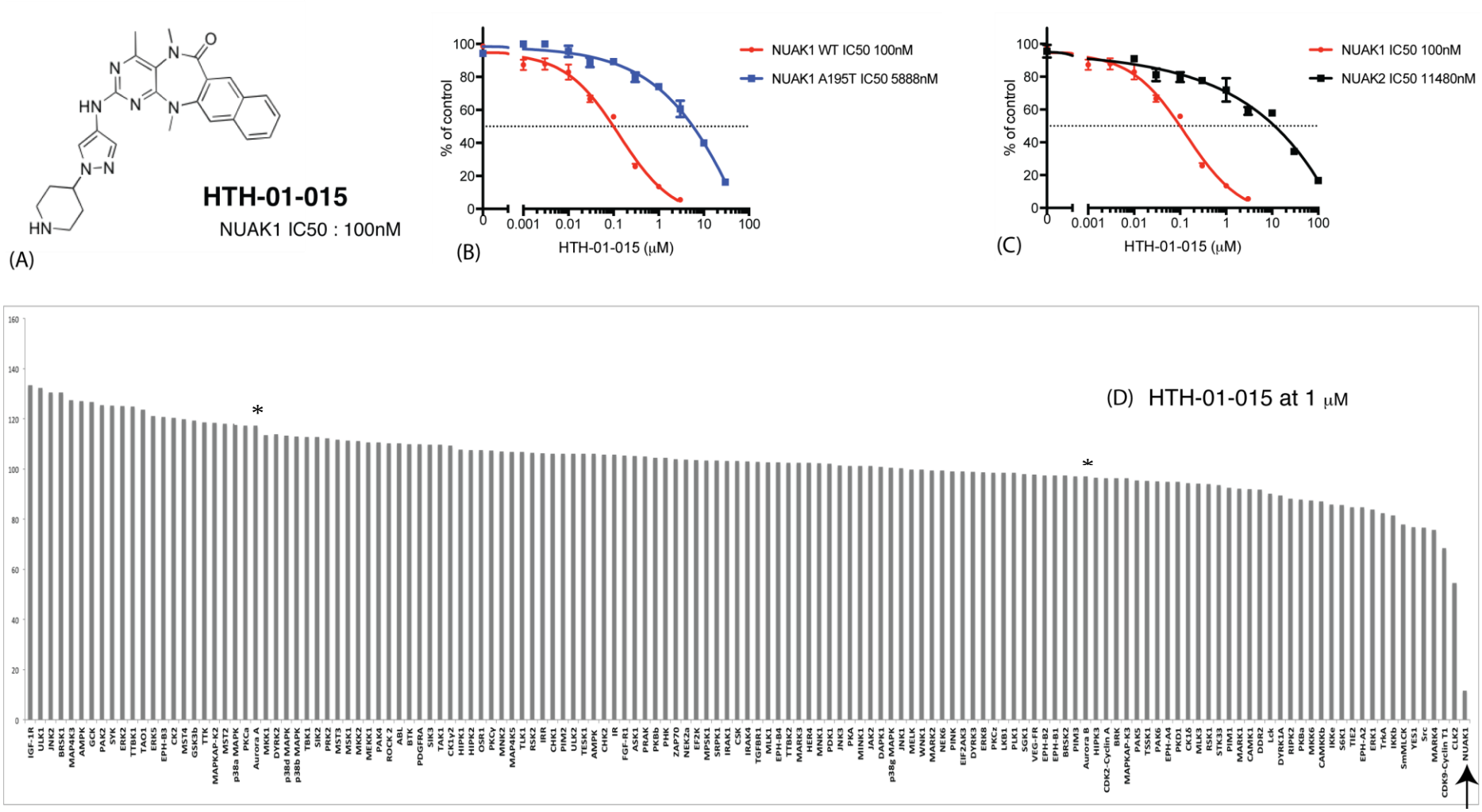

Figure 3.12 : HTH-01-015 is a highly potent and remarkably selective inhibitor of NUAK1. A) Structure of HTH-01-015. B) NUAK1 IC50 with HTH-01-015 was carried out using NUAK1 WT and NUAK1 [A195T]. C) NUAK2 IC50 with HTH-01-015 was carried out using NUAK2 WT and NUAK1WT in parallel. D) The kinase specificity panel for HTH-01-015 was carried out as described in section 2.2.30.
(Arrow indicates NUAK1 and * indicates Aurora kinases)

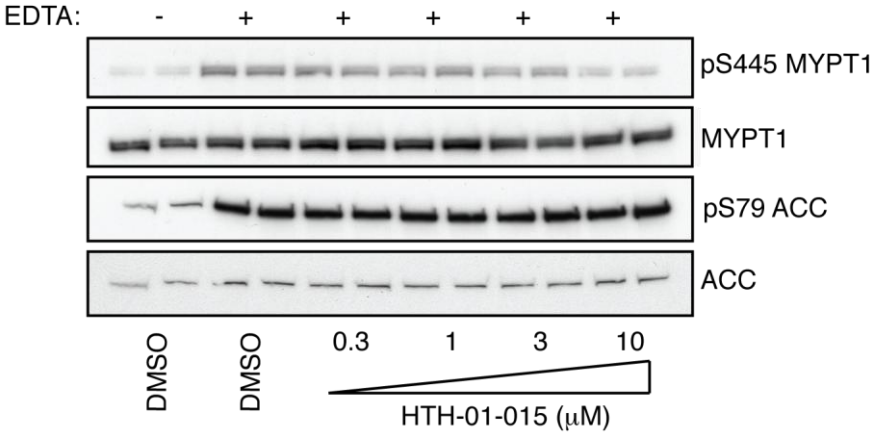

Figure 3.13 : HTH-01-015 inhibits NUAK1 in vivo. HEK293 cells treated with or without the indicated concentrations of HTH-01-015 for 8 hrs. The cells were induced with or without EDTA buffer mediated detachment to activate NUAK1. Cells were lysed and immunoblots were carried out with Ser445 MYPT1, MYPT1, Ser79 ACC and ACC antibodies.

To further test the efficacy of the inhibitor, HEK293 cells stably expressing NUAK1 WT and NUAK1 [A195T] cells were treated with various dilutions of the inhibitors and Ser445 MYPT1 phosphorylation was checked by immunoblotting. Unlike the NUAK1 WT expressing cells (Fig.3.14A), HEK293 cells expressing the drug-resistant NUAK1[A195T] did not exhibit any significant decrease of Ser445 MYPT1 phosphorylation even at 30 µM HTH-01-015 concentration (Fig.3.14B).

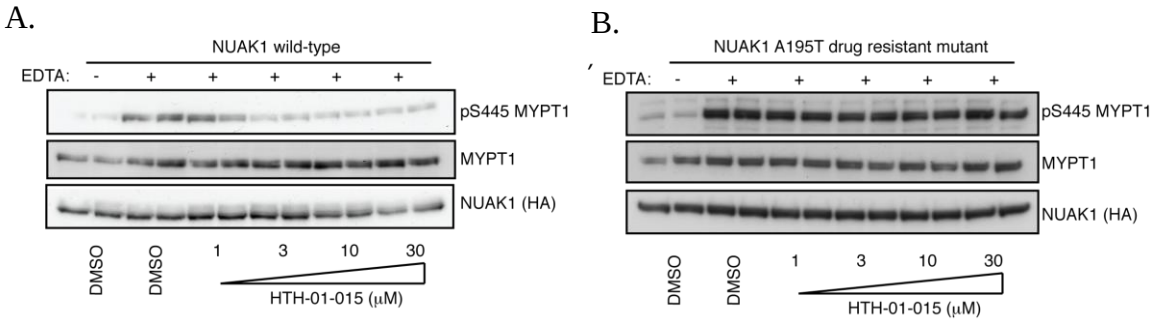

Figure 3.14 : HEK293 cells stably expressing NUAK1[A195T] cells do not exhibit reduction of Ser445 MYPT1 phosphorylation upon treatment with HTH-01-015. A) HEK293 cells expressing NUAK1 WT exhibits reduction of Ser445 MYPT1 phosphorylation between 3-30 µM. B) Cells expressing NUAK1[A195T] does not show any significant reduction of Ser445 MYPT1 phosphorylation even at 30 µM.

3.2.7. The BX-795 derived first generation 2,4,5-trisubstituted pyrimidine series of NUAK inhibitors were less specific for NUAK1

The 2,4,5-trisubstituted pyrimidine series of inhibitors were developed based on primarily the backbone of BX-795 and fusing some of the basic side chains of TG101348. These inhibitors were structurally diverse from the 7-membered ring series and hence provided as a perfect control to replicate and consolidate the *in vitro* and *in vivo* effects of NUAK1 inhibition. There were in total three inhibitors in the first generation of 2,4,5-trisubstituted pyrimidine series namely: SJB4-115, WZ4002 and HMSL10085.

HMSL10085 was relatively selective for NUAK1 with off-target effects on IGFR, BTK and HER4. HMSL10085 had a NUAK1 IC50 of 25 nM (Fig 3.15) and being less selective, it was not carried forward for cell based assays.

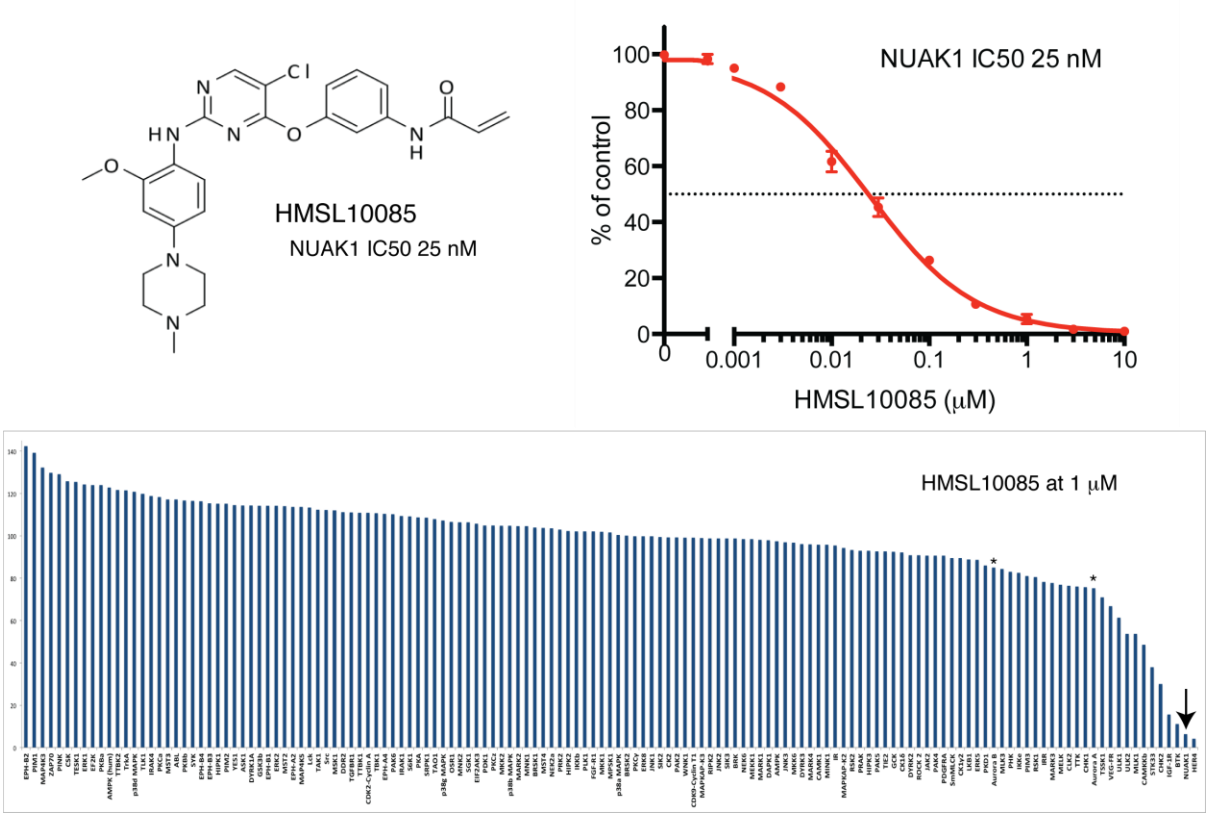

Figure 3.15 : HMSL10085 was a first generation 2,4,5-trisubstituted pyrimidine inhibitor of NUAK1. (Arrow indicates NUAK1 and * indicates Aurora kinases)

SJB4-115, similar to HMSL10085, potently inhibited NUAK1 with an in vitro IC50 of 67 nM (Fig. 3.16). SJB4-115, however was far less selective for NUAK1 as compared to HMSL10085 exhibiting off-target effects on JAK2, ERK8, TrkA, Lck, ULK1, Src and AMPK related kinase SIK2 (Fig. 3.16). As in HMSL10085, SJB4-115 was not tested further on cells.

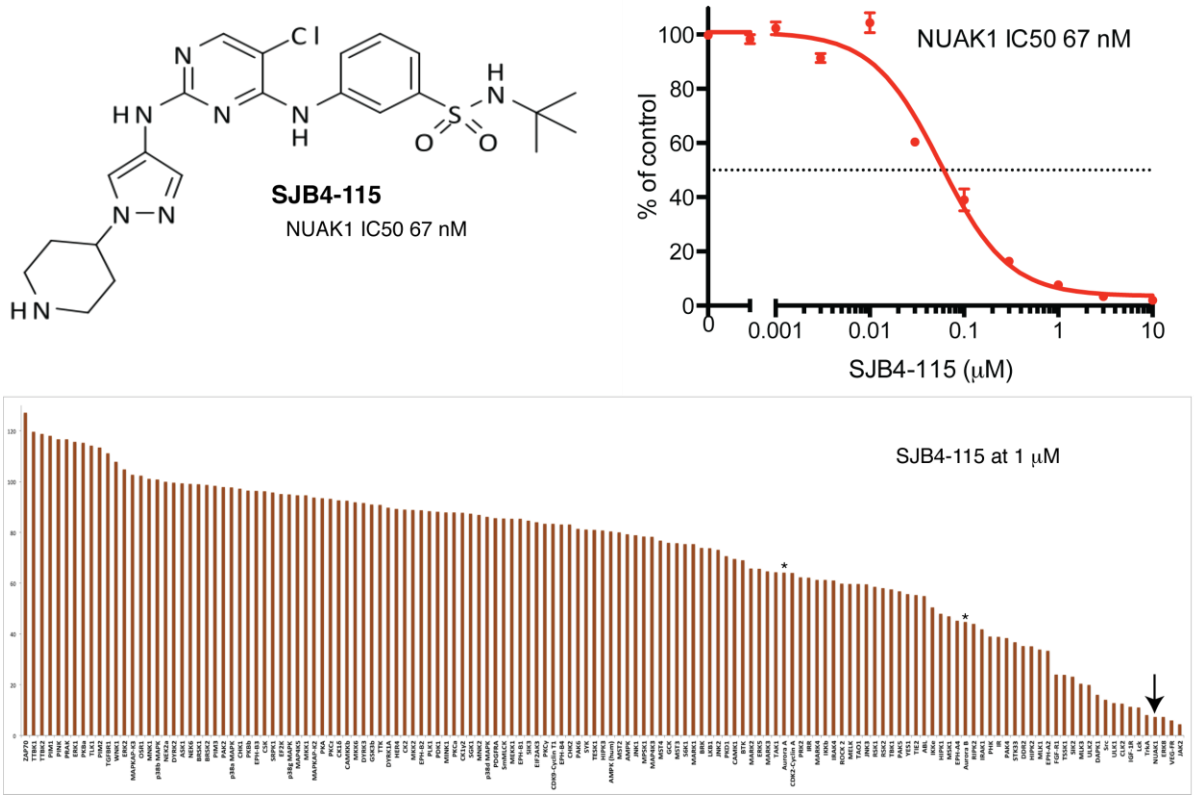

Figure 3.16 : SJB4-115 was a first generation 2,4,5-trisubstituted pyrimidine inhibitor of NUAK1 and less selective than HMSL10085. (Arrow indicates NUAK1 and * indicates Aurora kinases)

3.2.8. The third generation 2,4,5-trisubstituted pyrimidine series WZ4003 is a highly potent and remarkably specific inhibitor for both NUAK1 and NUAK2 isoforms.

One of the first generation 2,4,5-trisubstituted pyrimidine series of inhibitors is WZ4002 (Fig.3.1) that has previously been reported as a potent EGFR inhibitor, and Ambit screening against 400 kinases revealed that WZ4002 inhibits a sub-set of the TEC-family kinases as well (Zhou et al., 2009). The Ambit screening data also exhibited that WZ4002 inhibited NUAK1 by 82% and NUAK2 by 72% at 0.1 μM concentration (Zhou et al., 2009). Interestingly, a reversible analog of WZ4002 was used as a control probe with a hundred fold lower potency for EGFR inhibition, termed WZ4003 (Fig.3.17A) (Zhou et al., 2009). WZ4003 did not have significant inhibitory effect on EGFR or TEC-family kinases, but kinase profiling at the International Centre for Protein Kinase Profiling, University of Dundee revealed that WZ4003 did not lose the inhibitory effect on NUAK1 (Fig 3.17D).

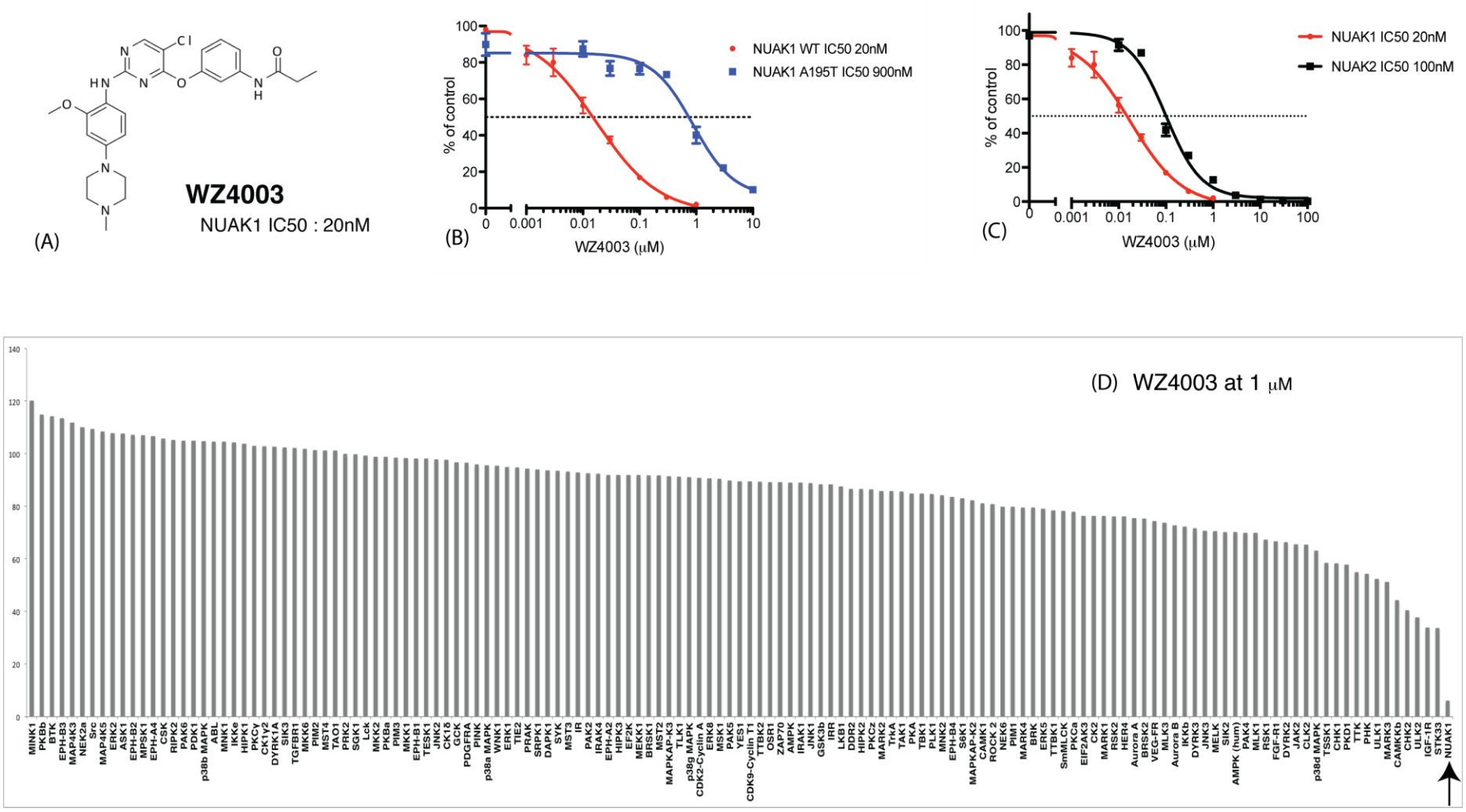

Figure 3.17 : WZ4003 is a highly potent and remarkably selective inhibitor of NUAK1 and NUAK2. A) Structure of WZ4003. B) NUAK1 IC50 with WZ4003 was carried out using NUAK1 WT and NUAK1 [A195T]. C) NUAK2 IC50 with WZ4003 was carried out using NUAK2 WT and NUAK1 WT in parallel. D) The kinase specificity panel for WZ4003 was carried out as described in section 2.2.30.

WZ4003 inhibited NUAK1 with an IC50 of 20 nM with the drug-resistant NUAK1 [A195T] exhibiting 45 times more resistance to inhibition (Fig. 3.17B). WZ4003 is the first potent and selective inhibitor of both the NUAK isoforms and inhibits NUAK2 in vitro with an IC50 of 100 nM (Fig. 3.17C). WZ4003 had a more potent inhibition of Ser445 MYPT1 phosphorylation between 1-10 μM (Fig. 3.18) and consistent with the screening data, Ser79 of ACC was unaffected suggesting minimal inhibition of AMPK (Fig 3.18).

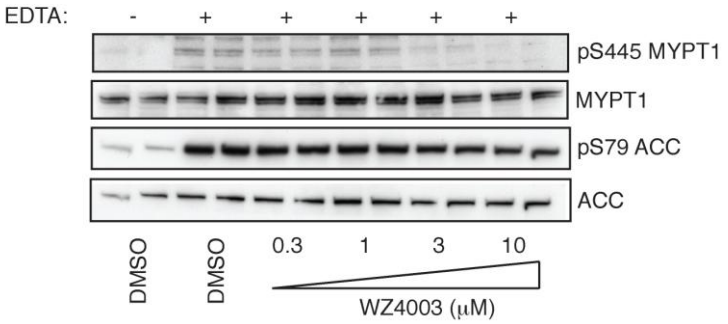

Figure 3.18 : WZ4003 inhibits NUAK activity in vivo. HEK293 cells treated with or without the indicated concentrations of WZ4003 for 16 hrs. The cells were induced with or without EDTA buffer mediated detachment to activate NUAK1. Cells were lysed and immunoblots were carried out with Ser445 MYPT1, MYPT1, Ser79 ACC and ACC antibodies.

To further test the efficacy of the inhibitor, HEK293 cells stably expressing NUAK1 WT and NUAK1 [A195T] cells were treated with various dilutions of WZ4003 and Ser445 MYPT1 phosphorylation was checked by immunoblotting. Unlike the NUAK1 WT expressing cells (Fig.3.19A), HEK293 cells expressing the drug-resistant NUAK1[A195T] did not exhibit any significant decrease of Ser445 MYPT1 phosphorylation even at 30 μM WZ4003 concentration (Fig.3.19B).

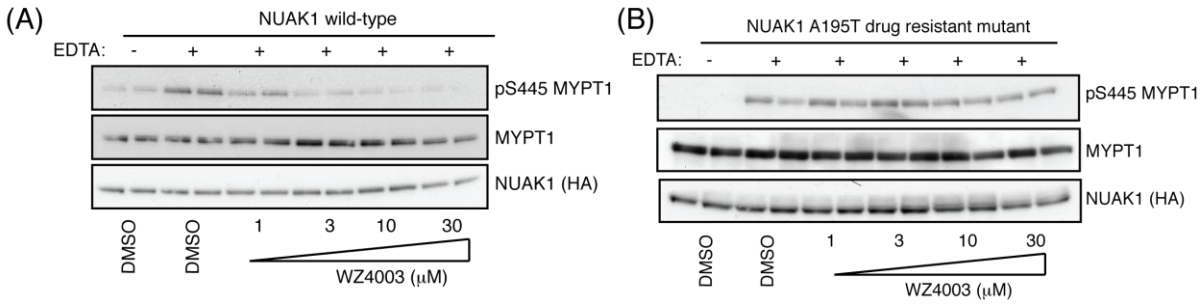

Figure 3.19 : HEK293 cells stably expressing NUAK1[A195T] cells do not exhibit reduction of Ser445 MYPT1 phosphorylation upon treatment with WZ4003. A) HEK293 cells expressing NUAK1 WT exhibits reduction of Ser445 MYPT1 phosphorylation between 3-30 µM concentration of WZ4003. B) Cells expressing NUAK1[A195T] does not show any significant reduction of Ser445 MYPT1 phosphorylation even at 30 µM concentration.

3.2.9. WZ4074, the imidizolopyrimidine series NUAK1 inhibitor was considerably less selective than HTH-01-015 or WZ4003.

The only imidizolopyrimidine series inhibitor WZ4074 potently inhibited NUAK1 with an IC50 of 33 nM but exhibited many off-target effects including BTK, HER4, MLK isoforms (Fig 3.20). The structure of WZ4074 is loosely based on sunitib and its derivatives and hence is structurally diverse than the 7-membered ring series or the 2,4,5-trisubstituted pyrimidine series of inhibitors.

WZ4074, owing to its non-selective profile, was not used in further cell based assays to check MYPT1 phosphorylation.

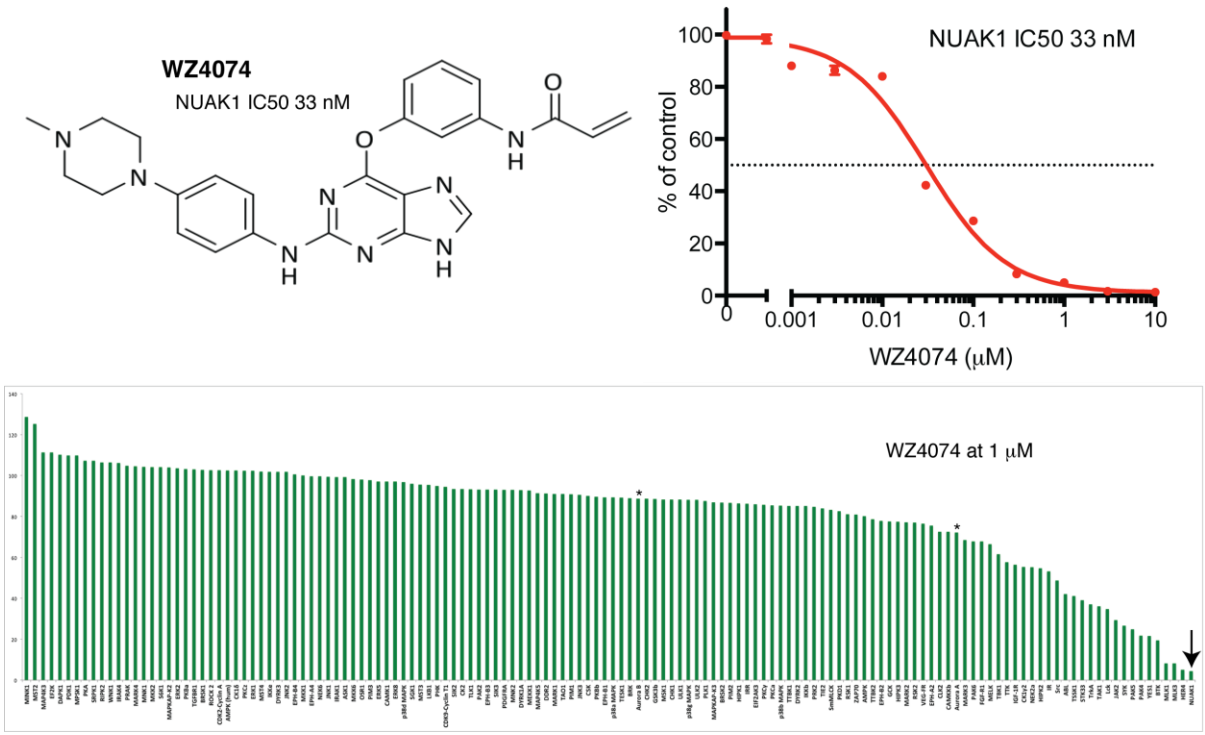

Figure 3.20: WZ4074 is the only inhibitor in the imidizolopyrimidine series and potently inhibits NUAK1 but is much less selective. (Arrow indicates NUAK1 and * indicates Aurora kinases).

3.2.10. Inhibition of NUAK1 impairs the migration properties of cells

Previous studies have revealed that RNAi mediated knockdown of NUAK1 slows down the rate of migration of cells especially in a wound-healing assay (Chang et al., 2012, Chen et al., 2013b, Lu et al., 2013). We employed wound-healing assays on $NUAK1^{+/+}$ and $NUAK1^{-/-}$ MEFs and compared the migration properties between wild-type and NUAK1 deficient cells (Fig. 3.21). Clearly, the $NUAK1^{-/-}$ MEFs migrated much slower into the 500 µm wound while within 15-16 hrs, the $NUAK1^{+/+}$ MEFs had already closed the wound (Fig. 3.21).

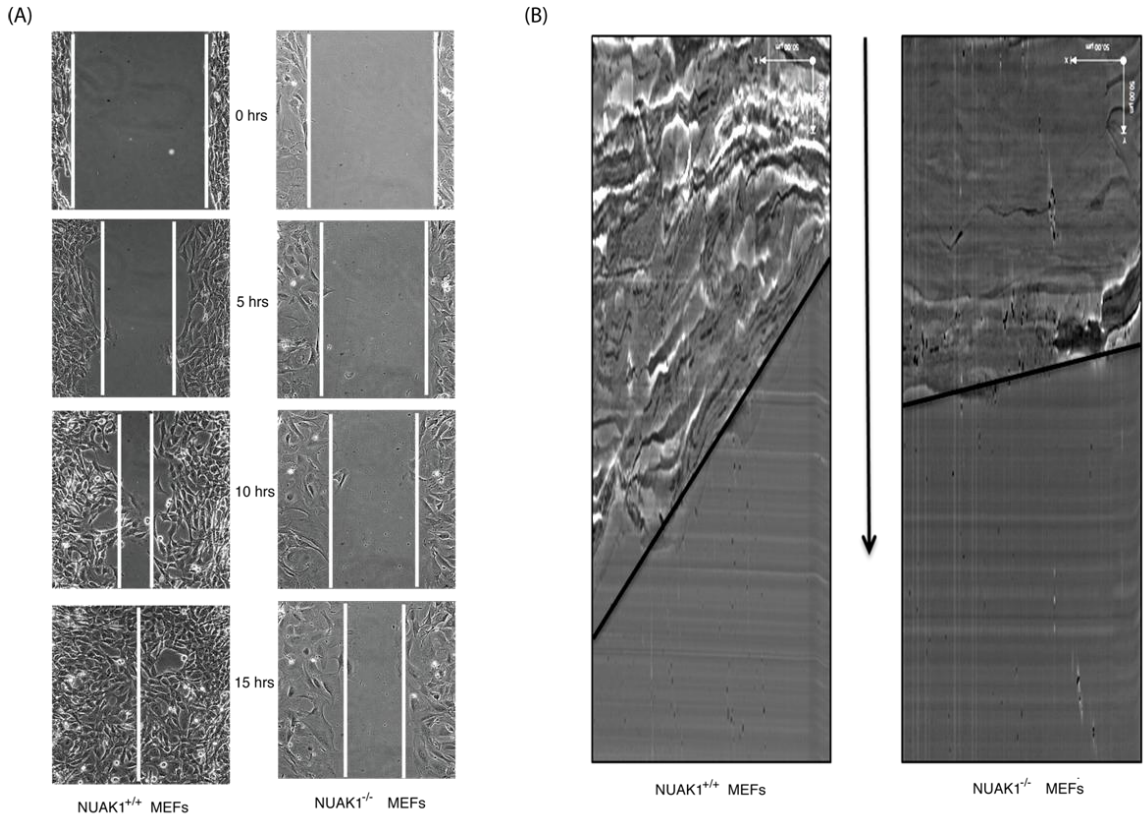

Figure 3.21 : NUAK1 deficient cells migrate slower than the wild-type. A) Wound-healing assay showing the total migration of cells into the 500 µm wound over 15 hours. B) Quantitative kymographs of A. where the arrow indicates direction of migration.

To see whether inhibitor treatment of cells (NUAK1$^{+/+}$ MEF and U2OS) would phenocopy the slow migration of NUAK1$^{-/-}$ MEFs, wound healing assay was carried out with or without the treatment of WZ4003 and HTH-01-015 on cells. NUAK1$^{+/+}$ MEFs on treatment with both WZ4003 and HTH-01-015, migrated much slower into the wound as is evident in Fig. 3.22.

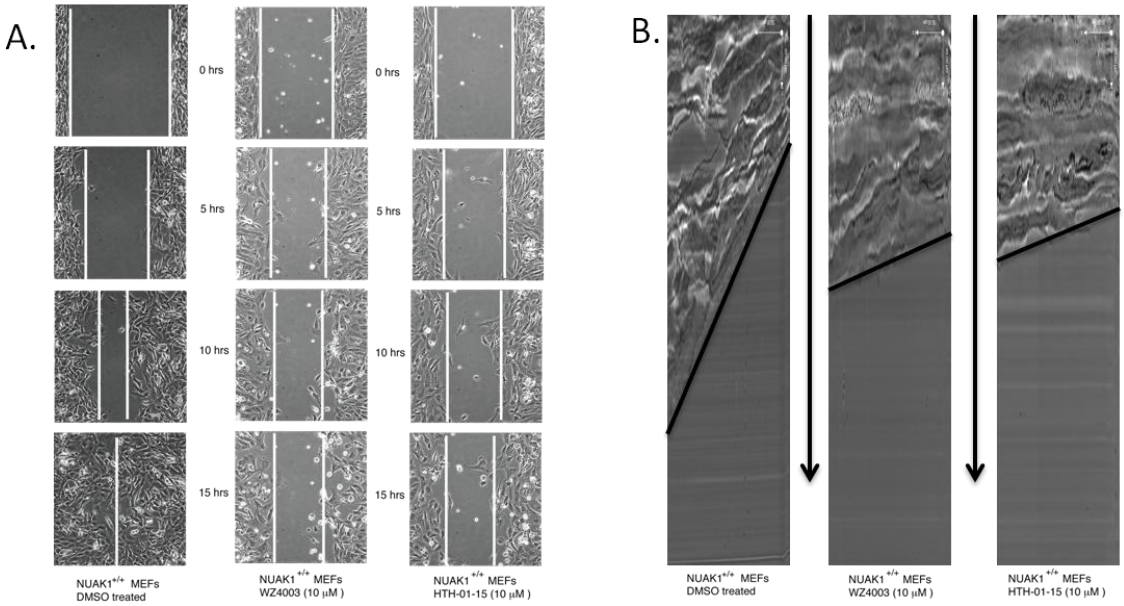

Figure 3.22 : Treatment of WZ4003 or HTH-01-015 phenocopies slower migration properties of NUAK1 deficient cells. A) Wound-healing assay showing the total migration of NUAK1$^{+/+}$ MEFs into the 500 µm wound over 15 hours. B) Quantitative kymographs of A. where the arrow indicates direction of migration.

Similar to the NUAK1$^{+/+}$ MEFs, treatment of WZ4003 and HTH-01-015 inhibitors to highly migratory U2OS cells exhibited the same slower phenotype in wound-healing assays (Fig. 3.23).

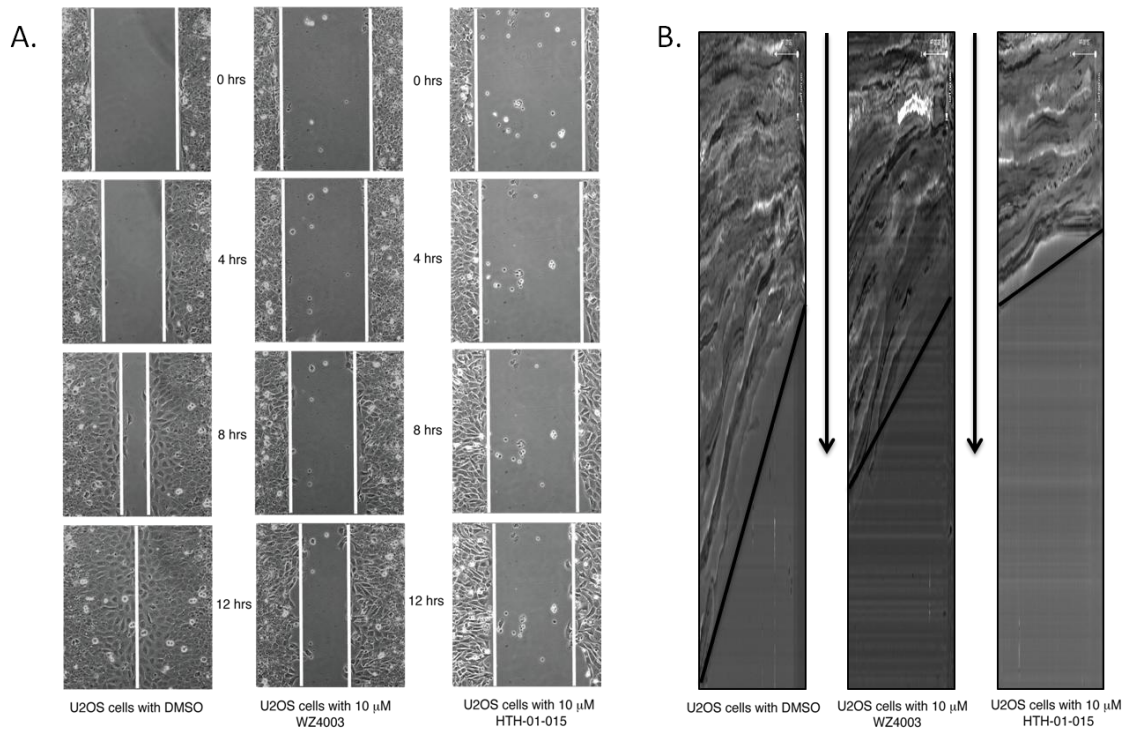

Figure 3.23: U2OS cells treated with NUAK1 inhibitors migrate slower into the wound. A) Wound-healing assay showing the total migration of cells into the 500 μm wound over 12 hours. B) Quantitative kymographs of A. where the arrows indicate direction of migration.

Phalloidin staining revealed that NUAK1$^{-/-}$ MEFs had more actin stress fibres than NUAK1$^{+/+}$ MEFs (Figure 3.24). This striking phenotype might explain the NUAK1$^{-/-}$ MEFs resistance to cell dissociation. To check whether that NUAK1 inhibitor treated NUAK1$^{+/+}$ MEFs could mimic the actin stress fibre phenotype of the NUAK1$^{-/-}$ MEFs, the NUAK1$^{+/+}$ MEFs were treated with or without 10 μM WZ4003 or HTH-01-015 and immunofluorescence was carried out using phalloidin-TRITC for actin staining. Both WZ4003 and HTH-01-015 treated cells exhibited more actin stress fibres as compared to the DMSO treated NUAK1$^{+/+}$ MEFs (Figure 3.24). Hence higher and more prominent actin stress fibres could contribute directly to the slower migration phenotype in NUAK1 deficient/ inhibited cells.

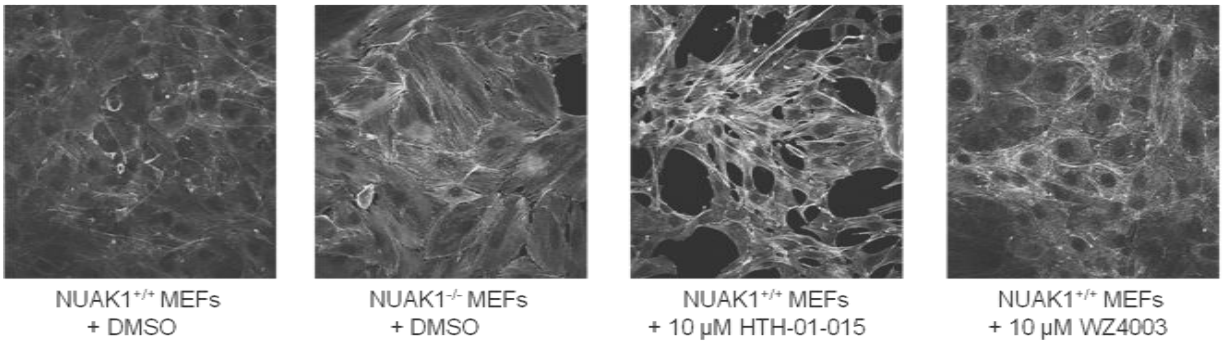

Figure 3.24: NUAK1 inhibitor treatments of NUAK1$^{+/+}$ MEFs lead to more prominent actin stress fibres consistent with the NUAK1$^{-/-}$ MEFs phenotype.

3.2.11. Inhibition of NUAK1 impairs cell proliferation

To compare the rate of cell proliferation in NUAK1 deficient/inhibited cells and normal cells, U2OS and NUAK1$^{+/+}$ MEFs cells with or without 10 µM WZ4003 or HTH-01-015 treated were used to assay cell proliferation over 5-6 days. For NUAK1$^{+/+}$ MEFs cell proliferation, NUAK1$^{-/-}$ MEFs were used as control cells to compare with the rate of proliferation in NUAK inhibitor treated NUAK1$^{+/+}$ MEFs. Inhibitor treated U2OS cells were found to proliferate at a significantly slower rate than the DMSO treated cells (Fig. 3.25A). Consistent with the U2OS cell proliferation data, NUAK inhibitor treated NUAK1$^{+/+}$ MEFs were proliferating at a dramatically slower rate than the DMSO treated NUAK1$^{+/+}$ MEFs. The NUAK inhibitor treated NUAK1$^{+/+}$ MEFs exhibited a rate of proliferation exactly similar to that of the NUAK1$^{-/-}$ MEFs (Fig. 3.25B).

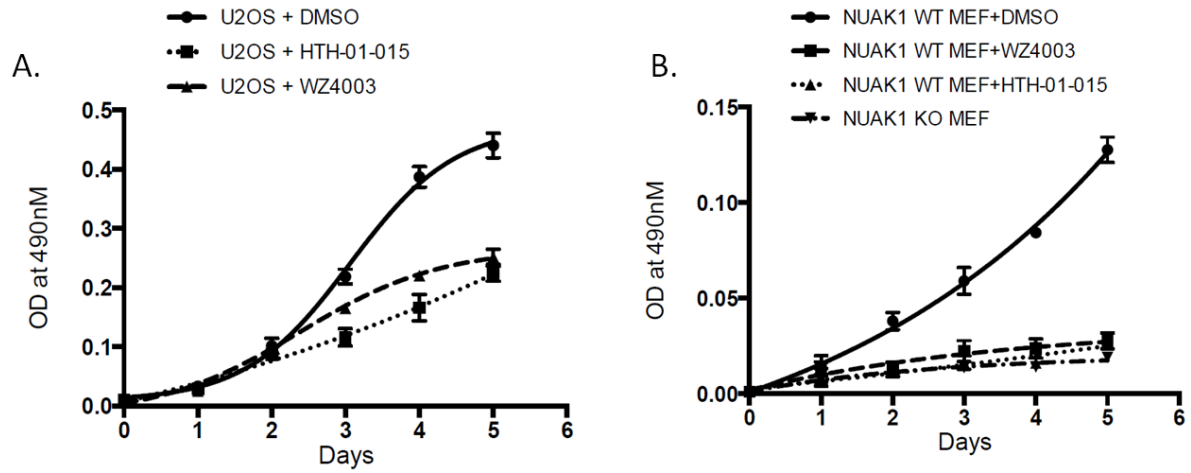

Figure 3.25 : NUAK1 inhibition impairs cell proliferation. A) Both WZ4003 and HTH-01-015 treated U2OS cells had reduced cell proliferation. B) NUAK1$^{+/+}$ MEFs treated with WZ4003 and HTH-01-015 mimicked the slow proliferation rate of NUAK1$^{-/-}$ MEFs.

3.2.12. Inhibition of NUAK1 reduces the invasive potential of U2OS cells

The invasive potential of U2OS cells treated with or without 10 µM HTH-01-015 and WZ4003 were compared using the growth factor reduced Matrigel^{TM} invasion chambers as mentioned in Section 2.2.29. The DMSO treated U2OS cells clearly invaded more potently into the Matrigel^{TM} matrix as compared to the NUAK inhibitor treated cells (Fig. 3.26). Snapshots of the inserts were taken and representative images are shown. Number of cells invading into the matrix were counted and represented as a standard deviation of the mean of triplicate images.

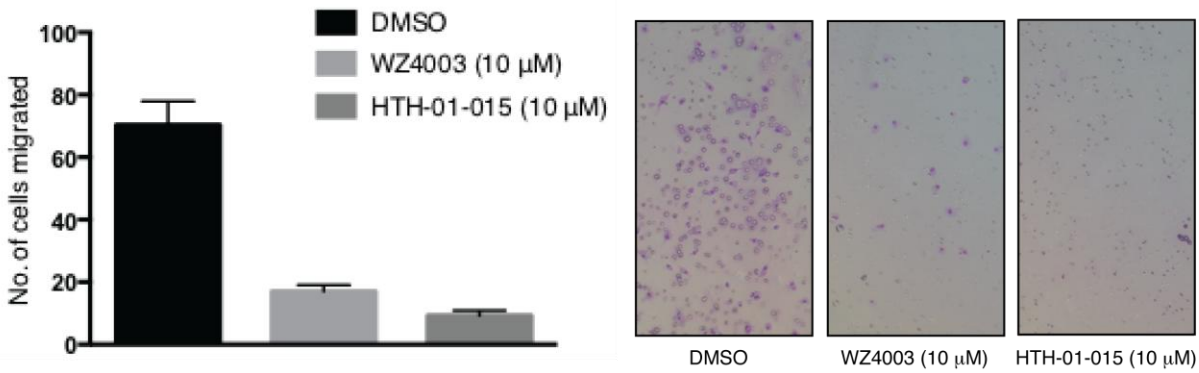

Figure 3.26 : NUAK1 inhibition reduced the invasive potential of U2OS cells by approximately 3 folds.

3.2.13. NUAK1 inhibition and its effect on deregulated MYC driven cancer cells

In 2011, Prof. Martin Eilers and Dr. Daniel Murphy's laboratory reported that NUAK1 was an essential factor involved in the survival of MYC driven tumours and cancer cells (Liu et al., 2012). They have shown that inhibition of NUAK1 either by RNAi or by using the inhibitor BX-795, cancer cells expressing deregulated oncogenic MYC underwent apoptosis (Liu et al., 2012). To test this new hypothesis, a panel of cancer cells were chosen to study the effect of the NUAK inhibitors on the ones over-expressing oncogenic MYC. Besides standard cancer cell lines, Dr. Victoria Cowling (MRCPPU, University of Dundee) provided me with IMEC (immortalised mammalian epithelian cells) expressing MYC and vector control (VEC) and TET21N neuroblastoma cells expressing doxycyclin inducible repressor of N-MYC (Lutz et al., 1996). To test the level of MYC in the cell lines, immunoblot was carried out and HEK293, HCT116 and SHSY5Y cells were found to overexpress c-MYC while U2OS, MDA-MB-231 and MDA-MB-468 expressed low levels of c-MYC (Fig 3.27A). TET21N cells were treated with or without 200 ng/ml doxycyclin and the expression of N-MYC was ascertained (Fig. 3.27B)

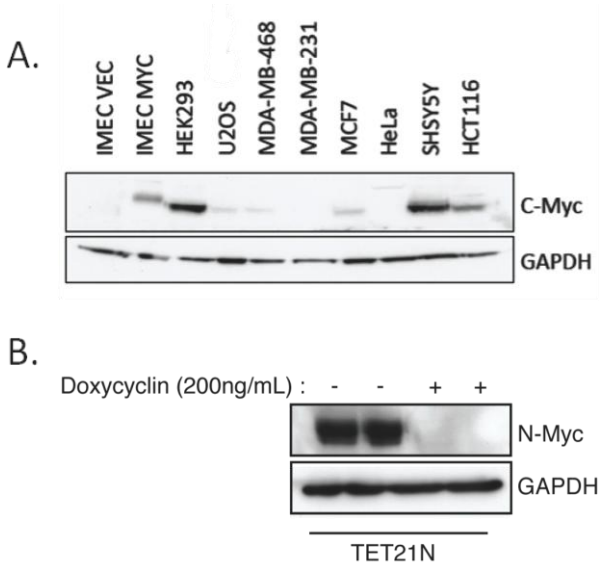

Figure 3.27 : Cell lines expressing oncogenic MYC. A) Various cancer cell lines were tested for MYC expression. B) Doxycyclin inducible repressor expressing TET21N cells were tested for N-MYC by immunoblotting with GAPDH as control.

3.2.13.1 shRNA mediated of knockdown of NUAK1 in TET21N induced cell death

Knockdown of NUAK1 was carried out in the high N-MYC expressing TET21N cells using two different shRNAs (section 2.2.9) and post puromycin selection, the cells were tested for growth and proliferation using the MTS assay (section 2.2.28). Strikingly, shRNA mediated knockdown of NUAK1 in TET21N cells led to rapid cell death within 5 days of selection (Fig. 3.28).

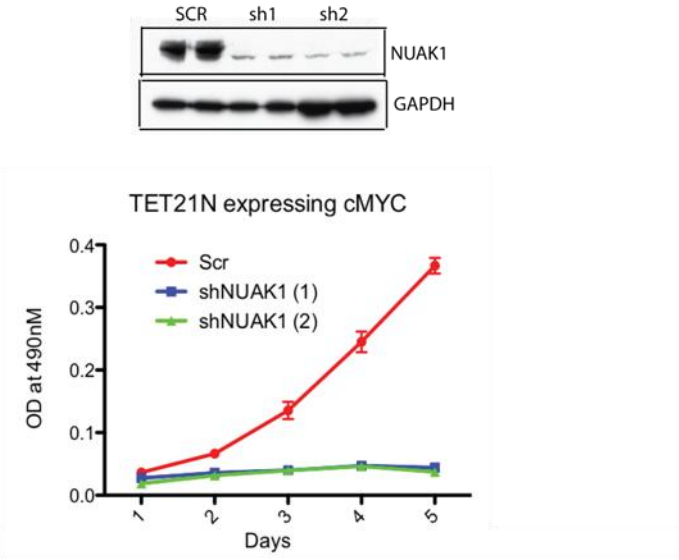

Figure 3.28 : shRNA knockdown of NUAK1 led to cell death in high N-MYC expressing TET21N cells. MTS assay was carried out over 5 days and optical density at 490 nM was used as the reading for cell proliferation.

An interesting observation was that the high sensitivity towards the shRNAs of NUAK1 in TET21N cells could not be rescued by addition of 200 ng/ml doxycyclin to repress the expression of MYC (Fig. 3.29). Hence, it was essential to ascertain whether this robust trigger of cell death was owing to NUAK1 inhibition alone or some off-target effects by the shRNA oligos.

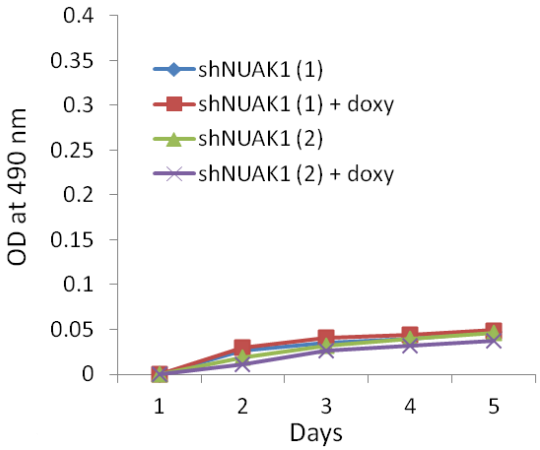

Figure 3.29 : MYC repression by 200ng/ml of doxycyclin could not rescue the TET21N cell death upon shRNA knockdown of NUAK1. MTS assay was carried out over 5 days and optical density at 490 nM was used as the reading for cell proliferation.

3.2.13.2. Second generation inhibitor XMD-18-42 induced apoptosis mediated cell death in high MYC expressing cancer cells.

The second generation 7-membered ring series inhibitor XMD-18-42 was initially used to probe into the role of NUAK1 in MYC driven tumour cells as the WZ4003 and HTH-01-015 compounds had not yet been elaborated. Interestingly, treatment of various concentrations of XMD-18-42 led to reduced cell proliferation and higher rate of cell death on IMEC MYC expressing cells as compared to the vector control (Fig. 3.30) although the cell death was not as striking as the shRNA data (Fig.3.28) . Cell proliferation rate was estimated using MTS assay (section 2.2.28).

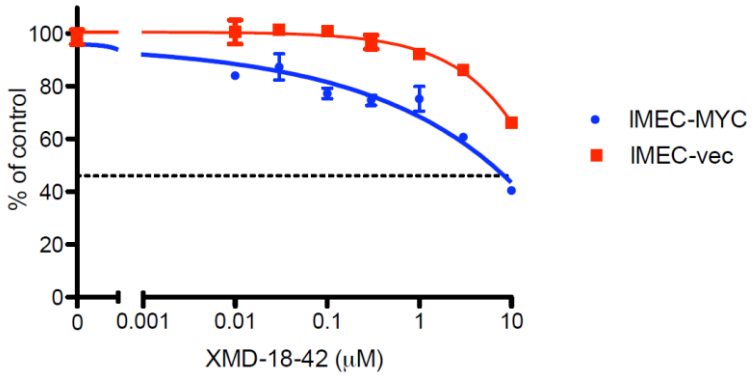

Figure 3.30. XMD-18-42 induced higher rate of cell death in MYC expressing IMEC cells as compared to the IMEC vector control cells. Dotted line represents Day 0 background counts. % of control represents % cell growth times Day 0 counts.

Consistent with the IMEC cells, XMD-18-42 also suppressed cell proliferation (Fig 3.31A) and induced higher rate of apoptosis (Fig 3.31B) in TET21N cells as compared to TET21N cells treated with doxycyclin (MYC repressed). Apoptosis was measured by staining cells with Caspase 3 antibody and number of active Caspase 3 cells were identified using flow cytometry (Section 2.2.26.2). Unlike the shRNA mediated cell death of TET21N in Fig.3.28, cell death induced by XMD-18-42 was far more modest (Fig. 3.31).

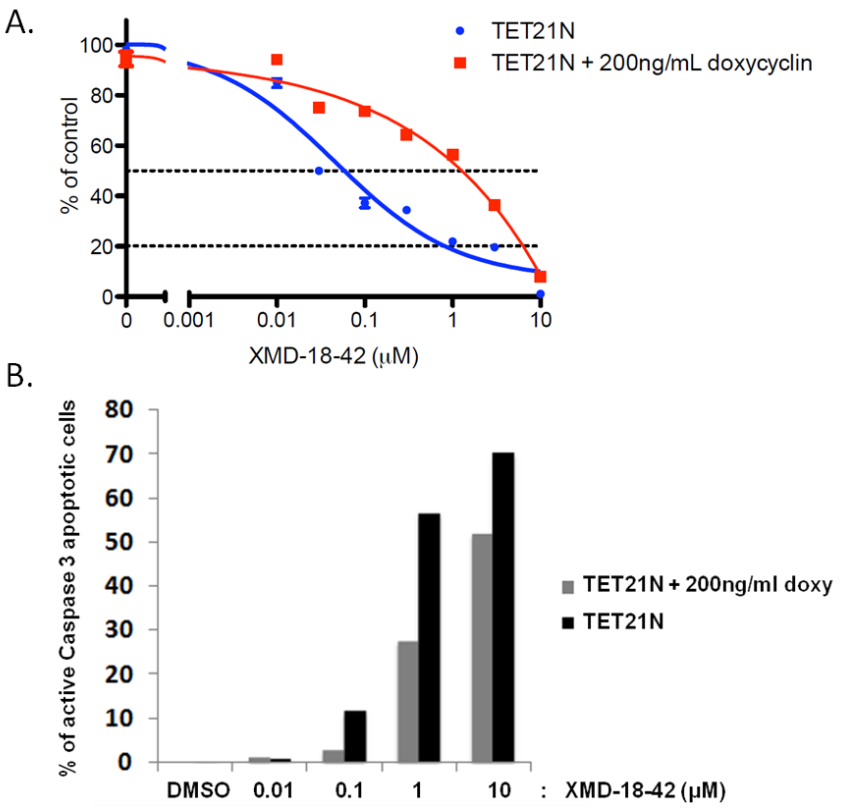

Figure 3.31 : XMD-18-42 induces faster rate of apoptosis in TET21N expressing high levels of N-MYC. A) MTS assay to study cell proliferation in TET21N cells with or without MYC suppression upon XMD-18-42 treatment. B) Flow cytometric measurement of active Caspase 3 expressing apoptotic cells was carried out to compare between TET21N cells with and without N-MYC suppression upon XMD-18-42 treatment.

To assess the role of NUAK1 in the apoptotic cell death induced by XMD-18-42, NUAK1 WT and NUAK1 [A195T] were stably overexpressed by retroviral transfection and puromycin selection in TET21N cells (Section 2.2.8). MTS assay was carried out upon XMD-18-42 treatment on TET21N NUAK1 WT and TET21N NUAK1 [A195T] with or without N-MYC suppression. TET21N cells expressing NUAK1 WT were moderately more sensitive to XMD-18-42 mediated cell death as compared to TET21N NUAK1 [A195T] or upon repression of N-MYC by doxycyclin (Fig. 3.32). Overall, this effect was not marked or consistent with the effect seen in the shRNA data (Fig. 3.28).

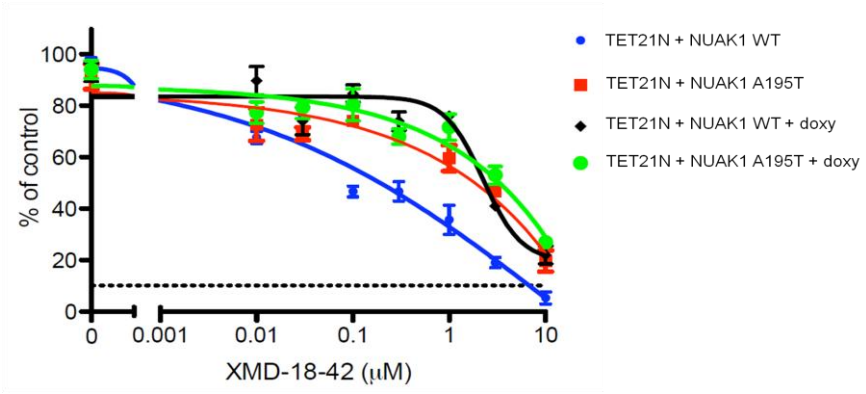

Figure 3.32 : TET21N cells stably expressing NUAK1 WT were more sensitive to XMD-18-42 induced cell death as compared to TET21N [A195T] and doxycyclin treated (MYC repressed) TET21N cells.

Besides IMECs and TET21N, effect of XMD-18-42 was tested on HEK293, HECT116, MCF-7 and MDA-MB-231 cells (Fig. 3.33A). As in Fig. 3.27A, HEK293 and HCT-116 had high expression of c-MYC while MCF-7 had low and MDA-MB-231 had lowest levels of c-MYC. Interestingly, XMD-18-42 seemed to have an effect somehwat directly proportional to the level of MYC in the cell lines. HEK293 and HCT-116 were most sensitive to the inhibitor, followed by MCF-7 while MDA-MB-231 had hardly any effect even at 10 µM inhibitor concentrations (Fig. 3.33A). To test the effect of XMD-18-42 on a larger panel of MYC driven cancer cell lines, Dr. Nathanael Gray's laboratory collaborated with Prof. Tom Look's laboratory at the Dana-Farber Cancer Centre (Harvard, USA). Prof. Tom Look's laboratory tested the effect of XMD-18-42 on a panel of 10 well established MYC driven tumour cells and found that a subset of MYC driven cancer cells were highly sensitive to XMD-18-42 (Fig.3.33B).

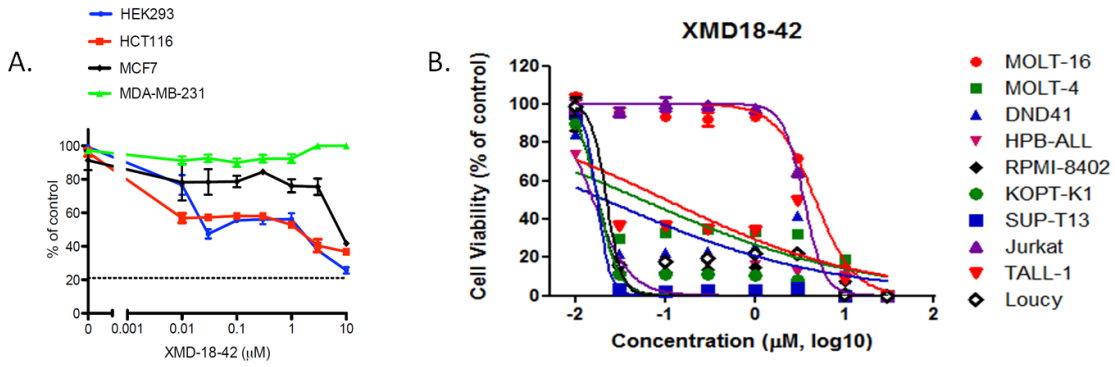

Figure 3.33 : XMD-18-42 induces cell death in a sub-set of MYC driven cancer cells. A) HEK293, HCT-116, MCF-7 and MDA-MB-231 cells were treated with XMD-18-42 and MTS cell proliferation assay was carried out. B) XMD-18-42 was tested by Prof. Tom Look's laboratory on the MYC driven cell line panel at Dana Farber Cancer Centre (Harvard, USA).

3.2.13.3. Aurora B inhibitor AZD1152-HQPA mimics XMD-18-42 induced cell death.

The major off-target effect that XMD-18-42 possess is on the Aurora kinases especially Aurora B (XMD-18-42 IC50 Aurora B 54 nM). Moreover, Aurora kinases have been previously reported to play significant role in maintaining the malignant state of MYC driven B-cell lymphomas (den Hollander et al., 2010). Hence to properly evaluate the roles of NUAK1 inhibition and Aurora B inhibition in the XMD-18-42 induced cell death, well established Aurora B inhibitor AZD1152-HQPA (Barasertib) (Yang et al., 2007) was used in parallel with the NUAK1 inhibitor. AZD1152-HQPA did not inhibit NUAK1 (retained >90% activity at 1 µM concentration) (Fig 3.34C) and possessed an IC50 of 15.5 nM for Aurora B and 193 nM for Aurora A.

AZD1152-HQPA clearly mimicked the cell death pattern induced by XMD-18-42 both in TET21N cells (Fig 3.34A) as well as in the Dana Farber Cancer Centre MYC

driven cell line panel (Fig. 3.34B) as tested by Prof Tom Look's laboratory (Harvard, USA). Since AZD1152-HQPA does not inhibit NUAK1 significantly, one could argue that the MYC dependent cell death was primarily owing to Aurora B inhibition and not just NUAK1 inhibition. To ascertain the contribution of NUAK1 inhibition in the cell death of MYC expressing cells, it was important to develop and test specific NUAK1 inhibitors which had no off-target on Aurora kinases.

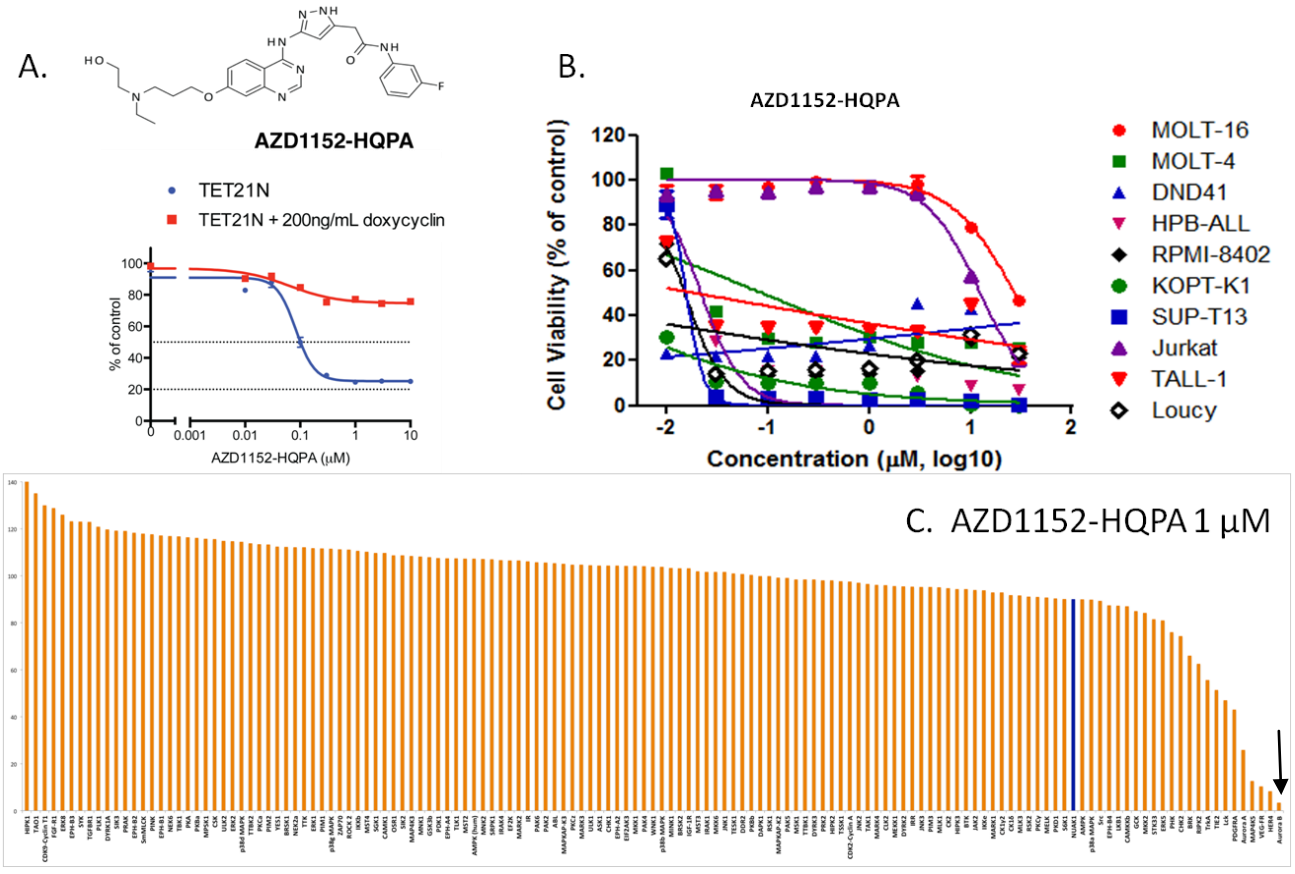

Figure 3.34: AZD1152-HQPA is a highly specific Aurora B inhibitor which mimicked the cell death pattern induced by NUAK1 inhibitor XMD-18-42. A) Structure of AZD1152-HQPA and MTS cell proliferation on TET21N cells upon AZD1152-HQPA treatment. B) Effect of AZD1152-HQPA on the deregulated MYC expressing cancer cell line panel at the Dana Farber Cancer Centre (Prof. Tom Look's laboratory, Harvard, USA). C) The kinase specificity panel for AZD1152-HQPA was carried out as described in section 2.2.30. Blue bar indicates NUAK1 and arrow indicates Aurora B.

3.2.13.4. NUAK1 inhibitors with insignificant off-target effects on Aurora kinases did not induce MYC expression selective cell death in TET21N cells

Various NUAK1 inhibitors of diverse structures were used to ascertain the contribution of NUAK1 inhibition in the MYC overexpression dependent cell death. The first and second generation 7-membered ring series of inhibitors JWE-071 and XMD-18-42 exhibited the MYC selective induction of cell death and both the inhibitors had major off-target effects on Aurora kinases (Fig. 3.4 and Fig. 3.8). The second generation XMD-18-83 had no off-target effects on Auroras (Fig. 3.9) and consequently did not exhibit any MYC selectivity (Fig. 3.35). Similar to XMD-18-83, the third generation 7-membered ring series highly selective and potent NUAK1 inhibitor HTH-01-015 also did not exhibit MYC selective cell death in TET21N cells (Fig. 3.35).

The 2,4,5-trisubstituted pyrimidine series of first and second generation NUAK inhibitors did not exhibit any specific MYC selective cell death in TET21N cells. HMSL10085, SJB4115 and WZ4003 have no off-target effects on Aurora kinases but are potent NUAK inhibitors (Fig. 3.35), hence absence of MYC selective cell death puts the whole concept of NUAK and MYC connection under a lot of controversy. Finally, the imidizolopyrimidine inhibitor WZ4074 did not have any significant effect on cell proliferation of either normal TET21N cells or on MYC repressed TET21N cells even at high 10 μM concentration (Fig. 3.35).

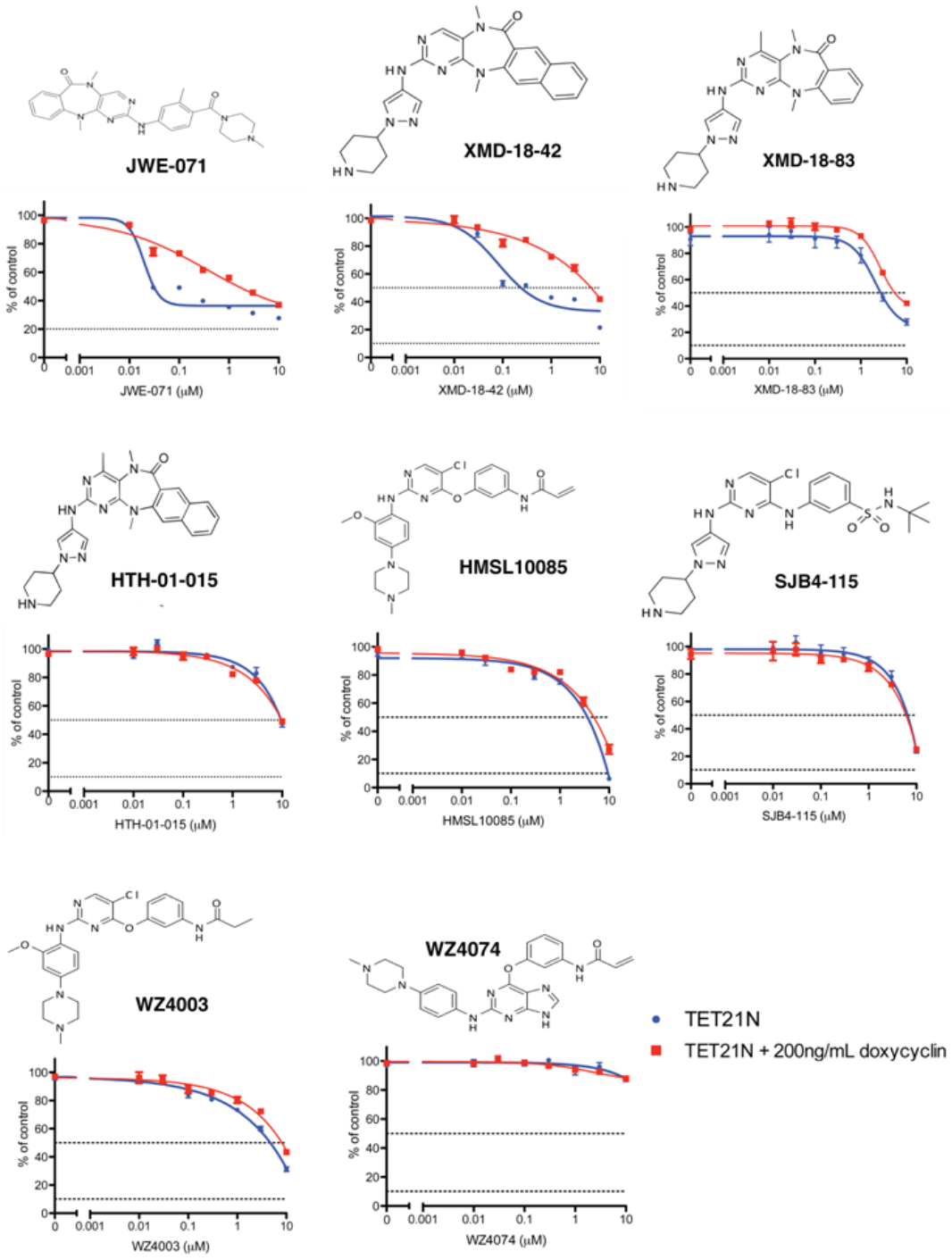

Figure 3.35: Specific NUAK1 inhibitors with no off-target effects on Aurora kinases did not exhibit MYC selective induction of cell death in TET21N cells

3.3. Discussion

Over the years, the LKB1 activated NUAK kinases have been found to be overexpressed in cancer, playing essential roles in cell migration, detachment and invasion properties (Kusakai et al., 2004a, Zagorska et al., 2010, Chang et al., 2012, Lu et al., 2013)and recently has been reported to be a vital antiapoptotic factor in deregulated MYC driven tumours (Liu et al., 2012). Moreover, all the 14 kinases in the AMPK family including NUAK isoforms could potentially possess overlapping substrates and regulatory properties owing to their highly homologous kinase domains and affinity towards the AMPK consensus phosphorylation motifs in the substrates (Zagorska et al., 2010). So, to properly dissect the role of the NUAK kinases and their potential contribution to cancer, it was important to develop highly specific small molecule tool compounds capable of selective inhibition of the NUAK isoforms. Initially, developing specific inhibitors to individual kinases within the AMPK family was deemed a rather challenging task owing to their highly homologous kinase domains. But the recent success of SIK (Clark et al., 2012) and MELK (Chung et al., 2012) inhibitors offered great encouragement that it may ultimately be possible to develop specific inhibitors to each of the AMPK family members. The only NUAK inhibitor in use is BX-795 which inhibits NUAK1 with nanomolar IC50 but is a rather generic inhibitor potently targetting many of the other AMPK family members, PDK1, TAK1, IKKε etc (Clark et al., 2009, Zagorska et al., 2010, Liu et al., 2012). Besides BX-795, Ambit Biosciences recently reported that may of the FDA approved anti-cancer drugs like sunitinib, dovitinib and TG101348 could potentially inhibit NUAKs with nanomolar IC50 but non-specific off-target effects on other kinases still persisting as a major issue (Davis et al., 2011).

To develop highly specific and potent inhibitors of NUAKs, we collaborated with Dr. Nathanael Gray's laboratory in Harvard, USA. The 7-membered ring backbone containing

LRRK2in1 was recently reported from our laboratory as a potent and highly selective inhibitor of LRRK2 a kinase mutated in Parkinson's disease (Deng et al., 2011). Interestingly, LRRK2in1 had off target effects on NUAK1 at 10 µM concentration. Based on the 7-membered ring backbone and on the trisubstituted pyrimidine backbone of BX-795, Dr. Gray's laboratory developed various generations of NUAK inhibitors (Fig. 3.1). IC50 values of all the inhibitors on NUAK1 in vitro is listed in the Table 3.2 below :

Table 3.2 : Summary of NUAK inhibitors. * indicates inhibitor possesses >10 off-targets, ** indicates inhibitor possesses 2-9 off-targets and *** indicates inhibitor possesses <2 off-targets in the Dundee protein kinase panel screening.

Series	Inhibitor	IC50 NUAK1 WT	IC50 NUAK1 A195T	IC50 NUAK2 WT	pS445 MYPT1 inhibition	Selectivity
7-membered ring	JWE-071	6 nM	1500 nM	-	10 µM	*
	XMD-17-51	1.5 nM	600 nM	-	10 µM	*
	DLW-01-125-01	7 nM	1500 nM	-	10 µM	*
	DLW-01-122-01	15 nM	2000 nM	-	10 µM	**
	XMD-18-42	30 nM	1000 nM	-	10 µM	**
	XMD -18-83	17 nM	-	-	-	*
	HTH-01-015	100 nM	5888 nM	> 11 µM	10 µM	***
2,4,5-trisubstituted pyrimidine	BX-795	5 nM	-	-	1-10 µM	*
	HMSL10085	25 nM	-	-	-	*
	SJB4-115	67 nM	-	-	-	*
	WZ4003	20 nM	900 nM	100 nM	3-10 µM	***
Imidizolopyrimidine	WZ4074	33 nM	-	-	-	*

To further test these inhibitors, a drug resistant mutant of NUAK1 was developed by mutating the Ala residue adjacent to subdomain VII DFG motif in the kinase domain to a bulky Thr residue. Based on previous studies, it has been hypothesized that mutating the Ala adjacent to the DFG motif into a Thr residue results in alteration of the stearic properties in the inhibitor docking pocket of the kinase without affecting the ATP-Mg^{2+} binding properties of the kinase (Nichols et al., 2009, Deng et al., 2011). Thus NUAK1 A195T mutant was developed which exhibited 40-400 times more resistance to the inhibitors as compared to the wild-type (Table 3.2) without altering the stability, expression levels or intrinsic kinase activity of NUAK1 (Fig. 3.3). In future, it would be interesting to generate inhibitor resistant

NUAK1 A195T knock-in mutations that could be used as a control to verify the cellular responses mediated by NUAK inhibitors which are desensitised by this mutation.

Since the only known well established substrate of NUAK is MYPT1, the inhibitors were tested for dose dependent inhibition of cell detachment induced pSer445 MYPT1 as an in vivo read out of NUAK activity. In previous work we have found that both NUAK1 and NUAK2 isoforms similarly phosphorylate and coimmunoprecipitate with MYPT1 (Zagorska et al., 2010). This may explain why in HEK293 cells we observe that the dual NUAK1 and NUAK2 WZ4003 inhibitor suppresses MYPT1 pSer445 phosphorylation more effectively (Fig, 3.18) than the NUAK1 selective HTH-01-015 inhibitor (Fig, 3.13). The effect of some of the inhibitors were also tested in cells stably overexpressing NUAK1 wild-type and A195T drug resistant mutant to compare. Besides pSer445 MYPT1, effect of NUAK inhibition in deregulated MYC expressing cancer cells were also observed with the inhibitors.

The first generation 7-membered ring series inhibitors potently inhibited NUAK1 and were more specific for NUAK as compared to BX-795 (Fig. 3.2). However, these inhibitors had an off-target effect on Aurora kinases. All four inhibitors JWE-071 (Fig. 3.4), XMD-17-51 (Fig. 3.5), DLW-01-122-01 (Fig. 3.7) and DLW-01-125-01 (Fig. 3.6) could inhibit NUAK1 induced pSer445 MYPT1 at 3-10 μM concentrations. Similar to the first generation, the second generation 7-membered ring series XMD-18-42 was very specific for NUAK1(Fig. 3.10) with off-target effects on Aurora kinases (Fig. 3.8). The first and second generation 7-membered ring series of inhibitors were initially tested in deregulated MYC expressing cancer cells. For this purpose, Dr. Victoria Cowling provided me with TET21N neuroblastoma cells expressing doxycyclin inducible repressor of N-MYC (Lutz et al., 1996) and IMEC cells expressing MYC or vector control (Fig. 3.27). Initially shRNAs targetting

NUAK1 was used in the N-MYC expressing TET21N cells. Interestingly, upon NUAK knockdown, the TET21N cells underwent cell death within 48 hours of puromycin selection (Fig. 3.28). But, upon treatment of doxycyclin to repress MYC expression, the cells could not be rescued (Fig. 3.29) which signifies that the cell death induced by shRNAs to NUAK1 was possibly independent of MYC expression. However, upon treatment of TET21N cells with JWE-071 (Fig. 3.35) or XMD-18-42 (Fig. 3.31), cells expressing MYC underwent a moderately faster rate of cell death as compared to MYC repressed TET21N cells. MTS assay and caspase3 apoptotic cell counting by flow cytometry were carried out in parallel to study TET21N cell death upon XMD-18-42 inhibitor treatments (Fig. 3.31). This was consistent in IMEC cells wherein XMD-18-42 induced MYC expressing IMEC cells to undergo moderately accelerated rate of cell death as compared to vector control (Fig. 3.30). Moreover, upon overexpressing NUAK1 A195T drug resistant mutant in TET21N cells, there was a moderate rescue of NUAK inhibitor induced cell death as seen in NUAK1 WT expressing TET21N cells (Fig. 3.32).

To further confirm whether there was indeed any link between MYC levels and the cell death caused by NUAK inhibitors, standard cells lines expressing varied levels of MYC were treated with XMD-18-42. Interestingly, there seemed to be a direct proportionality between rate of cell death and MYC expression (Fig. 3.33A). XMD-18-42 was further tested on the MYC driven cell line panel in Prof. Tom Look's laboratory at the Dana-Farber Cancer Centre and a subset of cancer cells were found to be highly sensitive to the inhibitor (Fig. 3.33B). However, Prof Tom Look's laboratory reported that the effects of XMD-18-42 on the MYC driven cell line panel was a mimic of the Aurora B inhibitor AZD-1152-HQPA (Fig. 3.34). Since XMD-18-42 had off-target effects on Aurora B (Fig. 3.8), Dr Gray's laboratory developed XMD-18-83 (Fig. 3.9) which could inhibit NUAK1 with similar potency as XMD-

18-42 but didnot possess any off-target effects on Aurora isoforms. Since XMD-18-83 was relatively less selective for NUAK1 as compared to XMD-18-42, Dr. Gray's laboratory developed 7-membered ring third generation inhibitor HTH-01-015 (Fig. 3.12) which was a hybrid of XMD-18-42 and XMD-18-83 which retained NUAK1 target potency while maintaining high selectivity.

HTH-01-015 was highly selective for NUAK1 and ablated pSer445 MYPT1 phosphorylation between 3-10 µM concentration in HEK293 cells (Fig. 3.13). HEK293 cells stably overexpressing NUAK1 A195T drug resistant mutant however didnot exhibit loss of pSer445 MYPT1 phosphorylation even at high 30 µM concentration of HTH-01-015 (Fig. 3.14) further confirming that pSer445 MYPT1 was indeed the best available read-out for the activity of NUAK1 in vivo. One interesting observation in the 7-membered ring series of NUAK inhibitors was that they didnot exhibit major inhibitory effect on NUAK2. DLW-01-122-01 and XMD-18-42 did not inhibit NUAK2 significantly (Fig. 3.11) whereas HTH-01-015 had an IC50 value of >11 µM in vitro for NUAK2 (Fig. 3.12C). There are no available crystal structures for the NUAK isoforms and since the inhibitors are ATP-competitive in nature, one can only speculate that some of the amino acids in the kinase domain of NUAK2 which are not homologous to NUAK1 (Gly173 in NUAK1 to Arg170 in NUAK2 or Thr73 in NUAK1 to Arg71 in NUAK2) could possibly be involved in altering the stearic properties of the inhibitor docking pocket in NUAK2 for the 7-membered ring series of inhibitors.

Besides the 7-membered ring series, Dr. Gray's laboratory also developed a series of trisubstituted pyrimidine series of inhibitors based on the structural backbone of BX-795 and TG-101348 (Fig. 3.1). The first generation pyrimidine series of inhibitors were less specific for NUAK1 (Fig. 3.15 and 3.16) as some of them like WZ4002 potently inhibited EGFR and

TEC-family kinases (Zhou et al., 2009). The second generation trisubstituted pyrimidine based inhibitor was a reversible analog of WZ4002 termed WZ4003 which was a highly potent and selective inhibitor of the NUAK isoforms (Fig. 3.17). Unlike the 7-membered ring series, WZ4003 potently inhibited both NUAK1 and NUAK2 (IC50 100 nM) (Fig. 3.17C) and ablated pSer445 MYPT1 phosphorylation between 3-10 µM (Fig. 3.18) which was rescued upon stably overexpressing NUAK1 A195T drug resistant mutant (Fig. 3.19).

Unlike XMD-18-42 or JWE-071, HTH-01-015 and WZ4003 treatment didnot exhibit any significant induction of MYC expression dependent cell death in TET21N cells (Fiig. 3.35). Most NUAK inhibitors which didnot possess any off-target effects on Aurora isoforms did not exhibit the MYC expression dependent cell death in TET21N cells (Fig. 3.35). This data signifies that the MYC dependent cell death observed upon treatment of XMD-18-42 and JWE-071 was owing primarily due to Aurora inhibition (den Hollander et al., 2010) and perhaps partly on NUAK1 inhibition. Also, one could argue that the highly selective NUAK inhibitors like HTH-01-015 and WZ4003 are not potent enough to exhibit the MYC dependent cell death. However, Nathanael Gray has also provided HTH-01-015 and WZ4003 to his colleagues at the Dana Farber Cancer Centre and they also reported no observed striking effects on panels of Myc driven tumour cells tested. A library of NUAK1 RNAi has been generated and the data is consistent with the no effects exhibited with the inhibitors. More work is required but this does cast some doubt on whether NUAKs are good drug targets for treatment of Myc driven tumours.

Since NUAK isoforms have been implicated in cell invasion and migration in cancer (Kusakai et al., 2004a, Kusakai et al., 2004b, Suzuki et al., 2004b, Namiki et al., 2011a, Namiki et al., 2011b, Chang et al., 2012, Lu et al., 2013), I wanted to test whether treatment

of cells with or without the inhibitors could have an effect on the proliferation, invasion and migration of various cells. We had previously reported that NUAK1$^{-/-}$ MEFs were more adherent than the NUAK1$^{+/+}$ MEFs and NUAK1$^{-/-}$ MEFs had more prominent actin stress fibre formation and did not exhibit pSer445 MYPT1 signal upon treatment with cell dissociation agonists like EDTA (Zagorska et al., 2010). Interestingly, NUAK1$^{-/-}$ MEFs exhibited a more adherent and a slower migration phenotype as compared to the NUAK1$^{+/+}$ MEFs (Fig. 3.21) and upon treatment of NUAK1$^{+/+}$ MEFs with 10 µM HTH-01-015 and WZ4003, the cells mimicked the slow migration phenotype of NUAK1$^{-/-}$ MEFs (Fig.3.22). The adherent and slower migration phenotype in the NUAK1 deficient and inhibited cells could be a result of more focal adhesion points and higher actin stress fibres formation as observed in Fig 3.24. Besides the MEFs, similar slower migration was observed in U2OS cells treated with or without 10 µM HTH-01-015 and WZ4003 (Fig. 3.23) thus further providing evidence of the possible role of NUAKs in cell migration.

Besides cell migration, treatment of U2OS and NUAK1$^{+/+}$ MEFs with 10 µM HTH-01-015 and WZ4003 led to slower rate of cell proliferation which in the case of MEFs is consistent with the slow proliferating NUAK1$^{-/-}$ MEFs (Fig. 3.25). Previous studies have exhibited the role of NUAK1 in cell proliferation wherein NUAK1 directly phosphorylates p53 at Ser15 and Ser392 (Hou et al., 2011). Further work is required to establish possible role of NUAK isoforms in the cell cycle and proliferation. Various groups have also shown that NUAK1 plays essential roles in cancer cell invasion which was further confirmed in U2OS cells. Treatment of U2OS cells with 10 µM HTH-01-015 and WZ4003 led to an approximately 70-80% decrease in the number of cells invading into the Matrigel matrix as compared to the DMSO treated control (Fig. 3.26).

Thus, the data in this chapter indicate that WZ4003 and HTH-01-015 represent useful tools to dissect the physiological functions of NUAK kinases. These compounds are remarkably selective inhibitors, however, ablation of MYPT1 pSer445 phosphorylation, effects on cell migration, invasion, proliferation and MYC dependant cell death analysis indicate that these compounds will need to be used at relatively high concentrations of 3 to 10 μM in order to maximally suppress NUAK activity in vivo. Since WZ4003 inhibits both NUAK1 and NUAK2 while HTH-01-015 is NUAK1 specific, comparing the effects of the inhibitors in vivo would also be insightful into the relative contribution of NUAK isoforms in physiological processes. In future, it would be interesting to develop more potent NUAK inhibitors with an EC50 of < 1 μM instead of 3 to 10 μM which could potentially provide further insight into the NUAK-MYC connection in cancer. Better potency is required to properly dissect the role of NUAK1 in regulating survival of MYC driven tumours. Furthermore, generation of NUAK1 drug resistant A195T knock-in cell lines would help in the identification of novel substrates of NUAKs via phosphoproteomic studies with and without treatment of inhibitors in parallel to wild-type cells.

Thus, the success of the NUAK specific compounds provide yet further evidence that it is indeed possible to generate exquisitely specific inhibitors of the individual AMPK family kinases.

4. Role of $SCF^{\beta TRCP}$ in regulating NUAK1 in the cell cycle

4.1. Introduction

Amidst the RING E3 ubiquitin ligases, the most widely studied ones are the anaphase promoting complex/cyclosome (APC/C) and the SKP1-Cullin-F-box (SCF) complexes (Fig 4.1).

The APC/C complex (Fig 4.1a) is primarily active in the cell cycle and the APC core is formed of atleast 14 different subunits of which APC2 acts as the primary scaffold, APC11 acts as the E2 recruiting subunit and substrate adaptors Cdh1 or CDC20 which recognise substrate destruction motifs or degrons (Barford, 2011, Teixeira and Reed, 2013). APC/C^{CDC20} preferentially targets the D-box on substrates (consensus RxxLxxxxN) while APC/C^{Cdh1} targets both D-box and the KEN box motifs (consensus KENxxxN/Q) (Glotzer et al., 1991, Pfleger and Kirschner, 2000).

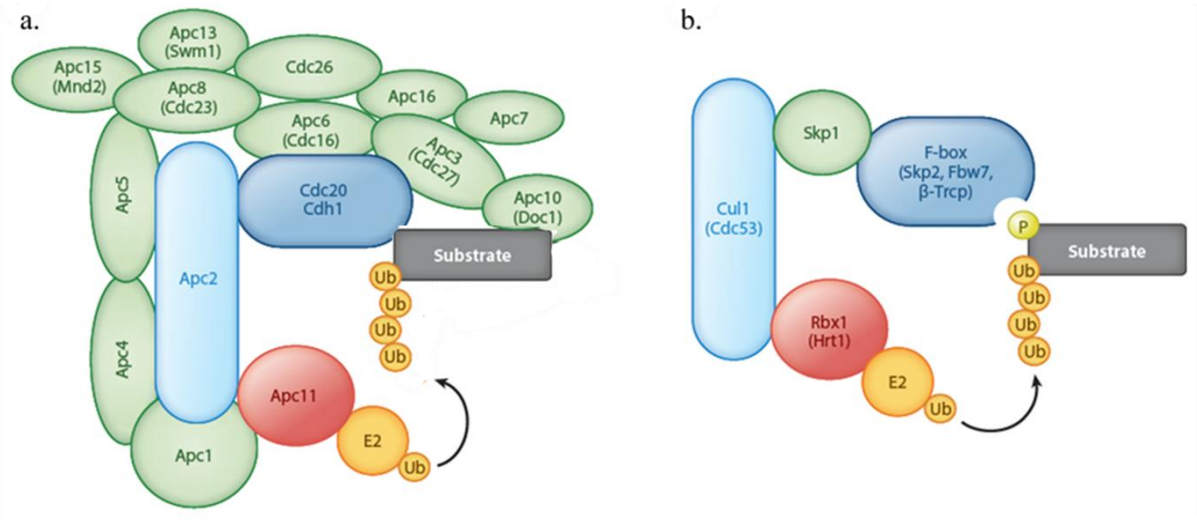

Figure 4.1 RING domain E3 ligases : a) The multisubunit APC/C complex which interacts with either Cdh1 or CDC20 substrate recognition subunits to target substrates for degradation primarily by Lys11 linked polyubiquitin chains. b) The SCF complex E3 ligases which generally require a phosphodegron on the substrates for docking followed by Lys48 linked polyubiquitylation and degradation. Image adapted from (Teixeira and Reed, 2013).

In mammals, there are six different types of CRLs or Cullin-RING E3 ligases of which SCF (SKP-Cullin-F-box) ubiquitin ligases are the most well characterised (Frescas and Pagano, 2008). The SCF E3 ubiquitin ligases consists of three essential subunits (Fig 4.1b). The RING-subunit ring box 1 or RBX1 catalyses the transfer of a ubiquitin-like NEDD8 molecule onto a conserved residue of the Cullin 1 (Cul1) scaffold which leads to autoactivation of the complex (Scott et al., 2010). S-phase kinase associated protein 1 or SKP1 is an adaptor which recruits the variable F-box or substrate recognition box on the SCF complex (Teixeira and Reed, 2013). Phosphorylation of specific motifs on the substrates, referred to as phosphodegrons, are generally the docking sites of the F-box sub-units of the SCF complex and almost all of the best studied SCF complexes leads to Lys48 link polyubiquitylation and degradation of its substrates (Frescas and Pagano, 2008).

The F-box subunit is the SCF substrate recognition motif which generally requires a post-translation modification (eg. phosphorylation) to interact with the substrate. The 69 identified F-box proteins have been classified into three major groups : FBXWs or the WD40 domain containing, FBXLs or leucine-rich repeat containing and FBXOs with diverse domains (Frescas and Pagano, 2008).

Amidst the 69 F-boxes identified to date, 9 SCF ubiquitin ligases have been extensively characterised of which βTRCP is the most highly studied exhibiting roles in cell cycle, DNA damage, apoptosis, transcription, translation, telomere length, viral replication, autophagy, cell growth and proliferation. A list of most studied $SCF^{\beta TRCP}$ substrates has been listed in Table 4.1. In mammals, there are two distinct homologues of βTRCP namely βTRCP1 (BTRC, FBXW1, FBW1A and FWD1) and βTRCP2 (FBXW11, FBW11, FBXW1B, FBX1B and HOS) with indistinguishable biochemical properties (Frescas and Pagano, 2008). βTRCP

binds to its substrate at a well conserved destruction motif or degron DSGxxS or its variants (DSG/DDG/ESGxxS/EEG/SSGxxS/E/D motifs) in which the Ser residues require prior phosphorylation by an upstream kinase (Table 4.1).

Table 4.1 : Substrates of $SCF^{\beta TRCP}$

Substrate	Function	Kinases	Reference
Atf4	Transcription		(Skaar et al., 2009)
Auf1	Cytokine translation		(Li et al., 2013)
β-catenin	WNT signalling	GSK3, CK1	(Skaar et al., 2009)
BimEL	Apoptosis induction	RSK1, RSK2	(Skaar et al., 2009)
Bora	Spindle stability	GSK3, PLK3	(Skaar et al., 2009)
Bst2	HIV infection		(Douglas et al., 2009)
Cdc25a	Cell cycle	CHK1, NEK11	(Sorensen et al., 2010)
Cdc25b	Cell cycle		(Skaar et al., 2009)
Claspin	DNA damage	PLK1	(Skaar et al., 2009)
Cortactin	Cell motility	ERK	(Zhao et al., 2012a)
Cyclin D1	Cell cycle		(Skaar et al., 2009)
Deptor	Cell growth and autophagy	CK1	(Wang et al., 2012b)
Dlg	Cell contact and polarity		(Skaar et al., 2009)
Ef2k	Translation	PKA, AMPK	(Wiseman et al., 2013)
Emi1	Cell cycle	PLK1	(Skaar et al., 2009)
FancM	DNA damage	PLK1	(Skaar et al., 2009)
Fgd1 & Fgd3	Cdc42 regulation		(Skaar et al., 2009)
Ghr	Growth hormone signalling		(Skaar et al., 2009)
H-Ras	GTPase, cell growth,signalling		(Skaar et al., 2009)
Hsf1	Transcription	PLK1	(Skaar et al., 2009)
HuR	mRNA stability	IKKα	(Chu et al., 2012)
Ifnr	Cytokine signalling		(Skaar et al., 2009)
IκBα	Immune signalling	IKKβ	(Skaar et al., 2009)
IL-10R1	Immune signalling		(Jiang et al., 2011)
Irak1	Immune signalling		(Cui et al., 2012)
Mcl1	Apoptosis inhibition	GSK3	(Skaar et al., 2009)
Mdm2	DNA damage	CK1	(Wang et al., 2012a)
Myc	Cell proliferation		(Popov et al., 2010)
Nrf2	Transcription	GSK3	(Chowdhry et al., 2012)
p100 & p105	Transcription	IKKα, IKKβ	(Skaar et al., 2009)
p53	Tumor suppressor	IKK2	(Skaar et al., 2009)
p63	Epithelial differentiation		(Skaar et al., 2009)
Pc2	Calcium signalling		(Skaar et al., 2009)
Pdcd4	Protein synthesis	S6K1	(Skaar et al., 2009)
Per1 & Per2	Circardian rhythm	CK1	(Skaar et al., 2009)
Pfkfb3	Glycolysis		(Tudzarova et al., 2011)
Phlpp1	Akt signalling		(Zhiqiang et al., 2012)
Plk4	Cell cycle	Auto-PLK4	(Mocciaro and Rape, 2012)

Prl-R	Growth hormone signalling		(Skaar et al., 2009)
Pro-caspase 3	Apoptosis		(Skaar et al., 2009)
Securin	Spindle checkpoint		(Skaar et al., 2009)
Rassf1c	DNA damage	GSK3	(Zhou et al., 2012)
Rcan1	Calcineurin-dependent signalling		(Skaar et al., 2009)
Rest	Cell cycle, differentiation		(Skaar et al., 2009)
Spar	Signal transduction	PLK2	(Skaar et al., 2009)
Smad3	TGF signalling		(Skaar et al., 2009)
Snail	EMT	GSK3	(Skaar et al., 2009)
Stat1	Transcription		(Skaar et al., 2009)
Taz	Transcription	LATS, GSK3	(Huang et al., 2012)
Trf1	Telomere length		(Wang et al., 2013)
Twist	EMT	IKKβ	(Zhong et al., 2013)
Uhrf1	DNA damage	CK1	(Chen et al., 2013a)
VEGFR	Angiogenesis and cell migration	CK1	(Shaik et al., 2012)
Wee1	Cell cycle	PLK1, CDK1	(Skaar et al., 2009)

βTRCP was first identified in Drosophila as Slimb which was found to negatively regulate Wnt and Hedgehog signalling pathway (Jiang and Struhl, 1998). In the absence of Wnt, a complex of GSK3β, CK1, APC, and axin associates with and phosphorylates β-catenin at the βTRCP interaction degron which targets β-catenin for ubiquitylation followed by 26S proteasomal degradation. In the presence of Wnt this process is blocked, leading to the accumulation of β-catenin, which functions as a coactivator for the transcription factor TCF/LEF-1. The β-catenin/TCF/LEF-1 complex then activates downstream genes in the Wnt pathway (Maniatis, 1999) (Fig. 4.2b). Besides Wnt pathway, $SCF^{\beta TRCP}$ also plays an essential role in the inflammatory NFκB activation pathway (Maniatis, 1999) (Fig. 4.2a). A variety of signals, like tumor necrosis factor-α (TNFα) lead to the activation of an IκB–kinase complex (IKK), which specifically phosphorylates Ser32 and Ser36 on the βTRCP interaction degron of IκBα. This phosphorylation leads to $SCF^{\beta TRCP}$ interaction, Lys48 linked polyubiquitylation at Lys21 and Lys22 of IκBα and degradation, resulting in the release and nuclear translocation of NFκB (Maniatis, 1999) (Fig. 4.2a).

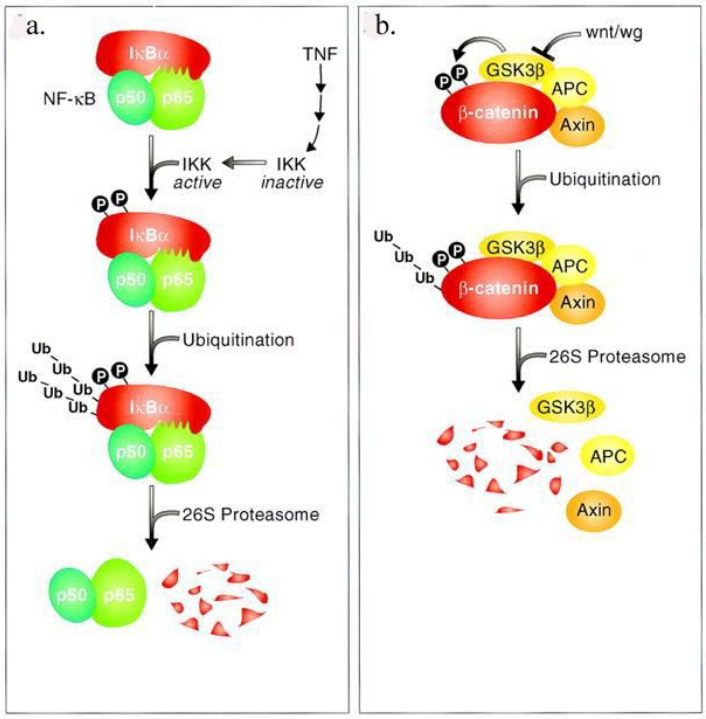

Figure 4.2. The role of the SCF$^{\beta TRCP}$ in the regulated degradation of (a) IκBα in NFκB activation pathway and (b) β-catenin in the Wnt signalling pathway. Image taken from (Maniatis, 1999).

SCF$^{\beta TRCP}$ also plays pivotal roles in S-G2 DNA damage checkpoints as well as in controlling the activity of CDK1 in various stages of cell cycle by targetting CDC25 phosphatases, claspin and Wee1 for degradation (Bassermann et al., 2013) which has been described in details in Section 1.6. Besides cell cycle, SCF$^{\beta TRCP}$ exhibits diverse substrate specificity and it was initially hypothesized that βTRCP could possess both tumour suppressor and oncogenic properties. But recently various studies have revealed that βTRCP1 is overexpressed in 56% of colorectal cancer tissues exhibiting decreased apoptosis (Ougolkov et al., 2004), in pancreatic cancer cells which have constitutively active NFκB (Muerkoster et al., 2005) and in hepatoblastomas (Koch et al., 2005). Some breast cancer cells exhibited βTRCP2 overexpression (Spiegelman et al., 2002).

In 2003, Prof. Keichi Nakayama's laboratory in Japan reported the βTRCP1$^{-/-}$ mice (Nakayama et al., 2003). The mice were generally viable but exhibited reduced fertility

owing to impaired spermatogenesis (Nakayama et al., 2003, Guardavaccaro et al., 2003). Further studies revealed that the βTRCP1$^{-/-}$ mice exhibited centrosome overduplication, and a longer transition through G2-M stage of cell cycle (Frescas and Pagano, 2008). The relatively modest phenotype exhibited by the βTRCP1$^{-/-}$ mice may be owing to the redundancy with βTRCP2 which can compensate for the loss of βTRCP1 and still target SCF$^{\beta TRCP}$ substrates for degradation (Frescas and Pagano, 2008).

Owing to the links between E3 ubiquitin ligases and cancer, various inhibitors have been developed like MG132, lactacystin and bortezomib which inhibit the proteasome thereby protecting E3 ubiquitin ligase substrates from degradation (Shirley et al., 2005). In 2003, bortezomib was approved by FDA for treatment against multiple myeloma and hence is the first and only proteasome inhibitor to enter the drug market (Orlowski and Kuhn, 2008). Recently MLN-4924, a specific CRL inhibitor has exhibited promising pre-clinical efficacy and has entered into multiple Phase I trials against various malignancies (Soucy et al., 2009a, Soucy et al., 2009b). The advantage of MLN-4924 over the other proteasome inhibitors is that the small molecule specifically inhibits the neddylation of the cullin and hence inhibits the CRL complexes only (Zhao et al., 2012b). Instead of targeting the proteasome, MLN-4924 inhibits NEDD8-activating enzyme by forming a covalent adduct with NEDD8 which can no longer be utilized to neddylate the cullin (Brownell et al., 2010). This leads to the accumulation of the substrates which are targetted specifically by CRLs for degradation (Zhao et al., 2012b).

In this chapter, I shall provide evidence of how NUAK1 is regulated over the cell cycle via its interactions with SCF$^{\beta TRCP}$ and try to elucidate any role which NUAK1 might possess in the cell cycle.

4.2. Results

4.2.1. Identification of NUAK1 interacting proteins using Orbitrap mass spectrometry

In order to identify novel regulators or interactors for NUAK1, I used the Flp-in U2OS cells to generate HA-NUAK1 expressing stable U2OS cell line. For the identification of physiological interactors of NUAK1, lysates from U2OS stable cells expressing HA-NUAK1 or HA-empty control cells were immunoprecipitated with anti-HA agarose (Figure 4.3). After in gel tryptic-digest, peptides were subjected to Orbitrap LC-MS mass fingerprint analysis. Table 4.2 shows the list of proteins that were present in the HA-NUAK1 lane but not in the control sample lane. The list was also filtered for proteins with a molecular weight matching the gel section in which they were identified. A Mascot score of >50 was taken as cut-off. As expected, the bait protein, NUAK1, was identified in the gel band corresponding to the molecular weight of NUAK1. Importantly, known interactors, USP9X (Al-hakim et al., 2008), myosin phoshatases MYPT1, MYPT2 and MBS85 (Zagorska et al., 2010), ubiquitin (Al-hakim et al., 2008) and PP1β (Zagorska et al., 2010) were identified with significant Mascot scores (Table. 4.2).

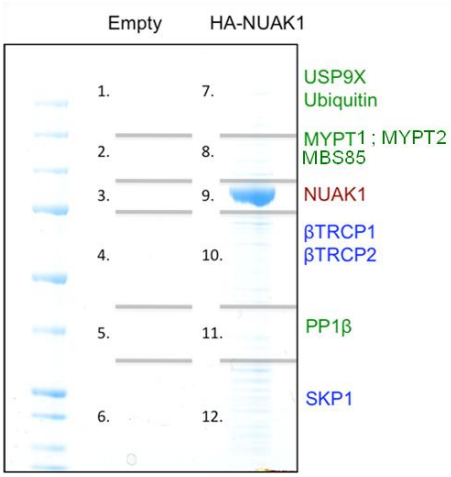

Figure 4.3 : Large scale immunoprecipitation of HA-NUAK1 for mass spectrometry. U2OS FLPIN cells control or with overexpression of HA-NUAK1 were lysed using 1% Triton-X lysis buffer. HA-NUAK1 was immunoprecipitated and electrophoresed on a polyacrylamide gel that was stained with Instant Blue. The gel was divided into the indicated pieces and proteins were identified within these sections by Orbitrap LC/MS. Published interactors are indicated in **green**, bait protein NUAK1 is in **red** and novel interactors are in **blue**.

In addition, NUAK1 was found to interact with βTRCP1 and βTRCP2 which are two isoforms of the substrate recognition F-box subunits of the $SCF^{\beta TRCP}$ E3 ubiquitin ligase complex as well as SKP1 which is an adaptor protein which interacts with the F-box domain of the F-box subunit and links it to the Cullin 1 in the SCF complex.

Table 4.2 : NUAK1-interacting proteins identified by mass spectrometry.
The gel pieces indicated in Figure 4.1 were digested with trypsin and proteins were identified by Orbitrap mass spectrometry. The identified proteins of importance that were present only in the NUAK1 immunoprecipitate (bands 7-12) but not in the control (bands 1-6) are listed. Mascot protein score where a value >50 is considered significant.

Gel Band	Symbol	Protein name	Mass [Da]	Mascot	Peptides	Reference
band 7	USP9X	USP9X	293699	327	15	(Al-hakim et al., 2008)
	MYH9	Myosin-9	227646	179	9	-
	UBB	Ubiquitin	18295	88	4	(Al-hakim et al., 2008)
band 8	PPP1R12A	Myosin phosphatase regulatory subunit 1 (MYPT1)	115610	2798	42	(Zagorska et al., 2010)
	PPP1R12B	Myosin phosphatase regulatory subunit 2 (MYPT2)	110793	289	18	(Zagorska et al., 2010)
	PPP1R12C	Myosin binding subunit 85 (MBS85)	85286	123	4	(Zagorska et al., 2010)
	UBB	Ubiquitin	18295	72	2	(Al-hakim et al., 2008)
band 9	NUAK1	NUAK family Snf1 like kinase 1	74772	4236	234	bait
band 10	**βTRCP1**	**β transducin repeat containing protein 1**	**66262**	**315**	**21**	-
	βTRCP2	**β transducin repeat containing protein 2**	**61772**	**208**	**17**	-
band 11	PPP1CB	Serine/threonine protein phosphatase PP1β catalytic subunit	37961	489	18	(Zagorska et al., 2010)
band 12	YWHAE	14-3-3 protein epsilon	29326	987	41	(Zagorska et al., 2010)
	SKP1	**S-phase kinase associated protein 1**	**18817**	**51**	**2**	-
	UBB	Ubiquitin	18295	56	2	(Al-hakim et al., 2008)

4.2.2. Verification of βTRCP as an interactor of NUAK1

To verify the interaction between NUAK1 and βTRCP at both the overexpressed and endogenous levels, I carried out co-immunoprecipitation experiments and looked for the interaction of endogenous NUAK1 and overexpressed FLAG-NUAK1 with endogenous βTRCP keeping endogenous MYPT1 as a control for co-immunoprecipitation. Endogenous NUAK1 was immunoprecipitated from 5 mgs of U2OS cell lysate and immunoblotting analysis revealed that it strongly interacted with MYPT1 and also exhibited a comparatively much weaker interaction with βTRCP (Fig. 4.4A). Overexpressed FLAG-NUAK1 strongly immunoprecipitated with MYPT1and PP1β (Fig. 4.4B). βTRCP clearly immunoprecipitated with overexpressed FLAG-NUAK1 (Fig. 4.4B).

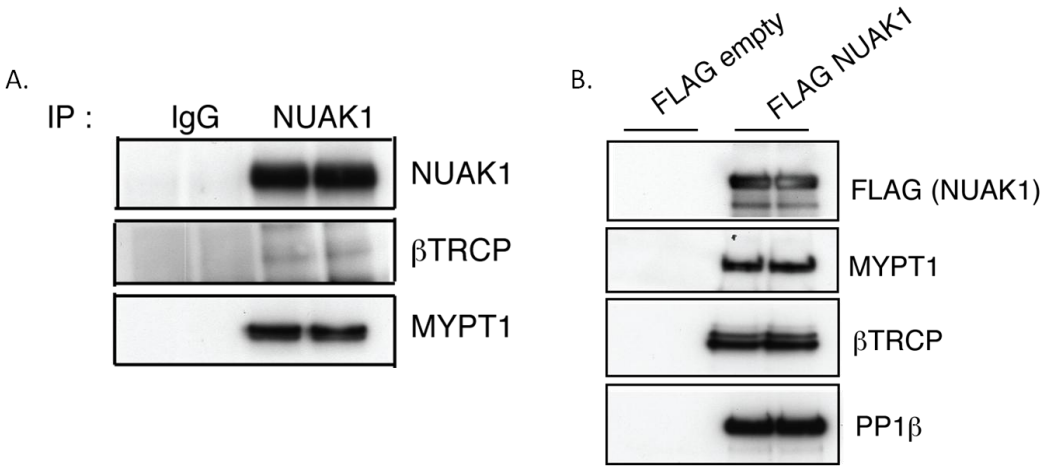

Figure 4.4 : βTRCP co-immunoprecipitates with NUAK1. A) Endogenous NUAK1 was immunoprecipitated from 2 mgs of U2OS cell lysate. Immunoprecipitates were analysed by immunoblotting with the indicated antibodies. B) Overexpressed FLAG-NUAK1 was immunoprecipitated from U2OS cells transfected with a construct for FLAG-NUAK1 for 36 hrs. Immunoprecipitates were analysed by immunoblotting with the indicated antibodies. βTRCP antibody was used which is a βTRCP1 and βTRCP2 dual antibody. βTRCP isoforms possess indistinguishable functions within a cell.

4.2.3. βTRCP interacts with NUAK1 and NUAK2 but not other AMPK related kinases

In order to determine if the interaction with βTRCP is specific to NUAK kinases or also occurs with other AMPK-related kinases, I transfected HEK293 cells with 10 meembers of

the AMPK family kinases (GST-tagged NUAK1, NUAK2, MARK1-4, BRSK1-2 and SIK1-2). βTRCP1 co-immunoprecipitated with the NUAKs (Figure 4.5). Other than the NUAK isoforms, the only other AMPK related kinase found to interact with βTRCP1 albeit very weekly was SIK2.

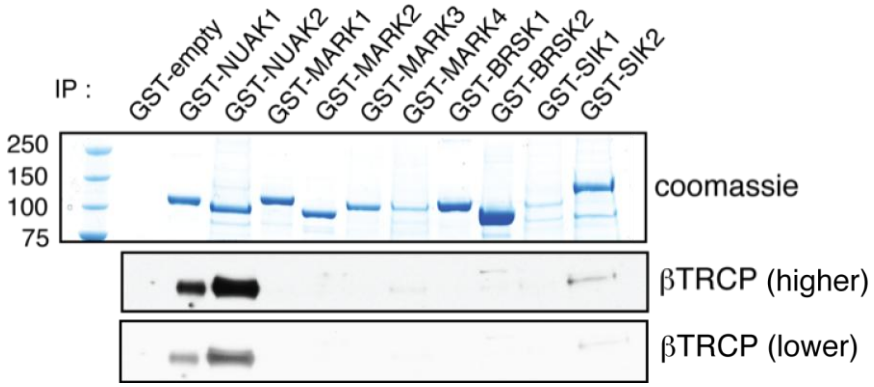

Figure 4.5 : βTRCP interacts with NUAKs but not other AMPK related kinases.
HEK293 cells were transfected with expression plasmids for GST-tagged AMPK related kinases. 36 hrs after transfection cells were lysed and GST-tagged proteins were immunoprecipitated from 5 mg of cell lysates. Immunoprecipitates were analysed by either coomassie staining for GST-tagged proteins or by immunoblotting with βTRCP antibody.

4.2.4. Mapping the $SCF^{\beta TRCP}$ interaction motif or 'degron' on NUAK1

As outlined in the introduction, βTRCP or the substrate recognition motif $SCF^{\beta TRCP}$ interacts with its substrate via conserved destruction domain or degron on the substrate which bears the canonical or slightly modified amino acid sequence of DSGxxS where the two Ser residues require prior phosphorylation by an upstream kinase.

I next inspected the sequence of both NUAK1 and NUAK2 to see whether they contained the βTRCP degron motif that could account for their interaction with βTRCP. Sequence analysis revealed that NUAK1 and NUAK2 possessed the highly conserved ESGYYS degron motif. Both in NUAK1 and NUAK2, the ESGYYS degron is highly conserved within the vertebrate

orthologues upto zebrafish (*Danio spp.*) (Fig. 4.6). In NUAK2 of zebrafish, the degron is modified into a ESSCCS motif which could still possess βTRCP interaction properties.

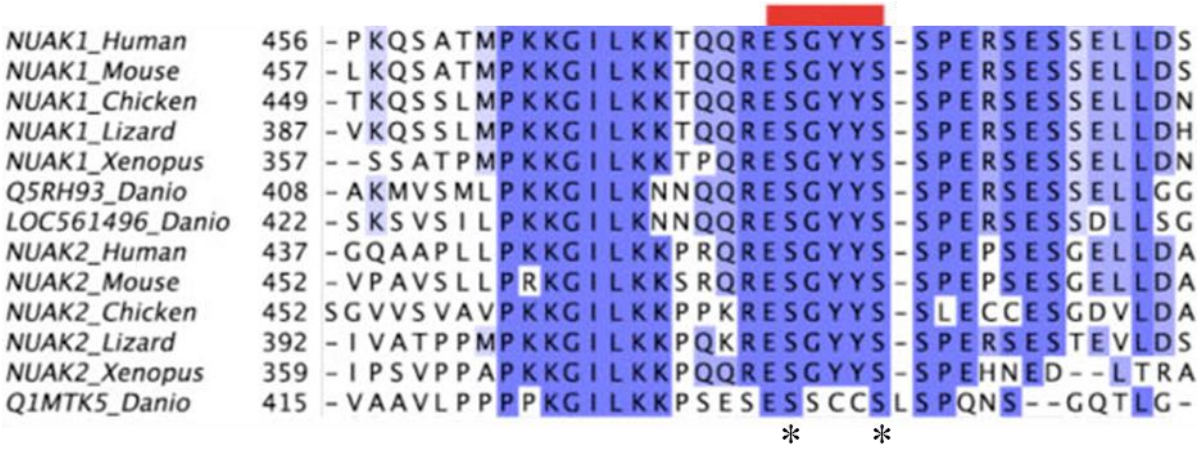

Figure 4.6 Alignment showing the conservation of the ESGYYS degron of NUAK1 and NUAK2 within vertebrate orthologues. The sequences used for alignment were obtained from Uniprot database. In zebrafish (Danio) there are two orthologues of NUAK1 (Q5RH93 and LOC561496) and one of NUAK2 (Q1MTK5). Red bar indicates the ESGYYS degron and * indicates the two Ser residues which are potential phosphorylation sites on the degron.

NUAK1and NUAK2 possess a slightly modified degron with the sequence of ESGYYS (Fig. 4.7A) which has been found to be conserved within vertebrates (Fig. 4.6). To justify whether the ESGYYS motif is indeed the βTRCP interaction motif in NUAK1, I carried out an alanine scan of the residues on the degron. On mutating the major residues on the degron, there was marked reduction in the interaction with βTRCP especially on mutating the Gly477 and the two Ser residues Ser476 and Ser480 (Fig. 4.7B). On mutating both the Ser residues to Ala, the interaction to βTRCP was virtually lost (Fig. 4.7B)

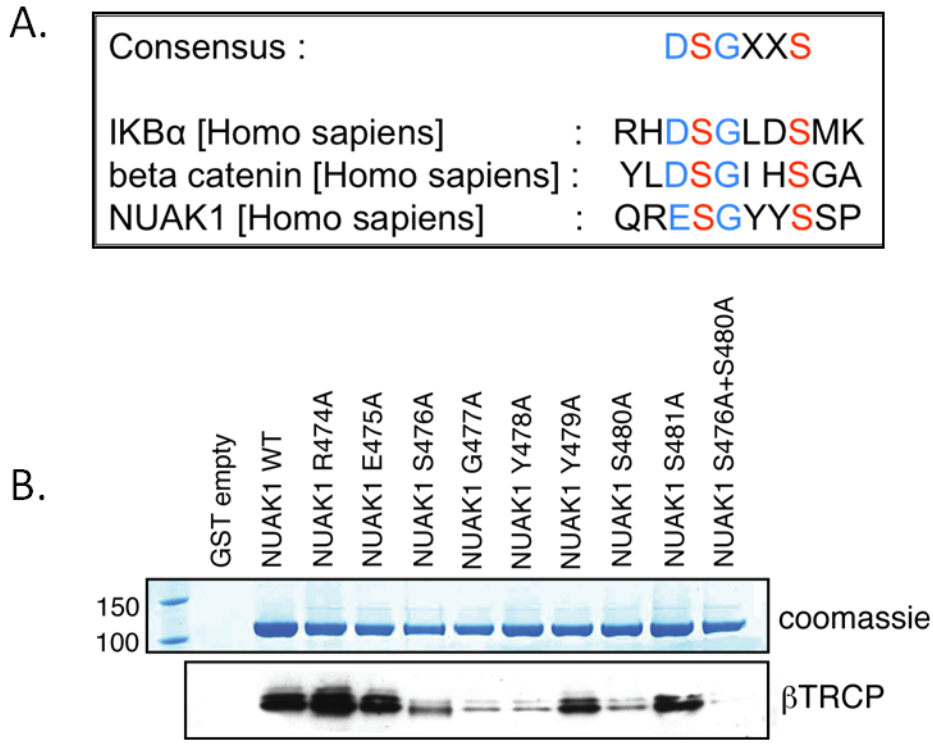

Figure 4.7 : Identification of the destruction motif or 'degron' of NUAK1 as a binding site for βTRCP. (A) NUAK1 was identified to possess a slight variant of the canonical $SCF^{\beta TRCP}$ binding domain DSGxxS which is present in the bonafide $SCF^{\beta TRCP}$ substrates IκBα and β-catenin. (B) HEK293 cells were transfected with expression plasmids for GST-tagged NUAK1 wild-type or indicated mutants. 36 hrs after transfection cells were lysed and GST-tagged proteins were immunoprecipitated from 10 mg of cell lysates. Immunoprecipitates were analysed by either Instant blue staining for the GST-tagged proteins or by immunoblotting with βTRCP antibody.

4.2.5. Phosphorylation of the NUAK1 degron is a requirement for βTRCP interaction

To identify whether phosphorylation was essential for βTRCP to bind to NUAK1, λ-phosphatase assay was employed. EDTA inactivated λ-phosphatase was used as control. HA-NUAK1 was immunoprecipitated from 10 mg of U2OS cell lysate and divided into three reactions (each in duplicates) and λ-phosphatase assay was carried out for 30 mins at 30 ºC. The reactions were washed 3x with 1% Triton lysis buffer to remove any dissociated βTRCP. Post λ-phosphatase reaction, immunoblotting for βTRCP revealed that λ-phosphatase treatment abolished interaction of NUAK1 with βTRCP and this was prevented by EDTA mediated inactivation of λ-phosphatase (Fig. 4.8).

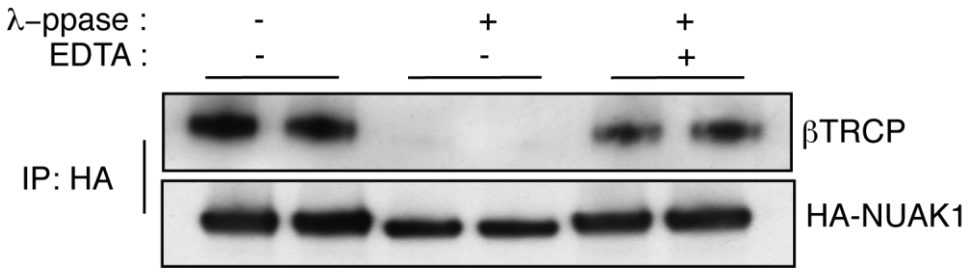

Figure 4.8 : Phosphorylation of NUAK1 is required for interaction with βTRCP. HA-NUAK1 was immunoprecipitated from stably expressing U2OS cells. λ-phosphatase assay was carried out with or without prior inactivation of λ-phosphatase with EDTA. The immunoprecipitates were washed thoroughly before immunoblotting. An electrophoretic mobility shift of NUAK1 was observed in λ-phosphatase treated NUAK1 immunoprecipitate.

4.2.6. Ser476 and Ser480 on the NUAK1 degron are potential phosphosites which may be under the regulation of interacting PP1β

To address whether the two Ser residues on the NUAK1 ESGYYS degron are indeed potential phosphosites in vivo, I immunoprecipitated GST-NUAK1 (wild-type and mutants) from transiently transfected overexpressing HEK293 cells and carried out high performance liquid chromatography with tandem mass spectrometry (LC-MS-MS) on an LTQ-Orbitrap mass spectrometer to identify phosphosites (Section 2.2.23.1) (Fig. 4.9). Phosphosites on NUAK1 wild-type was compared with Ser476Ala+Ser480Ala mutant. Extracted ion chromatogram analysis (XIC) of Ser476+Ser480 phosphopeptide (R.ESGYYSSPER.S+2P) was carried out to compare between the intensities of the phosphopeptides in NUAK1 WT and mutants. The total signal intensity of the phosphopeptide is plotted on the y-axis and retention time is plotted on the x-axis. The m/z (mass/charge ratio) value corresponding to the phosphopeptide was detected in NUAK1 WT between 625.8 to 626.8 with a retention time of approximately 11 mins. The phosphopeptide was not identified in Ser476Ala+Ser480Ala mutant (Fig 4.9).

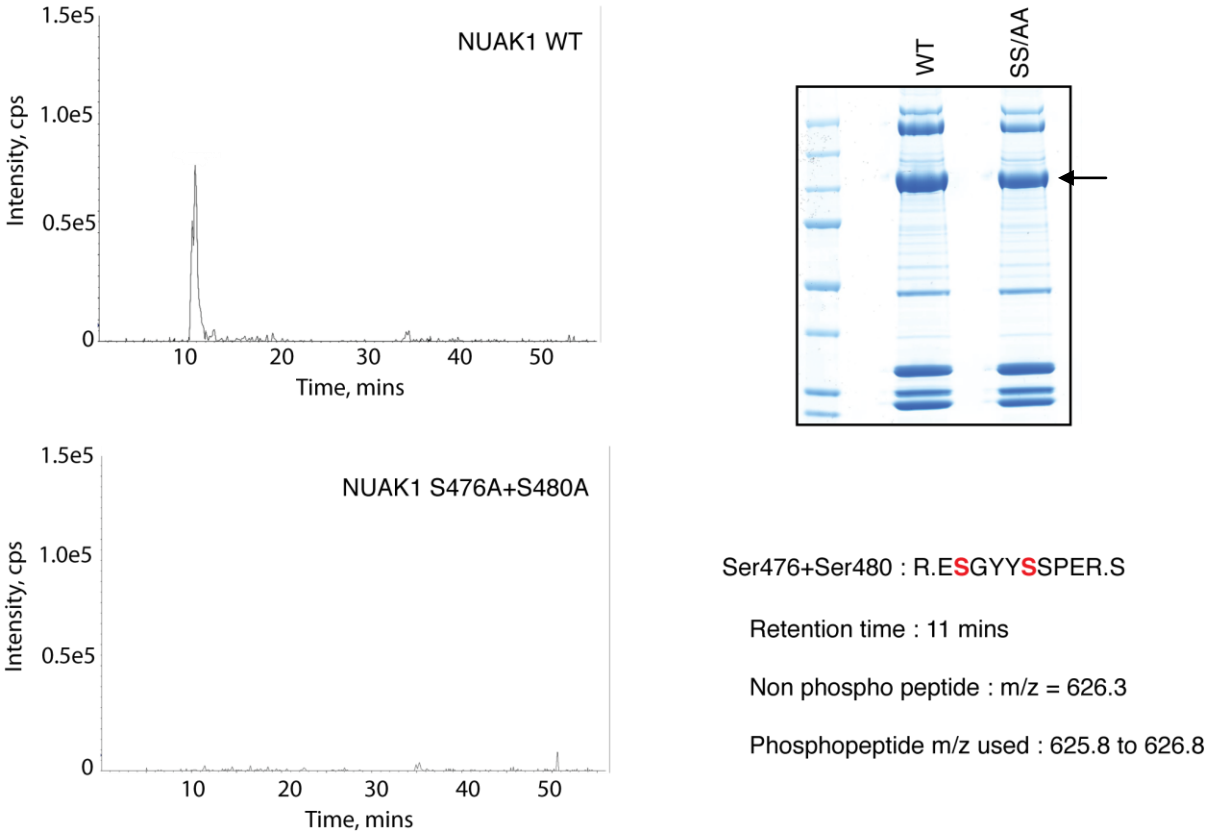

Figure 4.9 : The Ser476 and Ser480 on the βTRCP interacting degron of NUAK1 are potential phosphosites. NUAK1 WT and Ser476Ala+Ser480Ala mutant were immunoprecipitated from stably expressing U2OS cells and the protein band was excised for phosphopeptide analysis using LTQ Orbitrap. The tryptic peptide R.ESGYYSSPER.S+2P intensity between WT and SS/AA mutant was observed by XIC. Arrow indicated the NUAK1 band which was excised for LTQ-Orbitrap analysis.

4.2.7. Myosin phosphatase non-binding 3IL/KK mutant of NUAK1 has a stronger interaction with βTRCP

Since Fig 4.9 showed that Ser476 and Ser480 are potential in vivo phosphosites, I wanted to test whether the NUAK1 interacting MYPT1-PP1β phosphatase could possibly regulate βTRCP interaction with NUAK1. MYPT1-PP1β interacts with NUAK1 via the NUAK1 triple GILK motif. Interestingly, on comparing the degree of βTRCP interaction between the NUAK1 wild-type, Ser476Ala, Ser 480Ala, Ser476Ala+Ser480A and 3IL/KK (NUAK1 triple GILK mutant) mutants, there was clearly a much stronger interaction of 3IL/KK with βTRCP (Fig. 4.10). Thus, ablating the interaction of NUAK1 with MYPT1-PP1β complex

indeed increases the potential of NUAK1 to interact with βTRCP. Also, in the Ser476Ala+Ser480A mutant of NUAK1, although there is minimal βTRCP interaction, a robust increase in PP1β interaction was observed.

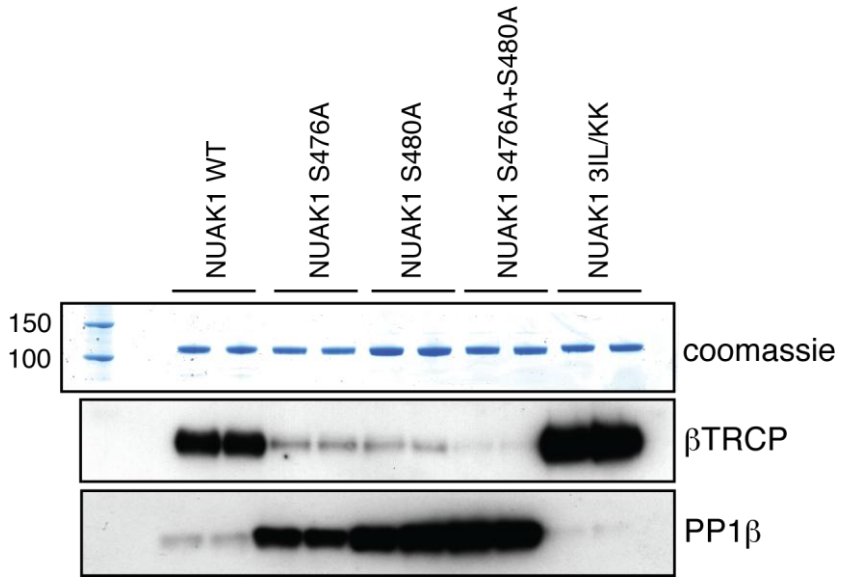

Figure 4.10 : Absence of phosphatase promotes NUAK1 interaction with βTRCP. GST tagged NUAK1 WT, S470A, S480A, SS/AA and 3IL/KK mutants were immunoprecipitated from transiently transfected HEK293 cells and resolved by SDS-PAGE followed by commassie staining or immunoblotting with βTRCP and PP1β antibodies.

4.2.8. Prolonged MLN-4924 treatment on cells leads to accumulation of endogenous NUAK1

To obtain further evidence that NUAK1 expression might be controlled by the $SCF^{\beta TRCP}$ E3 ubiquitin ligase complex, I decided to study how inhibition of Cullin-RING ligases (CRLs)would impact on the NUAK1 expression. To achieve this, I treated U2OS cells with NEDD8 inhibitor MLN-4924 which would inhibit Cullin 1 by inducing deneddylation. If NUAK1 was indeed a substrate of $SCF^{\beta TRCP}$, treatment of cells with MLN-4924 should lead to an increase in the expression levels of NUAK1. Indeed, upon treatment of U2OS cells with 3 μM MLN-4924 over 1,2,4,8 and 24 hours, there was a clear accumulation of NUAK1 over time (Fig. 4.11). By 4-8 hours, there was considerable accumulation of NUAK1 whereas closely related AMPK family kinase MARK1 had no change in expression levels (Fig. 4.11).

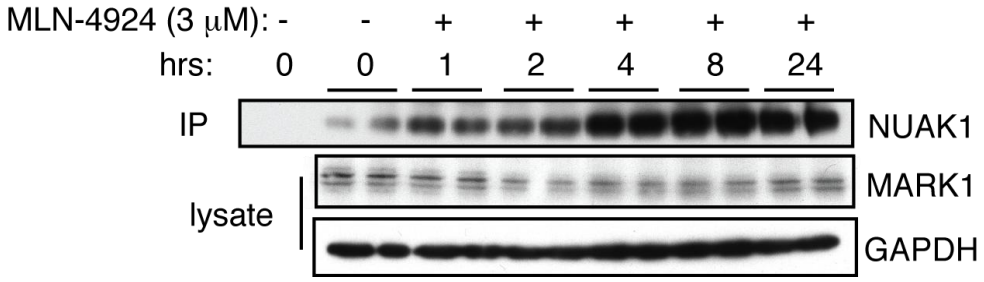

Figure 4.11 : Time course of MLN-4924 treatment on U2OS cells leads to accumulation of endogenous NUAK over time with no change in levels of closely related kinase MARK1. Endogenous NUAK1 was immunoprecipitated from U2OS cells treated with MLN-4924 over the indicated periods of time. Immunoblotting was carried out to detect NUAK1 levels in the immunoprecipitates and to detect MARK1 and GAPDH in the lysates.

4.2.9. Endogenous NUAK1 is degraded upon Calyculin A mediated hyperphosphorylation

Next, I wanted to establish whether increasing phosphorylation at Ser476 and Ser480 would lead to enhanced degradation of endogenous NUAK1. In order to do this, I treated U2OS cells with PP1 inhibitor Calyculin A with a final concentration of 50 nM over 0, 15 and 180 minutes. Phosphorylation of ERK was immunoblotted as a control for Calyculin A mediated hyperphosphorylation. Upon treatment with Calyculin A over 180 minutes, there was a significant degradation of NUAK1 (Fig. 4.12) suggesting that inhibition of phosphatases in cells may promote endogenous NUAK1 degradation possibly mediated via $SCF^{\beta TRCP}$.

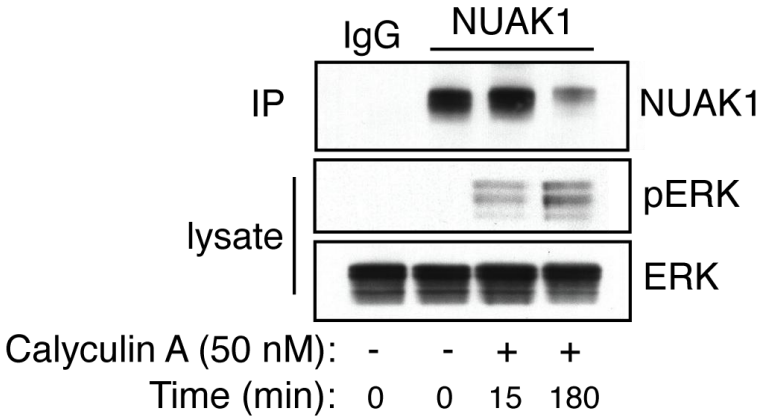

Figure 4.12 : Calyculin A mediated inhibition of phosphatases leads to degradation of NUAK1 over time. Endogenous NUAK1 was immunoprecipitated from U2OS cells treated with Calyculin A (50 nM) over the indicated periods of time. Immunoblotting was carried out to detect NUAK1 levels in the immunoprecipitates and to detect pERK and total ERK in the lysates.

4.2.10. Hyperphosphorylation leads to polyubiquitylation and degradation of NUAK1 which is reversed by MLN-4924

Since endogenous NUAK1 is degraded upon inhibition of phosphatases in cells, I wanted to check whether this hyperphosphorylation mediated degradation of NUAK1 was due to SCF E3 ligases. If SCF complexes are indeed involved in endogenous NUAK1 degradation, then MLN-4924 treatment should inhibit neddylation of the Cullin1 of SCF complex and thus protect NUAK1 from hyperphosphorylation mediated degradation. I carried out a time course of Calyculin A treatment of U2OS cells with or without the presence of 3 μM MLN-4924. Endogenous NUAK1 was immunoprecipitated from 1 mg of the U2OS lysates and immunoblotting was carried out. Upon 2-4 hours of Calyculin A treatment, there was a robust decrease in NUAK1 levels as observed before (Fig. 4.12) and in the presence of 3 μM MLN-4924, this Calyculin A mediated degradation of NUAK1 was reversed (Fig. 4.13).

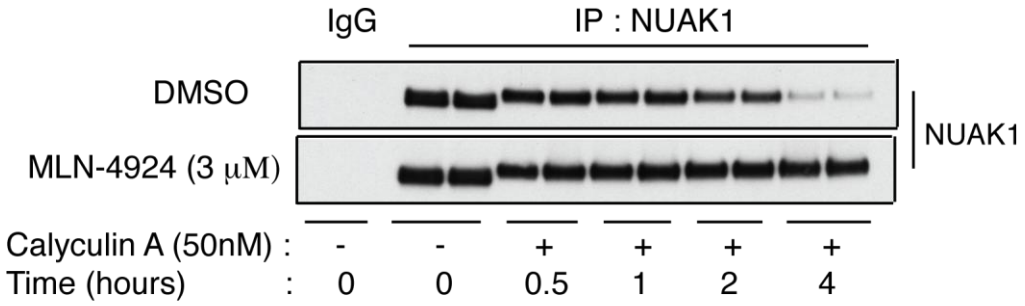

Figure 4.13 : Calyculin A mediated inhibition of phosphatases leads to degradation of NUAK1 over time which is reversed in the presence of NEDD8 inhibitor MLN-4924. Endogenous NUAK1 was immunoprecipitated from U2OS cells treated with Calyculin A (50 nM) and with or without MLN-4924 over the indicated periods of time. Immunoblotting was carried out to detect NUAK1 levels in the immunoprecipitates.

Since MLN-4924 inhibits the neddylation of Cullin 1, the SCF complex formation is jeopardised and hence there is transfer of ubiquitin chains onto the substrate. To check the endogenous polyubiquitylation of NUAK1 in Calyculin A treated U2OS cells with or without the presence of 3μM MLN-4924, similar experiment as in Fig. 4.13 was carried out and the

cells were lysed in reducing agent free lysis buffer supplemented with 5 mM N-ethylmaleimide (NEM). NEM is a deubiquitinase inhibitor and hence preserves the polyubiquitylation of proteins post-lysis. Endogenous NUAK1 was immunoprecipitated from 5 mg of cell lysates and immunoblotting was carried out using NUAK1 and Ubiquitin antibodies. There was a clear ubiquitylation of NUAK1 upon 30 mins of Calyculin A treatment and the ubiquitin signal was consequently reduced owing to degradation of NUAK1 over time (Fig. 4.14). However, in MLN-4924 treated cells, there was no significant signal of polyubiquitylation at any time point suggesting that NUAK1 was indeed polyubiquitylated and degraded by an SCF complex upon phosphatase inhibition (Fig, 4.14).

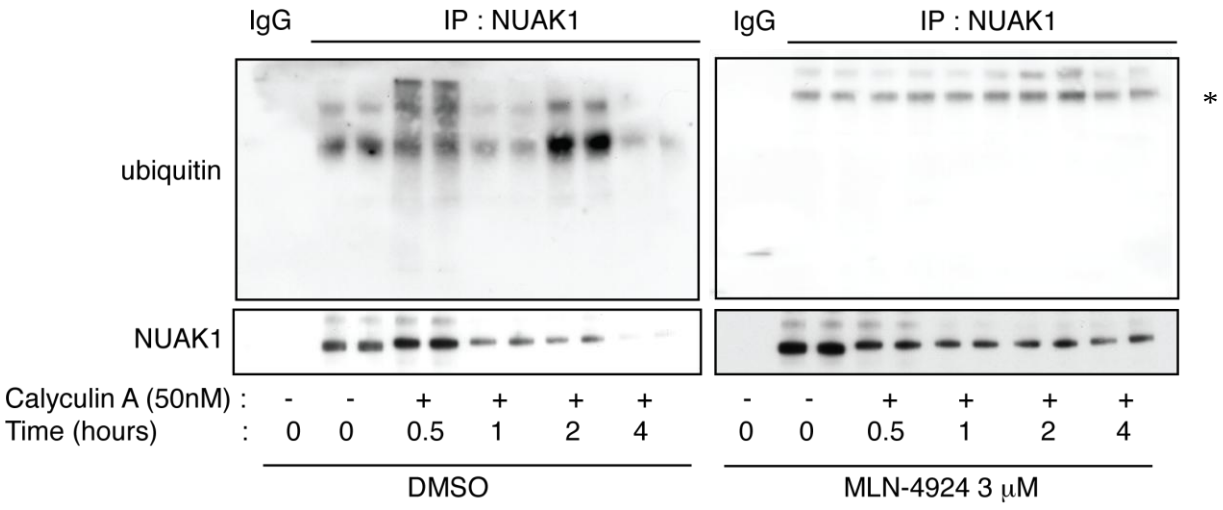

Figure 4.14 : Endogenous NUAK1 undergoes polyubiquitylation upon Calyculin A treatment which leads to its degradation over time which is reversed in the presence of NEDD8 inhibitor MLN-4924. Endogenous NUAK1 was immunoprecipitated from U2OS cells treated with Calyculin A (50 nM) and with or without MLN-4924 over the indicated periods of time. Immunoblotting was carried out to detect co-immunoprecipitation of ubiquitin with endogenous NUAK1. * indicates a non-specific band.

4.2.11. βTRCP1$^{-/-}$ MEFs exhibit double the level and activity of endogenous NUAK1

To obtain genetic evidence that NUAK1 is a substrate of SCF$^{\beta TRCP}$, βTRCP1 knock-out MEFs were tested for NUAK1 activity and expression levels. The βTRCP1 wild-type and knock-out MEFs were kindly provided by Dr.Keichi Nakayama (Japan) (Nakayama et al., 2003). βTRCP1 $^{-/-}$ cells clearly had approximately double the level and activity of endogenous NUAK1 as compared to the βTRCP1$^{+/+}$ MEFs (Fig. 4.15).

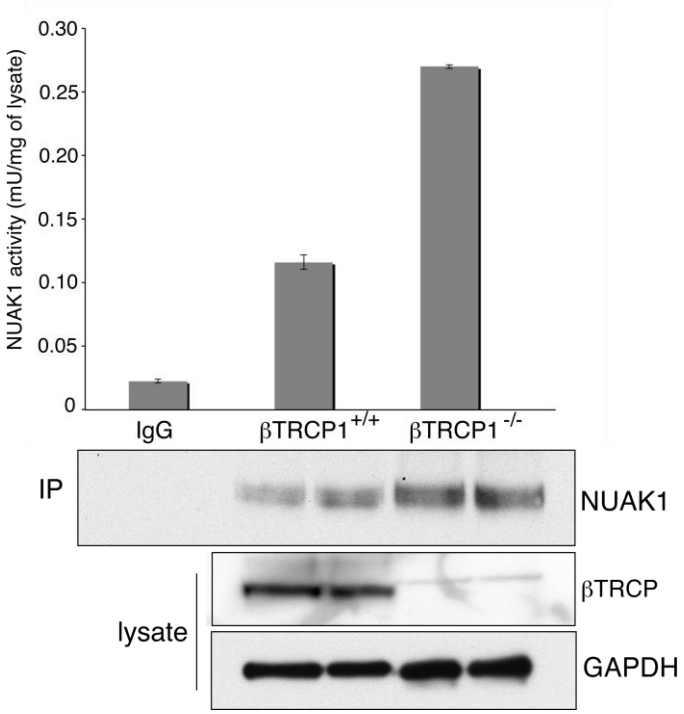

Figure 4.15 : βTRCP1$^{-/-}$ MEFs exhibit double the level and activity of endogenous NUAK1 as compared to the βTRCP1$^{+/+}$ MEFs. Endogenous NUAK1 was immunoprecipitated from 2 mgs of MEF lysates and kinase assay was carried out in triplicates along with immunoblotting. The lysates were subjected for immunoblotting with βTRCP and GAPDH antibodies.

4.2.12. U2OS cells stably expressing Ser476Ala+Ser480Ala+Ser481Ala mutant of NUAK1 exhibits faster proliferation rate and higher expression of NUAK1.

As in Fig. 4.7B, mutating the NUAK1 degron at the two Ser residues leads to a robust loss of βTRCP interaction. Hence, to compare between the NUAK1 WT and the βTRCP non-

interacting mutant, U2OS FLP-IN cells stably over-expressing HA-NUAK1 wild-type and HA-NUAK1 Ser476Ala+Ser480Ala+Ser481Ala mutant (SSS/AAA) were developed. The Ser481 was also mutated since an adjacent Ser residue to a βTRCP degron has been reported to partially compensate for the βTRCP interaction (Tudzarova et al., 2011). Interestingly, the U2OS FLP-IN cells expressing NUAK1 SSS/AAA expressed approximately double the level of NUAK1 (Fig. 4.16A) and had a moderately faster proliferation rate (Fig. 4.16B) as compared to the U2OS FLP-IN cells overexpressing NUAK1 WT.

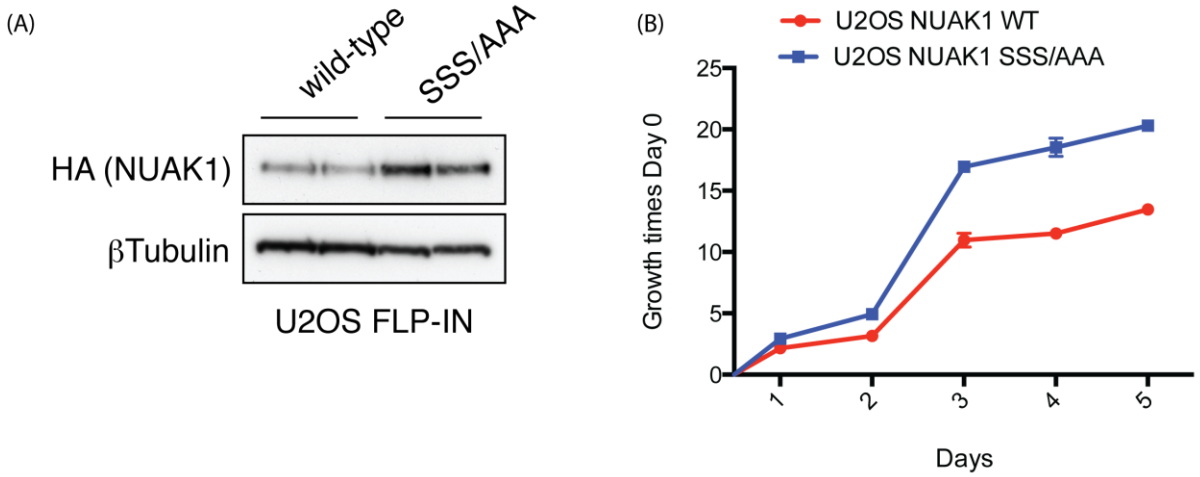

Figure 4.16 : U2OS FLP-IN cells overexpressing NUAK1 SSS/AAA mutant had a faster proliferation rate and expressed a higher level of NUAK1. A) Immunoblotting of cell lysates with HA and β-tubulin antibodies was carried out to compare between the expression levels of WT and SSS/AAA mutant of NUAK1. B) MTS cell proliferation assay was carried out to compare between cell proliferations of U2OS cells expressing NUAK1 WT and NUAK1 SSS/AAA mutant over 5 days. Data was represented as growth of cells times Day 0.

4.2.13. βTRCP non binding SSS/AAA mutant of NUAK1 is not degraded upon hyperphosphorylation induced with Calyculin A.

NUAK1 is degraded upon Calyculin A mediated PP1 inhibition which is protected in the presence of MLN-4924 (Fig. 4.13). To obtain evidence that phosphorylation of NUAK1 at βTRCP interacting residues was critical for regulating stability of NUAK1, I treated U2OS NUAK1 WT and U2OS NUAK1 SSS/AAA cells with 0, 0.5 or 3 hrs of Calyculin A treatment. Upon treatment with Calyculin A over 3 hrs, there was a significant degradation of

NUAK1 WT as compared to the 0.5 hr Calyculin A treatment, whereas there was hardly any NUAK1 degradation observed between 0.5 hr and 3 hrs Calyculin A treated U2OS NUAK1 SSS/AAA (Fig. 4.17).

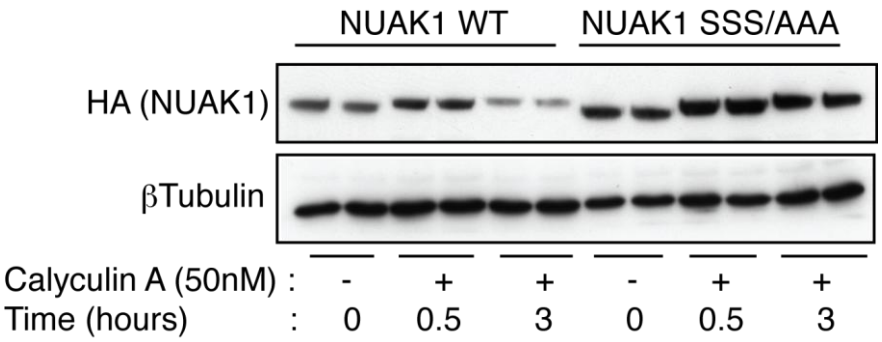

Figure 4.17 : NUAK1 SSS/AAA mutant is resistant towards hyperphosphorylation mediated degradation of NUAK1 upon treatment of Calyculin A over time. U2OS cells stably expressing NUAK1 WT or SSS/AAA mutant were treated with 50 nM Calyculin A over the indicated periods of time and immunoblotting was carried out with HA (NUAK1) and β-tubulin antibodies.

4.2.14. Inhibitor panel to identify the upstream kinase responsible for phosphorylating the NUAK1 degron.

Since $SCF^{\beta TRCP}$ targets a degron that requires prior phosphorylation, it was important to identify the upstream kinase(s) of NUAK1 which may be involved in phosphorylating Ser476 and Ser480 on the degron. To identify the upstream kinase responsible for phosphorylating NUAK1 at the βTRCP interaction residues, a lot of effort was spent initially towards raising phospho-antibodies against the Ser476+Ser480 residues of the NUAK1 degron. The antibodies raised, however, were not efficient enough to study NUAK1 phosphorylation either at overexpressed or at endogenous levels. Hence to identify the upstream kinase of NUAK1, I carried out a protein kinase inhibitor screen and identify the compounds which mimic the NUAK1 protection exhibited by MLN-4924. The inhibitor panel consisted of inhibitors which targetted kinases which has been previously been reported to be

phosphorylating $SCF^{\beta TRCP}$ substrates on the degron. MLN-4924 exhibits a robust protection of NUAK1 upon Calyculin A treatment. Any other kinase inhibitor which could protect NUAK1 to the same level could potentially lead to the identification of the upstream kinase of NUAK1 phosphorylating the degron. Amidst the protein kinase inhibitors tested, PLK inhibitor BI-2536 significantly protected NUAK1 from hyperphosphorylation mediated degradation. Besides BI-2536, IKK/GSK inhibitor BIO and ROCK inhibitor H1152 also exhibited moderate levels of NUAK1 protection (Fig. 4.18). Since BIO and H1152 were considerably less specific inhibitors (http://www.kinase-screen.mrc.ac.uk/), there were not used in further experiments.

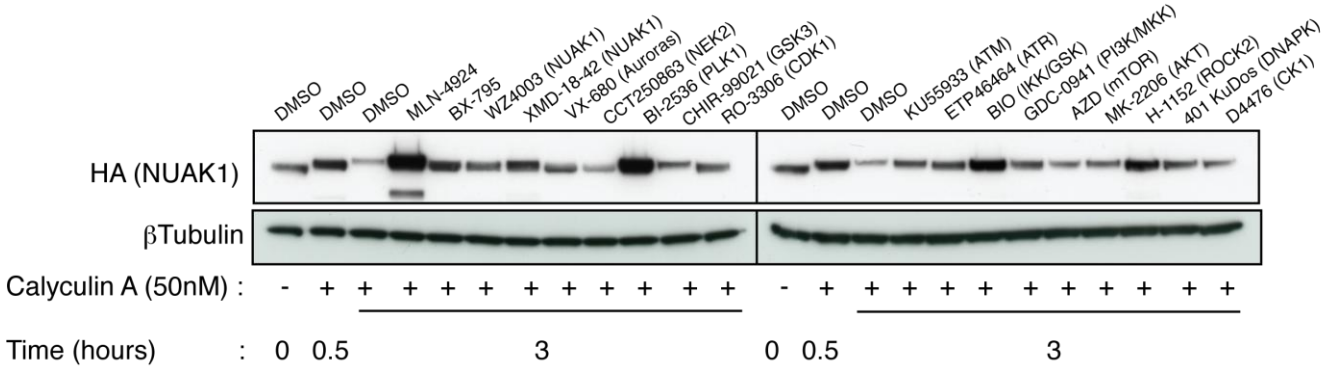

Figure 4.18 : Inhibitor panel treatment of U2OS NUAK1 WT cells to identify potential upstream kinases responsible for hyperphosphorylation mediated degradation of NUAK1. U2OS cells stably expressing HA-NUAK1 were treated with the indicated inhibitors for 6 hours before lysing them for immunoblot analysis. The inhibitors were used at 10 µM final except for MLN-4924 (3 µM), BI-2536 (1 µM) and D4476 (30 µM).

4.2.15. PLK1 immunoprecipitates with overexpressed NUAK1 in U2OS cells

Since Polo-kinases seem to be playing a role in protection of NUAK1 upon hyperphosphorylation, I wanted to see whether PLK1 immunoprecipitates with overexpressed NUAK1. GST-NUAK1 was immunoprecipitated from 5 mg of transiently transfected HEK293 cells and immunoblot was carried out to identify PLK1 and PP1β. PLK1 was found to immunoprecipitate with overexpressed NUAK1 (Fig 4.19) along with the previously known interactor PP1β (Zagorska et al., 2010).

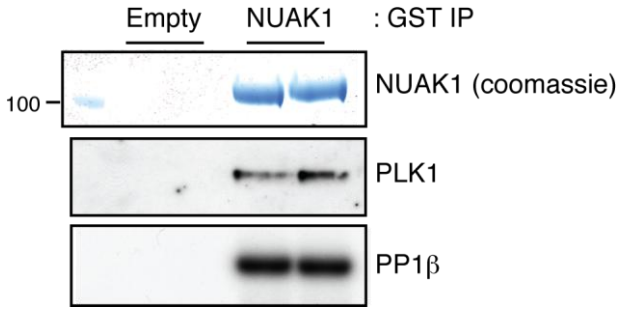

Figure 4.19 : PLK1 co-immunoprecipitates with overexpressed NUAK1. Overexpressed GST-NUAK1 was immunoprecipitated from transiently transfected HEK293 cells. GST-NUAK1 was identified on Instant Blue stained gel and immunoprecipitates were analysed by immunoblotting with the indicated antibodies.

4.2.16. NUAK1 accumulates in the S phase of the cell cycle.

Since polo kinases are responsible for phosphorylating the NUAK1 degron, the cell cycle might be the best starting point to identify the physiological process wherein $SCF^{\beta TRCP}$ might be playing a role in NUAK1 degradation. Since $SCF^{\beta TRCP}$ has been implicated as a key cell cycle regulator at G2 stage of cell cycle, I synchronised U2OS cells at G2 stage of cell cycle by double thymidine block followed by release in 10 µM RO-3306 (reversible CDK1 inhibitor) (Section 2.2.25). Endogenous NUAK1 was found to be degraded in the G2/M stage of cell cycle and levels steadily increase during later G1-S phase (Fig. 4.20). Immunoblot was carried out for G2 markers cyclin A and B1 and mitotic marker pSer10 H3. AMPK related kinase SIK2 and NUAK upstream kinase LKB1 levels were unchanged throughout the cell cycle. NUAK substrate MYPT1 levels also did not alter over the cell cycle.

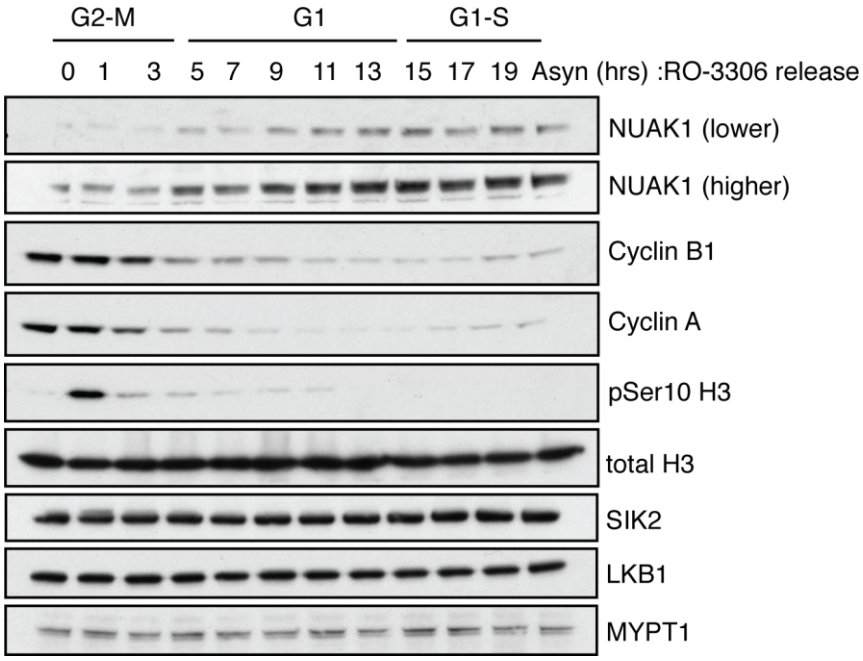

Figure 4.20 : Endogenous NUAK1 is degraded in the G2-M stage of cell cycle and accumulates in the S phase. U2OS cells were synchronised at G2/M stage of cell cycle by a double-thymidine block followed by release in reversible CDK1 inhibitor RO-3306. Immunoblotting was carried out with the indicated antibodies.

To examine this further, U2OS FLP-IN cells expressing HA-NUAK1 WT and SSS/AAA mutant were synchronised using double thymidine for G1-S and using double thymidine and release in 10 μM RO-3306 for G2 stage of the cell cycle. Propidium iodide stained flow cytometry analysis was carried out to ascertain the cell cycle progression of the U2OS cells. Interestingly, WT NUAK1 was found to be degraded in the G2-M-G1 stages of the cycle with clear accumulation in the S phase whereas the SSS/AAA mutant remained relatively constant at all stages of the cell cycle (Fig. 4.21). Thus, protection of the βTRCP non-binding mutant suggests that the $SCF^{\beta TRCP}$ may be playing significant roles in controlling NUAK1 expression in the cell cycle.

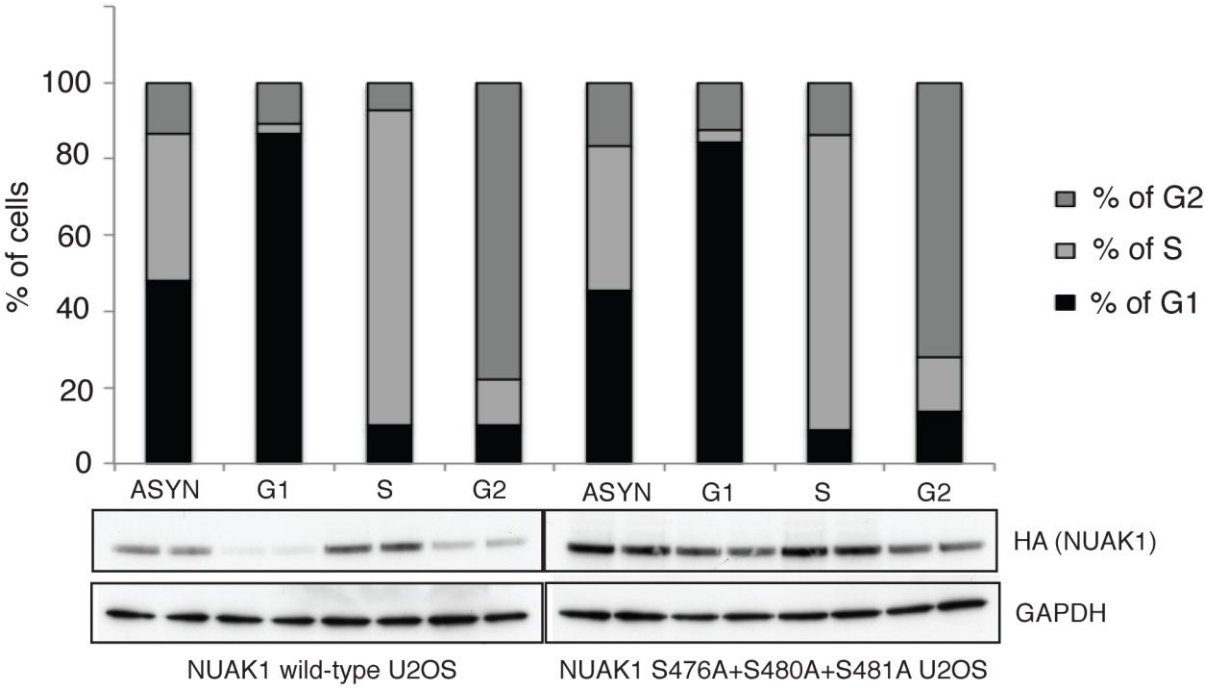

Figure 4.21 : NUAK1 WT is degraded in the G2-M-G1 stages of the cell cycle unlike the βTRCP non-binding SSS/AAA mutant. (ASYN : asynchronous) U2OS cells stably expressing HA-NUAK1 WT and SSS/AAA mutants were synchronised with double thymidine block release for G1 and S phase and double thymidine block followed by release in RO-3306 for G2/M phase. Cell cycle synchronisation efficiency was confirmed by flow cytometry propidium iodide staining. Immunoblotting was carried out with indicated antibodies.

Moreover, immunofluorescence of HA-NUAK1 in the synchronised U2OS FLP-IN cells suggest that during S-phase, along with a clear increase in the level of HA-NUAK1, there is also a significant translocation of NUAK1 into the nucleus (Fig. 4.22) and hence could possibly indicate novel functions of NUAK1 in the DNA replication phase of the cell cycle. The HA-NUAK1 Ser476Ala+Ser480Ala+Ser481Ala (SSS/AAA) expression levels and localisation within the cells remained relatively unchanged over the cell cycle stages.

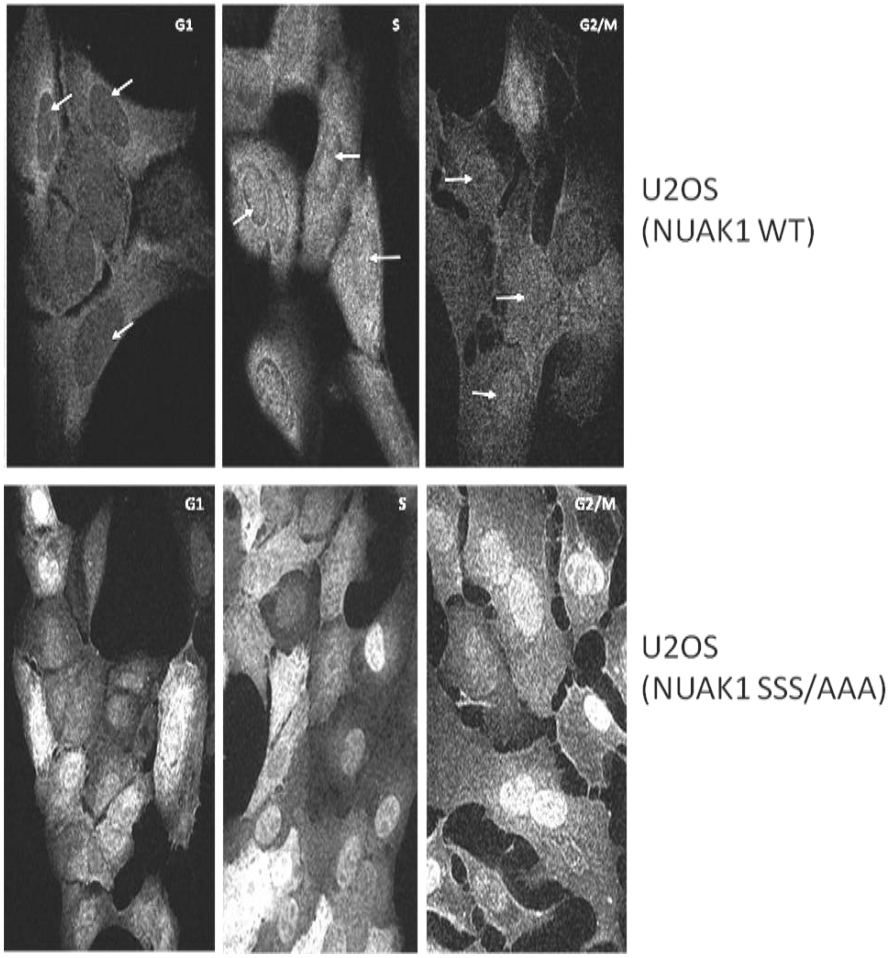

Figure 4.22 : Besides an increase in the level of NUAK1 in the S-phase, a distinct localisation of NUAK1 is observed in the nucleus of the cells in S-phase. U2OS cells stably expressing HA-NUAK1 WT and SSS/AAA mutants were synchronised with double thymidine block release for G1 and S phase and double thymidine block followed by release in RO-3306 for G2/M phase. Cells were fixed in 4% paraformaldehyde, permeabilised and immunofluorescence was carried out using HA-monoclonal antibody.

4.3 Discussion

NUAK1 is a much less studied kinase as compared to its family member and closely related kinase AMPK. The only rigorously characterised substrate known is MYPT1 which gets phosphorylated by NUAK1 upon cell detachment (Zagorska et al., 2010). NUAK1 is known to undergo ubiquitylation and interacts with USP9X which is thought to be the DUB responsible for deubiquitylating NUAK1 (Al-hakim et al., 2008). Recently, p53 was reported to be a direct substrate of NUAK1 wherein NUAK1 phosphorylates p53 at Ser15 and Ser392 leading to a cell cycle arrest at G1/S border and hence playing vital roles in cell proliferation (Hou et al., 2011). Besides cell proliferation, NUAK1 has been implicated in metastasis, invasion, tumour promotion and antiapoptotic roles in cancer (Kusakai et al., 2004a, Kusakai et al., 2004b, Chang et al., 2012, Liu et al., 2012, Lu et al., 2013) but very little is known regarding the biochemical mechanisms by which NUAK1 might confer its functions within the cancer cells.

In an attempt to identify novel interacting partners of NUAK1, mass fingerprint analysis was carried out and components of the $SCF^{\beta TRCP}$ RING E3 ubiquitin ligase complex was found to co-immunoprecipitate with NUAK1 (Fig. 4.3). βTRCP1, βTRCP2 and SKP1 was found in the NUAK1 interactome (Fig. 4.3 and 4.4). As outlined in the introduction, $SCF^{\beta TRCP}$ is instrumental in Wnt, Hedgehog, immune signalling, cell cycle and DNA damage pathways (Table 4.1, Fig. 4.2). Hence, the idea of NUAK1 interacting with a highly studied E3 ubiquitin ligase with diverse functions was indeed quite intriguing. Characteristic of majority $SCF^{\beta TRCP}$ substrates, NUAK1 also possess the DSGxxS (ESGYYS in NUAK1) degron which requires prior phosphorylation at the two Ser residues for βTRCP to interact (Fig. 4.7A). βTRCP was found to interact with both NUAK1 and NUAK2 (Fig. 4.5) and both the

NUAK isoforms possess the ESGYYS degron which is evolutionarily conserved in vertebrates upto zebrafish (*Danio spp*.) (Fig. 4.6). On performing an alanine scan over the degron, βTRCP interaction was lost upon introducing double mutation of the two Ser residues (Ser476 and Ser480) on the ESGYYS degron (Fig. 4.7B). The two Ser residues were also identified to be potential phosphorylation sites upon LTQ-Orbitrap mass spectrometry followed by extracted ion chromatogram (XIC) analysis (Fig. 4.9). The NUAK1 tryptic peptide R.ESGYYSSPER.S consisting of the degron sequence was found to be doubly phosphorylated with a mass by charge ratio between 625.8 to 626.8 and a retention time of approximately 11 mins (Fig. 4.9). Upon mutating the two Ser residues, the intensity peak for the phosphopeptide was lost hence suggesting that Ser476 and Ser480 were the two possible phosphosites instead of the other Tyr or Ser residues within the tryptic peptide (Fig. 4.9). Moreover, upon dephosphorylating NUAK1 with λ-phosphatase, there was a robust loss of βTRCP interaction which could be reversed upon inactivating λ-phosphatase with EDTA (Fig. 4.8). Hence phosphorylation at the Ser476 and Ser480 residues are essential for βTRCP to interact with NUAK1.

Since NUAK1 interacts with MYPT1-PP1β complex, I wanted to check whether interaction with the PP1β could be involved in keeping the degron of NUAK1 in a dephosphorylated state. To test this idea, I compared the βTRCP interaction of NUAK1 WT, single Ser to Ala mutants and double S476A + Ser480A with the MYPT1-PP1β non-binding 3IL/KK mutant of NUAK1. NUAK1 interacts with the PP1β subunit of MYPT1-PP1β via three conserved GILK motifs (Zagorska et al., 2010). Mutating the triple GILK motifs into GKKK, led to a clear loss of PP1β interaction but interestingly had significantly higher βTRCP interaction (Fig. 4.10). This data suggests that there is an intrinsic competition between βTRCP and PP1β to interact with NUAK1 and one could speculate that upon NUAK1 phosphorylation at

the degron, the MYPT1-PP1β complex might be dissociating from NUAK1. A lot of time was invested in developing the Ser476+Ser480 phosphospecific antibody for NUAK1, but the antibodies raised were not effective enough to identify phosphorylated NUAK1.

βTRCP was found to robustly co-immunoprecipitate with overexpressed NUAK1 (Fig. 4.4B) whereas the co-immunoprecipitation with endogenous NUAK1 was markedly less (Fig. 4.4A), hence one could argue that the interaction may only be an overexpression artefact. To obtain conclusive evidence that βTRCP is indeed playing essential roles in controlling expression level of endogenous NUAK1, I carried out a time course treating U2OS cells with NEDD8 inhibitor MLN-4924. MLN-4924 inhibits the neddylation of the cullin in the SCF complex which consequently fails to transfer ubiquitin chains to degrade the substrate. Hence MLN-4924 treatment of cells should ideally lead to an increase in the levels of NUAK1 if NUAK1 is indeed a $SCF^{\beta TRCP}$ substrate. Within 4 hours of 3 μM MLN-4924 treatment, there was significant increase in the protein levels of endogenous NUAK1 (Fig 4.11) which clearly suggested that NUAK1 was indeed regulated by an Cullin RING E3 ligase. Furthermore, upon treating U2OS cells with PP1 inhibitor calyculin A, endogenous NUAK1 was found to be degraded within 2-4 hrs of treatment (Fig. 4.12 and 4.13). The NUAK1 degradation could be reversed by introducing MLN-4924 to the system (Fig. 4.13). Upon blotting for endogenous ubiquitin, NUAK1 was found to be ubiquitylated within 30 mins of calyculin A treatment and consequently degraded over time (Fig. 4.14). In the presence of MLN4924, NUAK1 was not found to be ubiquitylated upon calyculin A treatment (Fig. 4.14) suggesting that the SCF complex is inactive owing to deneddylation of the cullin. Thus, NUAK1 is ubiquitylated and degraded upon hyperphosphorylation which can be reversed by MLN-4924. To further obtain genetic evidence that βTRCP is indeed degrading NUAK1, we received $\beta TRCP1^{-/-}$ MEF cells from Prof Keichi Nakayama's lab in

Japan. βTRCP1$^{-/-}$ MEF cells had approximately double the level of endogenous NUAK1 and double the activity (Fig. 4.15). The βTRCP2 isoform may still be playing a role in targetting NUAK1 for degradation as the two βTRCP isoforms are functionally indistinguishable. I tried to knock-down βTRCP2 isoform in the βTRCP1$^{-/-}$ MEF but the shRNAs to βTRCP2 was found to be lethal for the cells. Hence, the data suggests that SCF$^{\beta TRCP}$ may indeed be the E3 ligase responsible for regulating the endogenous level of NUAK1.

To obtain further evidence that the calyculin A mediated degradation of NUAK1 was indeed brought about by SCF$^{\beta TRCP}$, I developed U2OS cells stably expressing NUAK1 WT and βTRCP non-binding NUAK1 S476A+S480A+S481A mutant (SSS/AAA mutant). Ser481 was an additional mutation introduced in NUAK1, as Prof. Salvador Moncada's group in London had reported in their studies with PFKFB3 and βTRCP that an additional Ser residue adjacent to the βTRCP interaction degron could at times partially compensate for the loss of interaction with βTRCP upon mutating the two Ser residues in the degron (Tudzarova et al., 2011). NUAK1 SSS/AAA mutant expressing cells expressed double the level of NUAK1 (Fig. 4.16A) presumably owing to its inability to interact with SCF$^{\beta TRCP}$ and had a moderately faster proliferation rate as compared to NUAK1 WT expressing cells (Fig. 4.16B). Upon treatment of the cells with calyculin A over 3 hrs, NUAK1 WT was found to be degraded but SSS/AAA mutant did not exhibit significant degradation at 3 hrs of calyculin A treatment (Fig. 4.17) thus further consolidating the hypothesis that NUAK1 is degraded by SCF$^{\beta TRCP}$ upon hyperphosphorylation.

The evidence suggests that upon phosphorylation of Ser476 and Ser480, NUAK1 interacts with SCF$^{\beta TRCP}$ and undergoes degradation. Since SCF$^{\beta TRCP}$ has diverse roles in cells, it was important to identify the physiological process wherein NUAK1 needs to be targetted for

degradation via $SCF^{\beta TRCP}$. To approach this question, the first step was to identify the possible upstream kinase(s) responsible for phosphorylating NUAK1 at the degron. For this purpose, a panel of kinase inhibitors were employed which specifically target the kinases known to phosphorylate βTRCP substrates at the degron (Table 4.1). The idea was to identify the kinase inhibitors which could protect NUAK1 from calyculin A mediated degradation. As seen in the inhibitor panel, U2OS cells treated with PLK inhibitor BI2536 exhibited robust NUAK1expression (Fig. 4.18). Treatment with IKK/GSK inhibitor BIO and H1152 (ROCK inhibitor) also exhibited NUAK1 protection but these inhibitors were less specific and hence were not considered for further experiments (Fig. 4.18). Since BI2536 is a highly specific PLK inhibitor, and PLK1 is known to phosphorylate various βTRCP substrates, I wanted to gather further evidence via co-immunoprecipitation studies to identify whether PLK1 interacts with NUAK1. PLK1 indeed co-immunoprecipitates with overexpressed NUAK1 (Fig. 4.19), although it is yet unclear whether the interaction is direct or via a NUAK1 interactor like MYPT1-PP1β.

Since PLK1 has essential roles in the progression of cell cycle especially in the G2/M stage (Section 1.6), I synchronised U2OS cells in the cell cycle and found that endogenous NUAK1 was degraded in the G2/M stage of the cell cycle and slowly started accumulating in the late G1/S phase (Fig. 4.20). Strong signals of G2/M cyclins B1 and A and pSer10 H3 mitotic signal confirmed the proper synchronisation of cells in G2/M stage (Fig. 4.20). NUAK1 substrate MYPT1, NUAK1 related SIK2 or NUAK1 activating LKB1 kinase were unchanged in the cell cycle (Fig. 4.20). Further synchronisation experiments on U2OS cells expressing NUAK1 WT and NUAK1 SSS/AAA mutant showed that NUAK1 was degraded in G2/M stage till early G1 and accumulated in the S phase of the cell cycle (Fig. 4.21). NUAK1 SSS/AAA mutant levels, however, were relatively unchanged throughout the cell

cycle (Fig. 4.21). Upon staining the HA-NUAK1 in the synchronised U2OS cells for immunofluorescence, NUAK1 levels were found to be upregulated in the S phase (consistent with the immunoblot data) and there was a significant fraction of NUAK1 migrating to the nucleus (Fig. 4.22). NUAK1 migrating to the nucleus during the S or DNA synthetic phase of cell cycle suggests the possibility of NUAK1 to be playing important roles in the DNA damage or perhaps DNA synthesis processes of the cell. NUAK1 SSS/AAA levels were found to be constant throughout the cell cycle with strong NUAK1 signal in the nucleus at all the 3 stages of cell cycle (Fig. 4.22).

Thus upon PLK1 mediated phosphorylation, NUAK1 interacts with and is degraded by $SCF^{\beta TRCP}$ in the G2/M stage of the cell cycle and further work is required to identify the potential functions of NUAK1 in the cell cycle or perhaps in the cell cycle checkpoints and DNA damage pathways.

In future, it would be interesting to dissect the exact role that NUAK1 may be playing in the cell cycle or perhaps in the DNA damage checkpoints. For this purpose, the initial step would be to identify novel interactors of NUAK1 in the nucleus via phosphoproteomic studies.

5. Myosin phosphatase family as potential substrates of NUAK1

5.1. Introduction

Cellular motility, cytokinesis, cell detachment, smooth muscle contraction and many other cellular and muscle functions are activated by phosphorylation of Ser19 and Thr18 of the regulatory myosin light chain 2 (MLC2) of the contractile motor protein myosin II (Allen and Walsh, 1994, Hirano et al., 2003, Wilson et al., 2005). Phosphorylation at Ser19/Thr18 promotes the reversible interaction of myosin II with actin filaments via cross-bridges and leads to the conversion of chemical energy of ATP into mechanical force or movement (Grassie et al., 2011). Hence, the phosphorylation status of myosin II is the primary determinant for cellular motility. MLC2 phosphorylation is regulated via phosphorylation and consequent dephosphorylation activities of MLCK and various other kinases and myosin phosphatases whose catalytic activity is attributable to protein phosphatase type 1 catalytic subunit or PP1β (Cohen, 2002b, Bollen et al., 2010). In the case of myosin II, PP1β functions as a heterodimeric complex along with a member of the myosin phosphatase targeting subunit (MYPT) family (Shimizu et al., 1994).

The MYPT family consists of five members: MYPT1 (or PPP1R12A), MYPT2 (or PPP1R12B), myosin binding subunit of 85 kDa (MBS85 or PPP1R12C), MYPT3 (or PPP1R16A) and the TGFβ- inhibited membrane-associated protein (TIMAP or PPP1R16B) (Fig. 5.1). The MYPT family members reveal high level of sequence similarity and exhibit several structural and functional domains (Fig. 5.1). The N-terminal RVxF motif (PP1β-binding site) is found in all family members which is immediately followed by a region containing several ankyrin repeats which aids in protein interactions including phosphorylated myosin. MYPT1, MYPT2 and MBS85 contain C-terminal leucine zipper

sequences which are involved in dimerization and protein–protein interaction. The other two family members, MYPT3 and TIMAP, lack the leucine zipper domain but contain a C-terminal prenylation site which targets the proteins to membranes (Hartshorne et al., 2002, Grassie et al., 2011).

The MYPT family is primarily regulated by phosphorylation by a variety of protein serine/threonine kinases. MYPT1 is phosphorylated Thr696 and Thr853 by ROCK (Kimura et al., 1996) which leads to the dissociation of the phosphatase from myosin and consequently leads to decrease in activity (Ichikawa et al., 1996, Velasco et al., 2002a). Both the ROCK sites are conserved in MYPT2, while only that corresponding to T696 is conserved in MBS85, and neither site is found in TIMAP or MYPT3 (Fig. 5.1) (Grassie et al., 2011). Anna Zagorska a previous PhD student in the lab had shown that NUAK1 phosphorylates the myosin targeting subunit or MYPT1 after interacting with the PP1β subunit of the complex via the conserved GILK motifs. NUAK1 phosphorylates MYPT1 subunit at the three Ser445, Ser472 and Ser910 residues that promotes interactions with 14-3-3 isoforms which was hypothesized to inhibit the MYPT1-PP1β complex phosphatase activity on MLC2. Besides MYPT1 , the other isoforms of myosin phosphatase family MYPT2 and MBS85 also interact with NUAK1 (Zagorska et al., 2010) but the exact functional implications have not yet been deciphered.

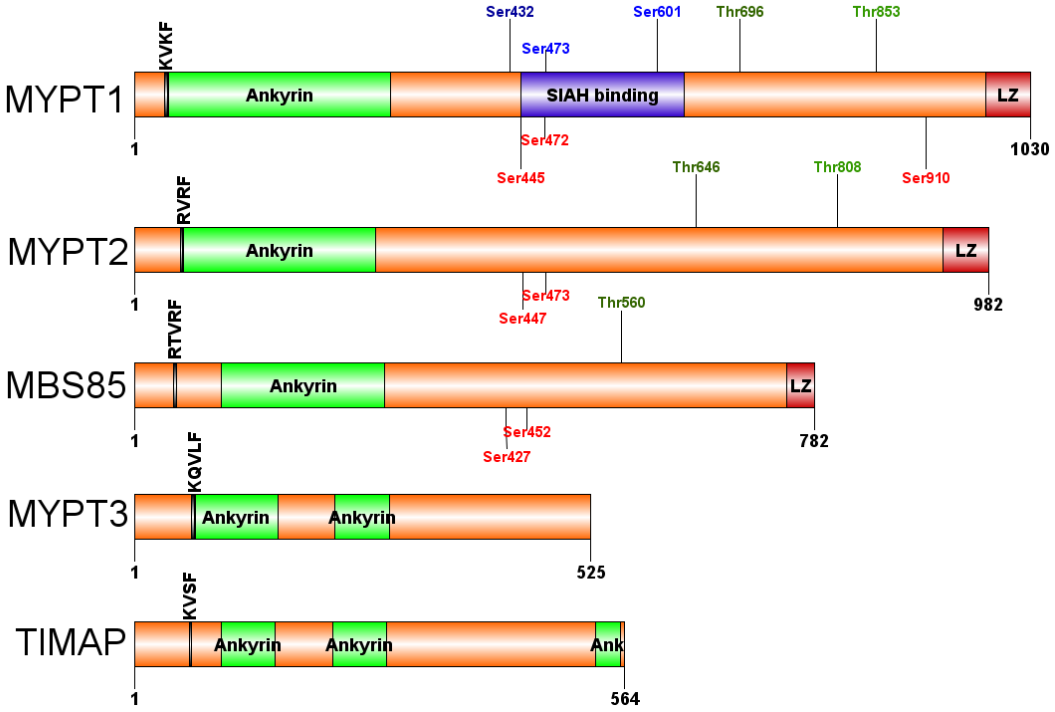

Figure 5.1 The domain structures of the MYPT family members with indicated phosphorylation sites.

5.1.1. MYPT1 or PPP1R12A

Smooth muscle MYPT1 was purified from chicken gizzard as a heterotrimeric complex composed of a 38 kDa PP1β catalytic subunit, regulatory subunit MYPT1(130 kDa) and a 20 kDa small subunit (M20) (Alessi et al., 1992, Hartshorne et al., 2002). MYPT1 interacts with PP1β at the N-terminus and with M20 at the C-terminus, thereby forming the holoenzyme of MYPT1-PP1β (Hartshorne et al., 2002). M20 is a splice variant of MYPT2 and has been detected only in smooth muscle myosin phosphatase (Moorhead et al., 1998). Determination of the crystal structure of PP1β in complex with a fragment (residues 1–299) corresponding to the N-terminus of MYPT1 (Terrak et al., 2004) showed that MYPT1 interacts with PP1β via the KVKF (RVxF) motif or via the myosin phosphatase N-terminal element or MyPhoNE (residues 10–17 in MYPT1) consensus sequence RxxQV/I/LK/RxY/W, which is conserved in all MYPT family members (Grassie et al., 2011).

MYPT1 contains a number of phosphorylation sites, of which the Thr696 and Thr853 cause inhibition of myosin phosphatase activity. Thr853 is a conserved ROCK phosphorylation site whereas several protein kinases, including ROCK, zipper-interacting protein kinase (ZIPK), myotonic dystrophy kinase and p21-activated protein kinases are known to phosphorylate the Thr696 residue (Grassie et al., 2011). During mitosis, MYPT1 is phosphorylated at several residues (Ser432, Ser473 and Ser601) by proline-directed kinases, such as cdc2 (Yamashiro et al., 2008) which creates a docking site for PLK1. Interaction with MYPT1-PP1β leads to dephosphorylation of the PLK1 activation residue Thr210 which leads to hindering of centrosome maturation and leads to mitotic arrest (Yamashiro et al., 2008).

MYPT1 undergoes proteasomal degradation upon interaction with E3 ubiquitin ligase sevenin-absentia-homolog 2 (SIAH2) (Twomey et al., 2010). SIAH2 interacts with MYPT1 via a central region of MYPT1 containing a SIAH-binding motif, which is not conserved in other MYPT family members. An activator protein p116Rip or M-RIP interacts directly with MYPT1 and myosin, thereby assists in the localisation of myosin phosphatase to myosin and increases myosin phosphatase activity on MLC2 (Koga and Ikebe, 2005). It has also been reported that 14-3-3s inhibit myosin phosphatase activity by dissociating myosin phosphatase from myosin, leading to delocalisation of MYPT1 from stress fibres (Koga and Ikebe, 2008). Recently our laboratory has shown that NUAK1 phosphorylates MYPT1 subunit at the three Ser445, Ser472 and Ser910 residues that promotes interactions with 14-3-3 isoforms which was suggested to inhibit the MYPT1-PP1β complex phosphatase activity on MLC2 (Zagorska et al., 2010). A key aim of the research presented in this chapter is to obtain physiological experimental evidence that phosphorylation of MYPT1 might indeed inhibit MYPT1-PP1β protein phosphatase activity.

5.1.2. MYPT family

Besides MYPT1, the four other members of the MYPT family are much less studied. They all have the conserved RVxF motif for PP1β interaction.

MYPT2 is predominantly expressed in striated (cardiac and skeletal) muscles and brain. MYPT2 has been shown to interact with PP1β and is the regulatory subunit of cardiac myosin phosphatase (Moorhead et al., 1998, Mizutani et al., 2010). MYPT2-PP1β blocks angiotensin II-induced sarcomere organization in cultured cardiomyocytes and localises at the A band and Z-line of cardiac muscles and also in mitochondria (Okamoto et al., 2006).

MBS85 is an 85 kDa ubiquitously expressed protein that was discovered as a substrate of MRCKα which mediates Cdc42-induced actin reorganization (Tan et al., 2001). Recent studies have shown that MBS85 undergoes AMPKα2 mediated phosphorylation at Ser452 which promotes 14-3-3 interaction and is essential for proper progression of mitosis (Banko et al., 2011). The AMPK phosphorylation site Ser452 on MBS85 was conserved with Ser472 of MYPT1 and could possibly be a NUAK1 phosphosite as well and hence required further attention.

TIMAP is primarily localized to the plasma membrane of endothelial cells and undergoes TGFβ-mediated transcriptional repression (Grassie et al., 2011). TIMAP was reported to bind laminin receptor (LAMR1) and recruit PP1β for LAMR1 dephosphorylation (Kim et al., 2005). Activity of the TIMAP-PP1β complex seems to be regulated by PKA and GSK3 mediated phosphorylation at Ser333 and Ser337 (Li et al., 2007, Csortos et al., 2008).

MYPT3 is predominantly membrane-associated and is expressed primarily in the heart, brain and kidneys (Grassie et al., 2011). Contrary to other MYPT family members, MYPT3 binding to PP1β inhibits its catalytic activity towards MLC2 (Skinner and Saltiel, 2001) and requires PKA mediated phosphorylation of MYPT3 to increase the activity of PP1β towards phosphorylated MLC2 (Yong et al., 2006).

MYPT2 and MBS85 has been found to immunoprecipitate with overexpressed NUAK1 in mass-spectrometric experiments as well as in co-immunoprecipitations (Zagorska et al., 2010). Hence, I was interested in exploring whether MYPT2 and MBS85 were potential substrates of NUAK1.

5.2. Results

5.2.1. MYPT1-PP1β wild-type and triple Ser mutant complexes were co-purified from bacterial and exhibited similar phosphatase specific activity

Although MYPT1-PP1β beautifully expresses in mammalian cells, I decided to purify the complex from bacterial system because MYPT1 is known to interact with various kinases in vivo and hence the major sites may remain pre-phosphorylated and consequently pose problems while carrying out biochemical phosphatase assays. In order to express recombinant MYPT1-PP1β complex for functional analysis, I decided to express the two subunits of the complex together in a polycistronic bacterial expression vector. GST-MYPTI-His-PP1β wild-type (WT) and GST-MYPTI-His-PP1β triple serine-alanine mutant (Ser445Ala+Ser472Ala+Ser910Ala or SSS/AAA) in which all NUAK1 phosphorylation sites are mutated, were overexpressed and purified using autoinduction media from *E.coli* BL-21 tranformed with the polycistronic pOPTH expression vector (Fig.5.2A) containing the cDNA of the proteins. MYPT1 complex was purified by GST-sepharose affinity chromatography and the GST tag was cleaved from MYPT1 with Precission protease. The purified proteins were resolved by SDS gel electrophoresis (Fig.5.2B) and the purified complexes were estimated to be approximately 20% pure. The identity of MYPT1 (130kDa) and the PP1β (37kDa) bands were confirmed by QTRAP mass spectrometry analysis.

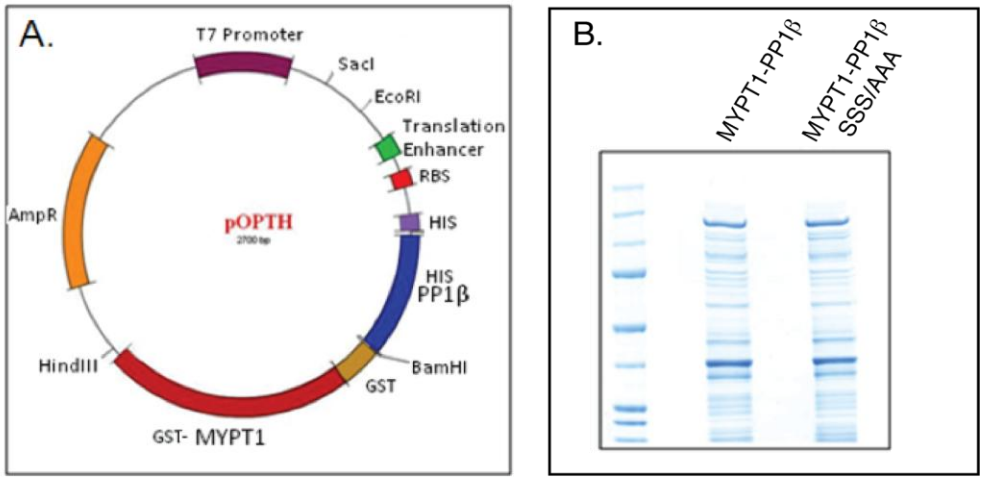

Figure 5.2 : Overexpression of MYPT1-PP1β complexes : (A) The construct used to overexpress recombinant MYPT1-PP1β wild-type (WT) and SSS/AAA mutant (mutated at the three NUAK1 phosphosites Ser445+Ser472+Ser910 to alanine) complexes from *E.coli* was a polycistronic pOPTH vector with a T7 promoter, translation enhancer element and ampicillin resistance gene. A GST tag was linked to MYPT1 and a hexa-His tag on the PP1β. (B) The coomassie gel showing the overexpressed wild-type and triple serine mutant GST-MYPT1-His-PP1β after a GST-affinity purification and GST cleavage by Precission protease.

In order to establish that the purified recombinant MYPT1-PP1β complexes (WT and SSS/AAA) were active, varying amounts of the complexes were incubated with ^{32}P-GST-MLC2 that had been phosphorylated to stoichiometric levels with ROCK kinase. The reaction was carried out for 10min at 30 °C. Reactions were terminated by addition of 20% TCA to precipitate the protein and the amount of ^{32}P inorganic phosphate released in the supernatant by virtue of phosphatase activity was assessed. A linear reaction condition was achieved between the % release of phosphate from the ^{32}P-GST-MLC2 into the supernatant and the amount in ng (nanograms) of MYPT1-PP1β (Fig 5.3). The wild type MYPT1-PP1β had a specific activity of 1100 U/mg and that of the SSS/AAA was found to be 1000 U/mg, thus indicating that mutating the NUAK1 phosphorylation site did not influence the intrinsic activity of the MYPT1-PP1β complex.

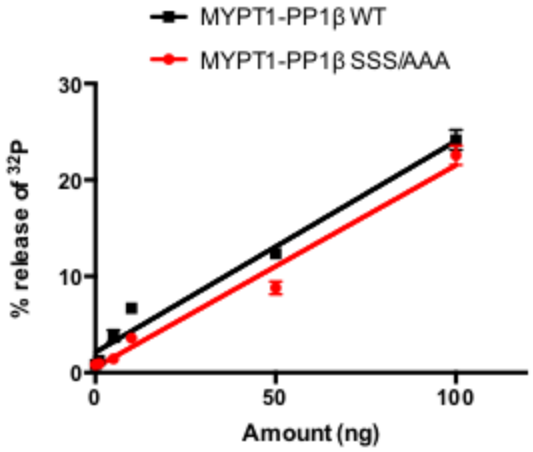

Fig 5.3 : The purified MYPT1-PP1β complexes were active. MYPT1-PP1β wild-type and SSS/AAA were overexpressed and purified in parallel. Various amounts of the purified MYPT1-PP1β complex (both WT and SSS/AAA) were treated with ^{32}P-GST-MLC2 and a linear reaction was established between the protein phosphatase amount in reaction (0.5ng to 100ng) and % release of phosphate from ^{32}P-GST-MLC2 into the supernatant. The specific activity of each of the wild-type and SSS/AAA mutant was calculated by considering 20% purity. The specific activity of wild type MYPT1-PP1β was 1100 U/mg and that of SSS/AAA was 1000 U/mg.

To further confirm that NUAK1 was unable to phosphorylate the MYPT1-PP1β SSS/AAA, an autoradiography was carried out using NUAK1 on the bacterially purified MYPT1-PP1β WT and SSS/AAA in parallel using [γ^{32}P]ATP. Immunoblots were carried out for MYPT1 total, MYPT1 Ser445, Ser472, Ser910 and NUAK1 (Fig. 5.4). MYPT1-PP1β SSS/AAA could not be phosphorylated significantly by NUAK1.

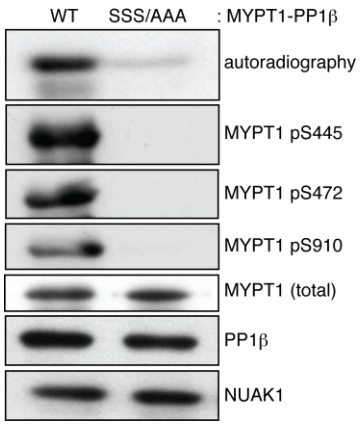

Figure 5.4 : MYPT1-PP1β SSS/AAA complex is not phosphorylated by NUAK1 significantly : NUAK1 phosphorylates the MYPT1-PP1β complex at Ser445, Ser472 and Ser910. NUAK1 showed significantly lower phosphorylation of the MYPT1-PP1β triple serine mutant (SSS/AAA) complex as shown in the autoradiography and the phosphoblots.

5.2.2. Phosphorylation by NUAK1 inhibits MYPT1-PP1β phosphatase activity

In order to investigate whether NUAK1 phosphorylation of MYPT1 influenced its phosphatase activity, MYPT1-PP1β complex was incubated with or without NUAK1 with 0.1 μM [γ-32P]ATP-Mg under the conditions that MYPT1 complex undergoes maximum stoichiometric phosphorylation of 3 moles of phosphate per mole of complex. Reaction was terminated by addition of excess EDTA to chelate the Mg and intrinsic MYPT1 phosphatase activity was assessed following 100 fold dilution. 14-3-3s were used in the assay as it was reported that 14-3-3 interaction was essential for the inhibition of MYPT1 binding to myosin II (Koga and Ikebe, 2008). Under these conditions, it was found that NUAK1 induced a moderate but reproducible and statistically significant (~40%) inhibition of the phosphatase activity of the complex towards MLC2 (Fig 5.5). The mutant with all the three NUAK1 phosphosites mutated to alanine, however, didnot show any inhibition of phosphatase activity on NUAK1 phosphorylation (Fig 5.5).

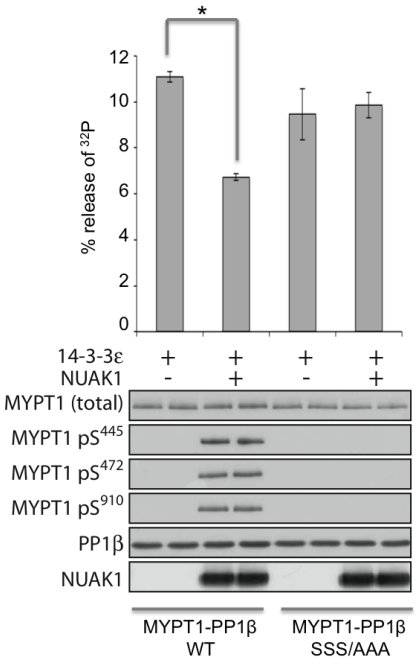

Figure 5.5 : NUAK1 phosphorylation at Ser445, Ser472 and Ser910 of MYPT1-PP1β complex inhibits the phosphatase activity : The phosphatase activities of the MYPT1-PP1β wild-type and SSS/AAA mutant were compared with or without NUAK1 phosphorylation. There was a significant inhibition of phosphatase activity of the NUAK1 phosphorylated MYPT1-PP1β wild-type complex unlike the SSS/AAA mutant which showed no inhibition post NUAK1 phosphorylation.

5.2.3. NUAK1 phosphorylates MYPT2 and MBS85 in vitro at phosphosites conserved with MYPT1

NUAK1 has been found to phosphorylate MYPT1 at residues that lie within an optimal AMPK consensus motif LX(R/K)(S/T)X(pS)XXX(L/I) (Dale et al., 1995, Hardie et al., 2012). Sequence alignment suggests that this AMPK consensus motif is found in MYPT2 and MBS85 but not in MYPT3 and TIMAP. Fig 5.5 shows the residues in MYPT2 and MBS85 that align with the Ser445 and Ser472 residues on MYPT1 that NUAK1 phosphorylates. Consistent with this, NUAK1 phosphorylates MYPT2 (Fig. 5.7) and MBS85 (Fig. 5.8).

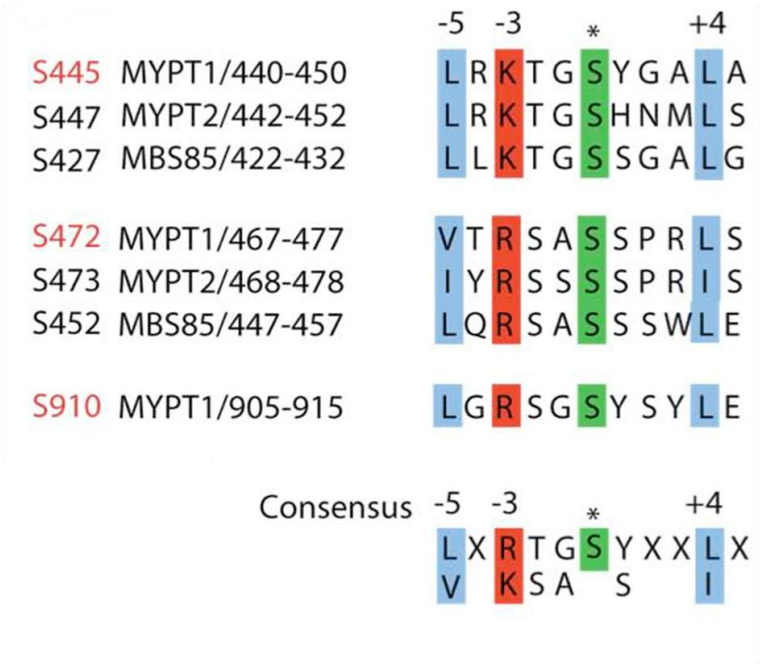

Figure 5.6 NUAK1 phosphosites are conserved in MYPT1, MYPT2 and MBS85 isoforms. The Ser445 and Ser472 sites on MYPT1 was found to be conserved in MYPT2 and MBS85 but not in MYPT3 and TIMAP. Thus MYPT2 and MBS85 may be potential NUAK1 substrates. All the potential NUAK1 sites on MYPT isoforms are conserved AMPK phosphorylation motifs. Image adapted from (Zagorska et al., 2010).

In order to map the phosphorylation sites, MYPT2 and MBS85 were radiolabelled by NUAK1 using [γ^{32}P]ATP (specific activity 10,000-15,000 cpm/pmol) in vitro, and then digested with Trypsin. The resulting peptides were then subjected to HPLC, mass spectrometric analysis and solid phase Edman sequencing (Section 2.2.23.2). This analysis revealed that NUAK1 phosphorylates MYPT2 at Ser447 and Ser473 (Fig 5.7) and MBS85 at Ser427 and Ser452 (Fig. 5.8) in vitro.

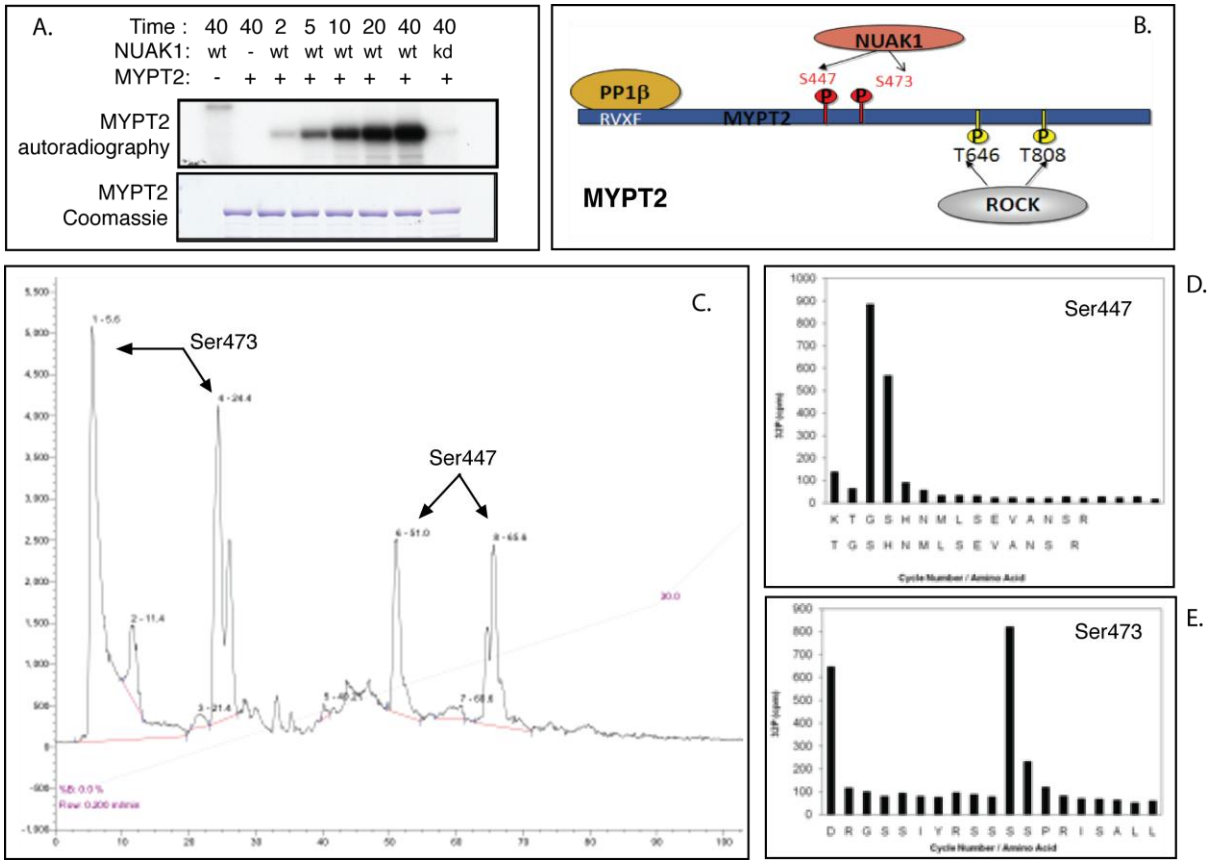

Figure 5.7. NUAK1 phosphorylates MYPT2 at Ser447 and Ser 473. (A) Time course of phosphorylation of MYPT2 by NUAK1 with [γ^{32}P]ATP, incubated at the given time points, has been shown in an autoradiography. A kinase inactive (kd) NUAK1(Asp196Ala) was used in place of wild-type NUAK1 as a negative control. (B) The schematic domain structure of MYPT2 showing the conserved ankyrin repeat domain, leucine zipper motif, PP1β binding RVXF motif and the inhibitory regions with NUAK1 and ROCK phosphosites. (C) MYPT2 phosphorylated by NUAK1 with [γ^{32}P]ATP was in gel digested by trypsin and hplc of the peptides were carried out. Two peaks corresponding to each of the two phosphopeptides were found. (D) The solid phase Edman sequencing of the hplc derived Ser 447 phosphopeptides are shown. (E) same as D, except for Ser473 Edman sequencing is shown. The second peaks of the tryptic digest were miscleavages wherein two phosphopeptides with the same phosphosite were identified.

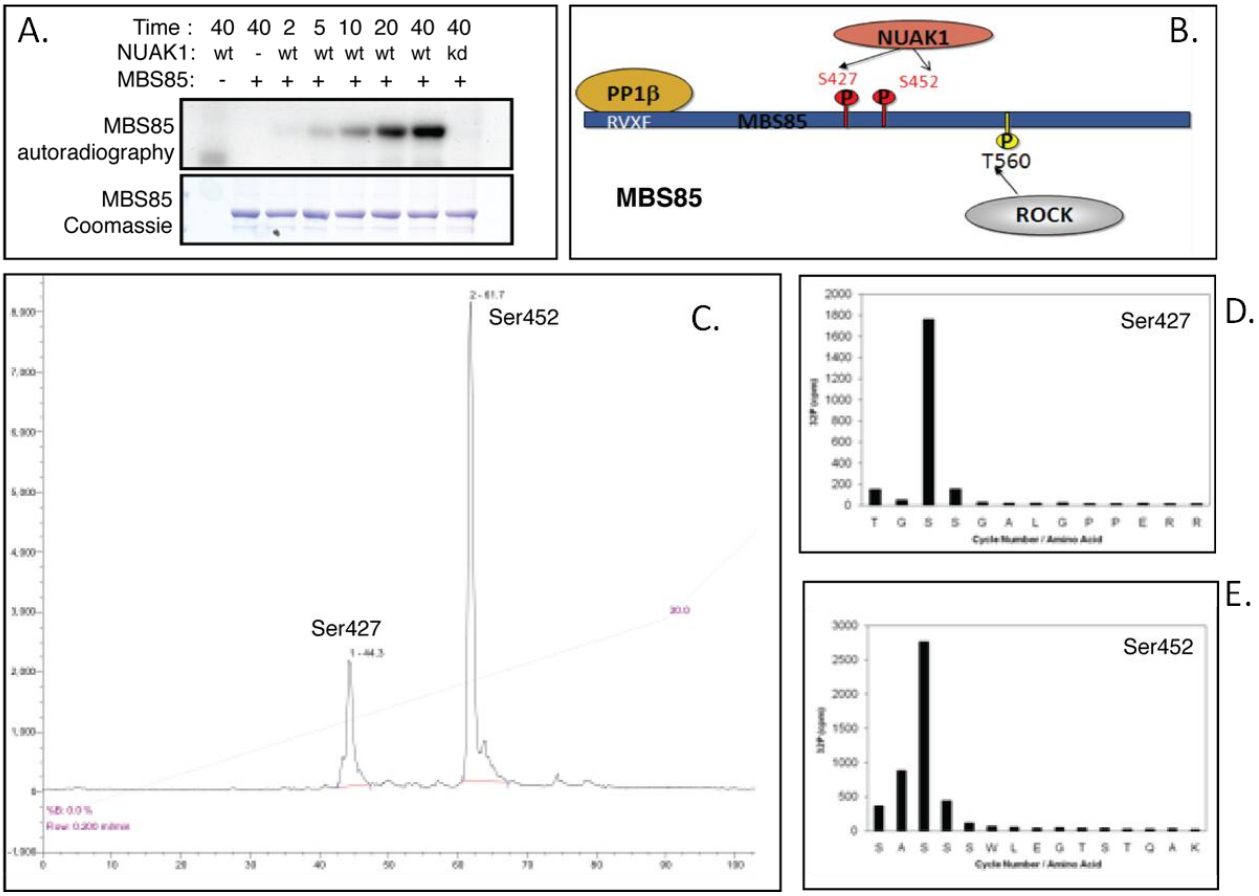

Figure 5.8. NUAK1 phosphorylates MBS85 at Ser427 and Ser 452. (A) Time course of phosphorylation of MBS85 by NUAK1 with [γ^{32}P]ATP, incubated at the given time points, has been shown in an autoradiography. A kinase inactive (kd) NUAK1(Asp196Ala) was used in place of wild-type NUAK1 as a negative control. (B) The schematic domain structure of MBS85 showing the conserved ankyrin repeat domain, leucine zipper motif, PP1β binding RVXF motif and the inhibitory regions with NUAK1 and ROCK phosphosites. (C) MBS85 phosphorylated by NUAK1 with [γ^{32}P]ATP was in gel digested by trypsin and hplc of the peptides were carried out. One peak corresponding to each of the two phosphopeptides were found. (D) The solid phase Edman sequencing of the hplc derived Ser 427 phosphopeptides are shown. (E) same as D, except for Ser452 Edman sequencing is shown.

5.2.4. NUAK1 phosphorylates MYPT3 at an AMPK consensus motif

In order to map the phosphorylation sites, MYPT3 was radiolabelled by NUAK1 using [γ^{32}P]ATP (specific activity 10,000-15,000 cpm/pmol) in vitro as before, and then digested with Trypsin. The resulting peptides were then subjected to HPLC, mass spectrometric analysis and solid phase Edman sequencing (Section 2.2.23.2). This analysis revealed that

NUAK1 phosphorylates MYPT3 at Ser433 (Fig 5.9) at typical AMPK phosphorylation motif LDRSV**S**YQLSP (Ser433 in red). A radioactive signal was observed at Ser431 on the Edman sequencing, but carrying out a hplc on NUAK1 phosphorylated trypic peptides of MYPT3 S433A showed that Ser431 may not be an in vitro phosphosite for NUAK1 (Fig. 5.9D).

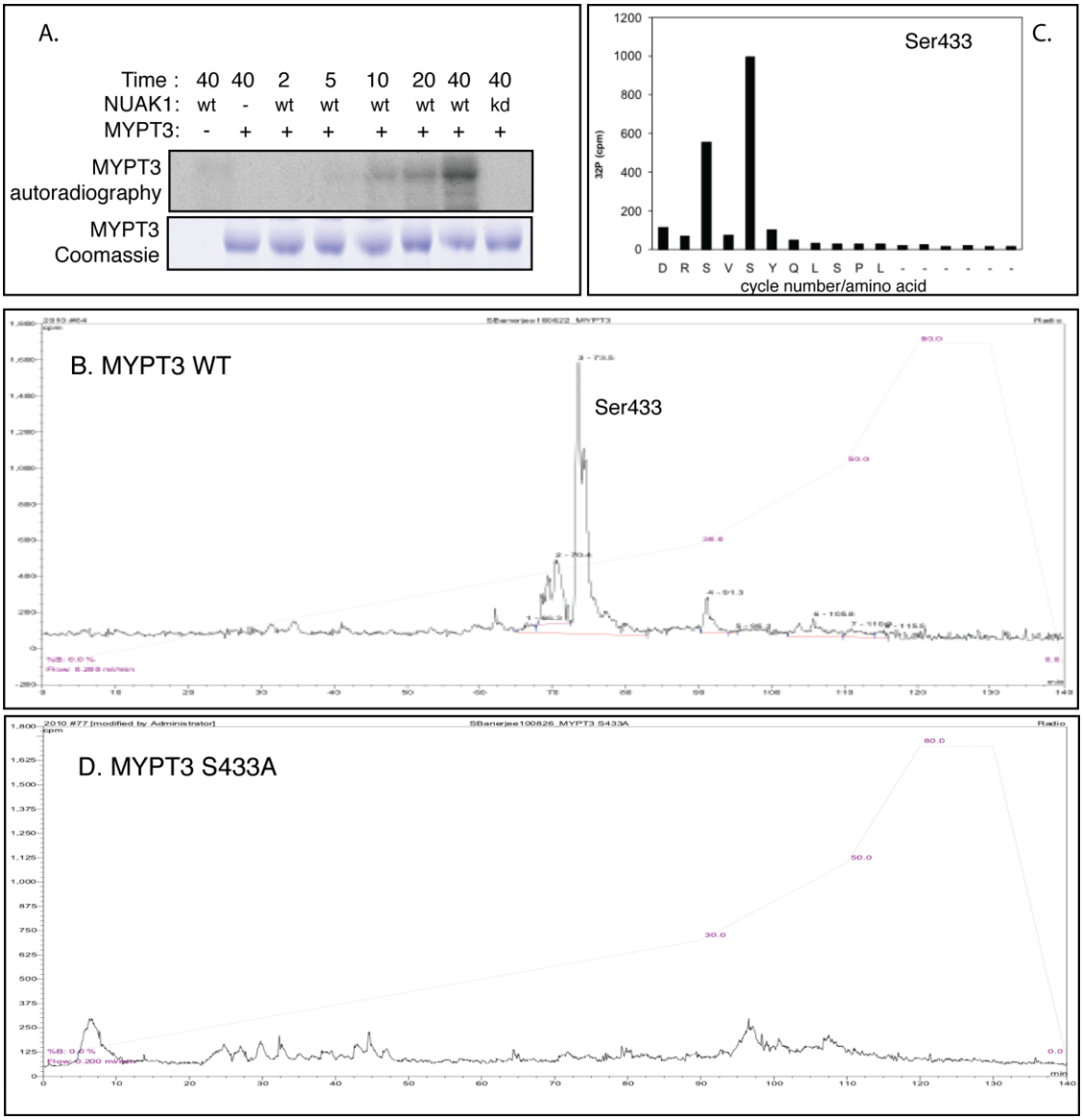

Figure 5.9. NUAK1 phosphorylates MYPT3 at Ser433. (A) Time course of phosphorylation of MYPT3 by NUAK1 with [γ^{32}P]ATP, incubated at the given time points, has been shown in an autoradiography. A kinase inactive (kd) NUAK1(Asp196Ala) was used in place of wild-type NUAK1 as a negative control. (B) MYPT3 phosphorylated by NUAK1 with [γ^{32}P]ATP was in gel digested by trypsin and hplc of the peptides were carried out. One peak corresponding to the single phosphopeptide was found. (C) The solid phase Edman sequencing of the hplc derived Ser 433 phosphopeptide is shown. (D) MYPT3 S433A mutant phosphorylated by NUAK1 with [γ^{32}P]ATP was in gel digested by trypsin and hplc of the peptides were carried out.

5.2.5. NUAK1 does not phosphorylate TIMAP with a high stoichiometry

Compared to MYPT1, MYPT2, MYPT3 and MBS85, the other MYPT isoform TIMAP is not significantly phosphorylated by NUAK1 in vitro. Bacterially purified TIMAP was phosphorylated by NUAK1 in vitro. Time course of phosphorylation of MYPT3 and TIMAP by NUAK1 with [γ^{32}P]ATP was carried out. A kinase inactive (kd) NUAK1(Asp196Ala) was used in place of wild-type NUAK1 as a negative control. Compared to the autoradiography signal of the other MYPT1 phosphoryated with NUAK1, MYPT3 and TIMAP were much weaker and exhibited hardly any ^{32}P incorporation at 40 mins of kinase reaction (Fig. 5.10).

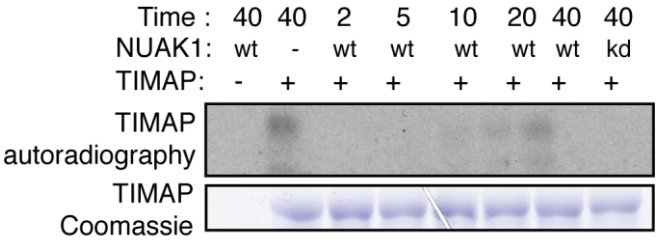

Figure 5.10. NUAK1 doesnot phosphorylate TIMAP. Time course of phosphorylation of TIMAP by NUAK1 with [γ^{32}P]ATP has been shown in an autoradiography. A kinase inactive (kd) NUAK1 was used in place of wild-type NUAK1 as a negative control. TIMAP was not phosphorylated by NUAK1 to the extent of the other MYPT isoforms.

5.3. Discussion

Myosin phosphatases are a family of five isoforms primarily responsible for dephosphorylating and inactivating myosin in diverse tissues (Grassie et al., 2011). Previous works from Dr. Mitsuo Ikebe's laboratory has shown that p116RIP and 14-3-3 isoforms are essential interactors of MYPT1-PP1β complex which determine the localisation of the phosphatase to myosin II (Koga and Ikebe, 2005, Koga and Ikebe, 2008). ROCK plays a critical role in phosphorylating MYPT1 isoform at Thr696 and Thr853 which leads to inhibition of the phosphatase activity of MYPT1-PP1β towards phosphorylated myosin light chain 2 (Feng et al., 1999, Velasco et al., 2002b). Recently, Anna Zagorska, a former PhD student of our laboratory had shown that NUAK1 controls the cell adhesion properties of the cells by controlling the phosphatase activity of MYPT1-PP1β (Zagorska et al., 2010). NUAK1 has specific and distinct phosphosites on MYPT1 Ser445, Ser472 and Ser910 (Stoichiometry of 1.5) (Fig. 5.4) which are independent of the inhibitory ROCK phosphosites Thr696 and Thr853 (Zagorska et al., 2010).

To study the effect of NUAK1 on the phosphatase activity of MYPT1-PP1β in vitro on radiolabelled MLC2 substrate, I co-purified MYPT1-PP1β complex from bacteria (Fig. 5.2). Although MYPT1-PP1β complex can be purified from mammalian systems, there is always a possibility of contamination with interacting kinases and pre-phosphorylation of essential residues on MYPT1. MYPT1-PP1β complex was for the first time expressed together in the same construct; earlier works on the complex had been carried out mostly by separate bacterial expression of the two proteins and carrying out an in vitro binding. MYPT1-PP1β WT and S445A+S472A+S910A mutant complexes were purified in parallel (Fig. 5.2) and their specific activity was calculated and found to be comparable ~1000-1100 U/mg (Fig 5.3). The MYPT1-PP1β complex phosphatase activity is moderately inhibited (~40%) by

NUAK1 phosphorylation at the MYPT1 Ser445, Ser472 and Ser910 phosphosites and hence the MYPT1 complex is unable to dephosphorylate myosin light chain (Fig. 5.5). The inhibition, although moderate, was statistically significant and reproducible. Full length myosin II instead of the MLC2 subunit could possibly be a more physiological substrate for the phosphatase assay and is one aspect which might require more attention in future. MYPT1- PP1β complex mutated at the three NUAK1 phosphosites to alanine does not show any inhibition of phosphatase activity on phosphorylating with NUAK1 (Fig. 5.5).

Dr. Anne Brunet's laboratory reported that one of the myosin phosphatase isoform MBS85 was a substrate of AMPKα2 and phosphorylation of MBS85 at Ser452 by AMPKα2 induced 14-3-3 interaction with MBS85 and regulated the progression of mitosis (Banko et al., 2011). Interestingly, Ser452 in MBS85 was conserved with MYPT1 NUAK1 phosphorylation site of Ser472 (Fig. 5.6). Both MYPT2 and MBS85 had Ser residues which were conserved with the MYPT1 NUAK1 phosphosites (Fig. 5.6). To identify whether NUAK1 phosphorylated MYPT2 and MBS85 as well, I carried out phospho-peptide mapping followed by Edman sequencing. NUAK1 strongly phosphorylated MYPT2 and MBS85 in vitro. MYPT2 phosphomapping revealed Ser447 and Ser473 (stoichiometry of 1.2) (Fig. 5.7) as potential phosphosites whereas MBS85 phosphomapping showed Ser427 and Ser452 (stoichiometry of 0.8) (Fig. 5.8) as potential NUAK1 phosphosites. MYPT3 was relatively weakly phosphorylated by NUAK1 at Ser433 which was a typical AMPK consensus phosphorylation motif but not conserved with the other MYPT isoforms (Fig. 5.9). NUAK1, however, did not phosphorylate TIMAP with high enough stoichiometry (Fig. 5.10). Hence, AMPK and NUAK may be playing dual roles in phosphorylating myosin phosphatase isoforms especially Ser452 of MBS85 in cells and further work is required to properly dissect the mechanism.

Thus, the present work has established that NUAK1 phosphorylates and inhibits MYPT1-PP1β phosphatase activity in vitro and the other MYPT isoforms MYPT2 and MBS85 are substrates of NUAK1 in vitro. Further investigation is required looking into a possible NUAK1-MYPT isoform interactions in controlling myosin II activity.

6. Summary

The primary aspect my work has been to dissect the physiological roles, identification of interacting partners and methods of regulation of AMPK-related kinase NUAK1. Since NUAK1 substrate specificity is very closely related to most of the other AMPK family members, in collaboration with Dr. Nathanael Gray's laboratory I have developed highly selective inhibitors of NUAK kinases (detailed in chapter 3). Based on the chemical backbone of generic inhibitors, HTH-01-015 (NUAK1 selective) and WZ4003 (NUAK1 and NUAK2 dual inhibitor) could potentially be exciting tools to dissect the possible roles of NUAK1 in cancer.

Besides pharmacological inhibition, in chapter 4, I further identified NUAK1 to be regulated in the cell cycle upon phosphorylation by PLK1 at the G2/M stage which triggers NUAK1 interaction with $SCF^{\beta TRCP}$. $SCF^{\beta TRCP}$ interaction leads to ubiquitylation and degradation of NUAK1 at G2/M stage of cell cycle. NUAK1 tends to accumulate in cells at the S-phase of the cell cycle and localises to the nucleus, thus indicating possible roles in the DNA synthetic or DNA damage checkpoint regulation of cell cycle. Further work is required to elucidate the exact roles of NUAK1 in the cell cycle.

Finally, Anna Zagorska a previous student had identified MYPT1-PP1β as a physiological substrate of NUAK1 and in chapter 5, I have shown that NUAK1 regulates the phosphatase activity of MYPT1-PP1β in vitro towards myosin light chain 2 substrate. Furthermore, I have shown that the other MYPT isoforms MYPT2, MBS85 and possibly MYPT3 are substrates of NUAK1 in vitro. Further work is required to validate these in vitro substrates as potential in vivo physiological substrates and to identify the possible roles of the interactions.

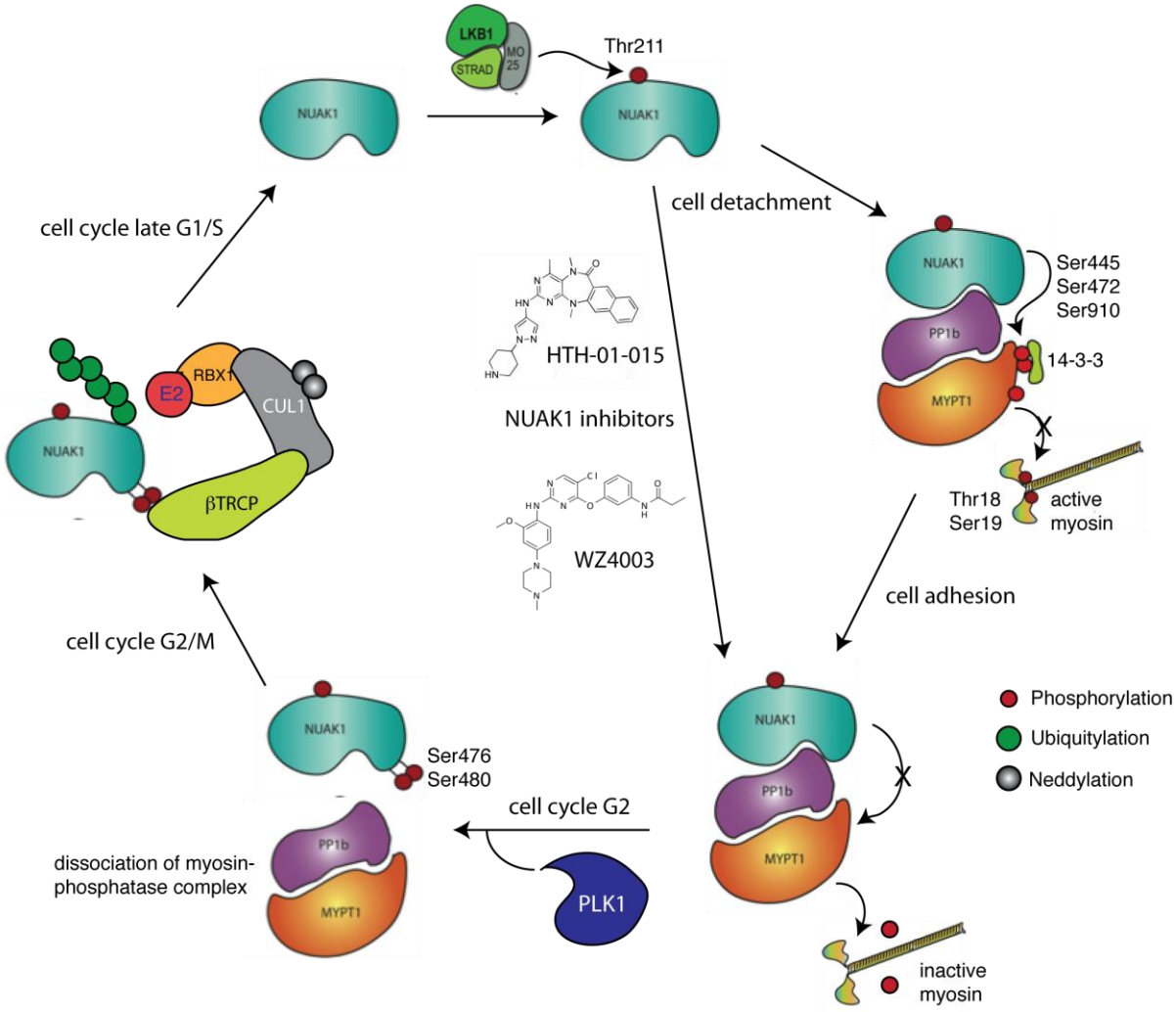

Figure 6. Schematic representation of phosphorylation, activation, ubiquitylation and small molecule inhibition of NUAK1.

7. Bibliography

ABBAS, T. & DUTTA, A. 2011. CRL4(Cdt2) Master coordinator of cell cycle progression and genome stability. *Cell Cycle,* 10**,** 241-249.

ABBAS, T., SIVAPRASAD, U., TERAI, K., AMADOR, V., PAGANO, M. & DUTTA, A. 2008. PCNA-dependent regulation of p21 ubiquitylation and degradation via the CRL4(Cdt2) ubiquitin ligase complex. *Genes & Development,* 22**,** 2496-2506.

ACQUAVIVA, C. & PINES, J. 2006. The anaphase-promoting complex/cyclosome: APC/C. *Journal of Cell Science,* 119**,** 2401-2404.

AL-HAKIM, A. K., GORANSSON, O., DEAK, M., TOTH, R., CAMPBELL, D. G., MORRICE, N. A., PRESCOTT, A. R. & ALESSI, D. R. 2005. 14-3-3 cooperates with LKB1 to regulate the activity and localization of QSK and SIK. *Journal of Cell Science,* 118**,** 5661-5673.

AL-HAKIM, A. K., ZAGORSKA, A., CHAPMAN, L., DEAK, M., PEGGIE, M. & ALESSI, D. R. 2008. Control of AMPK-related kinases by USP9X and atypical Lys29/Lys33-linked polyubiquitin chains. *Biochem J,* 411**,** 249-260.

ALBANESE, C., JOHNSON, J., WATANABE, G., EKLUND, N., VU, D., ARNOLD, A. & PESTELL, R. G. 1995. TRANSFORMING P21(RAS) MUTANTS AND C-ETS-2 ACTIVATE THE CYCLIN D1 PROMOTER THROUGH DISTINGUISHABLE REGIONS. *Journal of Biological Chemistry,* 270**,** 23589-23597.

ALESSI, D., MACDOUGALL, L. K., SOLA, M. M., IKEBE, M. & COHEN, P. 1992. THE CONTROL OF PROTEIN PHOSPHATASE-1 BY TARGETING SUBUNITS - THE MAJOR MYOSIN PHOSPHATASE IN AVIAN SMOOTH-MUSCLE IS A NOVEL FORM OF PROTEIN PHOSPHATASE-1. *European Journal of Biochemistry,* 210**,** 1023-1035.

ALESSI, D. R., SAKAMOTO, K. & BAYASCAS, J. R. 2006. LKB1-dependent signaling pathways. *Annual Review of Biochemistry,* 75**,** 137-163.

ALLEN, B. G. & WALSH, M. P. 1994. The biochemical basis of the regulation of smooth-muscle contraction. *Trends Biochem Sci,* 19**,** 362-8.

BAIN, J., PLATER, L., ELLIOTT, M., SHPIRO, N., HASTIE, C. J., MCLAUCHLAN, H., KLEVERNIC, I., ARTHUR, J. S. C., ALESSI, D. R. & COHEN, P. 2007. The selectivity of protein kinase inhibitors: a further update. *Biochemical Journal,* 408**,** 297-315.

BANKO, M. R., ALLEN, J. J., SCHAFFER, B. E., WILKER, E. W., TSOU, P., WHITE, J. L., VILLEN, J., WANG, B., KIM, S. R., SAKAMOTO, K., GYGI, S. P., CANTLEY, L. C., YAFFE, M. B., SHOKAT, K. M. & BRUNET, A. 2011. Chemical genetic screen for AMPKalpha2 substrates uncovers a network of proteins involved in mitosis. *Mol Cell,* 44**,** 878-92.

BARFORD, D. 2011. Structural insights into anaphase-promoting complex function and mechanism. *Philosophical Transactions of the Royal Society B-Biological Sciences,* 366**,** 3605-3624.

BARNES, A. P., LILLEY, B. N., PAN, Y. A., PLUMMER, L. J., POWELL, A. W., RAINES, A. N., SANES, J. R. & POLLEUX, F. 2007. LKB1 and SAD kinases define a pathway required for the polarization of cortical neurons. *Cell,* 129**,** 549-563.

BARR, A. R. & GERGELY, F. 2007. Aurora-A: the maker and breaker of spindle poles. *Journal of Cell Science,* 120**,** 2987-2996.

BASHIR, T., DORRELLO, N. V., AMADOR, V., GUARDAVACCARO, D. & PAGANO, M. 2004. Control of the SCFSkp2-Cks1 ubiquitin ligase by the APC/C-Cdh1 ubiquitin ligase. *Nature,* 428**,** 190-193.

BASSERMANN, F., EICHNER, R. & PAGANO, M. 2013. The ubiquitin proteasome system - Implications for cell cycle control and the targeted treatment of cancer. *Biochim Biophys Acta*.

BASSERMANN, F., VON KLITZING, C., ILLERT, A. L., MUENCH, S., MORRIS, S. W., PAGANO, M., PESCHEL, C. & DUYSTER, J. 2007. Multisite phosphorylation of nuclear interaction partner of ALK (NIPA) at G(2)/M involves cyclin B1/Cdk1. *Journal of Biological Chemistry,* 282**,** 15965-15972.

BIONDI, R. M., KOMANDER, D., THOMAS, C. C., LIZCANO, J. M., DEAK, M., ALESSI, D. R. & VAN AALTEN, D. M. F. 2002. High resolution crystal structure of the human PDK1 catalytic domain defines the regulatory phosphopeptide docking site. *Embo Journal,* 21**,** 4219-4228.

BOLLEN, M., PETI, W., RAGUSA, M. J. & BEULLENS, M. 2010. The extended PP1 toolkit: designed to create specificity. *Trends Biochem Sci,* 35**,** 450-8.

BONN, S., HERRERO, S., BREITENLECHNER, C. B., ERLBRUCH, A., LEHMANN, W., ENGH, R. A., GASSEL, M. & BOSSEMEYER, D. 2006. Structural analysis of protein kinase A mutants with Rho-kinase inhibitor specificity. *Journal of Biological Chemistry,* 281**,** 24818-24830.

BORDEN, K. L. B. 2000. RING domains: Master builders of molecular scaffolds? *Journal of Molecular Biology,* 295**,** 1103-1112.

BOUDEAU, J., BAAS, A. F., DEAK, M., MORRICE, N. A., KIELOCH, A., SCHUTKOWSKI, M., PRESCOTT, A. R., CLEVERS, H. C. & ALESSI, D. R. 2003. MO25 alpha/beta interact with STRAD

alpha/beta enhancing their ability to bind, activate and localize LKB1 in the cytoplasm. *Embo Journal,* 22**,** 5102-5114.

BOUDEAU, J., SCOTT, J. W., RESTA, N., DEAK, M., KIELOCH, A., KOMANDER, D., HARDIE, D. G., PRESCOTT, A. R., VAN AALTEN, D. M. F. & ALESSI, D. R. 2004. Analysis of the LKB1-STRAD-MO25 complex. *Journal of Cell Science,* 117**,** 6365-6375.

BRADFORD, M. M. 1976. RAPID AND SENSITIVE METHOD FOR QUANTITATION OF MICROGRAM QUANTITIES OF PROTEIN UTILIZING PRINCIPLE OF PROTEIN-DYE BINDING. *Analytical Biochemistry,* 72**,** 248-254.

BREMM, A., FREUND, S. M. V. & KOMANDER, D. 2010. Lys11-linked ubiquitin chains adopt compact conformations and are preferentially hydrolyzed by the deubiquitinase Cezanne. *Nature Structural & Molecular Biology,* 17**,** 939-U47.

BRIGHT, N. J., THORNTON, C. & CARLING, D. 2009. The regulation and function of mammalian AMPK-related kinases. *Acta Physiologica,* 196**,** 15-26.

BROWNELL, J. E., SINTCHAK, M. D., GAVIN, J. M., LIAO, H., BRUZZESE, F. J., BUMP, N. J., SOUCY, T. A., MILHOLLEN, M. A., YANG, X., BURKHARDT, A. L., MA, J., LOKE, H. K., LINGARAJ, T., WU, D., HAMMAN, K. B., SPELMAN, J. J., CULLIS, C. A., LANGSTON, S. P., VYSKOCIL, S., SELLS, T. B., MALLENDER, W. D., VISIERS, I., LI, P., CLAIBORNE, C. F., ROLFE, M., BOLEN, J. B. & DICK, L. R. 2010. Substrate-assisted inhibition of ubiquitin-like protein-activating enzymes: the NEDD8 E1 inhibitor MLN4924 forms a NEDD8-AMP mimetic in situ. *Mol Cell,* 37**,** 102-11.

BUDHIDARMO, R., NAKATANI, Y. & DAY, C. L. 2012. RINGs hold the key to ubiquitin transfer. *Trends Biochem Sci.* England: 2011 Elsevier Ltd.

BUSINO, L., DONZELLI, M., CHIESA, M., GUARDAVACCARO, D., GANOTH, D., DORRELLO, N. V., HERSHKO, A., PAGANO, M. & DRAETTA, G. F. 2003. Degradation of Cdc25A by beta-TrCP during S phase and in response to DNA damage. *Nature,* 426**,** 87-91.

CAMPBELL, D. G. & MORRICE, N. A. 2002. Identification of protein phosphorylation sites by a combination of mass spectrometry and solid phase Edman sequencing. *Journal of biomolecular techniques : JBT,* 13**,** 119-30.

CASTRO, A., ARLOT-BONNEMAINS, Y., VIGNERON, S., LABBE, J. C., PRIGENT, C. & LORCA, T. 2002. APC/Fizzy-Related targets Aurora-A kinase for proteolysis. *Embo Reports,* 3**,** 457-462.

CHANG, X.-Z., YU, J., LIU, H.-Y., DONG, R.-H. & CAO, X.-C. 2012. ARK5 is associated with the invasive and metastatic potential of human breast cancer cells. *Journal of Cancer Research and Clinical Oncology*, 138**,** 247-254.

CHEN, H., MA, H., INUZUKA, H., DIAO, J., LAN, F., SHI, Y. G., WEI, W. & SHI, Y. 2013a. DNA damage regulates UHRF1 stability via the SCF(beta-TrCP) E3 ligase. *Mol Cell Biol,* 33**,** 1139-48.

CHEN, P., LI, K., LIANG, Y., LI, L. & ZHU, X. 2013b. High NUAK1 expression correlates with poor prognosis and involved in NSCLC cells migration and invasion. *Experimental Lung Research,* 39**,** 9-17.

CHOWDHRY, S., ZHANG, Y., MCMAHON, M., SUTHERLAND, C., CUADRADO, A. & HAYES, J. D. 2012. Nrf2 is controlled by two distinct beta-TrCP recognition motifs in its Neh6 domain, one of which can be modulated by GSK-3 activity. *Oncogene*.

CHRESTA, C. M., DAVIES, B. R., HICKSON, I., HARDING, T., COSULICH, S., CRITCHLOW, S. E., VINCENT, J. P., ELLSTON, R., JONES, D., SINI, P., JAMES, D., HOWARD, Z., DUDLEY, P., HUGHES, G., SMITH, L., MAGUIRE, S., HUMMERSONE, M., MALAGU, K., MENEAR, K., JENKINS, R., JACOBSEN, M., SMITH, G. C. M., GUICHARD, S. & PASS, M. 2010. AZD8055 Is a Potent, Selective, and Orally Bioavailable ATP-Competitive Mammalian Target of Rapamycin Kinase Inhibitor with In vitro and In vivo Antitumor Activity. *Cancer Research,* 70**,** 288-298.

CHU, P. C., CHUANG, H. C., KULP, S. K. & CHEN, C. S. 2012. The mRNA-stabilizing factor HuR protein is targeted by beta-TrCP protein for degradation in response to glycolysis inhibition. *J Biol Chem,* 287**,** 43639-50.

CHUNG, S., SUZUKI, H., MIYAMOTO, T., TAKAMATSU, N., TATSUGUCHI, A., UEDA, K., KIJIMA, K., NAKAMURA, Y. & MATSUO, Y. 2012. Development of an orally-administrative MELK-targeting inhibitor that suppresses the growth of various types of human cancer. *Oncotarget,* 3**,** 1629-40.

CIECHANOVER, A., HELLER, H., ELIAS, S., HAAS, A. L. & HERSHKO, A. 1980. ATP-DEPENDENT CONJUGATION OF RETICULOCYTE PROTEINS WITH THE POLYPEPTIDE REQUIRED FOR PROTEIN-DEGRADATION. *Proceedings of the National Academy of Sciences of the United States of America-Biological Sciences,* 77**,** 1365-1368.

CLARK, K., MACKENZIE, K. F., PETKEVICIUS, K., KRISTARIYANTO, Y., ZHANG, J., CHOI, H. G., PEGGIE, M., PLATER, L., PEDRIOLI, P. G. A., MCIVER, E., GRAY, N. S., ARTHUR, J. S. C. & COHEN, P. 2012. Phosphorylation of CRTC3 by the salt-inducible kinases controls the interconversion

of classically activated and regulatory macrophages. *Proceedings of the National Academy of Sciences of the United States of America,* 109**,** 16986-16991.

CLARK, K., PLATER, L., PEGGIE, M. & COHEN, P. 2009. Use of the Pharmacological Inhibitor BX795 to Study the Regulation and Physiological Roles of TBK1 and I kappa B Kinase epsilon A DISTINCT UPSTREAM KINASE MEDIATES SER-172 PHOSPHORYLATION AND ACTIVATION. *Journal of Biological Chemistry,* 284**,** 14136-14146.

CLURMAN, B. E., SHEAFF, R. J., THRESS, K., GROUDINE, M. & ROBERTS, J. M. 1996. Turnover of cyclin E by the ubiquitin-proteasome pathway is regulated by cdk2 binding and cyclin phosphorylation. *Genes & Development,* 10**,** 1979-1990.

COHEN, P. 2002a. Protein kinases - the major drug targets of the twenty-first century? *Nature Reviews Drug Discovery,* 1**,** 309-315.

COHEN, P. 2010. Guidelines for the effective use of chemical inhibitors of protein function to understand their roles in cell regulation. *Biochemical Journal,* 425**,** 53-54.

COHEN, P. & ALESSI, D. R. 2013. Kinase Drug Discovery - What's Next in the Field? *Acs Chemical Biology,* 8**,** 96-104.

COHEN, P. T. 2002b. Protein phosphatase 1--targeted in many directions. *J Cell Sci,* 115**,** 241-56.

CSORTOS, C., CZIKORA, I., BOGATCHEVA, N. V., ADYSHEV, D. M., POIRIER, C., OLAH, G. & VERIN, A. D. 2008. TIMAP is a positive regulator of pulmonary endothelial barrier function. *Am J Physiol Lung Cell Mol Physiol,* 295**,** L440-50.

CUI, W., XIAO, N., XIAO, H., ZHOU, H., YU, M., GU, J. & LI, X. 2012. beta-TrCP-mediated IRAK1 degradation releases TAK1-TRAF6 from the membrane to the cytosol for TAK1-dependent NF-kappaB activation. *Mol Cell Biol,* 32**,** 3990-4000.

D'ANGIOLELLA, V., DONATO, V., FORRESTER, F. M., JEONG, Y.-T., PELLACANI, C., KUDO, Y., SARAF, A., FLORENS, L., WASHBURN, M. P. & PAGANO, M. 2012. Cyclin F-Mediated Degradation of Ribonucleotide Reductase M2 Controls Genome Integrity and DNA Repair. *Cell,* 149**,** 1023-1034.

D'ANGIOLELLA, V., DONATO, V., VIJAYAKUMAR, S., SARAF, A., FLORENS, L., WASHBURN, M. P., DYNLACHT, B. & PAGANO, M. 2010. SCFCyclin F controls centrosome homeostasis and mitotic fidelity through CP110 degradation. *Nature,* 466**,** 138-U161.

DALE, S., WILSON, W. A., EDELMAN, A. M. & HARDIE, D. G. 1995. SIMILAR SUBSTRATE RECOGNITION MOTIFS FOR MAMMALIAN AMP-ACTIVATED PROTEIN-KINASE, HIGHER-PLANT HMG-COA REDUCTASE KINASE-A, YEAST SNF1, AND MAMMALIAN CALMODULIN-DEPENDENT PROTEIN-KINASE-I. *Febs Letters,* 361**,** 191-195.

DAVIS, M. I., HUNT, J. P., HERRGARD, S., CICERI, P., WODICKA, L. M., PALLARES, G., HOCKER, M., TREIBER, D. K. & ZARRINKAR, P. P. 2011. Comprehensive analysis of kinase inhibitor selectivity. *Nat Biotechnol.* United States.

DEMETRI, G. D., VAN OOSTEROM, A. T., GARRETT, C. R., BLACKSTEIN, M. E., SHAH, M. H., VERWEIJ, J., MCARTHUR, G., JUDSON, I. R., HEINRICH, M. C., MORGAN, J. A., DESAI, J., FLETCHER, C. D., GEORGE, S., BELLO, C. L., HUANG, X., BAUM, C. M. & CASALI, P. G. 2006. Efficacy and safety of sunitinib in patients with advanced gastrointestinal stromal tumour after failure of imatinib: a randomised controlled trial. *Lancet.* England.

DEN HOLLANDER, J., RIMPI, S., DOHERTY, J. R., RUDELIUS, M., BUCK, A., HOELLEIN, A., KREMER, M., GRAF, N., SCHEERER, M., HALL, M. A., GOGA, A., VON BUBNOFF, N., DUYSTER, J., PESCHEL, C., CLEVELAND, J. L., NILSSON, J. A. & KELLER, U. 2010. Aurora kinases A and B are up-regulated by Myc and are essential for maintenance of the malignant state. *Blood.* United States.

DENG, X., DZAMKO, N., PRESCOTT, A., DAVIES, P., LIU, Q., YANG, Q., LEE, J.-D., PATRICELLI, M. P., NOMANBHOY, T. K., ALESSI, D. R. & GRAY, N. S. 2011. Characterization of a selective inhibitor of the Parkinson's disease kinase LRRK2. *Nature Chemical Biology,* 7**,** 203-205.

DONZELLI, M., SQUATRITO, M., GANOTH, D., HERSHKO, A., PAGANO, M. & DRAETTA, G. F. 2002. Dual mode of degradation of Cdc25 A phosphatase. *Embo Journal,* 21**,** 4875-4884.

DOUGLAS, J. L., VISWANATHAN, K., MCCARROLL, M. N., GUSTIN, J. K., FRUH, K. & MOSES, A. V. 2009. Vpu directs the degradation of the human immunodeficiency virus restriction factor BST-2/Tetherin via a {beta}TrCP-dependent mechanism. *J Virol,* 83**,** 7931-47.

DREWES, G., EBNETH, A., PREUSS, U., MANDELKOW, E. M. & MANDELKOW, E. 1997. MARK, a novel family of protein kinases that phosphorylate microtubule-associated proteins and trigger microtubule disruption. *Cell,* 89**,** 297-308.

DUROCHER, Y., PERRET, S. & KAMEN, A. 2002. High-level and high-throughput recombinant protein production by transient transfection of suspension-growing human 293-EBNA1 cells. *Nucleic Acids Research,* 30.

EYERS, P. A., VAN DEN IJSSEL, P., QUINLAN, R. A., GOEDERT, M. & COHEN, P. 1999. Use of a drug-resistant mutant of stress-activated protein kinase 2a/p38 to validate the in vivo specificity of SE 203580. *Febs Letters,* 451**,** 191-196.

FAN, D., MA, C. & ZHANG, H. 2009. The molecular mechanisms that underlie the tumor suppressor function of LKB1. *Acta Biochimica Et Biophysica Sinica,* 41**,** 97-107.

FELDMAN, R. I., WU, J. M., POLOKOFF, M. A., KOCHANNY, M. J., DINTER, H., ZHU, D. G., BIROC, S. L., ALICKE, B., BRYANT, J., YUAN, S. D., BUCKMAN, B. O., LENTZ, D., FERRER, M., WHITLOW, M., ADLER, M., FINSTER, S., CHANG, Z. & ARNAIZ, D. O. 2005. Novel small molecule inhibitors of 3-phosphoinositide-dependent kinase-1. *Journal of Biological Chemistry,* 280**,** 19867-19874.

FENG, J. H., ITO, M., ICHIKAWA, K., ISAKA, N., NISHIKAWA, M., HARTSHORNE, D. J. & NAKANO, T. 1999. Inhibitory phosphorylation site for Rho-associated kinase on smooth muscle myosin phosphatase. *Journal of Biological Chemistry,* 274**,** 37385-37390.

FISCHER, E. H. & KREBS, E. G. 1955. Conversion of phosphorylase b to phosphorylase a in muscle extracts. *The Journal of biological chemistry,* 216**,** 121-32.

FOLKES, A. J., AHMADI, K., ALDERTON, W. K., ALIX, S., BAKER, S. J., BOX, G., CHUCKOWREE, I. S., CLARKE, P. A., DEPLEDGE, P., ECCLES, S. A., FRIEDMAN, L. S., HAYES, A., HANCOX, T. C., KUGENDRADAS, A., LENSUN, L., MOORE, P., OLIVERO, A. G., PANG, J., PATEL, S., PERGL-WILSON, G. H., RAYNAUD, F. I., ROBSON, A., SAGHIR, N., SALPHATI, L., SOHAL, S., ULTSCH, M. H., VALENTI, M., WALLWEBER, H. J. A., WAN, N. C., WIESMANN, C., WORKMAN, P., ZHYVOLOUP, A., ZVELEBIL, M. J. & SHUTTLEWORTH, S. J. 2008. The identification of 2-(1H-indazol-4-yl)-6-(4-methanesulfonyl-piperazin-1-ylmethyl)-4-morphol in-4-yl-thieno 3,2-d pyrimidine (GDC-0941) as a potent, selective, orally bioavailable inhibitor of class I PI3 kinase for the treatment of cancer. *Journal of Medicinal Chemistry,* 51**,** 5522-5532.

FRESCAS, D. & PAGANO, M. 2008. Deregulated proteolysis by the F-box proteins SKP2 and beta-TrCP: tipping the scales of cancer. *Nature Reviews Cancer,* 8**,** 438-449.

FUJIMOTO, T., YURIMOTO, S., HATANO, N., NOZAKI, N., SUEYOSHI, N., KAMESHITA, I., MIZUTANI, A., MIKOSHIBA, K., KOBAYASHI, R. & TOKUMITSU, H. 2008. Activation of SAD kinase by Ca2+/calmodulin-dependent protein kinase kinase. *Biochemistry,* 47**,** 4151-4159.

GLOTZER, M., MURRAY, A. W. & KIRSCHNER, M. W. 1991. CYCLIN IS DEGRADED BY THE UBIQUITIN PATHWAY. *Nature,* 349**,** 132-138.

GOLDKNOPF, I. L. & BUSCH, H. 1977. ISOPEPTIDE LINKAGE BETWEEN NONHISTONE AND HISTONE-2A POLYPEPTIDES OF CHROMOSOMAL CONJUGATE-PROTEIN-A24. *Proceedings of the National Academy of Sciences of the United States of America,* 74**,** 864-868.

GOLDSTEIN, G., SCHEID, M., HAMMERLING, U., BOYSE, E. A., SCHLESINGER, D. H. & NIALL, H. D. 1975. ISOLATION OF A POLYPEPTIDE THAT HAS LYMPHOCYTE-DIFFERENTIATING PROPERTIES AND IS PROBABLY REPRESENTED UNIVERSALLY IN LIVING CELLS. *Proceedings of the National Academy of Sciences of the United States of America,* 72**,** 11-15.

GRASSIE, M. E., MOFFAT, L. D., WALSH, M. P. & MACDONALD, J. A. 2011. The myosin phosphatase targeting protein (MYPT) family: a regulated mechanism for achieving substrate specificity of the catalytic subunit of protein phosphatase type 1delta. *Arch Biochem Biophys,* 510**,** 147-59.

GRIFFIN, R. J., FONTANA, G., GOLDING, B. T., GUIARD, S., HARDCASTLE, I. R., LEAHY, J. J. J., MARTIN, N., RICHARDSON, C., RIGOREAU, L., STOCKLEY, M. & SMITH, G. C. M. 2005. Selective benzopyranone and pyrimido 2,1-alpha isoquinolin-4-one inhibitors of DNA-dependent protein kinase: Synthesis, structure-activity studies, and radiosensitization of a human tumor cell line in vitro. *Journal of Medicinal Chemistry,* 48**,** 569-585.

GUARDAVACCARO, D., KUDO, Y., BOULAIRE, J., BARCHI, M., BUSINO, L., DONZELLI, M., MARGOTTIN-GOGUET, F., JACKSON, P. K., YAMASAKI, L. & PAGANO, M. 2003. Control of meiotic and mitotic progression by the F box protein beta-Trcp1 in vivo. *Developmental Cell,* 4**,** 799-812.

HANKS, S. K. & HUNTER, T. 1995. PROTEIN KINASES .6. THE EUKARYOTIC PROTEIN-KINASE SUPERFAMILY - KINASE (CATALYTIC) DOMAIN-STRUCTURE AND CLASSIFICATION. *Faseb Journal,* 9**,** 576-596.

HARDIE, D. G. 2007. AMP-activated/SNF1 protein kinases: conserved guardians of cellular energy. *Nature Reviews Molecular Cell Biology,* 8**,** 774-785.

HARDIE, D. G., ROSS, F. A. & HAWLEY, S. A. 2012. AMPK: a nutrient and energy sensor that maintains energy homeostasis. *Nature Reviews Molecular Cell Biology,* 13**,** 251-262.

HARLOW, E. & LANE, D. 1999. Using antibodies: A laboratory manual. *Using antibodies: A laboratory manual***,** xiv+495p-xiv+495p.

HARRINGTON, E. A., BEBBINGTON, D., MOORE, J., RASMUSSEN, R. K., AJOSE-ADEOGUN, A. O., NAKAYAMA, T., GRAHAM, J. A., DEMUR, C., HERCEND, T., DIU-HERCEND, A., SU, M., GOLEC, J. M. C. & MILLER, K. M. 2004. VX-680, a potent and selective small-molecule inhibitor of the Aurora kinases, suppresses tumor growth in vivo. *Nature Medicine,* 10**,** 262-267.

HARTSHORNE, D. J., MURANYI, A. & WU, Y. 2002. Regulation of myosin phosphatase. *Biophysical Journal,* 82**,** 872.

HATAKEYAMA, S. & NAKAYAMA, K. I. 2003. U-box proteins as a new family of ubiquitin ligases. *Biochemical and Biophysical Research Communications,* 302**,** 635-645.

HAUF, S., WAIZENEGGER, I. C. & PETERS, J. M. 2001. Cohesin cleavage by separase required for anaphase and cytokinesis in human cells. *Science,* 293**,** 1320-1323.

HAWLEY, S. A., BOUDEAU, J., REID, J. L., MUSTARD, K. J., UDD, L., MAKELA, T. P., ALESSI, D. R. & HARDIE, D. G. 2003. Complexes between the LKB1 tumor suppressor, STRAD alpha/beta and MO25 alpha/beta are upstream kinases in the AMP-activated protein kinase cascade. *Journal of biology,* 2**,** 28-28.

HAWLEY, S. A., DAVISON, M., WOODS, A., DAVIES, S. P., BERI, R. K., CARLING, D. & HARDIE, D. G. 1996. Characterization of the AMP-activated protein kinase kinase from rat liver and identification of threonine 172 as the major site at which it phosphorylates AMP-activated protein kinase. *Journal of Biological Chemistry,* 271**,** 27879-27887.

HAWLEY, S. A., FULLERTON, M. D., ROSS, F. A., SCHERTZER, J. D., CHEVTZOFF, C., WALKER, K. J., PEGGIE, M. W., ZIBROVA, D., GREEN, K. A., MUSTARD, K. J., KEMP, B. E., SAKAMOTO, K., STEINBERG, G. R. & HARDIE, D. G. 2012. The Ancient Drug Salicylate Directly Activates AMP-Activated Protein Kinase. *Science,* 336**,** 918-922.

HAWLEY, S. A., SELBERT, M. A., GOLDSTEIN, E. G., EDELMAN, A. M., CARLING, D. & HARDIE, D. G. 1995. 5'-AMP ACTIVATES THE AMP-ACTIVATED PROTEIN-KINASE CASCADE AND CA2+/CALMODULIN ACTIVATES THE CALMODULIN-DEPENDENT PROTEIN-KINASE-I

CASCADE, VIA 3 INDEPENDENT MECHANISMS. *Journal of Biological Chemistry,* 270**,** 27186-27191.

HEMMINKI, A. 1999. The molecular basis and clinical aspects of Peutz-Jeghers syndrome. *Cellular and Molecular Life Sciences,* 55**,** 735-750.

HEMMINKI, A., MARKIE, D., TOMLINSON, I., AVIZIENYTE, E., ROTH, S., LOUKOLA, A., BIGNELL, G., WARREN, W., AMINOFF, M., HOGLUND, P., JARVINEN, H., KRISTO, P., PELIN, K., RIDANPAA, M., SALOVAARA, R., TORO, T., BODMER, W., OLSCHWANG, S., OLSEN, A. S., STRATTON, M. R., DE LA CHAPELLE, A. & AALTONEN, L. A. 1998. A serine/threonine kinase gene defective in Peutz-Jeghers syndrome. *Nature,* 391**,** 184-7.

HICKSON, I., YAN, Z., RICHARDSON, C. J., GREEN, S. J., MARTIN, N. M. B., ORR, A. I., REAPER, P. M., JACKSON, S. P., CURTIN, N. J. & SMITH, G. C. M. 2004. Identification and characterization of a novel and specific inhibitor of the ataxia-telangiectasia mutated kinase ATM. *Cancer Research,* 64**,** 9152-9159.

HIDAKA, H., INAGAKI, M., KAWAMOTO, S. & SASAKI, Y. 1984. ISOQUINOLINESULFONAMIDES, NOVEL AND POTENT INHIBITORS OF CYCLIC-NUCLEOTIDE DEPENDENT PROTEIN-KINASE AND PROTEIN KINASE-C. *Biochemistry,* 23**,** 5036-5041.

HIRANO, K., DERKACH, D. N., HIRANO, M., NISHIMURA, J. & KANAIDE, H. 2003. Protein kinase network in the regulation of phosphorylation and dephosphorylation of smooth muscle myosin light chain. *Mol Cell Biochem,* 248**,** 105-14.

HIRANO, M., KIYONARI, H., INOUE, A., FURUSHIMA, K., MURATA, T., SUDA, Y. & AIZAWA, S. 2006. A new serine/threonine protein kinase, Omphk1, essential to ventral body wall formation. *Developmental Dynamics,* 235**,** 2229-2237.

HORIKE, N., TAKEMORI, H., KATOH, Y., DOI, J., MIN, L., ASANO, T., SUN, X. J., YAMAMOTO, H., KASAYAMA, S., MURAOKA, M., NONAKA, Y. & OKAMOTO, M. 2003. Adipose-specific expression, phosphorylation of Ser(794) in insulin receptor substrate-1, and activation in diabetic animals of salt-inducible kinase-2. *Journal of Biological Chemistry,* 278**,** 18440-18447.

HOU, X., LIU, J. E., LIU, W., LIU, C. Y., LIU, Z. Y. & SUN, Z. Y. 2011. A new role of NUAK1: directly phosphorylating p53 and regulating cell proliferation. *Oncogene,* 30**,** 2933-2942.

HSU, J. Y., REIMANN, J. D. R., SORENSEN, C. S., LUKAS, J. & JACKSON, P. K. 2002. E2F-dependent accumulation of hEmi1 regulates S phase entry by inhibiting APC(Cdh1). *Nature Cell Biology,* 4**,** 358-366.

HUANG, W., LV, X., LIU, C., ZHA, Z., ZHANG, H., JIANG, Y., XIONG, Y., LEI, Q. Y. & GUAN, K. L. 2012. The N-terminal phosphodegron targets TAZ/WWTR1 protein for SCFbeta-TrCP-dependent degradation in response to phosphatidylinositol 3-kinase inhibition. *J Biol Chem,* 287**,** 26245-53.

HUIBREGTSE, J. M., SCHEFFNER, M., BEAUDENON, S. & HOWLEY, P. M. 1995. A FAMILY OF PROTEINS STRUCTURALLY AND FUNCTIONALLY RELATED TO THE E6-AP UBIQUITIN PROTEIN LIGASE. *Proceedings of the National Academy of Sciences of the United States of America,* 92**,** 2563-2567.

HUMBERT, N., NAVARATNAM, N., AUGERT, A., DA COSTA, M., MARTIEN, S., WANG, J., MARTINEZ, D., ABBADIE, C., CARLING, D., DE LAUNOIT, Y., GIL, J. & BERNARD, D. 2010. Regulation of ploidy and senescence by the AMPK-related kinase NUAK1. *Embo Journal,* 29**,** 376-386.

HURLEY, R. L., ANDERSON, K. A., FRANZONE, J. M., KEMP, B. E., MEANS, A. R. & WITTERS, L. A. 2005. The Ca2+/calmodulin-dependent protein kinase kinases are AMP-activated protein kinase kinases. *Journal of Biological Chemistry,* 280**,** 29060-29066.

ICHIKAWA, K., HIRANO, K., ITO, M., TANAKA, J., NAKANO, T. & HARTSHORNE, D. J. 1996. Interactions and properties of smooth muscle myosin phosphatase. *Biochemistry,* 35**,** 6313-20.

IKEDA, F. & DIKIC, I. 2008. Atypical ubiquitin chains: new molecular signals - 'Protein modifications: Beyond the usual suspects' review series. *Embo Reports,* 9**,** 536-542.

ILLERT, A. L., ZECH, M., MOLL, C., ALBERS, C., KREUTMAIR, S., PESCHEL, C., BASSERMANN, F. & DUYSTER, J. 2012. Extracellular Signal-regulated Kinase 2 (ERK2) Mediates Phosphorylation and Inactivation of Nuclear Interaction Partner of Anaplastic Lymphoma Kinase (NIPA) at G(2)/M. *Journal of Biological Chemistry,* 287.

INAZUKA, F., SUGIYAMA, N., TOMITA, M., ABE, T., SHIOI, G. & ESUMI, H. 2012. Muscle-specific Knock-out of NUAK Family SNF1-like Kinase 1 (NUAK1) Prevents High Fat Diet-induced Glucose Intolerance. *Journal of Biological Chemistry,* 287**,** 16379-16389.

INNOCENTI, P., CHEUNG, K.-M. J., SOLANKI, S., MAS-DROUX, C., ROWAN, F., YEOH, S., BOXALL, K., WESTLAKE, M., PICKARD, L., HARDY, T., BAXTER, J. E., AHERNE, G. W., BAYLISS, R.,

FRY, A. M. & HOELDER, S. 2012. Design of Potent and Selective Hybrid Inhibitors of the Mitotic Kinase Nek2: Structure-Activity Relationship, Structural Biology, and Cellular Activity. *Journal of Medicinal Chemistry,* 55**,** 3228-3241.

INOUE, E., MOCHIDA, S., TAKAGI, H., HIGA, S., DEGUCHI-TAWARADA, M., TAKAO-RIKITSU, E., INOUE, M., YAO, I., TAKEUCHI, K., KITAJIMA, I., SETOU, M., OHTSUKA, T. & TAKAI, Y. 2006. SAD: A presynaptic kinase associated with synaptic vesicles and the active zone cytomatrix that regulates neurotransmitter release. *Neuron,* 50**,** 261-275.

INOUE, H., NOJIMA, H. & OKAYAMA, H. 1990. HIGH-EFFICIENCY TRANSFORMATION OF ESCHERICHIA-COLI WITH PLASMIDS. *Gene,* 96**,** 23-28.

ISHIHARA, H., MARTIN, B. L., BRAUTIGAN, D. L., KARAKI, H., OZAKI, H., KATO, Y., FUSETANI, N., WATABE, S., HASHIMOTO, K., UEMURA, D. & ET AL. 1989. Calyculin A and okadaic acid: inhibitors of protein phosphatase activity. *Biochem Biophys Res Commun,* 159**,** 871-7.

JACOBS, M., HAYAKAWA, K., SWENSON, L., BELLON, S., FLEMING, M., TASLIMI, P. & DORAN, J. 2006. The structure of dimeric ROCK I reveals the mechanism for ligand selectivity. *J Biol Chem.* United States.

JALEEL, M., MCBRIDE, A., LIZCANO, J. M., DEAK, M., TOTH, R., MORRICE, N. A. & ALESSI, D. R. 2005. Identification of the sucrose non-fermenting related kinase SNRK, as a novel LKB1 substrate. *Febs Letters,* 579**,** 1417-1423.

JALEEL, M., VILLA, F., DEAK, M., TOTH, R., PRESCOTT, A. R., VAN AALTEN, D. M. F. & ALESSI, D. R. 2006. The ubiquitin-associated domain of AMPK-related kinases regulates conformation and LKB1-mediated phosphorylation and activation. *Biochemical Journal,* 394**,** 545-555.

JENNE, D. E., REIMANN, H., NEZU, J., FRIEDEL, W., LOFF, S., JESCHKE, R., MULLER, D., BACK, W. & ZIMMER, M. 1998. Peutz-Jeghers syndrome is caused by mutations in a novel serine threonine kinase. *Nature Genetics,* 18**,** 38-44.

JI, H., RAMSEY, M. R., HAYES, D. N., FAN, C., MCNAMARA, K., KOZLOWSKI, P., TORRICE, C., WU, M. C., SHIMAMURA, T., PERERA, S. A., LIANG, M.-C., CAI, D., NAUMOV, G. N., BAO, L., CONTRERAS, C. M., LI, D., CHEN, L., KRISHNAMURTHY, J., KOIVUNEN, J., CHIRIEAC, L. R., PADERA, R. F., BRONSON, R. T., LINDEMAN, N. I., CHRISTIANI, D. C., LIN, X., SHAPIRO, G. I., JAENNE, P. A., JOHNSON, B. E., MEYERSON, M., KWIATKOWSKI, D. J., CASTRILLON,

D. H., BARDEESY, N., SHARPLESS, N. E. & WONG, K.-K. 2007. LKB1 modulates lung cancer differentiation and metastasis. *Nature,* 448**,** 807-U7.

JIANG, H., LU, Y., YUAN, L. & LIU, J. 2011. Regulation of interleukin-10 receptor ubiquitination and stability by beta-TrCP-containing ubiquitin E3 ligase. *PLoS One,* 6**,** e27464.

JIANG, J. & STRUHL, G. 1998. Regulation of the Hedgehog and Wingless signalling pathways by the F-box/WD40-repeat protein Slimb. *Nature,* 391**,** 493-6.

JIN, L., WILLIAMSON, A., BANERJEE, S., PHILIPP, I. & RAPE, M. 2008. Mechanism of ubiquitin-chain formation by the human anaphase-promoting complex. *Cell,* 133**,** 653-665.

JOAZEIRO, C. A. P. & WEISSMAN, A. M. 2000. RING finger proteins: Mediators of ubiquitin ligase activity. *Cell,* 102**,** 549-552.

KATAJISTO, P., VAAHTOMERI, K., EKMAN, N., VENTELA, E., RISTIMAKI, A., BARDEESY, N., FEIL, R., DEPINHO, R. A. & MAKELA, T. P. 2008. LKB1 signaling in mesenchymal cells required for suppression of gastrointestinal polyposis. *Nature Genetics,* 40**,** 455-459.

KATOH, Y., TAKEMORI, H., LIN, X., TAMURA, M., MURAOKA, M., SATOH, T., TSUCHIYA, Y., MIN, L., DOI, J., MIYAUCHI, A., WITTERS, L. A., NAKAMURA, H. & OKAMOTO, M. 2006. Silencing the constitutive active transcription factor CREB by the LKB1-SIK signaling cascade. *Febs Journal,* 273**,** 2730-2748.

KEMPHUES, K. J., PRIESS, J. R., MORTON, D. G. & CHENG, N. 1988. IDENTIFICATION OF GENES REQUIRED FOR CYTOPLASMIC LOCALIZATION IN EARLY C-ELEGANS EMBRYOS. *Cell,* 52**,** 311-320.

KIM, K., LI, L., KOZLOWSKI, K., SUH, H. S., CAO, W. & BALLERMANN, B. J. 2005. The protein phosphatase-1 targeting subunit TIMAP regulates LAMR1 phosphorylation. *Biochem Biophys Res Commun,* 338**,** 1327-34.

KIMURA, K., ITO, M., AMANO, M., CHIHARA, K., FUKATA, Y., NAKAFUKU, M., YAMAMORI, B., FENG, J., NAKANO, T., OKAWA, K., IWAMATSU, A. & KAIBUCHI, K. 1996. Regulation of myosin phosphatase by Rho and Rho-associated kinase (Rho-kinase). *Science,* 273**,** 245-8.

KIPREOS, E. T. 2005. Ubiquitin-mediated pathways in C. elegans. *WormBook***,** 1-24.

KISHI, M., PAN, Y. A., CRUMP, J. G. & SANES, J. R. 2005. Mammalian SAD kinases are required for neuronal polarization. *Science,* 307**,** 929-932.

KLEYLEIN-SOHN, J., WESTENDORF, J., LE CLECH, M., HABEDANCK, R., STIERHOF, Y.-D. & NIGG, E. A. 2007. Plk4-induced centriole biogenesis in human cells. *Developmental Cell,* 13**,** 190-202.

KNIGHTON, D. R., ZHENG, J. H., TENEYCK, L. F., ASHFORD, V. A., XUONG, N. H., TAYLOR, S. S. & SOWADSKI, J. M. 1991. CRYSTAL-STRUCTURE OF THE CATALYTIC SUBUNIT OF CYCLIC ADENOSINE-MONOPHOSPHATE DEPENDENT PROTEIN-KINASE. *Science,* 253**,** 407-414.

KOCH, A., WAHA, A., HARTMANN, W., HRYCHYK, A., SCHULLER, U., WHARTON, K. A., JR., FUCHS, S. Y., VON SCHWEINITZ, D. & PIETSCH, T. 2005. Elevated expression of Wnt antagonists is a common event in hepatoblastomas. *Clin Cancer Res,* 11**,** 4295-304.

KOEPP, D. M., SCHAEFER, L. K., YE, X., KEYOMARSI, K., CHU, C., HARPER, J. W. & ELLEDGE, S. J. 2001. Phosphorylation-dependent ubiquitination of cyclin E by the SCFFbw7 ubiquitin ligase. *Science,* 294**,** 173-177.

KOGA, Y. & IKEBE, M. 2005. p116Rip decreases myosin II phosphorylation by activating myosin light chain phosphatase and by inactivating RhoA. *J Biol Chem,* 280**,** 4983-91.

KOGA, Y. & IKEBE, M. 2008. A Novel Regulatory Mechanism of Myosin Light Chain Phosphorylation via Binding of 14-3-3 to Myosin Phosphatase. *Mol. Biol. Cell,* 19**,** 1062-1071.

KOMANDER, D. & RAPE, M. 2012. The Ubiquitin Code. *Annual Review of Biochemistry, Vol 81,* 81**,** 203-229.

KOMANDER, D., REYES-TURCU, F., LICCHESI, J. D. F., ODENWAELDER, P., WILKINSON, K. D. & BARFORD, D. 2009. Molecular discrimination of structurally equivalent Lys 63-linked and linear polyubiquitin chains. *Embo Reports,* 10**,** 466-473.

KREBS, E. G. & FISCHER, E. H. 1956. The phosphorylase b to a converting enzyme of rabbit skeletal muscle. *Biochimica et biophysica acta,* 20**,** 150-7.

KRUISWIJK, F., YUNIATI, L., MAGLIOZZI, R., LOW, T. Y., LIM, R., BOLDER, R., MOHAMMED, S., PROUD, C. G., HECK, A. J. R., PAGANO, M. & GUARDAVACCARO, D. 2012. Coupled Activation and Degradation of eEF2K Regulates Protein Synthesis in Response to Genotoxic Stress. *Science Signaling,* 5.

KUSAKAI, G., SUZUKI, A., OGURA, T., KAMINISHI, M. & ESUMI, H. 2004a. Strong association of ARK5 with tumor invasion and metastasis. *Journal of Experimental & Clinical Cancer Research,* 23**,** 263-268.

KUSAKAI, G., SUZUKI, A., OGURA, T., MIYAMOTO, S., OCHIAI, A., KAMINISHI, M. & ESUMI, H. 2004b. ARK5 expression in colorectal cancer and its implications for tumor progression. *American Journal of Pathology,* 164**,** 987-995.

LASHO, T. L., TEFFERI, A., HOOD, J. D., VERSTOVSEK, S., GILLILAND, D. G. & PARDANANI, A. 2008. TG101348, a JAK2-selective antagonist, inhibits primary hematopoietic cells derived from myeloproliferative disorder patients with JAK2V617F, MPLW515K or JAK2 exon 12 mutations as well as mutation negative patients. *Leukemia.* England.

LEFEBVRE, D. L., BAI, Y. H., SHAHMOLKY, N., SHARMA, M., POON, R., DRUCKER, D. J. & ROSEN, C. F. 2001. Identification and characterization of a novel sucrose-non-fermenting protein kinase/AMP-activated protein kinase-related protein kinase, SNARK. *Biochemical Journal,* 355**,** 297-305.

LI, H.-F., KIM, J.-S. & WALDMAN, T. 2009. Radiation-induced Akt activation modulates radioresistance in human glioblastoma cells. *Radiation Oncology,* 4.

LI, L., KOZLOWSKI, K., WEGNER, B., RASHID, T., YEUNG, T., HOLMES, C. & BALLERMANN, B. J. 2007. Phosphorylation of TIMAP by glycogen synthase kinase-3beta activates its associated protein phosphatase 1. *J Biol Chem,* 282**,** 25960-9.

LI, M., SHIN, Y.-H., HOU, L., HUANG, X., WEI, Z., KLANN, E. & ZHANG, P. 2008. The adaptor protein of the anaphase promoting complex Cdh1 is essential in maintaining replicative lifespan and in learning and memory. *Nature Cell Biology,* 10**,** 1083-1089.

LI, M. L., DEFREN, J. & BREWER, G. 2013. Hsp27 and F-Box Protein beta-TrCP Promote Degradation of mRNA Decay Factor AUF1. *Mol Cell Biol,* 33**,** 2315-26.

LIN, D. I., BARBASH, O., KUMAR, K. G. S., WEBER, J. D., HARPER, J. W., KLEIN-SZANTO, A. J. P., RUSTGI, A., FUCHS, S. Y. & DIEHL, J. A. 2006. Phosphorylation-dependent ubiquitination of cyclin D1 by the SCFFBX4-alpha B crystallin complex. *Molecular Cell,* 24**,** 355-366.

LINDON, C. & PINES, J. 2004. Ordered proteolysis in anaphase inactivates Plk1 to contribute to proper mitotic exit in human cells. *Journal of Cell Biology,* 164**,** 233-241.

LISTOVSKY, T., OREN, Y. S., YUDKOVSKY, Y., MAHBUBANI, H. M., WEISS, A. M., LEBENDIKER, M. & BRANDEIS, M. 2004. Mammalian Cdh1/Fzr mediates its own degradation. *Embo Journal,* 23**,** 1619-1626.

LIU, L., ULBRICH, J., MUELLER, J., WUESTEFELD, T., AEBERHARD, L., KRESS, T. R., MUTHALAGU, N., RYCAK, L., RUDALSKA, R., MOLL, R., KEMPA, S., ZENDER, L., EILERS,

M. & MURPHY, D. J. 2012. Deregulated MYC expression induces dependence upon AMPK-related kinase 5. *Nature,* 483**,** 608-U131.

LIU, S., BEKKER-JENSEN, S., MAILAND, N., LUKAS, C., BARTEK, J. & LUKAS, J. 2006. Claspin operates downstream of TopBP1 to direct ATR signaling towards Chk1 activation. *Molecular and Cellular Biology,* 26**,** 6056-6064.

LIZCANO, J. M., GORANSSON, O., TOTH, R., DEAK, M., MORRICE, N. A., BOUDEAU, J., HAWLEY, S. A., UDD, L., MAKELA, T. P., HARDIE, D. G. & ALESSI, D. R. 2004. LKB1 is a master kinase that activates 13 kinases of the AMPK subfamily, including MARK/PAR-1. *Embo Journal,* 23**,** 833-843.

LU, S., NIU, N., GUO, H., TANG, J., GUO, W., LIU, Z., SHI, L., SUN, T., ZHOU, F., LI, H., ZHANG, J. & ZHANG, B. 2013. ARK5 promotes glioma cell invasion, and its elevated expression is correlated with poor clinical outcome. *European Journal of Cancer,* 49**,** 752-763.

LUKAS, C., SORENSEN, C. S., KRAMER, E., SANTONI-RUGIU, E., LINDENEG, C., PETERS, J. M., BARTEK, J. & LUKAS, J. 1999. Accumulation of cyclin B1 requires E2F and cyclin-A-dependent rearrangement of the anaphase-promoting complex. *Nature,* 401**,** 815-818.

LUTZ, W., STOHR, M., SCHURMANN, J., WENZEL, A., LOHR, A. & SCHWAB, M. 1996. Conditional expression of N-myc in human neuroblastoma cells increases expression of alpha-prothymosin and ornithine decarboxylase and accelerates progression into S-phase early after mitogenic stimulation of quiescent cells. *Oncogene,* 13**,** 803-12.

MACKENZIE, K. F., CLARK, K., NAQVI, S., MCGUIRE, V. A., NOEEHREN, G., KRISTARIYANTO, Y., VAN DEN BOSCH, M., MUDALIAR, M., MCCARTHY, P. C., PATTISON, M. J., PEDRIOLI, P. G. A., BARTON, G. J., TOTH, R., PRESCOTT, A. & ARTHUR, J. S. C. 2013. PGE(2) Induces Macrophage IL-10 Production and a Regulatory-like Phenotype via a Protein Kinase A-SIK-CRTC3 Pathway. *Journal of Immunology,* 190**,** 565-577.

MACKINTOSH, C. 2004. Dynamic interactions between 14-3-3 proteins and phosphoproteins regulate diverse cellular processes. *Biochemical Journal,* 381**,** 329-342.

MAILAND, N., BEKKER-JENSEN, S., BARTEK, J. & LUKAS, J. 2006. Destruction of claspin by SCF beta TrCP restrains Chk1 activation and facilitates recovery from genotoxic stress. *Molecular Cell,* 23**,** 307-318.

MAILAND, N. & DIFFLEY, J. F. X. 2005. CDKs promote DNA replication origin licensing in human cells by protecting Cdc6 from APC/C-dependent proteolysis. *Cell,* 122**,** 915-926.

MALUMBRES, M. 2011. PHYSIOLOGICAL RELEVANCE OF CELL CYCLE KINASES. *Physiological Reviews,* 91**,** 973-1007.

MALUMBRES, M. & BARBACID, M. 2001. To cycle or not to cycle: a critical decision in cancer. *Nat Rev Cancer,* 1**,** 222-31.

MANIATIS, T. 1999. A ubiquitin ligase complex essential for the NF-kappaB, Wnt/Wingless, and. *Genes Dev,* 13**,** 505-10.

MANNING, G., WHYTE, D. B., MARTINEZ, R., HUNTER, T. & SUDARSANAM, S. 2002. The protein kinase complement of the human genome. *Science,* 298**,** 1912-+.

MARGOTTIN-GOGUET, F., HSU, J. Y., LOKTEV, A., HSIEH, H. M., REIMANN, J. D. R. & JACKSON, P. K. 2003. Prophase destruction of Emi1 by the SCF beta TrCP/Slimb ubiquitin ligase activates the anaphase promoting complex to allow progression beyond prometaphase. *Developmental Cell,* 4**,** 813-826.

MATENIA, D. & MANDELKOW, E.-M. 2009. The tau of MARK: a polarized view of the cytoskeleton. *Trends in Biochemical Sciences,* 34**,** 332-342.

MATSUOKA, S., HUANG, M. X. & ELLEDGE, S. J. 1998. Linkage of ATM to cell cycle regulation by the Chk2 protein kinase. *Science,* 282**,** 1893-1897.

MCGARRY, T. J. & KIRSCHNER, M. W. 1998. Geminin, an inhibitor of DNA replication, is degraded during mitosis. *Cell,* 93**,** 1043-1053.

METZGER, M. B., HRISTOVA, V. A. & WEISSMAN, A. M. 2012. HECT and RING finger families of E3 ubiquitin ligases at a glance. *J Cell Sci.* England.

MILLER, J. J., SUMMERS, M. K., HANSEN, D. V., NACHURY, M. V., LEHMAN, N. L., LOKTEV, A. & JACKSON, P. K. 2006. Emi1 stably binds and inhibits the anaphase-promoting complex/cyclosome as a pseudosubstrate inhibitor. *Genes & Development,* 20**,** 2410-2420.

MIZUTANI, H., OKAMOTO, R., MORIKI, N., KONISHI, K., TANIGUCHI, M., FUJITA, S., DOHI, K., ONISHI, K., SUZUKI, N., SATOH, S., MAKINO, N., ITOH, T., HARTSHORNE, D. J. & ITO, M. 2010. Overexpression of myosin phosphatase reduces Ca(2+) sensitivity of contraction and impairs cardiac function. *Circ J,* 74**,** 120-8.

MOCCIARO, A. & RAPE, M. 2012. Emerging regulatory mechanisms in ubiquitin-dependent cell cycle control. *Journal of Cell Science,* 125**,** 255-263.

MOORHEAD, G., JOHNSON, D., MORRICE, N. & COHEN, P. 1998. The major myosin phosphatase in skeletal muscle is a complex between the beta-isoform of protein phosphatase 1 and the MYPT2 gene product. *FEBS Lett,* 438**,** 141-4.

MUERKOSTER, S., ARLT, A., SIPOS, B., WITT, M., GROSSMANN, M., KLOPPEL, G., KALTHOFF, H., FOLSCH, U. R. & SCHAFER, H. 2005. Increased expression of the E3-ubiquitin ligase receptor subunit betaTRCP1 relates to constitutive nuclear factor-kappaB activation and chemoresistance in pancreatic carcinoma cells. *Cancer Res,* 65**,** 1316-24.

MURPHY, J. M., KORZHNEV, D. M., CECCARELLI, D. F., BRIANT, D. J., ZARRINE-AFSAR, A., SICHERI, F., KAY, L. E. & PAWSON, T. 2007. Conformational instability of the MARK3 UBA domain compromises ubiquitin recognition and promotes interaction with the adjacent kinase domain. *Proceedings of the National Academy of Sciences of the United States of America,* 104**,** 14336-14341.

NAJAFOV, A., SOMMER, E. M., AXTEN, J. M., DEYOUNG, M. P. & ALESSI, D. R. 2011. Characterization of GSK2334470, a novel and highly specific inhibitor of PDK1. *Biochemical Journal,* 433**,** 357-369.

NAKAYAMA, K., HATAKEYAMA, S., MARUYAMA, S., KIKUCHI, A., ONOE, K., GOOD, R. A. & NAKAYAMA, K. I. 2003. Impaired degradation of inhibitory subunit of NF-kappa B (I kappa B) and beta-catenin as a result of targeted disruption of the beta-TrCP1 gene. *Proc Natl Acad Sci U S A,* 100**,** 8752-7.

NAMIKI, T., COELHO, S. G. & HEARING, V. J. 2011a. NUAK2: an emerging acral melanoma oncogene. *Oncotarget,* 2**,** 695-704.

NAMIKI, T., TANEMURA, A., VALENCIA, J. C., COELHO, S. G., PASSERON, T., KAWAGUCHI, M., VIEIRA, W. D., ISHIKAWA, M., NISHIJIMA, W., IZUMO, T., KANEKO, Y., KATAYAMA, I., YAMAGUCHI, Y., YIN, L., POLLEY, E. C., LIU, H., KAWAKAMI, Y., EISHI, Y., TAKAHASHI, E., YOKOZEKI, H. & HEARING, V. J. 2011b. AMP kinase-related kinase NUAK2 affects tumor growth, migration, and clinical outcome of human melanoma. *Proceedings of the National Academy of Sciences of the United States of America,* 108**,** 6597-6602.

NEEF, R., GRUNEBERG, U., KOPAJTICH, R., LI, X., NIGG, E. A., SILLJE, H. & BARR, F. A. 2007. Choice of Plk1 docking partners during mitosis and cytokinesis is controlled by the activation state of Cdk1. *Nature Cell Biology,* 9**,** 436-U132.

NICHOLS, R. J., DZAMKO, N., HUTTI, J. E., CANTLEY, L. C., DEAK, M., MORAN, J., BAMBOROUGH, P., REITH, A. D. & ALESSI, D. R. 2009. Substrate specificity and inhibitors of LRRK2, a protein kinase mutated in Parkinson's disease. *Biochemical Journal,* 424**,** 47-60.

O'REGAN, L., BLOT, J. & FRY, A. M. 2007. Mitotic regulation by NIMA-related kinases. *Cell Division,* 2.

OHMURA, T., SHIOI, G., HIRANO, M. & AIZAWA, S. 2012. Neural tube defects by NUAK1 and NUAK2 double mutation. *Developmental Dynamics,* 241**,** 1350-1364.

OKAMOTO, R., KATO, T., MIZOGUCHI, A., TAKAHASHI, N., NAKAKUKI, T., MIZUTANI, H., ISAKA, N., IMANAKA-YOSHIDA, K., KAIBUCHI, K., LU, Z. J., MABUCHI, K., TAO, T., HARTSHORNE, D. J., NAKANO, T. & ITO, M. 2006. Characterization and function of MYPT2, a target subunit of myosin phosphatase in heart. *Cellular Signalling,* 18**,** 1408-1416.

ORLOWSKI, R. Z. & KUHN, D. J. 2008. Proteasome inhibitors in cancer therapy: lessons from the first decade. *Clin Cancer Res,* 14**,** 1649-57.

OUGOLKOV, A., ZHANG, B., YAMASHITA, K., BILIM, V., MAI, M., FUCHS, S. Y. & MINAMOTO, T. 2004. Associations among beta-TrCP, an E3 ubiquitin ligase receptor, beta-catenin, and NF-kappaB in colorectal cancer. *J Natl Cancer Inst,* 96**,** 1161-70.

PAGANO, M., TAM, S. W., THEODORAS, A. M., BEERROMERO, P., DELSAL, G., CHAU, V., YEW, P. R., DRAETTA, G. F. & ROLFE, M. 1995. ROLE OF THE UBIQUITIN-PROTEASOME PATHWAY IN REGULATING ABUNDANCE OF THE CYCLIN-DEPENDENT KINASE INHIBITOR P27. *Science,* 269**,** 682-685.

PESCHIAROLI, A., DORRELLO, N. V., GUARDAVACCARO, D., VENERE, M., HALAZONETIS, T., SHERMAN, N. E. & PAGANO, M. 2006. SCF beta TrCP-mediated degradation of claspin regulates recovery from the DNA replication checkpoint response. *Molecular Cell,* 23**,** 319-329.

PFLEGER, C. M. & KIRSCHNER, M. W. 2000. The KEN box: an APC recognition signal distinct from the D box targeted by Cdh1. *Genes & Development,* 14**,** 655-665.

PLECHANOVOVA, A., JAFFRAY, E. G., TATHAM, M. H., NAISMITH, J. H. & HAY, R. T. 2012. Structure of a RING E3 ligase and ubiquitin-loaded E2 primed for catalysis. *Nature,* 489**,** 115-U135.

POPOV, N., SCHULEIN, C., JAENICKE, L. A. & EILERS, M. 2010. Ubiquitylation of the amino terminus of Myc by SCF(beta-TrCP) antagonizes SCF(Fbw7)-mediated turnover. *Nat Cell Biol,* 12**,** 973-81.

RAPE, M. & KIRSCHNER, M. W. 2004. Autonomous regulation of the anaphase-promoting complex couples mitosis to S-phase entry. *Nature,* 432**,** 588-595.

REGAN, J., BREITFELDER, S., CIRILLO, P., GILMORE, T., GRAHAM, A. G., HICKEY, E., KLAUS, B., MADWED, J., MORIAK, M., MOSS, N., PARGELLIS, C., PAV, S., PROTO, A., SWINAMER, A., TONG, L. & TORCELLINI, C. 2002. Pyrazole urea-based inhibitors of p38 MAP kinase: From lead compound to clinical candidate. *Journal of Medicinal Chemistry,* 45**,** 2994-3008.

RENA, G., BAIN, J., ELLIOTT, M. & COHEN, P. 2004. D4476, a cell-permeant inhibitor of CK1, suppresses the site-specific phosphorylation and nuclear exclusion of FOXO1a. *EMBO Rep,* 5**,** 60-5.

RING, D. B., JOHNSON, K. W., HENRIKSEN, E. J., NUSS, J. M., GOFF, D., KINNICK, T. R., MA, S. T., REEDER, J. W., SAMUELS, I., SLABIAK, T., WAGMAN, A. S., HAMMOND, M. E. W. & HARRISON, S. D. 2003. Selective glycogen synthase kinase 3 inhibitors potentiate insulin activation of glucose transport and utilization in vitro and in vivo. *Diabetes,* 52**,** 588-595.

RODRIGUEZ-ASIAIN, A., RUIZ-BABOT, G., ROMERO, W., CUBI, R., ERAZO, T., BIONDI, R. M., BAYASCAS, J. R., AGUILERA, J., GOMEZ, N., GIL, C., CLARO, E. & LIZCANO, J. M. 2011. Brain Specific Kinase-1 BRSK1/SAD-B associates with lipid rafts: modulation of kinase activity by lipid environment. *Biochimica Et Biophysica Acta-Molecular and Cell Biology of Lipids,* 1811**,** 1124-1135.

RUNE, A., OSLER, M. E., FRITZ, T. & ZIERATH, J. R. 2009. Regulation of skeletal muscle sucrose, non-fermenting 1/AMP-activated protein kinase-related kinase (SNARK) by metabolic stress and diabetes. *Diabetologia,* 52**,** 2182-2189.

SANDERS, M. J., GRONDIN, P. O., HEGARTY, B. D., SNOWDEN, M. A. & CARLING, D. 2007. Investigating the mechanism for AMP activation of the AMP-activated protein kinase cascade. *Biochemical Journal,* 403**,** 139-148.

SASAGAWA, S., TAKEMORI, H., UEBI, T., IKEGAMI, D., HIRAMATSU, K., IKEGAWA, S., YOSHIKAWA, H. & TSUMAKI, N. 2012. SIK3 is essential for chondrocyte hypertrophy during skeletal development in mice. *Development,* 139**,** 1153-1163.

SASAKI, Y., SUZUKI, M. & HIDAKA, H. 2002. The novel and specific Rho-kinase inhibitor (S)-(+)-2-methyl-1- (4-methyl-5-isoquinoline)sulfonyl -homopiperazine as a probing molecule for Rho-kinase-involved pathway. *Pharmacology & Therapeutics,* 93**,** 225-232.

SCHEFFNER, M., NUBER, U. & HUIBREGTSE, J. M. 1995. PROTEIN UBIQUITINATION INVOLVING AN E1-E2-E3 ENZYME UBIQUITIN THIOESTER CASCADE. *Nature,* 373**,** 81-83.

SCHULMAN, B. A. & HARPER, J. W. 2009. Ubiquitin-like protein activation by E1 enzymes: the apex for downstream signalling pathways. *Nature Reviews Molecular Cell Biology,* 10**,** 319-331.

SCOTT, D. C., MONDA, J. K., GRACE, C. R. R., DUDA, D. M., KRIWACKI, R. W., KURZ, T. & SCHULMAN, B. A. 2010. A Dual E3 Mechanism for Rub1 Ligation to Cdc53. *Molecular Cell,* 39**,** 784-796.

SCOTT, J. W., ROSS, F. A., LIU, J. K. D. & HARDIE, D. G. 2007. Regulation of AMP-activated protein kinase by a pseudosubstrate sequence on the gamma subunit. *Embo Journal,* 26**,** 806-815.

SCREATON, R. A., CONKRIGHT, M. D., KATOH, Y., BEST, J. L., CANETTIERI, G., JEFFRIES, S., GUZMAN, E., NIESSEN, S., YATES, J. R., TAKEMORI, H., OKAMOTO, M. & MONTMINY, M. 2004. The CREB coactivator TORC2 functions as a calcium- and cAMP-sensitive coincidence detector. *Cell,* 119**,** 61-74.

SEKI, A., COPPINGER, J. A., JANG, C.-Y., YATES, J. R., III & FANG, G. 2008. Bora and the kinase Aurora A cooperatively activate the kinase Plk1 and control mitotic entry. *Science,* 320**,** 1655-1658.

SENGA, T., SIVAPRASAD, U., ZHU, W. G., PARK, J. H., ARIAS, E. E., WALTER, J. C. & DUTTA, A. 2006. PCNA is a cofactor for Cdt1 degradation by CUL4/DDB1-mediated N-terminal ubiquitination. *Journal of Biological Chemistry,* 281**,** 6246-6252.

SHACKELFORD, D. B. & SHAW, R. J. 2009. The LKB1-AMPK pathway: metabolism and growth control in tumour suppression. *Nature Reviews Cancer,* 9**,** 563-575.

SHAIK, S., NUCERA, C., INUZUKA, H., GAO, D., GARNAAS, M., FRECHETTE, G., HARRIS, L., WAN, L., FUKUSHIMA, H., HUSAIN, A., NOSE, V., FADDA, G., SADOW, P. M., GOESSLING, W., NORTH, T., LAWLER, J. & WEI, W. 2012. SCF(beta-TRCP) suppresses angiogenesis and thyroid cancer cell migration by promoting ubiquitination and destruction of VEGF receptor 2. *J Exp Med,* 209**,** 1289-307.

SHAW, R. J., KOSMATKA, M., BARDEESY, N., HURLEY, R. L., WITTERS, L. A., DEPINHO, R. A. & CANTLEY, L. C. 2004. The tumor suppressor LKB1 kinase directly activates AMP-activated kinase and regulates apoptosis in response to energy stress. *Proceedings of the National Academy of Sciences of the United States of America,* 101**,** 3329-3335.

SHELLY, M., CANCEDDA, L., HEILSHORN, S., SUMBRE, G. & POO, M.-M. 2007. LKB1/STRAD promotes axon initiation during neuronal polarization. *Cell,* 129**,** 565-577.

SHIMIZU, H., ITO, M., MIYAHARA, M., ICHIKAWA, K., OKUBO, S., KONISHI, T., NAKA, M., TANAKA, T., HIRANO, K., HARTSHORNE, D. J. & ET AL. 1994. Characterization of the myosin-binding subunit of smooth muscle myosin phosphatase. *J Biol Chem,* 269**,** 30407-11.

SHIRLEY, R. B., KADDOUR-DJEBBAR, I., PATEL, D. M., LAKSHMIKANTHAN, V., LEWIS, R. W. & KUMAR, M. V. 2005. Combination of proteasomal inhibitors lactacystin and MG132 induced synergistic apoptosis in prostate cancer cells. *Neoplasia,* 7**,** 1104-11.

SKAAR, J. R., D'ANGIOLELLA, V., PAGAN, J. K. & PAGANO, M. 2009. SnapShot: F Box Proteins II. *Cell,* 137**,** 1358, 1358.e1.

SKINNER, J. A. & SALTIEL, A. R. 2001. Cloning and identification of MYPT3: a prenylatable myosin targetting subunit of protein phosphatase 1. *Biochem J,* 356**,** 257-67.

SOMMER, E. M., DRY, H., CROSS, D., GUICHARD, S., DAVIES, B. R. & ALESSI, D. R. 2013. Elevated SGK1 predicts resistance of breast cancer cells to Akt inhibitors. *Biochem J*.

SORENSEN, C. S., MELIXETIAN, M., KLEIN, D. K. & HELIN, K. 2010. NEK11: linking CHK1 and CDC25A in DNA damage checkpoint signaling. *Cell Cycle,* 9**,** 450-5.

SOUCY, T. A., SMITH, P. G., MILHOLLEN, M. A., BERGER, A. J., GAVIN, J. M., ADHIKARI, S., BROWNELL, J. E., BURKE, K. E., CARDIN, D. P., CRITCHLEY, S., CULLIS, C. A., DOUCETTE, A., GARNSEY, J. J., GAULIN, J. L., GERSHMAN, R. E., LUBLINSKY, A. R., MCDONALD, A., MIZUTANI, H., NARAYANAN, U., OLHAVA, E. J., PELUSO, S., REZAEI, M., SINTCHAK, M. D., TALREJA, T., THOMAS, M. P., TRAORE, T., VYSKOCIL, S., WEATHERHEAD, G. S., YU, J., ZHANG, J., DICK, L. R., CLAIBORNE, C. F., ROLFE, M., BOLEN, J. B. & LANGSTON, S. P. 2009a. An inhibitor of NEDD8-activating enzyme as a new approach to treat cancer. *Nature,* 458**,** 732-U67.

SOUCY, T. A., SMITH, P. G. & ROLFE, M. 2009b. Targeting NEDD8-activated cullin-RING ligases for the treatment of cancer. *Clin Cancer Res,* 15**,** 3912-6.

SPIEGELMAN, V. S., TANG, W., CHAN, A. M., IGARASHI, M., AARONSON, S. A., SASSOON, D. A., KATOH, M., SLAGA, T. J. & FUCHS, S. Y. 2002. Induction of homologue of Slimb ubiquitin ligase receptor by mitogen signaling. *J Biol Chem,* 277**,** 36624-30.

STEEGMAIER, M., HOFFMANN, M., BAUM, A., LENART, P., PETRONCZKI, M., KRSSAK, M., GUERTLER, U., GARIN-CHESA, P., LIEB, S., QUANT, J., GRAUERT, M., ADOLF, G. R.,

KRAUT, N., PETERS, J.-M. & RETTIG, W. J. 2007. BI 2536, a potent and selective inhibitor of polo-like kinase 1, inhibits tumor growth in vivo. *Current Biology,* 17**,** 316-322.

STEINBERG, G. R. & KEMP, B. E. 2009. AMPK in Health and Disease. *Physiological Reviews,* 89**,** 1025-1078.

STEWART, S. & FANG, G. W. 2005. Destruction box-dependent degradation of Aurora B is mediated by the anaphase-promoting complex/cyclosome and Cdh1. *Cancer Research,* 65**,** 8730-8735.

STUDIER, F. W. 2005. Protein production by auto-induction in high-density shaking cultures. *Protein Expression and Purification,* 41**,** 207-234.

SUMARA, I., QUADRONI, M., FREI, C., OLMA, M. H., SUMARA, G., RICCI, R. & PETER, M. 2007. A Cul3-based E3 ligase removes aurora B from mitotic chromosomes, regulating mitotic progression and completion of cytokinesis in human cells. *Developmental Cell,* 12**,** 887-900.

SUTHERLAND, E. W., JR. & WOSILAIT, W. D. 1955. Inactivation and activation of liver phosphorylase. *Nature,* 175**,** 169-70.

SUZUKI, A., KUSAKAI, G., KISHIMOTO, A., LU, J., OGURA, T., LAVIN, M. F. & ESUMI, H. 2003. Identification of a novel protein kinase mediating Akt survival signaling to the ATM protein. *Journal of Biological Chemistry,* 278**,** 48-53.

SUZUKI, A., KUSAKAI, G., KISHIMOTO, A., SHIMOJO, Y., MIYAMOTO, S., OGURA, T., OCHIAI, A. & ESUMI, H. 2004a. Regulation of caspase-6 and FLIP by the AMPK family member ARK5. *Oncogene,* 23**,** 7067-7075.

SUZUKI, A., LU, H., KUSAKAI, G. I., KISHIMOTO, A., OGURA, T. & ESUMI, H. 2004b. ARK5 is a tumor invasion-associated factor downstream of Akt signaling. *Molecular and Cellular Biology,* 24**,** 3526-3535.

SUZUKI, A., OGURA, T. & ESUMI, H. 2006. NDR2 acts as the upstream kinase of ARK5 during insulin-like growth factor-1 signaling. *Journal of Biological Chemistry,* 281**,** 13915-13921.

TAKEMORI, H., DOI, J., HORIKE, N., KATOH, Y., MIN, L., LIN, X. Z., WANG, Z. N., MURAOAKA, M. & OKAMOTO, M. 2003. Salt-inducible kinase-mediated regulation of steroidogenesis at the early stage of ACTH-stimulation. *Journal of Steroid Biochemistry and Molecular Biology,* 85**,** 397-400.

TAN, I., NG, C. H., LIM, L. & LEUNG, T. 2001. Phosphorylation of a novel myosin binding subunit of protein phosphatase 1 reveals a conserved mechanism in the regulation of actin cytoskeleton. *J Biol Chem,* 276**,** 21209-16.

TASSAN, J. P. & LE GOFF, X. 2004. An overview of the KIN1/PAR-1/MARK kinase family. *Biology of the Cell,* 96**,** 193-199.

TEIXEIRA, L. K. & REED, S. I. 2013. Ubiquitin Ligases and Cell Cycle Control. *Annu Rev Biochem*.

TERRAK, M., KERFF, F., LANGSETMO, K., TAO, T. & DOMINGUEZ, R. 2004. Structural basis of protein phosphatase 1 regulation. *Nature,* 429**,** 780-4.

TOKUNAGA, F., SAKATA, S.-I., SAEKI, Y., SATOMI, Y., KIRISAKO, T., KAMEI, K., NAKAGAWA, T., KATO, M., MURATA, S., YAMAOKA, S., YAMAMOTO, M., AKIRA, S., TAKAO, T., TANAKA, K. & IWAI, K. 2009. Involvement of linear polyubiquitylation of NEMO in NF-kappa B activation. *Nature Cell Biology,* 11**,** 123-U40.

TOLEDO, L. I., MURGA, M., ZUR, R., SORIA, R., RODRIGUEZ, A., MARTINEZ, S., OYARZABAL, J., PASTOR, J., BISCHOFF, J. R. & FERNANDEZ-CAPETILLO, O. 2011. A cell-based screen identifies ATR inhibitors with synthetic lethal properties for cancer-associated mutations. *Nature Structural & Molecular Biology,* 18**,** 721-U124.

TOTSUKAWA, G., YAMAKITA, Y., YAMASHIRO, S., HARTSHORNE, D. J., SASAKI, Y. & MATSUMURA, F. 2000. Distinct roles of ROCK (Rho-kinase) and MLCK in spatial regulation of MLC phosphorylation for assembly of stress fibers and focal adhesions in 3T3 fibroblasts. *J Cell Biol,* 150**,** 797-806.

TRUDEL, S., LI, Z. H., WEI, E., WIESMANN, M., CHANG, H., CHEN, C., REECE, D., HEISE, C. & STEWART, A. K. 2005. CHIR-258, a novel, multitargeted tyrosine kinase inhibitor for the potential treatment of t(4;14) multiple myeloma. *Blood.* United States.

TSENG, A. S., ENGEL, F. B. & KEATING, M. T. 2006. The GSK-3 inhibitor BIO promotes proliferation in mammalian cardiomyocytes. *Chem Biol.* England.

TSUCHIHARA, K., OGURA, T., FUJIOKA, R., FUJII, S., KUGA, W., SAITO, M., OCHIYA, T., OCHIAI, A. & ESUMI, H. 2008. Susceptibility of Snark-deficient mice to azoxymethane-induced colorectal tumorigenesis and the formation of aberrant crypt foci. *Cancer Sci.* England.

TUDZAROVA, S., COLOMBO, S. L., STOEBER, K., CARCAMO, S., WILLIAMS, G. H. & MONCADA, S. 2011. Two ubiquitin ligases, APC/C-Cdh1 and SKP1-CUL1-F (SCF)-beta-TrCP, sequentially regulate glycolysis during the cell cycle. *Proc Natl Acad Sci U S A,* 108**,** 5278-83.

TWOMEY, E., LI, Y., LEI, J., SODJA, C., RIBECCO-LUTKIEWICZ, M., SMITH, B., FANG, H., BANI-YAGHOUB, M., MCKINNELL, I. & SIKORSKA, M. 2010. Regulation of MYPT1 stability by the E3 ubiquitin ligase SIAH2. *Exp Cell Res,* 316**,** 68-77.

UEBI, T., ITOH, Y., HATANO, O., KUMAGAI, A., SANOSAKA, M., SASAKI, T., SASAGAWA, S., DOI, J., TATSUMI, K., MITAMURA, K., MORII, E., AOZASA, K., KAWAMURA, T., OKUMURA, M., NAKAE, J., TAKIKAWA, H., FUKUSATO, T., KOURA, M., NISH, M., HAMSTEN, A., SILVEIRA, A., BERTORELLO, A. M., KITAGAWA, K., NAGAOKA, Y., KAWAHARA, H., TOMONAGA, T., NAKA, T., IKEGAWA, S., TSUMAKI, N., MATSUDA, J. & TAKEMORI, H. 2012. Involvement of SIK3 in Glucose and Lipid Homeostasis in Mice. *Plos One,* 7.

VALLENIUS, T., VAAHTOMERI, K., KOVAC, B., OSICEANU, A.-M., VILJANEN, M. & MAKELA, T. P. 2011. An association between NUAK2 and MRIP reveals a novel mechanism for regulation of actin stress fibers. *Journal of Cell Science,* 124**,** 384-393.

VASSILEV, L. T. 2006. Cell cycle synchronization at the G(2)/M phase border by reversible inhibition of CDK1. *Cell Cycle,* 5**,** 2555-2556.

VELASCO, G., ARMSTRONG, C., MORRICE, N., FRAME, S. & COHEN, P. 2002a. Phosphorylation of the regulatory subunit of smooth muscle protein phosphatase 1M at Thr850 induces its dissociation from myosin. *FEBS Lett,* 527**,** 101-4.

VELASCO, G., ARMSTRONG, C., MORRICE, N., FRAME, S. & COHEN, P. 2002b. Phosphorylation of the regulatory subunit of smooth muscle protein phosphatase 1M at Thr850 induces its dissociation from myosin. *Febs Letters,* 527**,** 101-104.

VIJAYKUMAR, S., BUGG, C. E. & COOK, W. J. 1987. STRUCTURE OF UBIQUITIN REFINED AT 1.8 A RESOLUTION. *Journal of Molecular Biology,* 194**,** 531-544.

WANG, C., XIAO, H., MA, J., ZHU, Y., YU, J., SUN, L., SUN, H., LIU, Y., JIN, C. & HUANG, H. 2013. The F-box protein beta-TrCP promotes ubiquitination of TRF1 and regulates the ALT-associated PML bodies formation in U2OS cells. *Biochem Biophys Res Commun*.

WANG, Z., INUZUKA, H., ZHONG, J., FUKUSHIMA, H., WAN, L., LIU, P. & WEI, W. 2012a. DNA damage-induced activation of ATM promotes beta-TRCP-mediated Mdm2 ubiquitination and destruction. *Oncotarget,* 3**,** 1026-35.

WANG, Z., ZHONG, J., GAO, D., INUZUKA, H., LIU, P. & WEI, W. 2012b. DEPTOR ubiquitination and destruction by SCF(beta-TrCP). *Am J Physiol Endocrinol Metab,* 303**,** E163-9.

WANG, Z. N., TAKEMORI, H., HALDER, S. K., NONAKA, Y. & OKAMOTO, M. 1999. Cloning of a novel kinase (SIK) of the SNF1/AMPK family from high salt diet-treated rat adrenal. *Febs Letters,* 453**,** 135-139.

WATANABE, N., ARAI, H., NISHIHARA, Y., TANIGUCHI, M., HUNTER, T. & OSADA, H. 2004. M-phase kinases induce phospho-dependent ubiquitination of somatic Wee1 by SCF beta-TrCP. *Proceedings of the National Academy of Sciences of the United States of America,* 101**,** 4419-4424.

WATERHOUSE, A. M., PROCTER, J. B., MARTIN, D. M., CLAMP, M. & BARTON, G. J. 2009. Jalview Version 2--a multiple sequence alignment editor and analysis workbench. *Bioinformatics.* England.

WEI, W., AYAD, N. G., WAN, Y., ZHANG, G. J., KIRSCHNER, M. W. & KAELIN, W. G. 2004. Degradation of the SCF component Skp2 in cell-cycle phase G1 by the anaphase-promoting complex. *Nature,* 428**,** 194-198.

WENZEL, D. M., LISSOUNOV, A., BRZOVIC, P. S. & KLEVIT, R. E. 2011. UBCH7 reactivity profile reveals parkin and HHARI to be RING/HECT hybrids. *Nature,* 474**,** 105-U136.

WILSON, D. P., SUTHERLAND, C., BORMAN, M. A., DENG, J. T., MACDONALD, J. A. & WALSH, M. P. 2005. Integrin-linked kinase is responsible for Ca2+-independent myosin diphosphorylation and contraction of vascular smooth muscle. *Biochem J,* 392**,** 641-8.

WINGO, S. N., GALLARDO, T. D., AKBAY, E. A., LIANG, M. C., CONTRERAS, C. M., BOREN, T., SHIMAMURA, T., MILLER, D. S., SHARPLESS, N. E., BARDEESY, N., KWIATKOWSKI, D. J., SCHORGE, J. O., WONG, K. K. & CASTRILLON, D. H. 2009. Somatic LKB1 mutations promote cervical cancer progression. *PLoS One,* 4**,** e5137.

WISEMAN, S. L., SHIMIZU, Y., PALFREY, H. C. & NAIRN, A. C. 2013. Proteasomal degradation of eukaryotic elongation factor-2 kinase (EF2K) is regulated by cAMP-PKA signaling and the SCFbetaTRCP ubiquitin E3 ligase. *J Biol Chem*.

WOODS, A., DICKERSON, K., HEATH, R., HONG, S. P., MOMCILOVIC, M., JOHNSTONE, S. R., CARLSON, M. & CARLING, D. 2005. Ca2+/calmodulin-dependent protein kinase kinase-beta acts upstream of AMP-activated protein kinase in mammalian cells. *Cell Metabolism,* 2**,** 21-33.

WOODS, A., JOHNSTONE, S. R., DICKERSON, K., LEIPER, F. C., FRYER, L. G. D., NEUMANN, D., SCHLATTNER, U., WALLIMANN, T., CARLSON, M. & CARLING, D. 2003. LKB1 is the upstream kinase in the AMP-activated protein kinase cascade. *Current Biology,* 13**,** 2004-2008.

YAMAMOTO, H., TAKASHIMA, S., SHINTANI, Y., YAMAZAKI, S., SEGUCHI, O., NAKANO, A., HIGO, S., KATO, H., LIAO, Y., ASANO, Y., MINAMINO, T., MATSUMURA, Y., TAKEDA, H. & KITAKAZE, M. 2008. Identification of a novel substrate for TNF alpha-induced kinase NUAK2. *Biochemical and Biophysical Research Communications,* 365**,** 541-547.

YAMASHIRO, S., YAMAKITA, Y., TOTSUKAWA, G., GOTO, H., KAIBUCHI, K., ITO, M., HARTSHORNE, D. J. & MATSUMURA, F. 2008. Myosin phosphatase-targeting subunit 1 regulates mitosis by antagonizing polo-like kinase 1. *Dev Cell,* 14**,** 787-97.

YANG, J., IKEZOE, T., NISHIOKA, C., TASAKA, T., TANIGUCHI, A., KUWAYAMA, Y., KOMATSU, N., BANDOBASHI, K., TOGITANI, K., KOEFFLER, H. P., TAGUCHI, H. & YOKOYAMA, A. 2007. AZD1152, a novel and selective aurora B kinase inhibitor, induces growth arrest, apoptosis, and sensitization for tubulin depolymerizing agent or topoisomerase II inhibitor in human acute leukemia cells in vitro and in vivo. *Blood.* United States.

YEH, L. A. & KIM, K. H. 1980. REGULATION OF ACETYL-COA CARBOXYLASE - PROPERTIES OF COA ACTIVATION OF ACETYL-COA CARBOXYLASE. *Proceedings of the National Academy of Sciences of the United States of America-Biological Sciences,* 77**,** 3351-3355.

YLIKORKALA, A., ROSSI, D. J., KORSISAARI, N., LUUKKO, K., ALITALO, K., HENKEMEYER, M. & MAKELA, T. P. 2001. Vascular abnormalities and deregulation of VEGF in Lkb1-deficient mice. *Science,* 293**,** 1323-6.

YONG, J., TAN, I., LIM, L. & LEUNG, T. 2006. Phosphorylation of myosin phosphatase targeting subunit 3 (MYPT3) and regulation of protein phosphatase 1 by protein kinase A. *J Biol Chem,* 281**,** 31202-11.

YU, P. B., HONG, C. C., SACHIDANANDAN, C., BABITT, J. L., DENG, D. Y., HOYNG, S. A., LIN, H. Y., BLOCH, K. D. & PETERSON, R. T. 2008. Dorsomorphin inhibits BMP signals required for embryogenesis and iron metabolism. *Nature chemical biology,* 4**,** 33-41.

ZAGORSKA, A., DEAK, M., CAMPBELL, D. G., BANERJEE, S., HIRANO, M., AIZAWA, S., PRESCOTT, A. R. & ALESSI, D. R. 2010. New Roles for the LKB1-NUAK Pathway in Controlling Myosin Phosphatase Complexes and Cell Adhesion. *Science Signaling,* 3.

ZENG, Y., FORBES, K. C., WU, Z. Q., MORENO, S., PIWNICA-WORMS, H. & ENOCH, T. 1998. Replication checkpoint requires phosphorylation of the phosphatase Cdc25 by Cds1 or Chk1. *Nature,* 395**,** 507-510.

ZEQIRAJ, E., FILIPPI, B. M., DEAK, M., ALESSI, D. R. & VAN AALTEN, D. M. F. 2009. Structure of the LKB1-STRAD-MO25 Complex Reveals an Allosteric Mechanism of Kinase Activation. *Science,* 326**,** 1707-1711.

ZHAO, J., WEI, J., MIALKI, R., ZOU, C., MALLAMPALLI, R. K. & ZHAO, Y. 2012a. Extracellular signal-regulated kinase (ERK) regulates cortactin ubiquitination and degradation in lung epithelial cells. *J Biol Chem,* 287**,** 19105-14.

ZHAO, Y., XIONG, X., JIA, L. & SUN, Y. 2012b. Targeting Cullin-RING ligases by MLN4924 induces autophagy via modulating the HIF1-REDD1-TSC1-mTORC1-DEPTOR axis. *Cell Death Dis,* 3**,** e386.

ZHIQIANG, Z., QINGHUI, Y., YONGQIANG, Z., JIAN, Z., XIN, Z., HAIYING, M. & YUEPENG, G. 2012. USP1 regulates AKT phosphorylation by modulating the stability of PHLPP1 in lung cancer cells. *J Cancer Res Clin Oncol,* 138**,** 1231-8.

ZHONG, J., OGURA, K., WANG, Z. & INUZUKA, H. 2013. Degradation of the transcription factor Twist, an oncoprotein that promotes cancer metastasis. *Discov Med,* 15**,** 7-15.

ZHOU, G. C., MYERS, R., LI, Y., CHEN, Y. L., SHEN, X. L., FENYK-MELODY, J., WU, M., VENTRE, J., DOEBBER, T., FUJII, N., MUSI, N., HIRSHMAN, M. F., GOODYEAR, L. J. & MOLLER, D. E. 2001. Role of AMP-activated protein kinase in mechanism of metformin action. *Journal of Clinical Investigation,* 108**,** 1167-1174.

ZHOU, W., ERCAN, D., CHEN, L., YUN, C.-H., LI, D., CAPELLETTI, M., CORTOT, A. B., CHIRIEAC, L., IACOB, R. E., PADERA, R., ENGEN, J. R., WONG, K.-K., ECK, M. J., GRAY, N. S. & JAENNE, P. A. 2009. Novel mutant-selective EGFR kinase inhibitors against EGFR T790M. *Nature,* 462**,** 1070-1074.

ZHOU, X., LI, T. T., FENG, X., HSIANG, E., XIONG, Y., GUAN, K. L. & LEI, Q. Y. 2012. Targeted polyubiquitylation of RASSF1C by the Mule and SCFbeta-TrCP ligases in response to DNA damage. *Biochem J,* 441**,** 227-36.

ZOU, H., MCGARRY, T. J., BERNAL, T. & KIRSCHNER, M. W. 1999. Identification of a vertebrate sister-chromatid separation inhibitor involved in transformation and tumorigenesis. *Science,* 285**,** 418-422.

ZOU, M. H., KIRKPATRICK, S. S., DAVIS, B. J., NELSON, J. S., WILES, W. G. T., SCHLATTNER, U., NEUMANN, D., BROWNLEE, M., FREEMAN, M. B. & GOLDMAN, M. H. 2004. Activation of the AMP-activated protein kinase by the anti-diabetic drug metformin in vivo. Role of mitochondrial reactive nitrogen species. *J Biol Chem.* United States.